The Anti-Obesity Effects of the Angiotensin-Converting Enzyme (ACE) Inhibitor Captopril – Metabolomics and Transcriptomics studies

Submitted by

SERPIL KUCUKTEPE

Bachelor of Biomedical Science with Honours

A thesis submitted in total fulfilment of the requirements for the degree of

Doctor of Philosophy

Department of Physiology, Anatomy and Microbiology

School of Life Sciences

College of Science, Health and Engineering

La Trobe University

Victoria, Australia

August 2019

Table of Contents

Chapter 1 1
Literature Review 1
Introduction 1
Obesity 2
Definition 2
Epidemiology 3
Aetiology 3
Current treatment options for Obesity 9
Negative energy balance 9
Pharmacotherapy 11
Bariatric surgery 11
Health implications of Obesity 11
Hypertension 12
Insulin resistance 14
Non-alcoholic fatty liver disease (NAFLD) 15
Physiology, pathophysiology & endocrinology of adipose and liver tissues 16
Physiology & pathophysiology of adipose tissue 16
Endocrinology of adipose tissue 19
Physiology & pathophysiology of liver tissue 21
Endocrinology of liver tissue 23
Molecular pathways to Obesity 24
Molecular pathways to weight loss: modulation of the Renin-angiotensin system 28
Conclusion 31
Aims and hypotheses 31
Chapter 2 33
General Materials and Methods 33
Mouse studies 33
Caenorhabditis elegans studies 34
Chapter 3 37
High dietary salt consumption impedes the weight loss efficacy of captopril in C57BL/6J mice maintained on a high-fat diet: A metabolomics study 37
Abstract 37
Introduction 38
Materials & methods 40
Animal subjects 40
Treatment groups 40
Tissue collection and storage 40

Extraction and Optimisation of mouse plasma for GC-MS 41
Polar metabolite derivatisation 41
Annotated untargeted metabolite analysis: GC-MS instrument conditions 41
Data processing (GC-MS) and statistical analyses 42
Statistical analysis 42
Results 44
Body weight 44
Organ mass 46
Feed Intake 50
Fluid Intake 52
Average daily Salt intake 53
Average daily Captopril dosage 53
Non-targeted metabolic profiling of plasma 54
Discussion 71
The effect of captopril and salt on bodyweight, organ mass, feed and water consumption 71
The effect of captopril and salt on the plasma metabolomes of C57BL6/J mice 72
Conclusions 90
Chapter 4 92
High dietary salt consumption impedes the weight loss efficacy of captopril in C57BL/6J mice maintained on a high-fat diet: liver and adipose tissue transcriptomics 92
Abstract 92
Introduction 93
Methods 95
Isolation of total RNA, library construction and RNA sequencing 95
RNAseq data analysis 95
Gene ontology 95
Results 97
Transcriptome analyses of mouse livers 97
Transcriptome analyses of mouse adipose tissues 116
Discussion 132
Liver tissue transcriptomics 132
Adipose tissue transcriptomics 146
Conclusion 153
Acknowledgements 153
Supplementary Data – Transcriptomics 154
Chapter 5 170
Captopril extends lifespan, reduces body fat and improves age-related deterioration and response to stress in *Caenorhabditis elegans* 170
Abstract 170

Introduction.....171
Methods.....172
Strains and maintenance.....172
Captopril treatment of agar plates.....172
Lifespan experiments.....172
Preparation of worm homogenates and biochemical assays.....173
Oil Red O preparation, *C. elegans* fixation, fat staining and analysis.....173
Determination of body length, pharyngeal pumping rate and motility.....174
Stress response assays.....174
Results.....175
The effect of captopril on lifespan of *C. elegans*.....175
The effect of captopril on fat storage in *C. elegans*.....179
The effect of captopril on age-related functional change and satiety.....183
The effect of captopril on lifespan and fat accumulation in *daf-16* and *flcn-1* loss-of-function *(lf)* mutants.....186
Discussion.....190
The effect of captopril on body fat storage and survival in *C. elegans*.....190
Captopril reduced triglyceride content in wild-type C. elegans.....190
Captopril reduced triglyceride content in flcn-1, but not daf-16 mutants.....190
Captopril extended the lifespan of wild-type C. elegans.....193
Captopril increased the lifespan of flcn-1, but not daf-16 mutants.....194
Captopril improved tolerance of *C. elegans* to oxidative and heat stress.....195
Captopril increased pharyngeal pumping rates in *C. elegans*.....197
Captopril reduced locomotor activity in *C. elegans*.....197
Conclusion.....199
Chapter 6.....201
General discussion.....201
References.....208
Appendix.....248

List of Tables

Table 1. Australian dietary recommendations for weight loss 10
Table 2 Baseline and post-mortem characteristics of mice: body, visceral fat, liver and kidney masses 49
Table 3. Average daily food intake 51
Table 4 Average daily fluid intake 52
Table 5 Average daily salt intake and captopril dose 53
Table 6 Discovery set (GC-MS): descriptive statistics 54
Table 7. Validation set (GC-MS): discriminating metabolites after correcting for multiple testing 62
Table 8 Metabolite relationship with phenotypic characteristics 66
Table 9. Top-20 biological process GO terms of downregulated DEGs significantly enriched in the liver 98
Table 10. Differentially expressed genes of liver ACE–Ang-II–AT_1 receptor and Ang(1-7)–ACE2–Mas receptor–HSL signaling axes 103
Table 11. Differentially expressed genes of carbon metabolism, TCA cycle and their interaction effect in liver tissue 107
Table 12. Differentially expressed genes of cell cycle regulation and p53 signaling, and their interaction effect in liver tissue 111
Table 13. Biological process GO terms of upregulated WL-related genes significantly enriched in the adipose tissue. 117
Table 14. Differentially expressed genes of adipose tissue ACE–Ang-II–AT_1-receptor and ACE2–Mas receptor–HSL signaling axes 123
Table 15. Differentially expressed genes associated with DNL, adipogenesis, obesity and body composition 125
Table 16. Differentially expressed genes involved in peroxisomeal processes, RNA transport, Spliceosome, Phenylalanine and BCAA metabolism. 129
Table 17 The effect of captopril on the lifespan of *C. elegans* 175
Table 18. The effect of captopril on stress responses in *C. elegans* 178
Table 19. The effect of captopril on fat storage and LD diameter in *C. elegans* 181
Table 20. The effect of captopril on age-related functional changes and satiety in *C. elegans* 185
Table 21. The effect of captopril on the lifespan of *daf-16* loss-of-function *C. elegans* 188
Table 22. The effect of captopril on the lifespan of *flcn-1* loss-of-function *C. elegans* 190

List of Figures

Figure 1. Intersection between *loci* associated at genome-wide significance with measures of adiposity and other metabolic traits. 5
Figure 2. Contribution of food groups to daily energy intake (% daily energy) in the current Western diet and predicted pre-agricultural ancestral diet 8
Figure 3. Components of the Renin-angiotensin system (RAS) 13
Figure 4. Key morphological characteristics of adipocytes. 19
Figure 5. Metabolic pathways of DNL in liver cells.....25
Figure 6. Receptor and non-receptor tyrosine and threonine kinases activated by AT_1-receptors .27
Figure 7.The effect of dietary salt and captopril on bodyweights of mice.....45
Figure 8. Absolute and relative organ weights.....47
Figure 9. Effect of dietary salt and captopril on feed intake 50
Figure 10. Effect of salt and captopril on average daily fluid intake 52
Figure 11. Correlation scatter plots modelling the relationship between plasma metabolite levels against phenotypic traits of mice 68
Figure 12. Correlation scatter plots modelling the relationship between plasma metabolite levels against phenotypic traits of mice (continued) 69
Figure 13. Correlation scatter plots modelling the relationship between plasma metabolite levels against phenotypic traits and other metabolites of mice 70
Figure 14. Glycolytic alterations detected in the plasma of mice 75
Figure 15. TCA cycle alterations detected in the plasma of mice.....77
Figure 16. Fructose metabolising pathway alterations detected in the plasma of mice 80
Figure 17. Inositol alterations detected in the plasma of mice.....83
Figure 18 Detected pentose phosphate pathway (PPP) and gluconate pathway alterations in the plasma of mice 88
Figure 19. Venn diagram of DEGs between HF, HFS, CAP and CAPS livers 98
Figure 20. Gene ontology enrichment analysis of upregulated weight loss-related DEGs in the livers of CAP mice.....100
Figure 21 Gene ontology enrichment analysis of downregulated weight loss-related DEGs in the livers of CAP mice.....101
Figure 22. KEGG pathway analysis of the top-5 weight loss-related DEGs that are downregulated in the livers of CAP mice.....102
Figure 23. Liver protein-protein ineraction network of the Ang-II–AT_1-receptor interacting G-protein cascade.....114
Figure 25. Liver protein-protein interaction network of DEGs involved in glucose metabolism and cell cycle regulation 115
Figure 25. Venn diagram of DEGs between HF, HFS, CAP and CAPS adipose tissues 117

Figure 26. Genes reversely regulated by salt in adipose tissue (downregulated by captopril, upregulated by salt) 118
Figure 27. Genes reversely regulated by salt in adipose tissue (upregulated by captopril, downregulated by salt) 119
Figure 28. Gene ontology enrichment analysis of upregulated weight loss-related DEGs in adipose tissues of CAP mice 120
Figure 29. Gene ontology enrichment analysis of downregulated weight loss-related DEGs in adipose tissues of CAP mice 121
Figure 30. KEGG pathway analysis of weight loss-related DEGs upregulated in the adipose tissues of CAP mice 122
Figure 31. KEGG pathway depiction of glycolysis and pentose-phosphate DEGs involved in the interaction between captopril and salt in the liver 138
Figure 32. KEGG pathway depiction of TCA cycle DEGs involved in the interaction between captopril and salt in the liver 139
Figure 33. KEGG pathway depiction of cell cycle DEGs involved in the interaction between captopril and salt in the liver 142
Figure 34. KEGG pathway depiction of DEGs involved in the p53 signaling pathway and their interaction with captopril and salt in the liver 145
Figure 35. KEGG pathway depiction of DEGs involved in peroxisomal processes and their interaction with captopril and salt 152
Figure 36. Survival curves of *C. elegans* exposed to captopril from L4 stage of life 175
Figure 37. Survival curves of *C. elegans* exposed to captopril from L1 stage of life 176
Figure 38. Survival curves of *C. elegans* exposed to captopril and paraquat from L4 stage of life 177
Figure 39. Survival curves of *C. elegans* exposed to captopril and heat stress from L4 stage of life 177
Figure 40. Bright field microscopy images of oil red O stained *C. elegans* exposed to captopril 179
Figure 41. Influence of varying levels of captopril on TG content of *C. elegans* 180
Figure 42. Influence of varying levels of captopril on TG content in intestinal regions of *C. elegans* 181
Figure 43. Fluorescent microscopy of intestinal lipid droplets captopril exposed *C. elegans* 182
Figure 44. Triglyceride-to-protein ratio of *C. elegans* exposed to captopril 182
Figure 45. Mean pharyngeal pumping rate *C. elegans* exposed to varlying levels of captopril ... 183
Figure 46. Distances travelled by *C. elegans* exposed to varying levels of captopril 184
Figure 47. Speeds of movement of *C. elegans* exposed to varying levels of captopril 184
Figure 48. Survival curves of *daf-16* loss-of-function *C. elegans* exposed to varying levels of captopril 186

Figure 49. Bright field microscopy images of oil red O stained *daf-16* loss-of-function strains exposed to captopril 187
Figure 50. Influence of captopril on TG content in *daf-16* loss-of-function *C. elegans*.....187
Figure 51. Survival curves of *flcn-1* loss-of-function *C. elegans* exposed to captopril.....188
Figure 52. Bright field microscopy images of oil red O stained *flcn-1* loss-of-function strains exposed to captopril 189
Figure 53 Influence of captopril on TG content in *flcn-1* loss-of-function *C. elegans*.....189

List of abbreviations

n

1, 4-Gnl – glucono-1, 4-lactone

6PGn – 6-phosphogluconolactone

6-PGL - 6-phosphogluconolactonase

6PGDH - 6-phosphogluconate dehydrogenase

A

AA – amino acid

AldoB – aldolase B

ACC – acetyl-CoA carboxylase

ACE – angiotensin-converting enzyme

ACO – aconitase

ACLY – ATP-citrate lyase

ADP – adenosine diphosphate

AGT – angiotensinogen

Akt – protein kinase B

AMP- adenosine monophosphate

AMPK – AMP-activated protein kinase

Ang – angiotensin

Ang-(1-7) – angiotensin (1-7)

Ang-I – angiotensin I

Ang-II – angiotensin II

AR – aldehyde/aldose reductase

AT – adipose tissue

AT_1 and AT_2 – angiotensin-II receptor type 1 & 2

atgl-1 – adipose triglyceride lipase 1

ATP – adenosine triphosphate

AU – arbitrary units

B

BAT – brown adipose tissue

BCAA – branched-chain amino acid

BMI – body mass index

BP – blood pressure

C

C – Carbon

CAD – coronary artery disease

cAMP – cyclic adenosine monophosphate

CDK – cyclin-dependent kinase

CO_2 – carbon dioxide

CoA – co-enzyme A

CPT1 – carnitine palmitoyltransferase 1

CrAT – carnitine acyltransferase

CRBP – cellular-retinol binding-protein

CRP – C-reactive protein

CS/CSY – citrate synthase

CVD – cardiovascular disease

D

DAG - diacylglycerol

daf-16 – forkhead box protein O gene (*C. elegans*)

DBP – diastolic blood pressure

DEGs – differentially expressed genes

DGAT – diacylglycerol O-acyltransferase

DIO – diet-induced obesity

DNA – deoxyribonucleic acid

DNL – *de novo* lipogenesis

DR – dietary restriction

E

E4P – erythrose 4-phosphate

EE – energy expenditure

EETs - epoxyeicosatruebiuc acids

e.g. – “example”

EI – energy intake

ENO – enolase

eNOS – endothelial nitric oxide synthase

F

FA – fatty-acid

FATP – fatty-acid transport protein

FASN – fatty acid synthase

FFA – free-fatty acid

FLCN – folliculin

flcn-1 – folliculin gene (*C. elegans*)

FOXO – Forkhead box protein O

G

G3P – glyceraldehyde 3-phosphate

G3PDH – glycerate 3-phosphate dehydrogenase

G6P – glucose 6-phosphate

G6PDH – glucose 6-phosphate dehydrogenase

GAPDH – glyceraldehyde 3-phosphate dehydrogenase

GC-MS – gas chromatography-mass spectrometry

GCK – gluconate kinase

GI – glycaemic index

GK – glycerol kinase

GLDH – glutamate dehydrogenase

GLUT – glucose transporter

GPDH – glyceraldehyde phosphate dehydrogenase

H

H^+ – hydrogen ion

H_2O – water

HDL – high-density lipoprotein

HF – high-fat

HFD – high-fat diet

HK – hexokinase

HSCs – hepatic stellate cells

HSF-1 – heat-shock factor-1

HSL – hormone sensitive lipase

HSP – heat shock protein

I

i.e. – "that is"

IDH – *iso*-citrate dehydrogenase

IFG – impaired fasting glucose

IIS – insulin/IGF-1 signaling

IL – interleukin

IMPase – inositol monophosphate phosphatase

IP – inositol phosphate

IPMK – inositol polyphosphate multikinase

IR – insulin resistance

IRS – insulin receptor substrate

InsR – insulin receptor

J

JNK – c-Jun N-terminal kinases

K

KO – knockout

KHK – ketohexokinase

L

LCAD – long-chain acyl-CoA dehydrogenase

LD – lipid droplet

LDH – lactate dehydrogenase

LDL – low-density lipoprotein

lf – loss of function

LPL – lipoprotein lipase

M

M – Molar

MAPK – mitogen-activated protein kinase

MAS – Angiotensin-(1-7) receptor

MCD – malonyl-CoA decarboxylase

MCM – minichromosome maintenance complex

MDH – malate dehydrogenase

ME1 – malic enzyme

MetS – metabolic syndrome

MIOX – *myo*-inositol oxygenase

MIPS – *myo*-inositol-1-phosphate synthase

mM – millimolar

mm – millimetre

MOGAT – monoacylglycerol O-acyltransferase

mRNA – messenger ribonucleic acid

N

NAD – nicotinamide adenine dinucleotide

NADPH – nicotinamide adenine dinucleotide phosphate

$NADP^+$ - nicotinamide adenine dinucleotide phosphate (reduced form)

NAFLD – non-alcoholic fatty liver disease

NASH – non-alcoholic steatohepatitis

NGM – nematode growth medium

NHS – national health survey

NO – nitric oxide

noxPPP – non-oxidative pentose phosphate pathway

NOX – NADPH oxidase

O

O_2^- - superoxide

OGDH – alpha-ketoglutarate dehydrogenase

OXPHOS – oxidative phosphorylation

oxPPP – Oxidative pentose-phosphate pathway

P

n-P – *n*-phosphate (*n* is numeric)

PAI-*n* – plasminogen activator inhibitor

PC – pyruvate carboxylase

PDH – pyruvate dehydrogenase

PFK – phosphofructokinase

PGC-1α - Peroxisome proliferator-activated receptor gamma coactivator 1-alpha

PGI – glucose phosphate isomerase

PGK – phosphoglycerate kinase

PGM – phosphoglycerate mutase

PIP_2 – phosphatidylinositol 4,5-bisphosphate

PK – pyruvate kinase

PP – pentose-phosphate

PPP – pentose-phosphate pathway

PPAR-α – peroxisome proliferator-activated receptor alpha

PPAR-δ – peroxisome proliferator-activated receptor delta

PPAR-γ – peroxisome proliferator-activated receptor gamma

PRR – (pro)renin receptor

PTS1 – peroxisomal targeting sequence type 1

PUFA – Polyunsaturated fatty acids

R

R5P – ribose-5-phosphate

RA – retinoid acid

RAR – retinoic acid receptors

RAS – Renin angiotensin system

RMR – resting metabolic rate

RNA – ribonucleic acid

RNAi – RNA interference

RPE - D-ribulose 6-phosphate empirase

RPI - D-ribulose 5-phosphate isomerase

ROS – reactive oxygen species

Ru5P – ribulose 5-phosphate

RXR – retinoid X receptor

S

SAT – subcutaneous adipose tissue

SBP – systolic blood pressure

SCD – stearoyl-CoA desaturase

SD – standard deviation

SDH – sorbitol dehydrogenase

sEH – soluble epoxide hydrolase

SEM – standard error of the mean

SGLT - sodium-dependent glucose cotransporter

SHPK - sedoheptulokinase

SIR - sirtuin

SOD – sulphur oxide dismutase

SREBF – sterol regulatory element-binding transcription factor

T

T2D – type-II diabetes

TALDO – transaldolase

tald-1 – transaldolase gene (*C. elegans*)

TCA – tricarboxylic acid cycle

TGFβ – transforming growth factor beta

TKT – transketolase

TLR – toll-like receptor

TNF-α – Tumor Necrosis Factor alpha

TPI – triose phosphate isomerase

U

UA – uric acid

UCP – uncoupling protein

V

VAT – visceral adipose tissue

VLDL – very-low density lipoprotein

VSMCs – vascular smooth muscle cells

W

WAT – white adipose tissue

WC – waist circumference

WD – Western style diet

WHO – World health organisation

WHR – waist-to-hip ratio

WL – weight loss

WT – wild-type

Abstract

The angiotensin-converting enzyme (ACE) plays a major part in blood pressure (BP) regulation through the renin-angiotensin system (RAS), which is typically upregulated in obesity. We have previously shown inhibition of ACE with captopril to lower BP, improve insulin sensitivity, promote anti-stress responses and reduce body fat content in rodent models of obesity. Albeit, the latter effect has not been reported in humans. We previously investigated the hypothesis that this may be due to excessive dietary salt consumption, and reported an interaction between salt and captopril whereby a high-salt diet counteracted the weight loss properties of captopril in the presence of a lower-salt diet. In order to better understand the metabolic pathways and molecular targets of captopril and its interaction with salt, in the first two experimental chapters of this thesis we explored the metabolomic changes in plasma and the transcriptomic changes in liver and adipose tissues of C57BL/6J mice treated with captopril following a standard or a high-salt obesogenic diet. In the final experimental chapter, we investigated the effect of captopril on body fat, stress responses and locomotive patterns of *Caenorhabditis elegans* (*C. elegans*) in which the mammalian homologue of the ACE gene (*acn-1*) functions independent of a RAS, and lacks the zinc-containing binding-site for captopril. Here we showed mice treated with captopril following a (standard-salt) Western style obesogenic diet significantly decreased bodyweight and fat mass to that of mice treated with captopril and a Western style obesogenic diet high in salt. Plasma metabolomes of mice indicated an interaction effect between captopril and salt involving metabolites primarily of carbohydrate/glucose origin as well as the tricarboxylic acid (TCA) cycle. In the second experimental chapter, liver transcriptomics revealed an interaction effect between captopril and salt involving the differential expression of genes related to glucose metabolism and the TCA cycle, as well as genes involved in cell cycle progression and p53 signaling. Adipose tissue transcriptomics revealed an interaction effect between captopril and salt involving the expression of genes related to peroxisomal biogenesis and peroxisomal-target sequence 1 (PTS1) containing genes primarily involved in the metabolism of fatty acids and reactive oxygen species (ROS). In the third and final experimental chapter, we showed that *C. elegans* treated with captopril displayed responses akin to that of captopril treated rodents, in that a reduction in body fat accompanied improvements in lifespan, age-related decline and stress responses. These effects appeared to be dependent on the DAF-16/FOXO transcription factor. These studies show an interaction between captopril and salt on tissue metabolism and gene expression, and suggests a role for captopril and salt in body fat regulation that may be independent of ACE (and a functional RAS). Whether bodyweight and body fat reduction is a direct consequence of ACE-inhibition requires further investigation, especially in the case of the *C. elegans*, albeit *in vivo* it is likely that the molecular targets of captopril are more extensive and has not been completely elucidated.

Statement of Authorship

Except where reference is made in the text of the thesis, this thesis contains no material published elsewhere or extracted in whole or in part from a thesis accepted for the award of any other degree or diploma. No other person's work has been used without due acknowledgment in the main text of the thesis. This thesis has not been submitted for the award of any degree or diploma in any other tertiary institution.

Conceptualising the research idea, designing experiments, conducting empirical research presented, data collection and analysis of samples and data as well as writing this thesis has predominantly been done by myself. Dr Markandeya Jois (La Trobe University, Victoria) contributed towards the initial idea for the project. Bioinformatics analysis of plasma metabolites was conducted by Dr Daniel Anthony Dias (RMIT University, Victoria), and bioinformatics analysis of tissue transcriptome data was conducted by Mr Jiang Quanlong (Chinese Academy of Sciences, Shanghai) under the supervision of A/Professor Bo Xian (Chinese Academy of Sciences, Shanghai).

Application to conduct experiments using *C. elegans* strains was approved by La Trobe Institutional Biosafety Committee with reference number GMSC15-07. The animal study reported in this thesis was approved by La Trobe University Animal Ethics Committee (AEC 14-32).

Serpil Kucuktepe

12/08/2019

Acknowledgements

I would like to express my sincerest appreciation to my mother, Fidan Yildirim, who instilled in me the values of education and devoted her entire life to my wellbeing. Without her, my accomplishments would not be possible and nor would they mean so much. Her only wish for me was to have the opportunities she herself was not afforded. Mum, from the bottom of my heart, I thank you for your patience, for believing in me, for your endless support, and I thank you for never giving up through all trials and tribulations. You are the strongest woman I know and I could not be any prouder of you.

My sincerest gratitude goes to my principal supervisor, the brilliant Dr Markandeya Jois, for not just giving me the opportunity to complete an Honours project but also a PhD project under his guidance. I am in awe of his generosity, his encouragement of freethought, and I appreciate him for allowing me to nurture and drive this project. I know it comes with great trust, and without you Mark, I would not have realised both my own and our potential as a team. Nobody could have asked for a better supporter and friend. I can genuinely say that above all, I have learned from you what it is to be an outstanding human being, and this is perhaps the most valuable lesson you could have given to me as your pupil. Thank you for all of your wisdom over these years and thank you for making this journey one that I will forever remember.

I would also like to thank my co-supervisor, A/Professor Warwick Grant, who has always been there for me in my times of need. You have so willingly taken me under your wing and made me a part of your lab, and it is for this reason I walk away having made some friendships and memories that will last a lifetime.

I would also like to show gratefulness to A/Professor Bo Xian, who has been an exceptional collaborator and a great friend. It is always a pleasure being in your presence, you are the definition of a ‘cool scientist’. My gratitude also goes out to Dr Daniel Dias for his kindness and willingness to be of assistance, his endless offers of enthusiasm and excitement is what re-ignites the passion for the work that we do. In my greatest time of need, you were both there. Thank you.

Thank you to my closest of friends, Michael Funari and Sharifa Khairie, for always supporting me, my vision, and always keeping faith. This was a team effort and you have been my rock and my strength throughout this entire process.

Last but definitely not least, I am so thankful to all of my lab members, past and present, with whom I will forever share the memory that is “The Jois Lab”; Piet Raedts, Surafel Melaku Tegegne, Monisha Samuel, Diana Teresa Navarro Perez, Rajneet Sohi, Matthew Flavel, Awais Ahmed, Devin Benheim, Fazel Almasi, Deniz Hayderian, Abdullah Almotayri, and Mihiri Munasinghe. I would also like to acknowledge members of the Grant Lab; Neha Sirwani, Gowtam Chalasani and Shilpa Kapoor. Thank you all for your assistance throughout different stages of this journey, and thank you for your beautiful friendship.

Chapter 1

Literature Review

Introduction

Obesity has fast reached epidemic proportions where more than 650 million adults worldwide are classified as obese (WHO, 2018). The 2014-15 National Health Survey (NHS) revealed one in three Australian adults were obese and two in three of those were afflicted with at least one related health problem (ABS, 2015). The increased prevalence of obesity has led to a subsequent surge in severe health risks and the incidence of the metabolic syndrome (Harris, 2013; WHO, 2018). The metabolic syndrome can be described as a clustering of at least three risk factors comprising abdominal obesity, insulin resistance, hypertension, or dyslipidemia and enhances the possibility for developing life-threatening morbidities to even lead to mortality (Danaei et al., 2009; Guh et al., 2009). Between 2005 and 2008, the total annual cost of obesity to Australia, which includes health system costs, carers' costs and loss of productivity costs, more than doubled to $58 billion (Access Economics, 2008; AIWH, 2017; Colagiuri et al., 2010). If current trends are to prevail it is estimated that by 2025, 35% of the adult population will be obese making obesity both a major public health and economic burden to Australians (Hayes, Lung, Bauman, & Howard, 2017; PwC, 2015).

The causes of obesity are multiple and complex with a deceivingly simple ultimate cause, that is the sustained consumption of calories in excess of those expended. Among environmental and genetic factors, chronic over-consumption of a Western style diet is one of the major causes of obesity in Australia and around the world (Bankman, 2017). Modifications to lifestyle, diet and exercise programs for weight loss and prevention of weight regain are most effective and adequate in curbing obesity, especially when combined with anti-obesity drugs to further modulate the energy equilibrium (Leblanc, O'Connor, Whitlock, Patnode, & Kapka, 2011; Wadden, Berkowitz, Sarwer, Prus-Wisniewski, & Steinberg, 2001). But as the prevalence of obesity increases and the regain of weight is common, these approaches are quickly coming to be seen as ineffective long-term solutions and therapeutic drugs that are currently on the market shows limited success (Rodgers, Tschop, & Wilding, 2012; Wadden et al., 2001).

Prescribed as an anti-hypertensive agent, captopril is a pharmacological angiotensin-converting enzyme (ACE) inhibitor which modulates the activity of the systemic renin-angiotensin system (RAS) (Zusman, 1987), and over activation of the RAS in obesity is consistently reported (Kalupahana & Moustaid-Moussa, 2012). In addition to lowering blood pressure, more recently captopril has been recognised for its role in preventing body fat gain and causing weight loss, improving insulin sensitivity and reducing tissue and systemic inflammation in rodent models of diet-induced obesity (DIO) (de Kloet et al., 2009; Mathai, Naik, Sinclair, Weisinger, & Weisinger, 2008; Premaratna et al., 2012; Stanley, 2013; Weisinger et al., 2009). Although a growing body of

evidence portrays captopril as an effective anti-obesity agent, there is no evidence of weight loss in humans.

The high-salt content of Western style foods strongly associates salt intake with obesity and metabolic complications, where obese individuals have been shown to consume up to four times the recommended daily intake (RDI) of 1,600 mg day^{-1} of sodium, which is equivalent to approximately 4.0g of salt (Oh, Koo, Han, Han, & Chin, 2017; Zhang, Wang, Li, Yu, & Song, 2018). Moreover, dietary salt has been known to regulate the systemic RAS (Drenjancevic-Peric et al., 2011) and there is evidence to suggest that a high-salt diet may moderate the anti-hypertensive efficacy of captopril (Swartz et al., 1980). This raises the hypothesis that a high-salt diet may offset the weight loss efficacy of captopril, as with its anti-hypertensive efficacy, and that this may embrace part of the reason as to why there is lack of reporting of weight loss in humans prescribed captopril. Therefore, a diet made lower in salt may enhance captopril's weight loss effect in obese humans and mice.

The aim of this project is to investigate captopril's interaction effect with dietary salt in C57BL6/J mouse models of DIO and assess whole animal responses at the metabolite and molecular level. In addition, we employed the *C. elegans* as it is devoid of a RAS and contains a homologue of the ACE gene, *i.e. acn-1*, to further address the pharmacological question of captopril and its body fat regulating potential. We also used the *C. elegans* worm to give indication of molecular pathways that are essential for captopril to facilitate a reduction in body fat.

Obesity

Obesity is resultant of an imbalance in energy homeostasis caused by (1) an increase in energy intake, (2) a decrease in energy expenditure, and (3) storage of calories on the body as fat. Obese individuals present a higher risk for developing chronic illnesses such as type-II diabetes (T2D), hepatic steatosis, hypertension, dyslipidaemia, cardiovascular diseases (CVD, *e.g.* coronary artery disease, CAD), pulmonary disorders, some forms of cancers and other ailments to be collectively recognised as a syndrome (Danaei et al., 2009). The regional distribution of body fat has to some capacity been associated with the development of such health issues where 'abdominal obesity' or 'upper body adiposity' is commonly accompanied with hormonal and metabolic abnormalities linked with T2D and CVD (Castro, Kolka, Kim, & Bergman, 2014).

Definition

The World Health Organisation (WHO) characterises obesity as the excessive accumulation of fat on the body of individuals to levels which substantially increases risk to health (WHO, 2018). Crude population measures of obesity includes the body mass index (BMI) or waist circumference (WC). The BMI expresses weight adjusted for height and is calculated by dividing a subject's weight (kg) by the square of their height (m^2) (Keys, Fidanza, Karvonen, Kimura, & Taylor, 1972). Limits defined by the WHO for overweight and obese individuals are those with a BMI >25kg/m^2 and

>30kg/m^2 respectively (WHO, 2018). The WC can give subjects an indication of body weight and relative risk of developing metabolic diseases, where a WC of 80-88cm for adult women and 94-102cm for adult men indicates obesity and increased risk of chronic disease (DoH, 2013; Pouliot et al., 1994).

Epidemiology

Having reached epidemic proportions, obesity reflects the profound changes in diet, lifestyle and behavioural patterns of humans in communities in recent decades (Wells, 2012). From 1995 to 2015, the proportion of obese adults in Australia increased from 18.5% to 27.9% and population projections estimates that this will increase to 35% by 2025 (ABS, 1995; Hayes et al., 2017). The change in adult prevalence of obesity is mirrored in children and adolescents, where rates in those aged 5-17 increased from 5% to 7.4% between the years of 1995 to 2014-15 (ABS, 1995, 2015).

Traditionally prevalent in wealthy countries, obesity has spread where now two thirds of the world's overweight and obese people live in developing countries (Ng et al., 2014). Despite the overall prevalence of obesity exceeding 50% in some South Pacific island countries, adult obesity in Egypt is highest in the world at 35% and childhood and adolescent obesity in the United States ranks highest at 13% (Afshin et al., 2017).

Obesity is associated with several risk factors, which shorten life expectancy by increasing an individual's chance of developing T2D and CVD (Mottillo et al., 2010). In 2016, CAD was the single leading cause of mortality responsible for 12% of all deaths in addition to contributing to one in four deaths (22%) in 2016 (ABS, 2017). There is indication that 85% of obese children become obese adults, and these children are at increased risk for early adulthood morbidity and mortality (Dietz, 1998; Weiss, Bremer, & Lustig, 2013). It has further been predicted that adolescents diagnosed with T2D lose 15 years from their remaining life expectancy in comparison to peers who do not have T2D (Springer et al., 2013).

Recent estimates indicate that in 2011-12 obesity alone cost key stakeholders in Australia $8.6 billion (AIWH, 2017), and if this trend prevails it is predicted that by 2025 the additional 2.4 million more obese people will continue to add $87.7 billion in accumulated total costs to Australian society (PwC, 2015).

Aetiology

Obesity is no longer viewed as a single disorder, rather a complex condition with multiple causes. An oversimplified view is that obesity is due to an energy imbalance such that in a given individual, if energy intake exceeds energy expenditure, the net result is positive energy balance which manifests accumulatively in the form of triglycerides (TG) in adipose tissue (Hofbauer, 2002). An all-inclusive explanation for obesity is the interactions occurring between human biology and genetics with the modern environment, simultaneously influencing energy intake and expenditure

(Huang & Hu, 2015; Jebb, 1997). Biological, genetic and various environmental/behavioural factors involved in the pathogenesis of obesity are discussed below.

Biological determinants

Genetic predisposition: monogenic, syndromic and polygenic obesity

Obesity may be classified as either polygenic, monogenic or syndromic, depending on its ultimate cause. Polygenic (common) obesity affecting the general population and arising when susceptible genotypes interact with obesity-promoting or 'obesogenic' environmental factors. The aetiology of monogenic and syndromic obesity is of genetic origin and is often due to gene disturbances operating within the leptin-melanocortin signaling pathway or as a symptom of multiple genetic defects (Krude et al., 1998; Montague et al., 1997; Rao, Lal, & Giridharan, 2014). Phenotypes commonly associated with impaired leptin-melanocortin signaling is hyperphagia, morbid obesity, and severe early-onset (congenital) obesity (Butler, 2016; Driscoll, Miller, Schwartz, & Cassidy, 1993; Farooqi & O'Rahilly, 2014). Henceforth, topics and discussions presented within this dissertation are related to the polygenic form of obesity.

The aetiology of polygenic obesity is multifactorial and can be broadly associated with the interplay between specific gene variants and multiple environmental stimuli (Carr et al., 2013; Dalle Molle et al., 2017; Frayling et al., 2007). When considered individually, each gene variant may have a modest effect on body fat gain whereas cumulative effects of specific genes can be further amplified by obesogenic environmental factors. To date over 150 independent loci associated with BMI and the development of obesity and metabolic diseases have been identified; see figure 1 below (Grarup, Sandholt, Hansen, & Pedersen, 2014; Pigeyre, Yazdi, Kaur, & Meyre, 2016; Rao et al., 2014). An example includes the 'fat mass and obesity' (*FTO*) gene, variants of which have been linked to adult and childhood obesity and T2D by inflicting an allelic 0.39 kg/m^2 increase in BMI (Frayling et al., 2007). Homozygosity for the allele is shown to be concomitant with a 3 kg increase in body weight and close to a 2-fold increase in the risk of developing obesity (Frayling et al., 2007; Zeggini et al., 2007). Overexpressing of *FTO* is strongly associated with behaviours such as pathological eating attitudes and physical inactivity in individuals (*e.g.* high frequency of binge-eating episodes), behaviours which are conducive to excessive bodyweight gain and obesity which are discussed further below (Bjørnland, Langaas, Grill, & Mostad, 2017; Castellini et al., 2017).

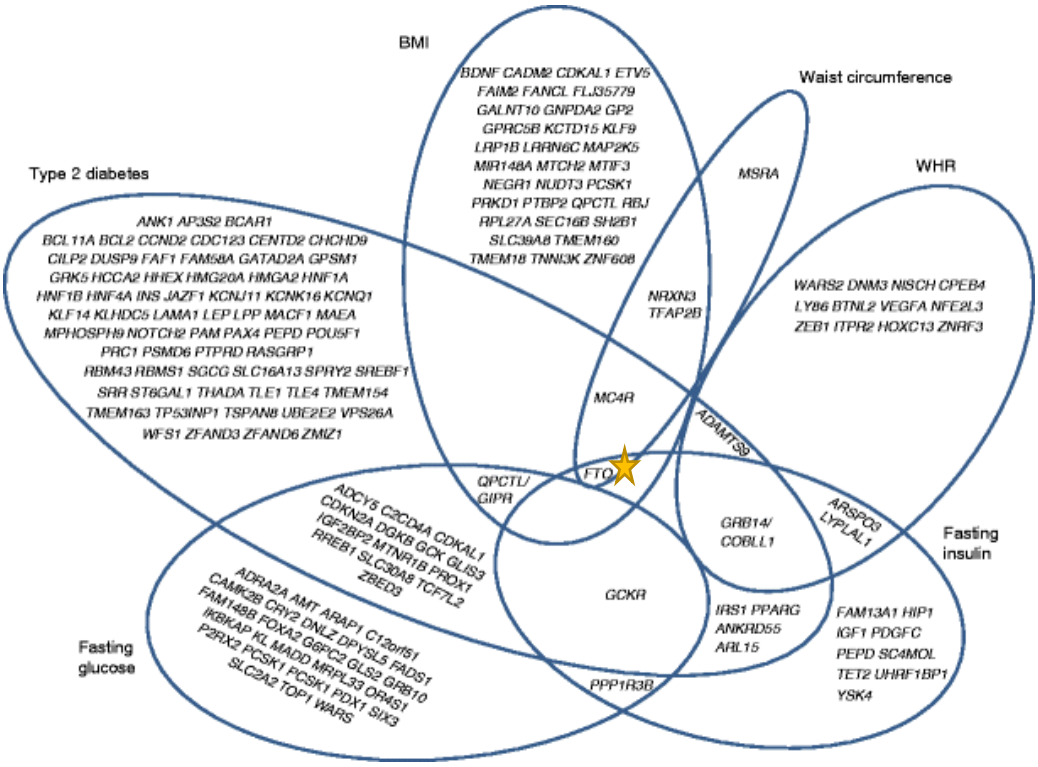

Figure 1. Venn diagram derived from Grarup et al. (2014), depicting the junction between *loci* associated at genome-wide significance with measures of adiposity, glucose homeostasis, T2D and other metabolic traits. Gene symbols are shown within the plot and FTO marked by star.

Environmental and behavioural determinants

Food and physical activity are two factors influenced by our built environment. The ingestion of high-fat (HF) energy-dense foods and reduced energy expenditure (EE) are the two factors currently conducive to obesity in Australia (AIHW, 2016). Excessive sodium consumption is also conducive to the declining cardiovascular health of Australians (NHFA, 2017; NHMRC, 2017) and emerging evidence suggests that high sodium consumption is independently associated with higher risk of obesity and central adiposity in humans (Ma, He, & MacGregor, 2015). Dietary and lifestyle risk factors for obesity are discussed below.

Lifestyle factors – physical inactivity and sedentary living

Markers of inactivity, including automobile dependency, TV viewing and sedentary occupations can influence bodyweight and the overall health of individuals at a community level (Ewing, Meakins, Hamidi, & Nelson, 2014; Ewing, Schmid, Killingsworth, Zlot, & Raudenbush, 2003).

There is evidence to link automobile dependency to declining levels of physical activity and obesity (Ewing et al., 2014; Mason, 2000). The "country sprawl index" defined by Ewing et al. (2003) describes a direct relationship between urban sprawl with BMI, physical activity and morbidity. As the sprawl index of "compact" countries increases at the population level, BMI declines owing to the low levels of vehicle ownership, shorter drives, higher transit and walking times and reduced

automobile dependencies of individuals (Ewing & Hamidi, 2014; Ewing et al., 2014). The opposite of this is observed for individuals living in sprawling countries, where the probability of obesity in young adults living in rural areas was 2.18 times that of comparable youth living in metropolitan areas of the United States (Ewing, Brownson, & Berrigan, 2006).

The hours spent on sedentary behaviours such as TV viewing, internet/computer use and desk-bound jobs has been identified as a risk factor for obesity. In the case with Australian children, a direct correlation between the number of hours spent watching television and bodyweight has been observed such that for each additional hour of television watched daily, the likelihood of a child being overweight increased 20-30% (Steffen, Dai, Fulton, & Labarthe, 2009). Moreover Australian adults who used the internet and computer for 3 or more hours a week were 1.5-2.5 times more likely to be overweight and obese compared to non-users (Vandelanotte, Sugiyama, Gardiner, & Owen, 2009). Australian workers in sedentary occupations who are sitting more than 6 hours a day have double the risk of being overweight or obese in comparison to those who spend less than one hour a day sitting (Brown, Miller, & Miller, 2003; Mummery, Schofield, Steele, Eakin, & Brown, 2005).

This evidence has led to the development of physical activity guidelines for overweight and obese individuals, suggesting both children and adults spend a minimum of 60-90 minutes on physical activity daily to lose bodyweight or maintain bodyweight loss (Haskell et al., 2007).

Dietary factors

Overfeeding, high-energy foods and the macronutrient composition of diets

Over-consumption of energy-dense foods with weak satiety value facilitates excess energy intake (EI) and is considered a predisposing factor to obesity (Stubbs, Ferres, & Horgan, 2000). Current nutritional guidelines in Australia recommends a daily energy intake of 8,700 kilojoules (kJ) for the average adult, yet this value varies depending on age, gender, body composition and physical activity level (NHMRC, 2017). On average however it is estimated that adults consume 815 excess kJ day^{-1}, and overweight and obese adults approximately 1,340 kJ day^{-1} (PHE, 2018). Dietary behaviours linked to creating excess EI includes: (1) high-intake and larger portion sizes of foods that are energy-dense, particularly foods high in saturated-, trans- and animal-fat, or high glycaemic index (GI) carbohydrates (Horton et al., 1995; Howarth, Huang, Roberts, & McCrory, 2005); (2) low-intake of high-fibre, low energy-dense foods such as fruits and vegetables (Davis, Hodges, & Gillham, 2006); (3) high-consumption of alcohol and sugar sweetened beverages (Bermudez & Gao, 2010; Traversy & Chaput, 2015).

Western style diet – a brief overview of current research perspectives

The current Western style diet (WD) may predispose modern populations to obesity and morbidity (Cordain et al., 2005). General characteristics of the WD today includes high intakes of red meat, processed foods, high-fat dairy and hydrogenated fats, eggs, refined cereal grains, artificially

sweetened foods and salt, with little intake of plant based foods, fish, legumes and whole grains (Bloomfield et al., 2015). Fathomably, the macro- and micro-nutrient composition of the WD is far from that of pre-agricultural dietary characteristics which conditioned the human genome. This has led to the notion that "*human energy homeostasis is maladapted to food excess and a sedentary lifestyle*" that is represented by the nutritional, cultural and behavioural patterns of modern societies today (Wilkin & Voss, 2004). Studies of hunter-gatherer populations provides information regarding dietary trends and estimated differences in dietary composition between pre-agricultural diets and the WD today (Cordain et al., 2000); see figure 2 for current and ancestral dietary macronutrient estimates. Implications of excess dietary salt consumption is reviewed below.

Emerging evidence suggests that the WD promotes hyperphagia by elevating peripheral endocannabinoid signaling via $G_{i/o}$ protein-coupled cannabinoid-type 1 receptor (*Cnr1*) activation (Argueta & DiPatrizio, 2017). Moreover, metabolites derived from vegetables and spices are able to bind peripheral cannabinoid-type 2 receptors (*Cnr2*) present in immune cells which may be protective against inflammatory stress (Pacher & Mechoulam, 2011). *Cnr1* deficiency in rodents is associated with leanness and resistance to DIO, and similarly, pharmacological blockade of *Cnr1* reduces food intake, bodyweight and increases adiponectin gene and protein expression (Bensaid et al., 2003; Ravinet Trillou, Delgorge, Menet, Arnone, & Soubrie, 2004). On the other hand, the precise role of *Cnr2* is still largely undetermined yet *Cnr2* deficient mice have greater increases in food intake and bodyweight but are largely protected from IR (Agudo et al., 2010). Thus foods able to regulate *Cnr1/Cnr2* receptor activation ratio may play a role in the WD and in its mediation of obesity and disease development.

There is suggestion that qualitative differences, particularly in that of carbohydrates consumed, between Westernised and the pre-agricultural "Paleolithic" diet may in large contribute to leptin resistance and obesity in humans today (Spreadbury, 2012). In line with this, systemic reviewing and meta-analyses has concluded that in free living people the *ad libitum* intake of free-sugars, *i.e.* added sugars and sugar components of foods, is a determinant of bodyweight (Te Morenga, Mallard, & Mann, 2012). Though starch is the main carbohydrate source in the WD, sugars in the form of mono- and disaccharides represents 20% of daily energy intake (Tappy, 2018) which is double the WHO recommendations (WHO, 2015). Whilst it is important to note that sugar is not solely responsible for the deleterious effects of the WD, there is indication that it is largely detrimental to health due to its ubiquitous and high presence in pre-packaged and processed foods/beverages that is commonly consumed amongst modern societies (Webber, 2003).

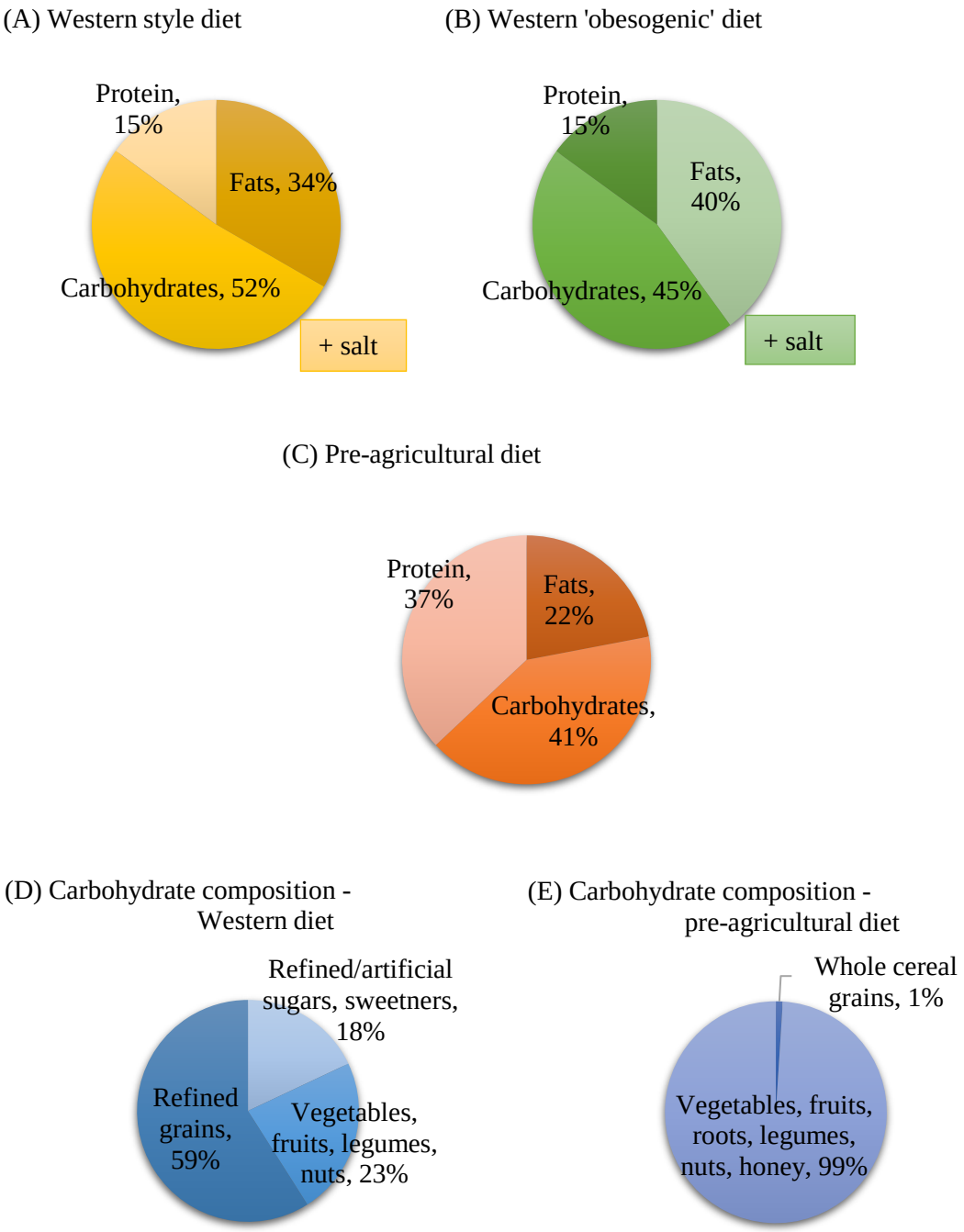

Figure 2. Contribution of food groups to % of daily energy intake in the current (A-B) Western diet and (C) predicted pre-agricultural ancestral diet. Qualitative differences in daily energy from carbohydrates between current (D) Western diets and (E) average ancestral diets. Data adapted from Konner and Eaton (2010) and Jew, AbuMweis, and Jones (2009).

Excess dietary salt (sodium) consumption and obesity

The connection between salt and obesity has accumulated over the years and there is evidence that high dietary intake is an independent risk factor for the development of obesity and central adiposity (Lanaspa et al., 2018; X. Zhang et al., 2018). On average, each 1.0 g of sodium ,equating to ~2.5 g of dietary salt, resulted in a 15% increase in the risk of obesity and 24% increase in the risk of

central adiposity (X. Zhang et al., 2018). Additionally, studies have shown a direct harmful effects of different levels of salt intake on factors contributing to cardiovascular health which includes serum lipids, insulin sensitivity, hypertension and the renin-angiotensin system (Kong, Baqar, Jerums, & Ekinci, 2016).

Consumption of salt in Western countries typically exceeds levels recommended by governments and international authorities (Brown, Tzoulaki, Candeias, & Elliott, 2009; Powles et al., 2013). Australian dietary guidelines have set adequate daily intake for salt to 1.17–2.30 g and a daily target of <5.0 g is advised for prevention of chronic diseases such as hypertension (NHMRC, 2017). Current population averages for salt consumption is estimated at 10.0 g day^{-1} whilst obese individuals have been reported as consuming levels of up to 13.0 g day^{-1} (NHMRC, 2017; Young & Barnason, 2016; H. Zhu et al., 2015). These reports show salt consumption among all Australians exceeds nutrient requirements and recommended targets.

A major source of excess salt is from pre-prepared processed, fast- and full-serviced restaurant foods, which are estimated to contribute up to 75-80% of the daily total by adding 0.8–1.0 g to each meal. Pre-prepared foods are also estimated as adding a net 836.8 kJ to total daily EI and these figures are even larger in obese adults (An, 2016; McLean, 2014). It is therefore not surprising that high salt intake in Australians is mirrored by the increase in accessibility and frequency of consumption of pre-prepared foods (ABS, 2008), which also correlates with the prevalence of central obesity and metabolic risk in young adults (Smith et al., 2009). Together, this suggests excessive salt consumption in Australians may be associated with the increase in accessibility and frequency of consumption of energy-dense pre-prepared foods which is in turn a predisposing factor to obesity.

Therefore dietary recommendations for obese patients often includes a reduced salt diet due to positive associations with increased palatability of foods, cardiovascular diseases, and measures of body size and body fat (Bolhuis, Lakemond, de Wijk, Luning, & de Graaf, 2012; Ma et al., 2015; NHFA, 2017; Oh et al., 2017; Yi, Firestone, & Beasley, 2015).

Current treatment options for Obesity

The National Preventative Health Strategy identifies the prevention of unhealthy weight gain as the most appropriate method by which to tackle obesity (NPHT, 2009). Given the extent of obesity in Australia, methods of weight loss interventions for the management of obesity is also of high importance particularly due to the associated health risks.

Negative energy balance

Successful non-pharmacological methods of management for obesity require obese individuals to modify dietary and physical activity behaviours. Combining an energy restricted diet with aerobic exercise appears to be more successful at aiding bodyweight and fat loss than either on its own, and

may be more beneficial in long-term bodyweight loss and maintenance (Johns, Hartmann-Boyce, Jebb, & Aveyard, 2014). Due to poor adherence to dietary and exercise strategies, maintaining weight loss beyond 1 year is rare (30%-35% of weight regained) and the majority of individuals who lose weight relapse to gain all or more weight within 4-5 years (Mann et al., 2007). See table 1 below for Australian dietary recommendations for weight loss.

The macronutrient composition of diets is also important as different foods with equal energy may have different effects on bodyweight and food intake through their effect on satiety and metabolism (Galgani & Ravussin, 2008; Rolls, Hetherington, & Burley, 1988; Rolls et al., 1994; Veldhorst et al., 2009). Typically, overweight and obese adults consume more total fat (38.7% versus 33.5%), saturated fat, and cholesterol and less carbohydrate (44.9% versus 52%) and dietary fibre than normal weight adults, whilst protein intake remains consistent (10-15%); see figure 2 for dietary macronutrient estimates (Davis et al., 2006). Conventional dietary macronutrient targets recommended for reducing the risk of developing obesity and chronic disease in Australia and New Zealand are: (1) 15-25% of daily EI from protein, (2) 20-35% of daily EI from fat, and (3) 45-65% daily EI from carbohydrates that are predominantly low in GI (NHMRC, 2017). These targets emphasise a low-fat, high-carbohydrate diet that is moderate in protein content due to its lower energy-density and enhanced effects on feelings of satiety (NHMRC, 2017; USDA, 2002).

An accumulating body of clinical evidence however supports a negative-energy balance diet in which 20 to 35% of EI is comprised of protein whilst fat and carbohydrate composition is personalised according to lifestyle and metabolic status (Astrup, 2005; Astrup, Raben, & Geiker, 2015; Brouns, 2018; Hu et al., 2012; Larsen et al., 2010; Sartorius, Sartorius, Madiba, & Stefan, 2018). Differing the contents of carbohydrates and fats in negative-energy balance has been shown to be equally as effective at lowering bodyweight and metabolic risk, yet diverse effects on various blood metabolites have been observed (Bravata et al., 2003; Hu et al., 2012; Noakes, Keogh, Foster, & Clifton, 2005; Sartorius et al., 2018). Compared with low-fat diets, individuals on low-carbohydrate diets generally exhibited a lower reduction in blood insulin and fasting glucose levels, total cholesterol and low-density lipoprotein (LDL) cholesterol but a greater increase in high-density lipoptotein (HDL) cholesterol and a greater decrease in TGs (Hu et al., 2012; Sacks et al., 2009; Santos, Esteves, da Costa Pereira, Yancy, & Nunes, 2012; Sartorius et al., 2018). Therefore dietary recommendations should be curated according to such reports, for instance a low-carbohydrate weight loss diet could be prescribed to obese persons with abnormal metabolic risk (Brouns, 2018).

Table 1. Australian dietary recommendations for weight loss (NHMRC, 2013a):

(1) low-GI high-fibre carbohydrates from a variety of fruits, vegetables and whole-grains;

(2) low-in-fat, especially saturated- and trans-fats from processed foods and refined oils;

(3) lean meats, poultry and fish as well as nuts and legumes;

(4) fewer foods/drinks with added salt, sugar and alcohol

Pharmacotherapy

Pharmacotherapy in the form of appetite suppressants and nutrient absorption inhibitors may be useful in aiding initial weight loss, maintaining weight loss, or preventing weight regain at the end of an intervention. Only three drugs have been approved by the Therapeutic Goods Administration (TGA) for the treatment of obesity in Australia which includes Phentermine (Duromine®, Metermine®), Orlistat (Xenical®) and Liraglutide (Saxenda®) (Ching Lee & Dixon, 2017). Phentermine acts as an appetite suppressant which in conjunction with an energy restricted diet can induce a 5-10% reduction in body weight and WC by 12-weeks of treatment (Kang, Park, Kang, Park, & Park, 2010). Orlistat acts as a pancreatic and gastric lipase inhibitor by reducing hydrolysis of TGs in to absorbable free-fatty acids (FFAs) and monoacylglycerols, decreasing overall fat absorption by 30%. A mean weight loss of 2.9-3.4% after 1-year of treatment can be accomplished with Orlistat alone (Apovian et al., 2015). Liraglutide is a glucagon-like peptide 1 receptor agonist that slows gastric emptying and supresses appetite, and as an adjunct to diet and exercise intervention, lead to a 3% and 8% reduction in BMI and bodyweight respectively after 1-year of treatment (Pi-Sunyer et al., 2015). Despite weight loss effects, pharmacological intervention with all three medications is not considered an effective long-term solution to obesity due to undesired side-effects and the weight loss achieved is insubstantial without behavioural modifications (Ching Lee & Dixon, 2017).

Bariatric surgery

Bariatric surgery is the most effective weight loss intervention for treating obesity, which aims to reduce the intake and uptake of energy by restricting gastric capacity and absorptive area of the bowel (NHMRC, 2013b). Different bariatric procedures produce varying degrees of weight loss trajectories, for instance comparing 10 year postoperative weight to baseline, long-term weight loss by gastric bypass surgery is greatest (25%±11%), followed by vertical banded gastroplasty (17%±11%), and fixed or variable banding procedures (13%±13%) (Sjostrom et al., 2007). Despite its efficacy, bariatric surgery in Australia is reserved for patients displaying extreme cases of obesity and is sequential to failed behavioural and pharmacological weight loss therapies (NHMRC, 2013b).

Health implications of Obesity

Obesity represents a major risk factor for the development of several pathologies, including insulin resistance (IR), non-alcoholic fatty liver disease (NAFLD) and hypertension, and when combined with glucose intolerance and dyslipidemia (hypertriglyceridemia and low HDL-cholesterol), these features collectively comprise part of the metabolic syndrome (MetS). Here we review the

pathophysiology of obesity-induced IR, NAFLD, with particular emphasis on hypertension and the classical renin-angiotensin system (RAS), and available treatment options for each condition.

Hypertension

In 2014-2015, 34% of the adult population in Australia had hypertension defined as a blood pressure (BP) of 140 mmHg or above for systolic and 90 mmHg or above for diastolic BP (ABS, 2015). Albeit the aetiology of hypertension reflects a number of factors, obesity is particularly important as obese individuals are more likely to develop hypertension than non-obese individuals (Elliott, 2006). There is also indication that hypertension *per se* may increase the risk of obesity, as weight gain is reported to be significantly higher in patients with hypertension than in normotensive individuals (Kannel, Brand, Skinner, Dawber, & McNamara, 1967).

The central deposition of adipose tissue has an important function in the pathogenesis of obesity-related hypertension (Kanai et al., 1990), in addition to the amount of intra-vascular deposition of fat, sympathetic nervous system activation, sodium retention, increased blood volume, enhanced renal sodium reabsorption, and RAS activation (da Silva, do Carmo, Dubinion, & Hall, 2009; Hall, 1997; Jiang, Lu, Zong, Ruan, & Liu, 2016). Increased oxidative stress may also inhibit the potent vasodilator, nitric oxide (NO), by covalently forming peroxynitrite and thereby increasing vascular resistance (Kojda & Harrison, 1999).

Classical renin-angiotensin system

Studies have implicated an overactive RAS in the development of obesity-related hypertension through peripheral and systemic circulating systems. The classically conceived role of systemic RAS, *i.e.* BP control, fluid and electrolyte balance, involves the enzymatic cleavage of circulating AGT (65% contributed by liver) by renin and ACE successively to form the main effector peptide Ang-II (Schmieder, Hilgers, Schlaich, & Schmidt, 2007; Yiannikouris et al., 2015). Conceivably, obese humans and rodents display elevated plasma AGT and Ang-II concentrations (Saiki et al., 2009; Umemura et al., 1997), ACE activity (Harp, Henry, & DiGirolamo, 2002), and upregulated Ang-II receptor 1 (AT_1) gene expression in vasculature (Mundy et al., 2007) as well as adipose tissue (Giacchetti et al., 2002).

Most of the physiological effects of Ang-II are mediated via two G-protein coupled receptors, AT_1 and AT_2, and the former is ubiquitously distributed in the body. The mechanism of Ang-II induced vasoconstriction entails stimulation of AT_1, leading to activation of phospholipase C, followed by G_q-protein mediated hydrolysis of phosphatidylinositol-4,5-biphosphate to generate the second messenger inositol-1,4,5-triphosphate (IP_3) and diacylglycerol (DAG). IP_3 triggers rapid intracellular release of calcium (Ca^{2+}) from the sarcoplasmic reticulum, mediated via the ryanodine receptor which opens Ca^{2+}-ATPase channels. Ca^{2+} binds to calmodulin and activates myosin light-chain (MLC) kinase and phospho-deactivates the chain to MLC phosphatase, enhancing the

interaction between actin and myosin filaments that causes vascular contraction to represent the pathogenesis of hypertension (Wynne, Chiao, & Webb, 2009).

The generation of Ang-II is not restricted to the systemic circulation but production also takes place in other tissues (Paul, Wagner, & Dzau, 1993). It has been reported that vasoconstriction of VAT vasculature by Ang-II stimulation of AT_1 is linked to obesity-induced hypertension (S. Y. Park et al., 2017), and adipose derived AGT may contribute 24-28% to circulating systemic levels to influence systolic BP by 10-15mmHg when following a normal diet (Yiannikouris et al., 2012).

AT_2 on the other hand is thought to counterbalance the AT_1 by forming a heterodimer with the receptor (AbdAlla, Lother, Abdel-tawab, & Quitterer, 2001), albeit due to low expression levels, the precise role of AT_2 has not been defined. Initial studies suggests activation of the AT_2 receptor triggers NO release in vascular smooth muscle cells (VSMCs) and inhibits nuclear factor κ-light-chain-enhancer of activated B cells (NF-κB) and the janus kinases/signal transducers and activators of transcription (JAK/STAT) signaling pathways (Herrera & Garvin, 2010; Horiuchi et al., 1999; Rompe et al., 2010), actions that may potentially counteract effects of the AT_1-receptor and promote cardiovascular protection (Stegbauer & Coffman, 2011). Several other angiotensin (Ang) peptides are generated by RAS, such as Ang-(1-7), and other non-classical pathways (enzymatic and non-enzymatic) may produce many of these RAS intermediates (Nehme, Zouein, Zayeri, & Zibara, 2019; Schmieder et al., 2007). These newer components of RAS are depicted in figure 3 below, and discussed in latter parts of this thesis.

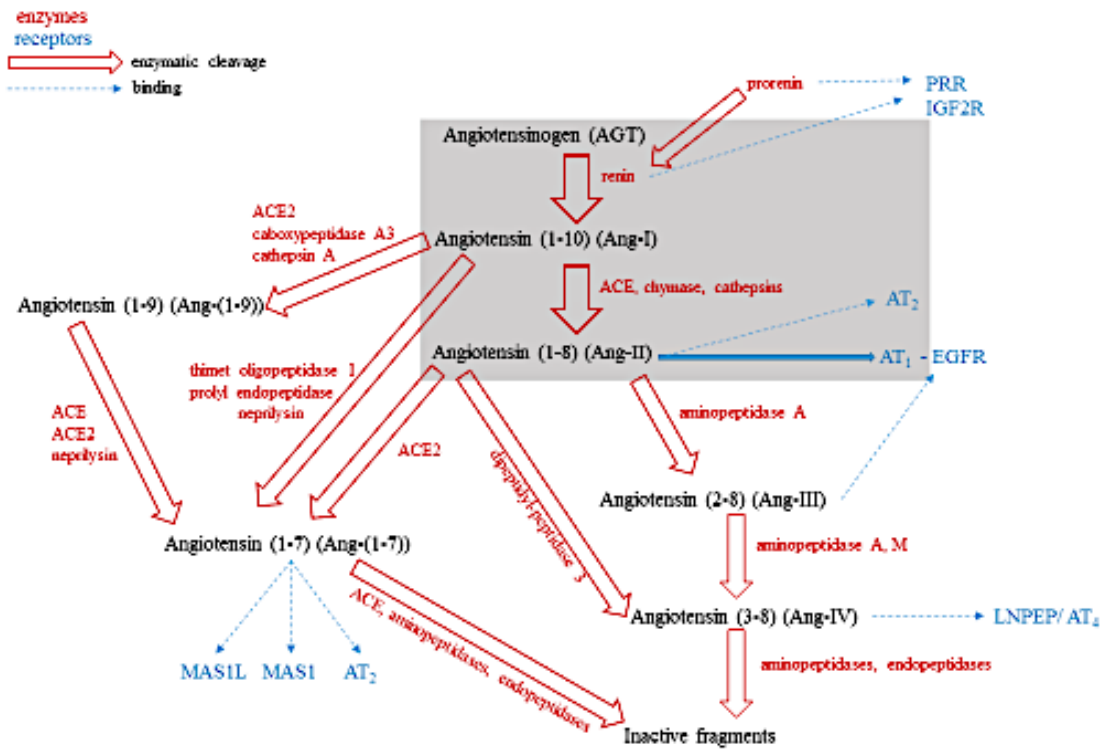

Figure 3. Components of the RAS. The classical pathway is shaded in grey. This figure was adapted from Nehme et al. (2019). Receptors: AT_1, angiotensin-II receptor type 1; AT_2, angiotensin-II

receptor type 2; AT_4, angiotensin-IV receptor; EGFR, epidermal growth factor receptor; IGF2R, insulin-like growth factor 2 receptor; LNPEP, leucyl/cystinyl aminopeptidase; MAS1L, Mas-related G-protein coupled receptor MRG; MAS1, Mas1 proto-oncogene, G-protein coupled receptor; PRR, (pro)renin receptor.

ACE-inhibitors are potential anti-hypertensives because they inhibit systemic Ang-II synthesis and increase adiponectin production to induce vasodilation to lower BP (Patrick, 2005). One such example is captopril, which alongside suppressing systemic RAS and improving hypertension in patients accompanies improvement of CVD and diabetes at peripheral sites, possibly due to increased adiponectin production (Arauz-Pacheco, Parrott, & Raskin, 2002; Kalupahana & Moustaid-Moussa, 2012). A recent study also showed that captopril interacts and alters the microbial population in the gut, elicits decreased posterior pituitary neuronal activity at central sites, and in this way sustains BP lowering effects even after captopril has been withdrawn, and this is suggested to be due to "recalibration" of the gut-brain axis (Yang et al., 2019). There is also a rationale for ACE-inhibition with captopril in the management of DIO, reviewed in latter parts of this thesis.

Insulin resistance

Insulin resistance (IR) is a requisite for the development of T2D, and is defined as the increased requirement for insulin to maintain glucose homeostasis (Butterworth, 2005a). Peripheral IR refers to diminished glucose uptake primarily by skeletal muscle, which mostly depends on the control of glucose transporter type 4 (GLUT4) expression and translocation to the plasma membrane. Hepatic IR describes impaired suppression of gluconeogenesis which largely accounts for hyperglycaemia and glucose intolerance (Kahn, Hull, & Utzschneider, 2006). Adipose tissue IR describes impaired repression of lipolysis in the presence of high levels of insulin, contributing to elevated plasma FFAs, *i.e.* hyperlipidaemia (Gastaldelli, Gaggini, & DeFronzo, 2017).

In obesity, chronic low-grade inflammation initiated by endoplasmic reticulum (ER) and oxidative stress, a reduction in adipose derived adiponectin and elevations in leptin and the FFA palmitate may be involved in the pathogenesis of IR (Alipourfard, Datukishvili, & Mikeladze, 2019). Furthermore, retinol-binding protein-4 released from adipocytes has been shown to induce muscle and hepatic IR through reduced phosphatidylinositol-3-OH kinase (PI3K) signaling and enhanced phosphoenoylpyruvate carboxykinase (PEPCK) expression respectively (Yang et al., 2005). In obesity, the production of adiponectin is decreased, and adiponectin acts as an insulin sensitiser by stimulating FA oxidation via an AMPK and PPAR-α-dependent manner (Kahn et al., 2006) which will be further addressed in this thesis.

In addition to the above mentioned adipose-derived factors, augmented release of cytokines tumor necrosis factor α (TNF-α), interleukin 6 (IL-6), monocyte chemoattractant protein 1 (MCP-1) and other products of macrophages and cells around adipose tissue is thought to contribute to the onset

of IR. Both TNF-α and IL-6 act via receptor-mediated processes to stimulate inflammatory pathways such as IκBα kinase β (IKKβ)/NF-κB and c-Jun N-terminal kinase 1 (JNK), leading to the upregulation of potential mediators of inflammation that can cause IR. In addition to activation by TNF-α and IL-6, these aforementioned signaling pathways are also responsive to FFAs, DAG, ceramide, ROS and hypoxia (Kahn et al., 2006; Ye, 2013).

As mentioned, a primary mechanism by which cells become IR is associated with elevated systemic and peripheral TNF-α expression and secretion (Hotamisligil, 1999b). TNF-α acts via its p55 receptor to inhibit IRS-1, and similarly activation of IKKβ and JNK1 involves IRS-1 inhibition by TNF-α to impair the insulin signaling pathway (Aguirre, Uchida, Yenush, Davis, & White, 2000; Gao et al., 2002). Obese mice with mutation in either TNF-α or its receptors had increased insulin-stimulated tyrosine phosphorylation of the insulin receptor in adipose and muscle tissue, thus were protected from obesity-induced development of IR (Hotamisligil, 1999a). The Ser^{307} residue of IRS-1 has been identified as a site for effects mediated by TNF-α. Ser phosphorylation of IRS-1 converts IRS-1 to a form that inhibits insulin-receptor tyrosine kinase activity, effectively reducing the action of insulin in target tissues by impairing the regulation of GLUT4 transcription (Hotamisligil, 1999b; Peraldi & Spiegelman, 1998). In addition, TNF-α inhibits PPAR-γ function in adipose tissue leading to the induction of IR (Zhang et al., 1996).

Current treatment strategies for the treatment of IR are aimed at enhancing insulin sensitivity, and includes treatment with metformin and thiazolidinediones (TZDs). Metformin has been shown to reduce liver gluconeogenesis, albeit not all of its effects can be explained via this mechanism. Metformin has been shown to act via both AMPK-dependent and -independent mechanisms that may include inhibition of fructose-1,6-bisphosphatase (by AMP) and mitochondrial respiration, and via alterations to gut microbiota (Rena, Hardie, & Pearson, 2017). TZDs behave as agonists for PPAR-γ, a nuclear receptor expressed primarily in adipose tissues that drives adipogenesis, lipid synthesis and storage via induction of lipogenic enzymes and glucoregulatory proteins, thus enhancing insulin sensitivity (Olefsky, 2000). The benefits of adipogenesis in the prevention of obesity-related complications is further addressed in latter parts of this dissertation.

Non-alcoholic fatty liver disease (NAFLD)

Obesity is highly associated with NAFLD which has become the most common liver disease worldwide, affecting approximately 25% of the population (Younossi et al., 2016). NAFLD is characterised by hepatic steatosis in the absence of significant alcohol consumption or other known liver diseases (Friedman, Neuschwander-Tetri, Rinella, & Sanyal, 2018). It was found that 76% of obese individuals exhibited fatty liver, and approximately 10% of patients with NAFLD develop non-alcoholic steatohepatitis (NASH), characterised by ceramide generation and severe inflammation with or without portal fibrosis, which significantly increases the risk of cirrhosis and cancer (Bedogni et al., 2005; Matteoni et al., 1999). IR and T2D has the clearest biological link to

NAFLD, where up to 75% of patients are hyperglycaemic, and impaired insulin signaling of adipose tissue contributes to high circulating FAs (due to dysregulated lipolysis of TGs) and delivery to the liver (Friedman et al., 2018; Portillo-Sanchez et al., 2015). Another major source of FAs is their synthesis from glucose and fructose in the liver by *de novo* lipogenesis (DNL), where the entry of glucose in to the DNL pathway is highly regulated whereas entry of fructose in to the DNL pathway is not regulated (absorbed by the liver from portal circulation), leading to a depletion of liver ATP and generation of uric acid (Abdelmalek et al., 2012).

Inhibition or downregulation of DNL enzymes, such as acetyl-CoA carboxylase (ACC) and steroyl-CoA response element binding protein-1c (SREBP-1c) is thought to be beneficial in treating NAFLD (Friedman et al., 2018). Moreover, restoring DNL in adipose tissue or diverting FAs and carbohydrates away from the liver in to peripheral tissues may also reduce their delivery to the liver. For instance metformin and TZDs have been shown to improve NAFLD and NASH due to enhanced hepatic oxidative capacity and enhanced adipocyte storage of fat respectively, albeit the latter is in expense of increased peripheral fat storage and weight gain (Snyder et al., 2018). Hepatic FA accumulation and DNL will be reviewed further.

Physiology, pathophysiology & endocrinology of adipose and liver tissues

Physiology & pathophysiology of adipose tissue

Adipose tissue (body fat) functions as a storage reserve for surplus energy as well as an endocrine organ producing and secreting adipose derived cytokines (adipokines) and metabolites to communicate with other tissues (Gesta, Tseng, & Kahn, 2007). The process of adipocyte differentiation, termed 'adipogenesis', is regulated by sequential activation of several transcription factors including nuclear receptor peroxisome proliferator-activated receptor γ (PPAR-γ) and CAAT-enhancer-binding proteins (C/EBP) (Rosen & MacDougald, 2006). Numerous environmental stimuli can influence PPAR-γ and C/EBPs expression to effect the degree and severity of body weight gain and obesity (Darlington, Ross, & MacDougald, 1998; Rosen & MacDougald, 2006). There are three major types of adipose tissue, white adipose tissue (WAT) brown adipose tissue (BAT), and brown in white or "beige" adipose tissue. Whilst both WAT and BAT are derived from the mesodermal cell types, they originate from different precursor cells; white adipocytes are derived from adipogenic lineage arising from *Myf5*$^{-}$ precursors, and brown from myogenic lineage arising from *Myf5*$^{+}$ precursors (Gesta et al., 2007; Rosell et al., 2014; Timmons et al., 2007). The origin and function of beige adipocytes is less clear, and recent studies in mice demonstrated derivation of beige adipocytes from progenitors, probably of adipogenic linage, expressing *Sma*, *Myh11*, *Pdgfra* or *Pdgfrb* (Ikeda, Maretich, & Kajimura, 2018).

As described above, three functionally distinct adipose subtypes are recognised in mammals. WATs are lipogenic and store excess energy in the form of accumulated TGs which can be metabolised in to FFAs in response to energy requirements (Kershaw & Flier, 2004). Conversely, BAT is restricted

to interscapular regions and contains high basal levels of mitochondrial uncoupling protein 1 (UCP1) involved in the generation of thermal energy from lipid and glucose metabolism (Choe, Huh, Hwang, Kim, & Kim, 2016; Enerback, 2010). Beige adipocytes on the other hand are distinct from BAT in that they arise as multilocular adipocytes within WAT and possess the capacity to express UCP1 at a high level upon adrenergic stimulation (Wu et al., 2012). Thus, WAT is the site of energy storage and both beige and BAT is the site of energy dissipation in the form of heat. The main morphological characteristics of mammalian white, brown and beige adipocytes is depicted in figure 4.

White adipose tissue

WAT is distributed viscerally and subcutaneously with regionally distinct molecular and physiological properties (Gesta et al., 2006). The anatomical location of WAT is associated with metabolic profiles such that increased deposition of visceral adipose tissue (VAT) correlates with increased risk for development of T2D, hypertension and hyperlipidemia, whereas increased deposition of subcutaneous adipose tissue (SAT) does not (Rosen & MacDougald, 2006; Ryden, Andersson, Bergstrom, & Arner, 2014). This comes as factors such as cytokines and FFAs released from VAT is directly exposed to the liver and circulation via the portal vein, making hypertrophic VAT important in the development of obesity and metabolic disease (Giacchetti et al., 2002; Item & Konrad, 2012). Adipose tissue expansion occurs via lipogenesis and/or adipogenesis to increase the liquid volume (hypertrophy) and/or the number of differentiating preadipocytes (Kershaw & Flier, 2004). Changes in the size and number of adipocytes affect the microenvironment of expanded adipose tissue to potentially dysregulate the secretion of adipocyte derived adipokines and cytokines such as leptin, adiponectin, TNF-α, IL-6, and MCP-1, depending on the degree of adiposity and insulin sensitivity (Huh, Park, Ham, & Kim, 2014). Most adipokines secreted are proinflammatory and are upregulated in the obese state, whereas few have anti-inflammatory activities (adiponectin) and are downregulated in the obese state (Foti & Locati, 2017).

There is strong evidence to suggest increased adipogenesis is a beneficial adaption to over-nutrition aimed at maintaining a healthier adipose tissue; this may be of benefit to metabolic health as newly differentiated adipocytes have better TG storage capacity and are thus more insulin-sensitive unlike hypertrophic adipocytes (Choe et al., 2016; Danforth, 2000; L. A. Muir et al., 2016). The number of preadipocytes able to differentiate in to white adipocytes is shown to correlate negatively with BMI and adipocyte cell size, such that extreme hypertrophy of VAT in obese individuals is associated with a reduction in the number of proliferative preadipocytes (Isakson, Hammarstedt, Gustafson, & Smith, 2009; L. A. Muir et al., 2016).

Brown adipose tissue

Classical BAT is found in highly vascularised depots with high levels of mitochondria and smaller lipid droplets to that of beige and WAT (Cedikova et al., 2016). BAT is most concentrated in

specific non-subcutaneous and narrow fascial regions in adults and studies show sympathetic innervation (activation) of BAT and UCP1 expression in obese patients to be inversely related to BMI and body fat content (El Hadi et al., 2016; Kozak & Anunciado-Koza, 2008; Leitner et al., 2017; Poekes, Lanthier, & Leclercq, 2015; Veilleux, Caron-Jobin, Noel, Laberge, & Tchernof, 2011). Active BAT is associated with increased EE and protection against obesity and T2D due to its high oxidative capacity (Cannon & Nedergaard, 2004; Kozak & Anunciado-Koza, 2008). This has made BAT a potential target for the treatment of obesity and metabolic disease (Bartelt et al., 2011; Poekes et al., 2015).

Beige adipose tissue

Beige adipocytes occur in WAT depots with the characteristics of both WAT and BAT, making it a therapeutic target in the treatment of obesity and T2D (Wang, Pan, Hung, Tung, & Ho, 2019). Occurring sporadically in SAT, beige adipocytes are induced in response to external and internal stimuli, such as chronic cold, exercise, and PR-domain zinc finger protein 16 (PRDM16), PPAR-γ and β3-adrenergic receptor agonism, resulting in the induction of UCP1 and dissipation of extra energy as heat (Ikeda et al., 2018; Ohno, Shinoda, Spiegelman, & Kajimura, 2012; Wang et al., 2019). In a process referred to as 'browning', there is evidence suggesting beige adipocytes may be derived from the trans-differentiation of WAT, as rats treated with a β3-adrenergic receptor agonist showed enhanced conversion of unilocular lipid droplets (of WAT) in to multilocular lipid droplets that are rich in UCP1-expressing mitochondria (Himms-Hagen et al., 2000). In obesity however, local and systemic inflammation of WAT inhibits the expression and activity of PPAR-γ, triggering adipocyte dysfunction and a pro-inflammatory environment that increases the expression of TNF-α, MCP-1, toll-like receptor 4 (TLR-4), interleukin 1β (IL-1β), and other inflammatory markers that reduce UCP1 expression and WAT thermogenicity (Villarroya, Cereijo, Gavalda-Navarro, Villarroya, & Giralt, 2018). In mice, TLR4 activation by lipopolysaccharide (LPS) was shown to repress β3-adrenergic browning of WAT, whereas deletion of TLR4 was protective of thermogenicity of WAT. Similarly, IL-1β was also shown to reduce UCP1 expression and blocking the IL-1 receptor protected the thermogenicity of WAT (Okla, Zaher, Alfayez, & Chung, 2018). Thus obesity-induced chronic inflammation of adipose tissue impairs the expression of UCP1 and browning potential, and strategies aimed at targeting adipose tissue inflammation has also become of therapeutic interest.

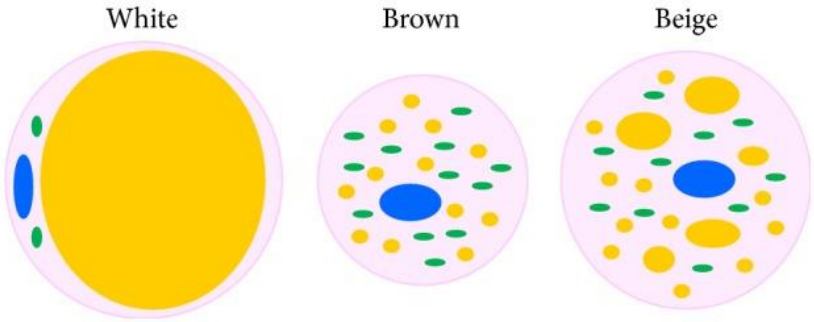

Figure 4. Key morphological characteristics of white, brown and beige adipocytes. White adipocytes contain a full unilocular LD (yellow) with few mitochondria (green) and a nucleus (blue). Brown adipocytes contain a greater number of mitochondria and multilocular LDs that are smaller in size. Upon stimulation, beige adipocytes increase the number of mitochondria and contain multilocular lipid droplets of variable sizes. Image adapted from Cedikova et al. (2016).

Endocrinology of adipose tissue

In addition to adipocytes, adipose tissue constitutes endothelial, neuronal and immune cells representative of its role in multiple biological processes (Kershaw & Flier, 2004). The microenvironment of adipose tissue may also reflect the status of energy stores by secreting various factors known to play a part in vascular disease, immunological responses, and appetite regulation. Two of the most common endocrine hormones expressed and secreted from adipocytes includes leptin and adiponectin, and there is an inverse relationship between circulating levels of the two (Matsubara, Maruoka, & Katayose, 2002). Circulating leptin concentrations correlate positively with BMI, WHR, body fat content, T2D, hypertension, serum insulin, FFAs, angiotensinogen (AGT), whereas adiponectin correlates negatively with the aforementioned (Diwan et al., 2018; Hall, Hildebrandt, & Kuo, 2001; Matsubara et al., 2002). Various other factors secreted from adipose tissue are derived from the non-adipocyte fraction such as interleukins, plasminogen activator inhibitor 1 (PAI-1), TNF-α, c-reactive protein (CRP), vascular endothelial growth factor (VEGF), prostaglandin E2 (PGE_2) and hepatocyte growth factor (HGF), the expression of which are all elevated in obese patients (Fain, Madan, Hiler, Cheema, & Bahouth, 2004). Both adiponectin and leptin will be discussed in relation to obesity.

Leptin

Leptin is a lipostatic hormone secreted mainly by WAT, contributing to energy balance by regulating food intake and energy consumption via receptor-mediated stimulation and suppression of hypothalamic anorexigenic pathways and orexigenic neuropeptides (*e.g.* neuropeptide Y), in addition to causing peripheral tissue metabolism to in turn diminish TG storage in adipocytes (Brennan & Mantzoros, 2006; Zhang et al., 1994). Circulating leptin levels is shown to correlate closely with adipocyte size and fat mass (Zhang, Guo, Diaz, Heo, & Leibel, 2002), and is acutely sensitive to dietary restriction and feeding (Friedman & Halaas, 1998). In non-obese humans, it is

reported that a day of fasting leads to a 50% drop in circulating levels of leptin causing appetite stimulation, and under conditions of acute positive energy balance, a rise of 40% is reported leading to appetite suppression (Chan, Heist, DePaoli, Veldhuis, & Mantzoros, 2003; Kolaczynski, Ohannesian, Considine, Marco, & Caro, 1996). On the other hand, circulating levels of leptin is increased in humans with obesity alongside adipose *Lep* gene expression (Lönnqvist, Arner, Nordfors, & Schalling, 1995). This increase in circulating leptin is thought to be secondary to 'leptin resistance', where in obese patients, resistance to the inhibitory effects of leptin on appetite facilitates hyperphagia further driving obesity (Considine et al., 1996; Kolaczynski et al., 1996).

In vitro, leptin also increases TG hydrolysis (lipolysis), FA and glucose oxidation, and reduces DNL from glucose in adipocytes (William, Ceddia, & Curi, 2002). Moreover, adenovirus-induced hyperleptinemia is shown to reduce body fat in normal rats (Orci et al., 2004). The mechanism of action is thought to involve the downregulation of key lipogenic and adipogenic genes and enzymes including ACC, fatty acid synthase (FASN), malic enzyme (ME), ATP-citrate lyase (ACL) and PPAR-γ, and the upregulation of thermogenic genes and enzymes including PPAR-γ coactivator 1α (PGC-1α), PPAR-α, UCP-1 and -2 (Ceddia et al., 2000; Orci et al., 2004; Wang, Lee, & Unger, 1999; Zhou, Wang, Higa, Newgard, & Unger, 1999). In addition to adipose tissue, leptin has also been shown to mediate an increase in FA oxidation in skeletal muscle and liver through activation of the α2 subunit of AMP-activated protein kinase (AMPK) (Minokoshi et al., 2002; Orci et al., 2004). The reverse regulation of these aforementioned proteins and enzymes of adipogenesis, DNL and FA oxidation is commonly reported in patients with polygenic obesity, and leptin replacement therapy has a very limited role in bodyweight and fat loss due to the fact that these patients are commonly hyperleptinemic and exhibit central leptin resistance (Paz-Filho, Mastronardi, & Licinio, 2015). Furthermore, leptin resistance often co-expresses with endothelial oxidative stress, T2D and hypertension (Katsiki, Mikhailidis, & Banach, 2018; Mittendorfer et al., 2011).

Adiponectin

Adiponectin is abundantly produced and secreted by adipose tissues, and plays a prominent role in the modulation of a number of metabolic processes including glucose uptake and FA catabolism, insulin sensitivity and energy expenditure (Foti & Locati, 2017; Nigro et al., 2014). Posttranslational modifications of the hormone results in three secreted isoforms that may vary in efficacy with respect to target tissues (Maeda et al., 1996). Existing as full-length or globular monomers, the latter form has the greatest impact on peripheral glucose uptake and FA oxidation via receptor-mediated signaling cascade involving binding of the adaptor protein APPL1 and the subsequent dephosphorylation of liver kinase B1 (LKB1) at Ser^{307}, thus enabling LKB1 translocation from nucleus to cytoplasm to stimulate AMPK activity (Achari & Jain, 2017; Deepa et al., 2011). The activation of AMPK is thought to be key in arbitrating most effects of adiponectin at the cellular level (Butterworth, 2005a), and low amounts of the globular form represents an independent risk for metabolic pathologies (Fruebis et al., 2001; Wu et al., 2018).

Plasma adiponectin concentration is reduced in obesity, T2D and hypertension, and correlates inversely with body fat content, IR and hyperinsulinemia (Arita et al., 1999; Wang et al., 2012; Weyer et al., 2001). Adiponectin mRNA (*Adipoq*) overexpression in 3T3-L1 cells is reported to promote the differentiation of preadipocytes in to adipocytes by prolonging PPAR-γ and C/EBP gene expression (Fu, Luo, Klein, & Garvey, 2005). In line with this, it was reported that genetically obese and IR *Ob*/*Ob* (leptin-deficient) mice overexpressing *Adipoq* showed healthy adipose tissue expansion that prevent the ectopic deposition of lipids and hyperlipidemia whilst improving insulin sensitivity (Kim et al., 2007). Moreover, the overexpression of adiponectin was not shown to inhibit bodyweight gain in HFD fed mice, although protection against the lipotoxic effects of lipid accumulation accompanied an increase in BAT mass (Combs et al., 2004). While there are many clinical reports of increased levels of circulating adiponectin following weight loss (Ma et al., 2016; Reinehr, Roth, Menke, & Andler, 2004), this appears to be secondary and perhaps points to a connection between adiponectin and body fat in relation to IR, rather than a key role for adiponectin in bodyweight regulation. Therefore, limited effect of adiponectin (on glucose uptake, FA oxidation and suppression of inflammatory cytokines) in the obese state, due to decreased systemic levels, may at least in part contribute to an overall negative impact on metabolic health.

Moreover adiponectin is also shown to enhance peripheral FA oxidation and glucose uptake by increasing PPAR-α and GLUT4 expression and translocation in adipose, liver and skeletal muscle tissues (Berg, Combs, Du, Brownlee, & Scherer, 2001; Ceddia et al., 2005; Fu et al., 2005; Yamauchi et al., 2001). This may in part constitute observed improvements in tissue sensitivity to insulin (a mechanism independent of AMPK activity).

In addition to its metabolic actions, studies demonstrate a negative correlation between plasma adiponectin levels with markers of systemic oxidative stress and inflammation, including TNF-α, IL-6, serum amyloid A (SAA), CRP, and NF-κB signaling (Frühbeck et al., 2017; Ouchi & Walsh, 2007). Conversely, pro-inflammatory cytokines like TNF-α are reported to downregulate *Adipoq* expression in adipocytes resulting in decreased circulating levels of adiponectin (Fantuzzi, 2008; Foti & Locati, 2017; Ouedraogo et al., 2006). These adiponectin-mediated reductions in inflammatory cytokines often accompanies improvement of insulin sensitivity, highlighting a role for adiponectin in the protection against cytokine-induced IR.

Physiology & pathophysiology of liver tissue

The liver plays a significant role in almost all organ systems in the body by interacting with endocrine and gastrointestinal systems to aid digestion and metabolism. These dietary nutrients may be transformed in to fuels and precursors which may be exported to other tissues via the circulation or lympatic system (Blanco & Blanco, 2017; Butterworth, 2005a). Metabolic processes will be re-visited in latter parts of this dissertation. Here we focus on mechanisms implicated in obesity-related functional abnormalities of the liver.

Increased visceral adiposity is primary in the pathogenesis of hepatic IR and steatotic liver diseases. Liver fat accumulation is largely dependent on re-circulating FFAs from the highly lipolytic and insulin insensitive VAT in to the portal circulation due to unopposed action of insulin on hormone-sensitive lipase (HSL) (Vatner et al., 2015). Thus the accumulation of TGs in hepatocytes is the result of both increased FFA influx and DNL, and it has been estimated that 59% of TGs in the liver arises from the recirculation of FFAs from adipose tissue, 26% from DNL from dietary carbohydrates and 15% from dietary lipids (Donnelly et al., 2005). Chronically exposing the liver to elevated FFAs can promote liver gluconeogenesis (Williamson, 1966), reduce enzymes involved in FA oxidation and increase hepatic DNL (Xu, Nakamura, Cho, & Clarke, 1999). This may be further exacerbated in the presence of hepatic IR resulting from the reduced efficiency of insulin to suppress hepatic glucose production (Qureshi & Abrams, 2007). Thus, steatosis and IR can potentiate one another creating a cycle of dysfunction.

The functional unit of the liver is the lobule which surrounds the portal triad (*i.e.* portal vein, hepatic artery and bile duct). Lobules are composed of hepatocytes that are divided in to three zones based on function and perfusion. Zone I, also known as the peri-portal region, is most perfuse and closest in proximity to the portal tracts making it highly oxygenated, thus plays a major role in oxidative metabolism such as β-oxidation of FAs, gluconeogenesis, amino acid (AA) catabolism, and cholesterol and bile formation. Zone II makes up the peri-central region sitting between zone I and III. Zone III is least perfuse and located around the central vein where oxygenation is poor, thus plays a major role in glycolysis, DNL, ketogenesis, glycogenesis, glutamine generation, detoxification and biotransformation of xenobiotics (Kalra & Tuma, 2019). Kupffer cells line the walls of the liver sinusoid and function as phagocytic macrophages involved in immunity and haemoglobin metabolism (Butterworth, 2005a).

Accordingly, histopathological studies have found a statistically significant relationship between the severity of liver steatosis with lobular inflammation and zone III fibrosis in obese adults exhibiting non-alcoholic fatty liver disease (NAFLD) (Chalasani et al., 2008). In contrast, zone I distribution of steatosis, inflammation and fibrosis is more common in pediatric cases of NAFLD (Brown & Kleiner, 2016). Additionally, the accumulation of lipids in Kupffer cells causes them to exhibit a pro-inflammatory phenotype with subsequent secretion of cytokines such as TNF-α, IL-1β and MCP-1 (Leroux et al., 2012). A causal link between TNF-α signaling and tissue specific IR has been suggested, and overexpression of TNF-α and its receptors has been reported in liver (and adipose) tissue of patients with NAFLD and non-alcoholic steatohepatitis (NASH), levels of which appear to correlate with the severity of disease and fibrosis (Lesmana et al., 2009; Tencerova et al., 2015; Valenti et al., 2002).

Albeit the molecular specifics and temporal order of events remains under investigation, yet it is clear that the VAT secretome of obese patients influences liver tissue so as to increase vulnerability

to hepatic lipotoxicity, oxidative stress and inflammation (Wree, Kahraman, Gerken, & Canbay, 2011). As in hypertrophic adipocytes, adipose derived FFA infiltration of the liver accompanies a reduction in the expression of PGC-1α as well as sirtuins (SIRT1 and SIRT3), which negatively affects mitochondrial biogenesis and FA oxidation causing mitochondrial dysfunction and abnormal respiration (Aharoni-Simon, Hann-Obercyger, Pen, Madar, & Tirosh, 2011; Sacerdoti et al., 2018). Similarly in cases of HFD-induced obesity, inhibition of hepatic PGC-1α expression caused a subsequent increase in NF-κB signaling and IL-6 expression and secretion to manifest liver inflammation (Barroso et al., 2018). Conversely, PGC-1α overexpression reduced hepatic TG storage and decreased plasma TG levels by elevating mitochondrial content/biogenesis and FA oxidation (Morris et al., 2012). These studies combined underscore an important molecular link between PGC-1α and hepatic metabolic and immune pathways that are distinguished during obesity.

Endocrinology of liver tissue

Angiotensinogen

The liver is responsible for secreting a plethora of important peptides, and one such example strongly noted in relation to obesity, hypertension, IR, oxidative inflammation and NAFLD is AGT (Dixon et al., 2003; Massiéra, Bloch-Faure, et al., 2001; Umemura et al., 1997). AGT, a substrate of the RAS, is the only known precursor to angiotensin (Ang) peptides, and in particular Ang-II displays a prominent role in systemic and local vasoconstriction and lipogenesis respectively. In obesity, circulating levels of AGT is increased alongside elevations in Ang-II, *i.e.* overactive RAS, to manifest hypertension (elevated systolic BP). Here, the classically conceived role of liver derived AGT with respect to BP regulation and obesity will be broadly reviewed.

According to the classical RAS (figure 3), renin produced by juxtaglomerular cells cleaves circulating AGT in to Ang-I, and this is thought to be the rate-limiting step of Ang-II release (catalysed by ACE) in to the circulation (Nehme et al., 2019). Whole body deficiency of AGT markedly reduces circulating AGT and Ang peptides to promote hypotension in mice (Tanimoto et al., 1994). Whilst several cell types have also been identified as producing AGT, hepatocyte-appear to contribute up to 63% to circulating levels in mice fed a standard murine diet, where AGT knockout models exhibit significantly reduced AGT and Ang-II levels in both the circulation and in the kidneys causing hypotension (Matsusaka et al., 2012; Yiannikouris et al., 2015). Moreover hepatocyte AGT deficiency was also shown to abolished obesity-induced increases in circulating AGT and Ang-II levels, which also caused hypotension despite obesity (Yiannikouris et al., 2015). Interestingly, AGT mRNA levels in the liver remains unaltered in mouse models of obesity (Yasue et al., 2010) and appears to be unresponsive to nutritional regulation, *i.e.* fasting and refeeding (Frederich, Kahn, Peach, & Flier, 1992). Besides pronounced decreases in BP, other studies have reported diminished bodyweight, liver steatosis and atherosclerosis induced by a hypercaloric WD in hepatocyte AGT deficient mice (Lu et al., 2016; Massiéra, Seydoux, et al., 2001; Wu et al., 2015).

These findings highlight that hepatocytes are the main source for AGT production and function *in vivo* with strong effect on BP and obesity-induced hypertension, albeit the effect of hepatocyte AGT on bodyweight regulation is not so clear given mRNA expression in the liver is unaffected.

Molecular pathways to Obesity

De novo lipogenesis

De novo lipogenesis (DNL) is the process by which carbon precursors of acetyl-CoA (primarily of carbohydrate origin) are synthesised in to FAs after activation to malonyl-CoA by ACC. Synthesis of FAs is catalysed by the FASN complex in which a condensation and decarboxylation reaction follows two reductions with nicotinamide adenine dinucleotide phosphate (NADPH) as a hydrogen donor until palmitate is formed (Hellerstein, Schwarz, & Neese, 1996). In rodents and primates, the liver is the major site contributing to whole-body lipogenesis and WAT is the primary site for TG storage. In humans, DNL was shown to contribute 1-3% of total body fat in the presence of a typical diet, and a 2- to 3-fold increase in DNL is observed upon consumption of a hyper-caloric diet rich in carbohydrates, wherein adipose tissue becomes a secondary site for DNL (Aarsland, Chinkes, & Wolfe, 1997; McDevitt et al., 2001; Shrago, Glennon, & Gordon, 1971). This has led to the hypothesis that DNL in adipose tissue may have a role in the disposal of excess energy in the form of carbohydrates and/or their metabolites when the liver exceeds its glycogen storage capacity (Strable & Ntambi, 2010).

Hepatic DNL and TG synthesis following a carbohydrate loading may lead to an increase in the synthesis and secretion of VLDLs which enter the circulation (McDevitt et al., 2001). When VLDLs travel to adipose tissues, TGs may undergo lipolysis by the action of the insulin-stimulated lipoprotein lipase (LPL) within vascular endothelium, and resultant FFAs can be transported (or undergo β-oxidation) in to adipocytes through the action of CD36 and fatty acid transport protein-1 (FATP1), where FFAs are re-esterified using glycerol-3-phosphate (generated from glucose) as a backbone to promote TG formation and storage in lipid droplets. Insulin may also stimulate adipocyte glucose uptake via GLUT4 which drives DNL in adipocytes through activation of the transcription factor SREBP-1c, whereby FFAs can be synthesised and esterified as described above (Hellerstein et al., 1996; Song, Xiaoli, & Yang, 2018). See figure 5 for metabolic pathways related to DNL in liver and adipose tissues.

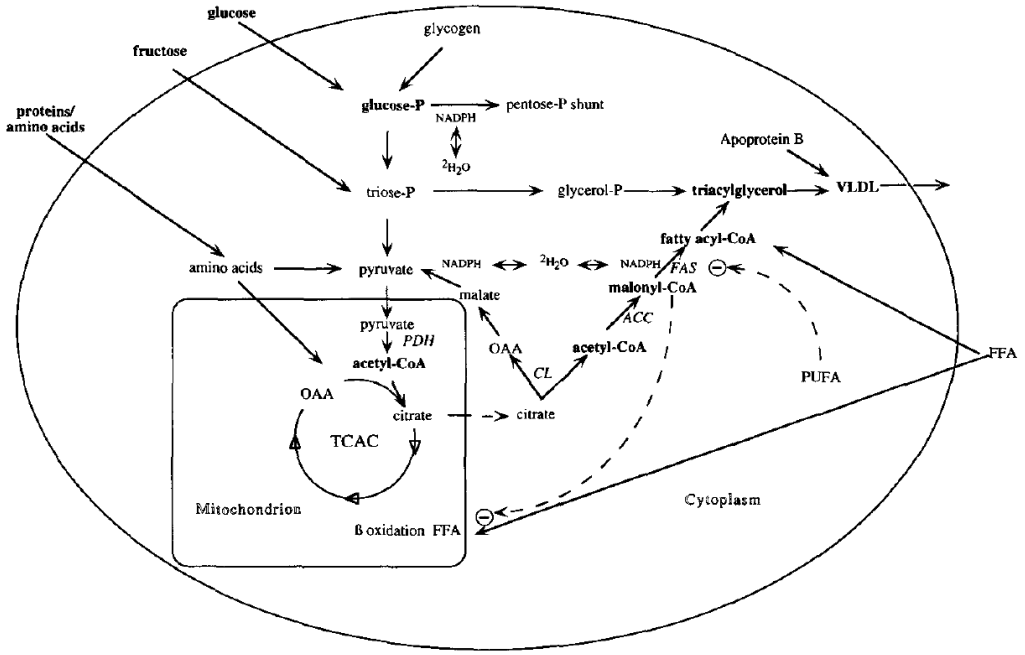

Figure 5. Metabolic pathways of DNL in a liver cell is shown with fructose uptake and VLDL secretory pathway; the pathway otherwise applies to adipocytes also. Abbreviations: P, phosphate; PDH, pyruvate dehydrogenase; TCAC, tricarboxylic acid cycle; OAA, oxaloacetate; FFA, free fatty acids; CPT-1, carnitine palmitoyl transferase 1; CL, ATP-citrate lyase; NADPH, nicotinamide adenine dinucleotide phosphate (reduced form); ACC, acetyl-coenzyme A (CoA) carboxylase; FAS, fatty acid synthase; PUFA, polyunsaturated fatty acids. (-) inhibitory action. Figure from Hellerstein et al. (1996).

Studies conducted in humans and rodents indicate that DNL in WAT is suppressed in obesity and T2D, as the expression of key lipogenic enzymes ACC and FASN, as well as GLUT4 and FA elongase 6 (ELOVL6) is markedly decreased (Eissing et al., 2013; Nadler et al., 2000). Another important lipogenic transcription factor is carbohydrate-responsive binding protein (ChREBP) which is activated by increased glucose flux, and is therefore associated with GLUT4 (Ortega-Prieto & Postic, 2019; Yamashita et al., 2001). ChREBP was shown to be markedly reduced in WAT of obese and T2D patients, and is therefore thought to be responsible for the reduced DNL gene expression in WAT of obese and T2D patients (Eissing et al., 2013). In contrast to WAT, DNL in the liver is upregulated in humans and rodent models of obesity, where it is considered to promote lipotoxicity, IR, NAFLD and atherogenic dyslipidemia (Diraison, Dusserre, Vidal, Sothier, & Beylot, 2002). As in WAT, ChREBP was also shown to regulate DNL in the human liver through elevated hepatic glucose flux, *e.g.* by fructose-rich or SREBP1-dependent induction of glucokinase, and this in turn induced FASN, ELOVL6 and stearoyl desaturase (SCD) in obese and IR humans (Eissing et al., 2013; Foretz et al., 1999), supporting the hypothesis that hepatic DNL can promote the development of NAFLD and systemic IR (Postic & Girard, 2008). Given the selective restoration of DNL in WAT by means of transgenic overexpression of inducible 6-phosphofructo-

2-kinase (iPFK2) is reported to reverse obesity-dependent IR (Huo et al., 2012), reduced DNL in WAT appears to be an important contributor to systemic IR and metabolic disease, thus inhibition of hepatic DNL may be a feasible approach in the treatment of obesity and related disorders.

Renin-angiotensin system and adipose tissue

The classical RAS is has been described, and the existence of a local RAS in different tissues has changed our functional understanding of the RAS. In earlier parts of this thesis, we reviewed the endocrinology of the liver with respect to the "inactive" RAS substrate, AGT, and described its systemic contribution and relationship to obesity. Similarly, combined with the occurrence of AGT, $AT_{1\,\&\,2}$ receptors, renin and ACE mRNA expression and activity, there is indication of a functional local RAS whereby Ang-II may be generated from within adipose tissue (Crandall, Herzlinger, Saunders, Armellino, & Kral, 1994; Harp & DiGirolamo, 1995; Karlsson et al., 1998).

Unlike the liver however where AGT mRNA expression appears unrelated to adiposity, adipose tissue mRNA expression and secretion of AGT is augmented in obese humans and rodents to correlate with WHR and diabetes (Boustany et al., 2004; Engeli et al., 2005; van Harmelen et al., 2000; Yasue et al., 2010). Genetic studies have also shown that transgenic mice overexpressing AGT in adipose tissue develop obesity with adipocyte hypertrophy, concurrent with systemic IR and augmented expression of lipogenic and pro-inflammatory genes, and whilst adipose-specific AGT gene knockout significantly reduced AGT expression and Ang-II generation in adipose tissue and plasma of mice fed a low-and high-fat diet, besides lowering SBP and preventing HFD-induced hypertension, bodyweight and fat mass remained unresponsive to adipose AGT-deficiency (Kalupahana et al., 2012; Massiéra, Bloch-Faure, et al., 2001; Yiannikouris et al., 2012). Conversely, whole-body knockout of AGT decreased bodyweight, adiposity, leptin, and insulin levels on a HFD compared to wildtype, and AGT gene silencing in cultured adipose cells and *in vivo* reduced molecular markers of lipid accumulation, adipogenesis and inflammation, as indicated by downregulation of *Fasn*, glycerol-3-phosphate dehydrogenase (*Gpd1*), serum amyloid A3 (*Saa3*), nucleotide binding oligomerisation domain (*Nod1*), *Stat1*, PPAR-γ (*Pparg*), sterol regulatory binding transcription factor (*Srebf1*), adipogenin (*Adig*), FA binding-protein 4 (*Fabp4*), TNF-α, IL-6 and MCP-1 mRNA and/or protein (Carroll et al., 2013; Massiéra, Seydoux, et al., 2001; Yiannikouris et al., 2012).

With respect to the main effector hormone of the RAS, i*n vitro* and *ex vivo* studies conducted in adipocytes have shown Ang-II to inhibit lipolysis through interaction with its AT_1-receptor whilst stimulating lipogenesis, ER stress and the secretion of pro-inflammatory cytokines as represented by increased *Fasn*, *Gpd1*, activating transcription factor 4 (*Atf4*), binding immunoglobulin protein (*Bip*), C/EBP homologous protein (*Chop*), IL-6, MCP-1 expression and NF-κB signaling (Goossens, Blaak, Arner, Saris, & van Baak, 2006; Jones, Standridge, & Moustaid, 1997; Menikdiwela et al., 2019; Tsuchiya et al., 2006). Similarly, *in vivo* studies have linked elevated

local and systemic generation of Ang-II to obesity and adipocyte hypertrophy (TG storage), concurrent with decreased plasma adiponectin, increased plasma leptin, local and systemic inflammation as well as IR, thereby possibly exacerbating adiposity (Boustany et al., 2004; Frederich et al., 1992; Furuhashi et al., 2003; Kalupahana et al., 2012; Ran et al., 2006; Saiki et al., 2009; Tsuchiya et al., 2006). More recently, salt-loading in adipocytes revealed an increase in several major metabolites involved in the RAS, including Ang-II and mineralocorticoid receptor, in addition to depressing AMPK activation and enhancing the expression levels of several early mentioned adipogenic, lipogenic and pro-inflammatory genes, *e.g.* ACC, FASN and TNF-α, as well as adipocyte-FA binding-protein (aP2) and salt-inducible kinase 2 (SIK-2), suggesting a high dose of intracellular salt may provoke adipose RAS activation and Ang-II synthesis (Lee, Sorn, Lee, & Kang, 2019), and thus high-salt provoked signaling (*i.e.* RAS) appears to promote molecular pathways of adipocyte hypertrophy and hyperplasia, a common feature of obesity.

While ACE is commonly deemed the main Ang-II forming enzyme in the circulation, in tissue, alternative serine proteases such as chymase, cathepsin D, cathepsin G and kallikrein, are shown to form Ang-II (Genest et al., 1983; Miura et al., 1994; Nehme et al., 2019). Chymase in particular has gained much attention due to its specificity and potency in the cardiovascular system. Divoux et al. (2012) and colleagues showed that the pathological characteristics of obese WAT, which includes markers fibrosis, macrophage accumulation and endothelial inflammation, were positively linked to accumulated mast cells with high chymase (and tryptase) activity, further linked with the pathophysiology of obesity and diabetes. More recently, Y. Zhang et al. (2018) showed that among enzymes involved in Ang-II generation, protein expression of ACE was higher in SAT whereas chymase was higher in VAT. This suggested that Ang-II generation in VAT may be more dependent on chymase than ACE, thus the therapeutic benefits of ACE-inhibitors in reducing Ang-II in VAT could be less effective. At present, widespread therapeutic application of chymase inhibitors is unavailable, and studies assessing chymase inhibition on bodyweight and fat regulation is limited to but one reporting successful treatment of NASH (Miyaoka et al., 2017).

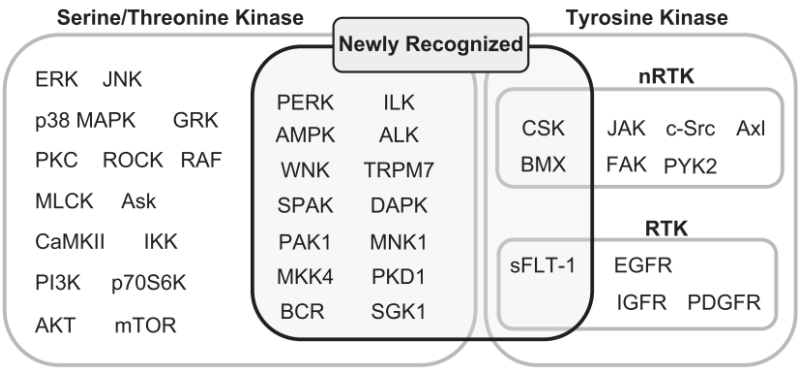

Figure 6. List of receptor and non-receptor tyrosine and threonine kinases activated AT_1-receptors. RTK, receptor tyrosine kinase; nRTK, non-receptor tyrosine kinase (Forrester et al., 2018; Higuchi et al., 2007).

Molecular pathways to weight loss: modulation of the Renin-angiotensin system

Counter-regulatory arm of the Renin-angiotensin system

Literature supports the existence of a counteracting interplay between ACE2/Ang-(1-7)/Mas and Ang-II/AT_1 signaling upon adipogenesis and lipogenesis. Ang-(1-7) is formed from Ang-II and Ang-I via the action of the ACE homologue, ACE2, and neutral endopeptidases, respectively (Nehme et al., 2019). Whilst Ang-II is pro-lipogenic, pro-proliferative, pro-inflammatory, and has vasoconstrictive effects, Ang-(1-7) is anti-lipogenic, anti-proliferative, anti-inflammatory and has vasodilatory effects, mediated via Mas receptor binding (Forrester et al., 2018; Frantz et al., 2018; Nehme et al., 2019; Simoes e Silva, Silveira, Ferreira, & Teixeira, 2013). Transgenic rats overexpressing Ang-(1-7) displayed heightened PPAR-γ and decreased LPL expression and activity in VAT to suggest higher FA oxidation, whereas the reverse was observed in Mas receptor-knockout mice. Moreover, a reduction in liver DNL and TG accumulation was concomitant with an increase in liver *Cpt1* and reduction in *Fasn* and *Fabp* expression, indicating Ang(1-7) has significant effects on pathways involved in lipid homeostasis (Moreira et al., 2017). Recently, Morimoto et al. (2018) showed that Ang-(1-7) treatment of mice maintained on a HFD had anti-obesity effects, as represented by increased thermogenesis (without upregulation of UCP1 expression in WAT), increased BAT mass (with augmented UCP1, PRDM16 and prohibitin expression), increased AMPK and phosphorylation of mammalian target of rapamycin (mTOR), resulting in improved lipid profiles and glucose tolerance concomitant with HSL activation and decreased perilipin expression. Thus targeting the ACE2/Ang-(1-7)/Mas-receptor axis has recently become of therapeutic interest in the treatment of obesity, hypertension and IR, especially over ACE-inhibitors, given the limiting adverse effects in patients (Gavras & Gavras, 1988; Loloi, Miller, Bingaman, Silberman, & Arnold, 2018).

Angiotensin-II receptor blockers (ARBs)

As described, the primary effects of Ang-II is mediated via activation of AT_1-receptors, and pharmacological intervention of Ang-II action via AT_1 blockers (ARBs) is reported to alleviate obesity and many of its symptoms. In humans, 26-weeks of AT_1-antagonism with valsartan reduced abdominal SAT adipocyte size whilst increasing the proportion of small adipocytes, and this was associated with a reduction in adipogenic and lipogenic gene expression including that of PPAR-γ, aP2 and C/EBPα, as well as markers of macrophage infiltration, *i.e.* CD11b, CD163 and CD206. Although a reduction in adipogenic genes does not align with a reduction in the number of adipocytes, reduced adipocyte size correlated with PPAR-γ expression and is therefore likely a relic of the steady state achieved, hence may not reflect molecular changes that may have occurred during early stages of treatment (Goossens et al., 2012). In rodents, treatment of rats with the ARB candesartan reduced bodyweight gain and fat mass due to adipose tissue hypotrophy, as indicated by decreased adipocyte size. These effects were accompanied by an increase in PPAR-γ mRNA and adiponectin mRNA and plasma levels, and a reduction in TNF-α mRNA and leptin mRNA and

plasma levels (Zorad et al., 2006). In other studies, AT_1-antagonism with telmisartan was shown to have an inhibitory effect toward Ang-II induced lipogenesis *in vitro* and HFD-induced bodyweight gain *in vivo*. These effects were associated with the activation of PPAR-α-dependent pathways in several tissues, leading to an upregulation in PPAR-γ, protein kinase A (PKA), UCP1, HSL, endothelial NO synthetase 3 (eNOS3) and CPT1α, activation of the ACE2/Ang-(1-7)/Mas-receptor axis, modulation of the MAPK pathway and downregulation of perilipin expression in adipose tissue, concomitant with an increase in the expression of UCP-2 and -3 in skeletal muscle to negatively affect bodyweight and glucose intolerance (Kang et al., 2015; Schuchard et al., 2015). These findings combined support the contention that blockade of AT_1-recptors may inhibit lipogenesis and lipid storage, improve lipid metabolism, adipokine secretion and inflammatory profiles, whilst also promoting adipogenesis (via PPAR-γ), which may be a central mechanism whereby to reduce the incidence of developing diseases associated with adipose tissue inflammation such as IR and T2D.

Angiotensin-converting enzyme (ACE) inhibitors

Pharmacological blockade of Ang-II synthesis via ACE-inhibition is reported to reduce adiposity and adipocyte size in rodents, but not in humans (Kalupahana & Moustaid-Moussa, 2012). In rats fed a fructose-rich diet, it has been demonstrated that ACE-inhibition with temocrapril has beneficial effects on adipose tissue function by inducing adipocyte hypotrophy, leading to improved insulin sensitivity without affecting bodyweight or epididymal fat content (Furuhashi et al., 2004). In other studies, ACE-inhibition with enalapril is reported to decrease bodyweight and fat mass as well as promote longevity in rats fed a low- and high-fat diet, and this correlated with reduced serum leptin levels and increased expression of antioxidant enzymes including catalase and superoxide dismutase (SOD), as well as PPAR-γ, adiponectin, HSL and FASN in adipose tissue, where the latter is suggested to be a compensatory mechanism for low levels of adipose TG content (Santos et al., 2009; E. L. Santos et al., 2008). In humans, combining enalapril treatment with a weight-loss regimen (low-caloric diet and aerobic exercise) for 12-months is reported to amplify bodyweight loss and plasma leptin, insulin and norepinephrine reductions by the end of the treatment period, albeit body composition, biochemical and molecular characteristics of tissues were not analysed (Masuo, Mikami, Ogihara, & Tuck, 2001).

Captopril

As the first orally active ACE-inhibitor to become commercially available, captopril is perhaps the most well studied ACE-inhibitor with respect to bodyweight and body fat regulation. Containing a sulfhydryl group and a modified proline with a thiol moiety that binds with the zinc ion within the active site of ACE, captopril differs from second generation ACE-inhibitors that are devoid of a sulphydryl group and compete with the renin substrate for ACE-binding sites (Patrick, 2005).

It has been reported that captopril can significantly reduce bodyweight and fat mass, in addition to preventing DIO in rodents (de Kloet et al., 2009; Kalupahana et al., 2012; Premaratna et al., 2011; Weisinger et al., 2009). Moreover, high-fructose fed rats treated with captopril were partially protected from MetS and abdominal fat gain, whilst serum glucose and insulin levels remained unchanged (Roncal et al., 2009). In particular, captopril treatment of mice has demonstrated that ACE-inhibition protects against HFD-induced obesity, glucose intolerance and NAFLD by causing adipocyte hypotrophy and reducing plasma/hepatic TGs, which may be mechanistically explained by an increase in peripheral (liver and skeletal muscle) FA metabolism as a result of a doubling of systemic adiponectin levels (Ackerman et al., 2005; Weisinger et al., 2009). Kohlstedt et al. (2009) demonstrated the signaling cascade underlying ACE-inhibition in cultured adipocytes is mediated by cellular-retinol binding protein 1 (CRBP1) whereby protein overexpression of CRBP1 activated retinol-dependent nuclear receptor proteins (RAR/RXR) followed by its heterodimerisation with PPAR-γ, promoting the upregulation of adiponectin. As reported, adiponectin promotes FA oxidation through AMPK, and in support of this hypothesis, Tabbi-Anneni, Buchanan, Cooksey, and Abel (2008) showed increased AMPK activation and decreased rate of glycolysis in the hearts of captopril-treated *Ob*/*Ob* mice, which may be sufficient to lower lipogenesis by limiting glycerol synthesis from glucose (Caminhotto, Sertié, Andreotti, Campaãa, & Lima, 2016). Moreover, low body fat levels, as represented by a decrease in TG content in adipose and liver tissue, correlated with a reduction in adipose leptin mRNA expression and circulating levels (and an increase in plasma adiponectin) in captopril treated mice maintained on a HFD, and this was observed alongside a reduction in the expression of inflammatory cytokines including MCP-1, IL-6 and TLR4 in peripheral tissues as well as upregulation of hepatic PGC-1α, HSL and long-chain acyl-CoA dehydrogenase (LCAD) mRNA, and downregulation of LPL; these findings are suggested to underlie the anti-obesity properties of captopril as well as the observed improvements in glucose tolerance, hepatic insulin sensitivity and reduction in hepatic gluconeogenesis (Premaratna et al., 2011). Studies have also partially attributed the weight-loss properties of captopril to an increase in the activity of the ACE2/Ang-(1-7)/Mas receptor axis (Oh, Kim, Park, Park, & Kim, 2012), albeit further studies are necessary to understand how captopril alters the lipid composition of adipocytes and other peripheral tissues, as well as tissue specific signaling activities that contribute to adipocyte hypotrophy and whole-body FA-oxidation leading to weight loss.

Conclusion

Obesity leads to major changes in body composition, such as excessive adipose and liver tissue TG accumulation to manifest peripheral IR and hypertension, which has a major impact on morbidity and mortality rates in both Western and developing populations. The co-existence of these pathologies suggests common metabolic pathway dysfunction. Studies suggest obesity is associated with low-grade chronic-inflammation, increased ER stress and dysregulation of adipokines, *e.g.* leptin and adiponectin, as well as lipotoxicity. Currently, management strategies of obesity includes lifestyle modifications, with diet and aerobic exercise as the first line of choice, followed by pharmacological intervention and lastly bariatric surgery. In this review, we presented the RAS as a key mechanism of WAT and hepatic dysfunction, and described salt-induced activation of adipose tissue RAS which comprised a common underlying mechanism of lipogenesis and adipogenesis leading to adipocyte growth and proliferation.

As described, the upregulation of the classical arm of the RAS promotes adipocyte hypertrophy via the activation of DNL and adipogenesis, inhibition of lipolysis, dysregulation of adipokine secretion, reduced glucose uptake and insulin insensitivity and induction of oxidative stress and inflammation. These effects are largely mediated by Ang-II and activation of the G-protein coupled AT_1-receptors, whilst pharmacological intervention of Ang-II synthesis and action via ACE-inhibition and AT_1-receptor antagonism respectively, is reported to alleviate obesity and many of its symptoms. In particular, the ACE-inhibitor captopril has been shown to promote lipolysis and FA-oxidation, improvements in plasma adipokine ratios, in addition to exhibiting anti-lipogenic, anti-proliferative and anti-inflammatory properties to overcome hypertension, IR, glucose intolerance, oxidative stress and inflammation to even offer protection against the development and progression of obesity.

Aims and hypotheses

Albeit the anti-obesity and weight loss effects of captopril has only been documented in rodent models of DIO, despite [captopril] having been prescribed as an antihypertensive in patients for over 30 years. Recent studies conducted in our laboratory suggests that this discrepancy between rodents and humans may involve an interaction effect between captopril and dietary salt, as a high-salt diet in DIO mice was shown to abolish the weight loss efficacy of captopril (Radcliffe, 2013 PhD thesis). To date, the mode/s of action of this interaction has not been thoroughly investigated. To this end, the aims of the experiments presented in chapters 3 and 4 is to identify key metabolites and molecular pathways involved in the interaction between captopril and salt leading to either weight loss or inhibition of weight loss [by dietary salt] by way of employing metabolomics and transcriptomics analyses, respectively. We hypothesise that key metabolites and genes involved in the development and progression of DIO will be reversely regulated by a high-salt diet in C57BL/6J mice administered captopril.

To date, the majority of studies with respect to ACE-inhibition with captopril on body fat composition has been demonstrated in rodents albeit animals including the *Caenohabditis elegans* (*C. elegans*) also expresses a homolog of the ACE (*acn-1*) which lacks the zinc-containing binding site for captopril. Moreover, given *C. elegans* are devoid of a circulatory system, *acn-1* is rendered catalytically inactive and functionally independent of a RAS (Bader, 2007; Coates, 2003; Coates, Siviter, & Isaac, 2000; Isaac, Siviter, Stancombe, Coates, & Shirras, 2000; Turner & Hooper, 2002). To date, only one study has reported on the positive effects of captopril on the lifespan of *C. elegans* via mechanisms that were dependent on the FOXO/*daf-16* transcription factor (Kumar et al., 2016). To this end, the aims of the final experiment presented in chapter 5 was to investigate whether the physiological response to captopril on body fat composition and health span, stress and locomotive patterns is conserved between *C. elegans* and rodents. We hypothesise that captopril will cause a reduction in body fat, increase health span, improve stress tolerance, and alter the locomotive patterns of *C. elegans* to a capacity that may be comparable to that of captopril administered rodents.

Chapter 2

General Materials and Methods

This chapter is a general summary of materials and methods used throughout the experiments reported in this thesis. Details methods for each experiment can be found in respective chapters.

Mouse studies

This study was approved by the La Trobe University Animal Ethics Committee, approval number AEC14-32.

Sample collection

Upon completion of the study, all mice were euthanised by CO_2 asphyxiation in a gas chamber. Blood samples were collected from the left ventricle of the heart in to syringes containing 5% (w/v) EDTA (Sigma Aldrich, USA) and transferred in to Eppendorf tubes placed on ice until preparation by centrifugation at 5,000 × *g* for 15 minutes to recover plasma which was then frozen at -20ºC until analysis.

Liver and adipose tissue (as well as brain, extensor digitorum longus muscle and hind-limb bone) was collected and stored in RNAlater (Qiagen GmbH, Hilden, Germany) for one hour and placed in -80ºC until transcriptomics analysis. Remainder of samples and mouse carcasses were snap frozen in LN_2 until being transferred in to a -80ºC freezer.

Extraction, optimisation, derivatisation and analysis of mouse plasma for GC-MS

Plasma was thawed at room temperature and simple liquid-liquid method was applied to extract amino acids, sugars, organic acids and secondary metabolites from mouse plasma. To 50µl of the mouse plasma, 150µl of absolute methanol containing 1µl internal standards ($^{13}C_6$-sorbitol/$^{13}C_5{}^{15}N$-valine in water, 0.2 mg mL^{-1}) was added. Prepared samples were evaporated to dryness *in vacuo* for subsequent TMS (trimethylsilyl) metabolite derivatisation. All samples were stored in darkness containing silica beads prior to GC-MS analysis. Prior to analysis, metabolites were dissolved in methoxyamine-hydrochloride and pyridine, and derivatised at 37ºC for 120 min, and injected into a GC–MS system (Gerstel PAL3 Autosampler, 7890B Agilent gas chromatograph and a 5977B Agilent quadrupole MS; Agilent, Santa Clara, USA) in splitless and split mode (1:20 split ratio). Chromatograms and mass spectra were processed using the Agilent MassHunter Workstation Software, Quantitative Analysis, Version B.07.01/Build 7.1.524.0. Mass spectra of eluting compounds were identified using a commercial, public and in-house mass spectra library. Resulting relative response ratios for each analysed metabolite were prepared as previously described by Aizat et al. (2014).

RNA-Seq library preparation, sequencing and analysis

Total RNA was extracted from liver and adipose tissue with the RNeasy kit (Qiagen GmbH, Hilden, Germany) according to manufacturer's protocol. RNA libraries were prepared using the TruSeq RNA Library Preparation Kit (Illumina, San Diego, CA). Multiple RNA samples were normalised to 10nM and pooled to create one RNA library. Reads generated by the sequencer, typically 100-150 base pair paired ended, were first mapped to the mouse transcriptome. The resulting table of numbers of alignments per gene per biological replicate per experimental condition was then analysed by a statistical algorithm. Sorted list of genes was subjected to gene ontology (GO) and pathway analyses using the Kyoto Encyclopaedia of Genes and Genomes (KEGG) database.

Caenorhabditis elegans studies

The required approval to maintain genetically modified organism was granted by La Trobe University Institute of Biosafety Committee (LTIBC), reference number GMSC15-017.

Materials, devices and equipment used in C. elegans experiments

Commonly used equipment, devices and consumables used throughtout *C. elegans* experiments included: Thermoline Scientific refrigerated incubators (15ºC and 20ºC); Thermo Scientific 4ºC fridge; Fisher and Paykel (-20ºC) and Thermofisher (-80ºC) freezers; Indiko Chemistry Analyser (Thermo Scientific); Precellys 24 lysis and homogenization (Peqlab, Erlangen, Germany); Corning Cell culture plates (3, 6 and 12 inch); Global Science centrifuge tubes (1.5 ml, 15 ml and 50 ml); Thermo Scientific pipettes; Interpath Aerosol Barrier Pipette Tips; Pioneer weighing scale; Thermo Scientific centrifuge; Thermo Scientific vortex; Alcohol burners; Lab made worm picks; J. Melvin Freed Brand microscope slides. Nikon up right and inverted microscopes fitted with a Nikon DS-Fi2 camera with bright light and fluorescence capabilities were utilized for monitoring development and data collection of *C. elegans* experiments.

Maintenance of C. elegans strains

Wild-type C. elegans Bristol N2 and *daf-16(mu86)* strain was acquired from the *Caenorhabditis* Genetic Centre (Minnesota, USA), *flcn-1(ok975)* mutants were kindly supplied by Professor Arnim Pause (McGill University, Quebec), and *dhs-3::gfp* by Professor Pingsheng Liu (Chinese Academy of Sciences, Beijing). All strains were maintained on Nematode Growth Medium (NGM) agar plates seeded with *E. coli* OP50 as a food source. NGM is prepared by dissolving 3g NaC1, 2.5g Bactopeptone (Difco) and 17g Bacto-agar in 975 ml distilled water. The mixture is autoclaved and cooled to 55ºC, to which 1 ml of cholesterol in absolute ethanol (5 mg/ml), 1 ml 1M $CaCl_2$, 1 ml 1M $MgSO_4$, and 25 ml 1M KPO_4 buffer (pH 6.0) is added in order. The two most commonly used buffers in the experiments were M9 and S-buffer. M9 buffer was made of 6 g Na_2HPO_4, 3 g KH_2PO_4, 5 g NaCl and 0.25 g $MgSO_4.7H_2O$ per liter of distilled water. S-buffer was composed of 0.1 M NaCl and 0.05 M KPO_4 and pH was adjusted to 6.0.

Lifespan experiments

Wild-type N2, daf-16 and flcn-1 mutants were used for lifespan analysis. All experiments were performed at 20ºC. Synchronised worms were grown on NGM and L4 larvae were transferred on to 30 mm experimental plated with a palmitic acid ring to prevent animals from escaping. Experimental plates consisted of three levels of captopril (Sigma Aldrich, USA), gentamicin (Thermo Fisher Scientific, AU) and 2'-deoxy-5-fluoroudine (FuDR; Sigma Aldrich, USA). Animals were observed under a Nikon upright light microscope. Lifespan experiments were performed three to five times.

Preparation of C. elegans homogenates and biochemical measurements

Worm homogenates and biochemical measurements were conducted as previously reported (Palgunow et al., 2012). Wild-type and mutant strains of *C. elegans* were cultivated under three levels of captopril (0.02%, 0.05%, 0.10%) until reaching L4 stage. For each replicate, ~3000 L4 larvae were collected in M9 buffer, pipetted in to sterile Eppendorf tubes and washed three times; worms were allowed to settle to the bottom of the tube between each wash. Animals were homogenised in 100µl buffer (150 mM NaCl; 1 mM EDTA; 50 mM Tris-HCl, pH 7.5; 0.5% CHAPS) using the Precellys 24 homogeniser and ceramic beads (1.4 mm). Cell debris was removed by centrifugation for 20 min. Homogenates were transferred to a chemical analyser for evaluation of triglycerides (TGs) and protein content in enzymatic assays (Indiko, Thermo Fisher Scientific). Protein content was measured using the Pierce® BCA protein assay kit (Thermo Fisher Scientific, USA) with bovine serum albumin (BSA) as protein standard and adapted to Indiko according to manufacturer's protocol.

Oil Red O preparation, C. elegans fixation, fat staining and analysis

Oil red O staining was conducted as previously reported (Walby, et al., 2014). A 0.5% Oil red O (Sigma Aldrich, USA) stock solution was prepared in absolute isoptopanol (Sigma Aldrich, USA), allowed to rock for a day and filtered twice through a 0.45µm filter (Millipore, USA). The day before use, stock was diluted to 60% in distilled water and filtered again through a 0.45 µm filter immediately before use.

Wild-type and mutant strain *C. elegans* were harvested at L4 stage in to 1.5ml tubes, washed three times in M9 buffer and allowed to settle by gravity. Worms were fixed by resuspending in 500µl of 60% isopropanol, allowed to settle, and supernatant was aspirated. 500µl of freshly filtered Oil red O working solution was added and worms were stained for 6-18 hours in a wet chamber (wet paper towel in a parafilm-wrapped plastic box). After staining, the supernatant was washed to which 250µl of 0.01% Triton X-100 (Sigma Aldrich, USA) in S-basal was added. For image acquisition, 3% agar pads were prepared on slides, and 3µl of mounting medium (Vector Labs) was added on to 24 x 24 mm cover slips. 5µl of the worm suspension was transferred on to the cover slip, mixed with the mounting medium and flipped on to agar pads. Images per condition were acquired on the Nikon

inverted microscope by mounting worms on to 3% agar pads on as many slides as necessary, and images were analysed using *ImageJ* software (v1.48).

Determination of body length, pharyngeal pumping rate and motility

For analysis of body length, Oil red O stained animals were measured using Image J software and length measurements derived by the sum-total of a number of segmented lines of known length, down the centre of the worm. For analysis of animal pharyngeal pumping rate, 20 animals per treatment group were analysed at L4 larval stage on a Nikon inverted microscope. The pharynx was filmed for 60 seconds at 100-fold magnification using Nikon DS-Fi2 camera, and the pharyngeal pumping rate (pumps/min) was counted on slowed films. For analysis of animal motility, worms were recorded for 20 seconds at 8-fold magnification using Nikon upright microscope fitted with a Nikon camera, and MBF WormLab software version 4.1 was used for video analysis of worms exposed to different levels of captopril. Locomotion parameters selected from the analysis included track length (μm) [forward + reversal] and speed (μm/s) [tracklength per second].

Stress response assays

Wild-type *C. elegans* were cultivated at 20ºC under control or 0.10% captopril and transferred to stressful conditions and monitored for survival. Thermotolerance assays were performed as described (McColl et al., 2010); briefly, L4 larvae were transferred to 34ºC and scored the percentage of dead and live animals starting at 6 hours and continuing every hour until all animals died. To perform oxidative stress assays, a total of 10 L4 larvae were transferred to experimental NGM plates containing 40mM paraquat and scored for survival every hour. Experiments were performed three times.

Statistical analysis

Unless otherwise stated, standard statistical analyses were performed using IBM Statistical Package for Social Science version 25.0 (SPSS, Chicago IL). For metabolomics and transcriptomics studies, significant interacting metabolites and genes of tissues were determined using the least significant difference (LSD) and Bonferroni *p*-value at $p<0.05$ of two-way analysis of variance (ANOVA), respectively. The relationship between plasma metabolites, genes, bodyweight, epididymal fat and liver masses were evaluated by means of bivariate correlations using Person's correlation coefficients, r (2-tailed). To correct the multiple comparison problem of GC-MS analysis of serum metabolites, a false-discovery rate (FDR)-corrected value was applied to variables according to Benjamini and Hochberg (BH) at a threshold of 0.20. Discriminative data analysis used was principal component analysis (PCA) using the open-source MetaboAnalystR program, version 4.0 (https://www.metaboanalyst.ca/).

For *C. elegans* studies, numerical data was analysed by repeated measures ANOVA and unpaired t-test (two-tailed), survival analyses were calculated by log-rank test where all differences were considered statistically significant at $p<0.05$.

Chapter 3

High dietary salt consumption impedes the weight loss efficacy of captopril in C57BL/6J mice maintained on a high-fat diet: A metabolomics study

Abstract

The ACE-inhibitor, captopril, is commonly prescribed to treat primary hypertension and has gained attention as a potential anti-obesity agent. Captopril treatment of obese rodents causes bodyweight and fat loss although paradoxically, there have been no such reports in hypertensive patients. Studies conducted in our laboratory recently showed the weight loss efficacy of captopril was abolished in DIO mice consuming in excess of 86.0 mg of dietary salt (NaCl) per day (Radcliffe, 2013 PhD Thesis), suggestive of an interaction effect between captopril and salt. This may explain the shortage of reports of weight loss in captopril administered patients given dietary salt intake is in excess in the average Western diet. The aim of this experiment was to investigate and identify key metabolites and metabolic pathways which may be involved in this interaction effect. We used a non-targeted GC-MS based metabolomics approach to investigate the interaction between captopril and salt on the plasma metabolite profiles of C57BL/6J mice maintained on a Western style obesogenic diet. A two-way ANOVA was applied to data to identify metabolites altered by the interaction between the two factors, and a FDR-corrected value was applied to variables according to Benjamini and Hochberg. Metabolite markers associated with bodyweight and body fat mass, represented by epididymal fat and liver masses, were identified using a Pearson's correlation coefficients test. Several metabolites were influenced differently to indicate interactions involving metabolic pathways predominantly relating to the metabolism of carbohydrates which may include glycolysis, fructose metabolism, inositol biosynthesis, the pentose phosphate and gluconate pathways as well as the TCA cycle and fatty acid metabolism. Significant inverse correlations were apparent between bodyweight and fat masses for plasma sucrose, fructose, erythritol, inositol, erythronate, glycerate, citrate, and 2-ketogluconate whilst 6-phosphogluconate, pyruvate and glutamine correlated positively. Together there was strong indication that the metabolic action of captopril may involve alterations in response to a restriction of glucose and fructose metabolism, causing a diversion of available substrates from intracellular phosphorylative routes towards extracellular oxidative pathways. This study supports our previous work showing the weight loss properties of captopril to be adversely affected by high dietary salt intake, and offers novel insight in to the metabolic states of captopril treated mice subjected to a normal salt or a high-salt intake.

Introduction

Obesity has become overwhelmingly prevalent globally without age, gender, geographical or ethnicity boundaries. According to the WHO obesity worldwide has nearly tripled to 13% since 1975 where more people today are dying from overweight and obesity than underweight (WHO, 2018). In Australian society, overweight and obesity has become a major risk factor for many of the leading causes of premature death and illness (AIHW, 2018). Generally considered to be a consequence of positive energy balance and abnormal lipid metabolism, current advances in the understanding of obesity and metabolism through "omics" technologies renders this view overly simplistic (Henstridge & Bozaoglu, 2017). A variety of critical metabolic pathways are perturbed in the development of obesity involving lipogenesis and lipolysis, adipocyte differentiation and hypertrophy, gluconeogenesis and glycolysis, oxidative stress and energy expenditure, whereas weight loss alters these metabolic characteristics from baseline (Kang, Yoo, Kim, Kim, & Lee, 2018; Xue & Ideraabdullah, 2016).

As outlined in Chapter 1, there is considerable evidence showing that the RAS is over-stimulated in both humans and animal models of DIO, and that this over-stimulation is associated with alterations in carbohydrate and lipid metabolism (Strazzullo & Galletti, 2004). Whilst blocking the RAS using the ACE-inhibitor captopril has been shown to cause significant bodyweight and fat loss in rodents (de Kloet et al., 2009; Premaratna et al., 2011; Weisinger et al., 2009), this effect has not been documented in humans. A hallmark of the Western diet is high-salt consumption (Martinez Steele et al., 2016; McMillan Price & Egger, 2017) that is additionally associated with an increase in the risk of developing obesity and its symptoms (Hulthén et al., 2010; Kim, Koo, Kim, & Chin, 2014; Ma et al., 2015). Rodent studies have shown short-term intake of a high-salt diet to cause weight loss (Kitada et al., 2017) and long-term intake of a high-salt diet to increase lipogenesis and body fat gain (Fonseca-Alaniz et al., 2007; Lanaspa et al., 2018). Whilst moderate dietary salt reduction has been reported as potentiating blood pressure reduction following captopril treatment of hypertensive patients, dietary salt is not thought to be involved in reducing captopril's [weight loss] efficacy in humans (Kristinsson et al., 1988). We showed that the weight loss effects of captopril is abolished when administered in combination with dietary salt levels that exceeds 86.0 mg day^{-1} (Radcliffe, 2013).

The aims of this study were to validate the interaction effect between dietary salt and captopril on bodyweight and fat loss in DIO C57BL/6J mice, and further uncover the effect of this interaction on plasma metabolite profiles. Combined with multivariate analyses, untargeted gas chromatography (GC) coupled with mass spectroscopy (MS) was performed on plasma samples in order to ascertain the metabolic impact of captopril and salt by comparison of endogenous metabolite levels. Metabolite markers associated with weight loss and fat mass were also evaluated by relating the degree of change of metabolites to body weight, epididymal fat and liver mass. We hypothesise that key metabolites involved in the progression of DIO will be reversely regulated by

a high-salt diet (>86.0 mg day^{-1}) in C57BL/6J mice administered captopril. Because metabolomics provides functional information about cellular physiology, findings may help to clarify how changes in metabolism/biochemistry contribute to the weight loss effects of captopril.

Materials & methods

All research procedures were conducted and approved under the guidelines set by the Animal Ethics Committee at La Trobe University (Bundoora) Melbourne, approval number AEC14-32.

Animal subjects

Fourty 3-week old post-weaned male C57BL/6J mice were obtained from Animal Resources Centre (Canning Vale, WA). Mice were then housed in groups of four in standard cages in the Central Animal House (La Trobe University) in a room under controlled ambient temperature (22±2.0ºC) and 12-hour light:dark cycle. Animals had *ad libitum* access to water and ready-prepared high-fat high-sucrose diet (19.4 kJ g^{-1}) formulated to mimic a "Western fast food diet" (SF00-219, Glenn Forrest, WA) for a duration of 20 weeks to allow the onset of DIO. Mice were then randomly assorted in to one of four treatment groups (n=10) and housed one per plastic cage. Mice were treated for a duration of four weeks and animal welfare was monitored routinely to ensure health, food and water accessibility. Water intake was measured daily and food intake was measured every other day. Bodyweight was measured bi-weekly. Water and food were refreshed 2-3 times per week as with cage bedding where sawdust and a cardboard roll was used to line the base and provide environmental enrichment. After the four-week treatment period all animals were euthanized via CO_2 asphyxiation and final bodyweights were recorded and blood and tissue samples were collected for further analysis as described in Chapter 2.

Treatment groups

Mice started treatment at an average bodyweight of 46.83±0.53g (p>0.05). All animals were maintained on high-fat high-sucrose feed SF00-219 for the duration of the experimental period. Two treatment groups received 20mg ml^{-1} (2.0%) dietary salt added in to their drinking water with or without 0.05mg ml^{-1} captopril, and two received standard drinking water with or without 0.05mg ml^{-1} captopril. The SF00-219 feed contained 2.6 mg g^{-1} sodium chloride.

One animal was prematurely euthanized for displaying ill-health (autopsy inconclusive) and another excluded due to enlarged thymus glands, a possible indicator of disease (n=38).

Tissue collection and storage

Mice were euthanized by CO_2 asphyxiation and final bodyweight were recorded. Blood was collected from the left atrium of the heart in to syringes treated with 0.171M EDTA (Sigma Aldrich, USA) solution, and blood was then transferred in to Eppendorph tubes and placed on ice. Whole blood was centrifuged at 5,000 × *g* (Heraeus Fresco 17, Thermo Scientific, USA) for 15 minutes at 4.0ºC and plasma was collected and frozen at -20ºC for metabolomic analysis. Tissues were collected (liver, epididymal adipose tissue, skeletal muscle, and kidney), weighed (liver, epididymal adipose tissue, and kidney) and recorded. Samples for analysis were portioned and saved in RNA*later* Stabilization Reagent (Qiagen GmbH, Hilden, Germany) and the remainder of samples

and mouse carcasses were submerged in liquid nitrogen immediately after collection. All tissues were stored at -80ºC until transcriptomic analysis.

Extraction and Optimisation of mouse plasma for GC-MS

Plasma was thawed at room temperature and vortex-mixed before use. A simple liquid-liquid method was applied to extract amino acids, sugars, organic acids and secondary metabolites from mouse plasma. To 50µl of the mouse plasma, 150µl of cold methanol (100%) containing 1µl internal standards ($^{13}C_6$-sorbitol/$^{13}C_5{}^{15}N$-valine in water, 0.2 mg mL^{-1}) was added and briefly vortexed. Then the mixture was placed on ice for 5-10 minutes and centrifuged at 13,000 rpm (4ºC) for 5 minutes to precipitate proteins. After centrifugation 150µl of supernatant was collected in to fresh Eppendorph tubes, and 50µl was added to pulled point glass vials (Agilent Technologies, part no. 5183-2085) and evaporated to dryness *in vacuo* for subsequent TMS (trimethylsilyl) metabolite chemical derivatisation. A pooled biological quality control (PBQC) was prepared by pooling a total volume of 250µl which was treated the same way as the samples prior to GC-MS analysis. All samples were stored in darkness containing silica beads prior to GC-MS analysis (Aizat et al., 2014).

Polar metabolite derivatisation

All samples were re-dissolved in 10 µL of 30 mg.mL^{-1} methoxyamine hydrochloride in pyridine and derivatized at 37 ˚C for 120 min with mixing at 500 rpm. Then, the samples were incubated for 30 min with mixing at 500 rpm after addition of both 20 µL *N,O-bis*-(trimethylsilyl)trifluoroacetamide (BSTFA) and 1 µL retention time standard mixture [0.029% (v/v) *n*-dodecane, *n*-pentadecane, *n*-nonadecane, *n*-docosane, *n*-octacosane, *n*-dotriacontane, *n*-hexatriacontane dissolved in pyridine]. Each derivatized sample was allowed to rest for 60 min prior to injection (Aizat et al., 2014).

Annotated untargeted metabolite analysis: GC-MS instrument conditions

Samples (1 µL) were then injected into a GC–MS system (Gerstel PAL3 Autosampler, 7890B Agilent gas chromatograph and a 5977B Agilent quadrupole MS; Agilent, Santa Clara, USA) in splitless and split mode (1:20 split ratio). The MS was adjusted according to the manufacturer's recommendations using *tris*-(perfluorobutyl)-amine (CF43). Chemical separation was achieved using a J&W Scientific VF-5MS column (30 m long with 10 m guard column, 0.25 mm inner diameter, 0.25 µm film thickness). The injection temperature was set at 250 ˚C; the MS transfer line at 290 ˚C, the ion source adjusted to 250 ˚C and the quadrupole at 150 ˚C. Helium (UHP 5.0) was used as the carrier gas at a flow rate of 1.0 mL min^{-1}. The following temperature program was used; injection at 70˚C, hold for 1 min, followed by a 7 ˚C min^{-1} oven temperature ramp to 325 ˚C and a final 6 min hold at 325 ˚C. Mass spectra were recorded at 2 scans s^{-1} with an 50–600 *m/z* scanning range (Aizat et al., 2014).

Data processing (GC-MS) and statistical analyses

Both chromatograms and mass spectra were processed using the Agilent MassHunter Workstation Software, Quantitative Analysis, Version B.07.01/Build 7.1.524.0. Mass spectra of eluting compounds were identified using the commercial mass spectra library NIST 08 (http://www.nist.gov), the public domain mass spectra library of Max-Planck- Institute for Plant Physiology, Golm, Germany (http://csbdb.mpimp-golm.mpg.de/csbdb/dbma/msri.html) and an *in-house* mass spectral library. All matching mass spectra were additionally verified by determination of the retention time by analysis of authentic standard substances. Resulting relative response ratios (area of analyte divided by area of the internal $^{13}C_6$ –sorbitol standard) for each analysed metabolite were prepared as previously described by Aizat et al. (2014)

The data were also normalized to the control group to compare fold differences between treatments. If a specific metabolite had multiple TMS derivatives, the metabolite with the greater detector response and better peak shape within the dynamic range of the instrument was selected (Aizat et al., 2014).

Dr Daniel Dias (RMIT University, VIC) was involved in the technical aspects and my involvement was with sample preparation and statistical analysis of data. Data was analysed according to statistical tests outlined below.

Statistical analysis

A two-way ANOVA tested the effect of captopril on bodyweight in mice that consumed an obesogenic Western style diet in combination with or without 2.0% dietary salt added in to their drinking water, also taking in to consideration the concentration of salt present in their feed. The reference groups did not receive captopril nor additional salt in drinking water.

All analysis was conducted by IBM Statistical Package for Social Science version 25.0 (SPSS, Chicago IL). Descriptive characteristics of mice and all other numerical data was analysed using multivariate analysis of variance (MANOVA) and a two-way ANOVA to compare the main effects of captopril and salt and the interaction effect between captopril and salt on body and organ weights, food and water consumption, captopril and salt intake, and the level of serum derived metabolites from all experimental mice. All effects were statistically significant at the 0.05 significance level. A logarithmic transformation was performed for the skewed variables and for descriptive purposes untransformed values were expressed as mean ± standard error of mean (SEM) unless otherwise stated. A Kruskal-wallis test was conducted for skewed variables and asymtotic significance at the 0.05 level is reported. To correct the multiple comparison problem of non-targeted GC-MS analysis of serum metabolites, a false discovery rate (FDR)-corrected value was applied to variables according to Benjamini and Hochberg (BH), as Bonferroni correction could be overly conservative (Broadhurst & Kell, 2006). Significant threshold for FDR-values was set at 0.20.

The relationship between plasma metabolites, bodyweight, epididymal fat and liver masses were evaluated by means of bivariate correlations using Pearson's correlation coefficients, r (2-tailed). Metabolite relationships with r>|(0.325)| were significant ($p<0.05$) and those with r>|(0.5)| were considered pertinent regarding their magnitude ($p<0.01$). Linear regression analysis was used to show the independent relationship of significant compounds/metabolites with bodyweight, epididymal fat and liver masses and other metabolic features.

Results

Body weight

As reported in table 2, the initial bodyweight of the CAPS treatment group was significantly higher than that of the HFS and CAP group. This was due to the removal of two animals from the study; one animal was culled prematurely for displaying signs of ill-health (autopsy inconclusive), and another was removed for presenting enlarged thymus glands which could indicate disease that may skew results. This does not deviate from the primary aims of this experiment, which is to determine the weight loss mechanism of captopril and its interaction with dietary salt at the metabolite level.

With the exception of the CAP treatment group, no substantial changes in bodyweight were observed within remaining groups after the treatment period ($p>0.05$). By the end of the study, HF group mice were 3.63% heavier than their pre-treatment bodyweights whilst CAP, CAPS and HFS treatment groups were 14.78%, 1.88% and 3.30% lighter than their pre-treatment bodyweights. Only the CAP group experienced significant bodyweight change ($p<0.05$). The administration of captopril in conjunction with a high-salt intake abolished the effect of captopril on bodyweight loss in CAPS group mice to resemble its respective HFS control ($p>0.05$). The addition of salt to drinking water appeared to curb body weight gain in the HFS treatment group against the HF group ($p<0.05$), however this could be a relic of differences in pre-treatment bodyweights of mice.

There was a significant main effect of captopril on bodyweight ($F(3, 37) = 6.758$, $p<0.05$). As shown in table 1 and figure 1B, there was a significant interaction between the two factors, captopril and salt, on bodyweight ($F(3, 37) = 20.939$, $p<0.05$). This means captopril has a significant effect on one treatment group (salt <86.0 mg day^{-1}) but not the other (salt >86.0 mg day^{-1}) on bodyweight, and this interaction is depicted graphically as a strong positive relationship between the two factors ($r=0.68$, $p<0.05$).

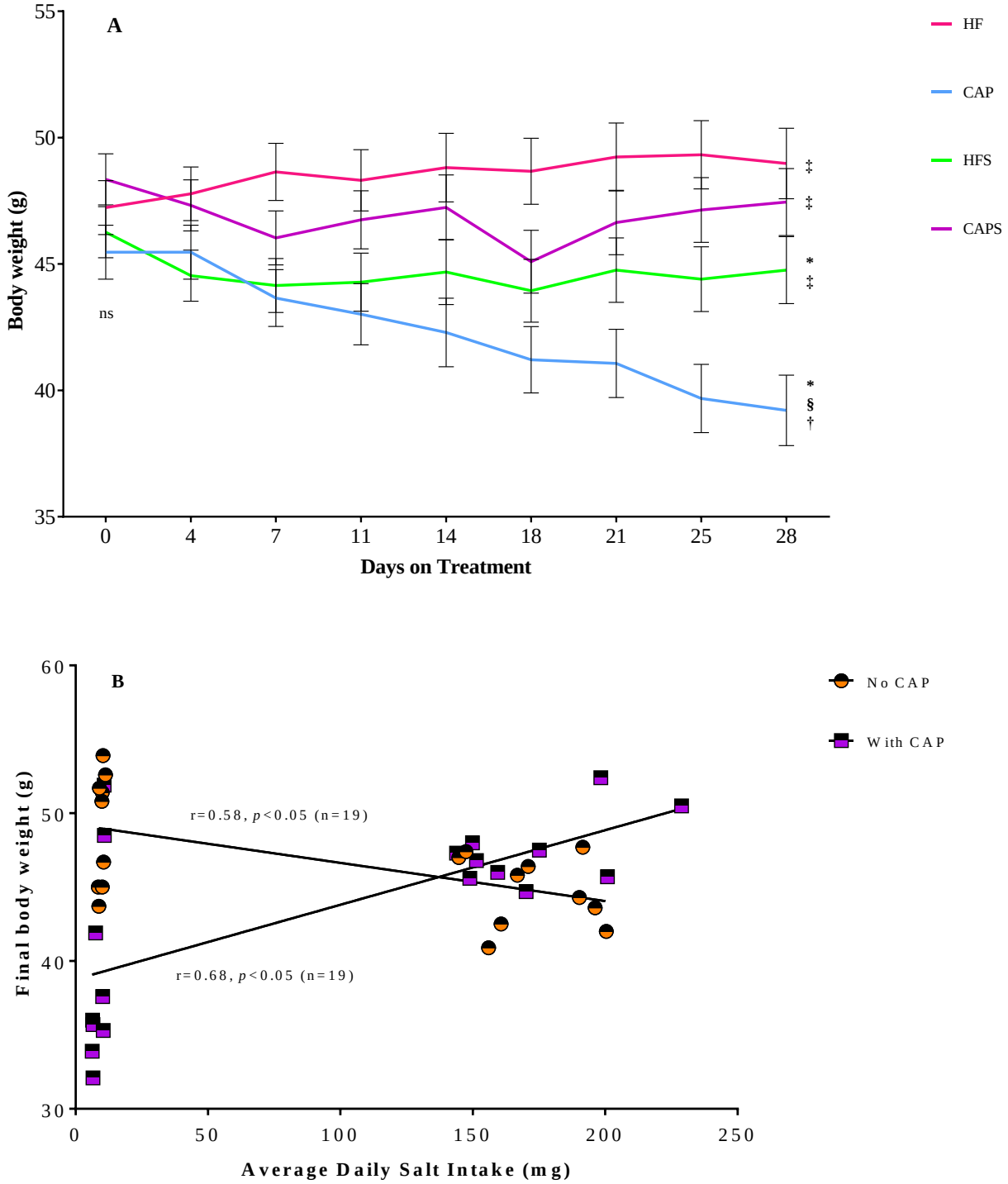

Figure 7.The effect of dietary salt and captopril on body weight. Data are represented as mean bodyweights ±SEM in grams (HF & CAP: n=9, HFS & CAPS: n=10). Statistical significances indicated by *p<0.05 CON compared to CAP, §p<0.05 CON compared to S, ‡p<0.05 CAP compared to S, †p<0.05 CAP compared to CAPS, ns p>0.05.

Organ mass

Absolute organ masses were recorded post-mortem and relative organ masses were determined per 100g final bodyweight. Note: C57BL6J mice receiving HFD developed enlarged livers that were pale (hepatic steatosis), and this change was not observed in the CAP group.

Figure 8 shows absolute epididymal fat mass, liver mass and relative liver mass decreased significantly in the HFS, CAP and CAPS treatment groups against the HF group ($p<0.05$). Relative epididymal fat mass did not differ between CAP and CAPS was well as CAPS and HFS treatment groups ($p>0.05$), and a significant reduction in relative epididymal fat mass was observed in CAP compared to the HF group ($p<0.05$). There was no significant change in absolute kidney masses in HFS mice compared to HF and CAPS group mice ($p>0.05$). A significant increase in relative kidney mass in HFS and CAP treatment groups was observed when compared to the HF group ($p<0.05$). Overall, the CAP treatment group significantly decreased absolute epididymal fat mass, liver mass, and increased absolute kidney mass in comparison to all groups ($p<0.05$).

As indicated in table 2, a significant main effect of captopril on epididymal fat mass ($F(3, 37)=8.61$, $p<0.05$), liver mass ($F(3, 37)=11.46$, $p<0.05$) and relative liver mass ($F(3, 37)=12.10$, $p<0.05$) was observed. There was a significant interaction effect between captopril and salt on visceral fat mass ($F(3, 37)=12.50$, $p<0.05$), liver mass ($F(3, 37)=18.77$, $p<0.05$), kidney mass ($F(1, 34)=4.55$, $p<0.05$), relative liver mass ($F(1, 34)=13.50$, $p<0.05$) and relative kidney mass ($F(3, 37)=4.17$, $p<0.05$). This suggests the effect of captopril on the aforementioned variables was dependent on the level of salt, such that mice in the CAP group carried less epididymal fat and reduced overall liver mass in comparison to CAPS. A strong positive correlation between final bodyweight with absolute epididymal fat mass ($r=0.687$, $p=0.000003$) and liver mass ($r=0.831$, $p=1.976\times10^{-10}$) is observed, and a strong positive correlation between absolute epididymal fat mass with liver mass ($r=0.588$, $p=0.000129$) is also observed.

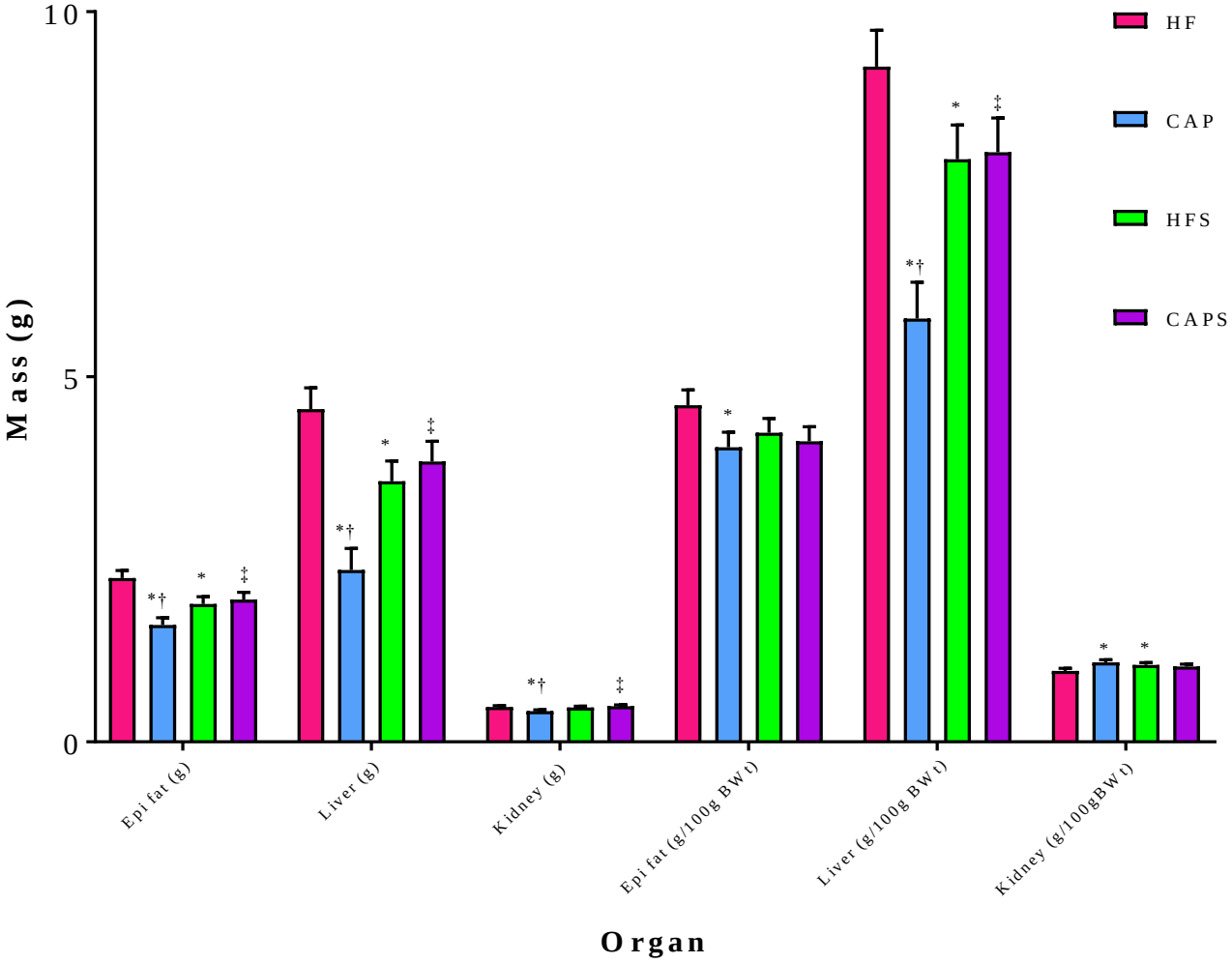

Figure 8. Absolute and relative organ weights. Statistical significances indicated by *p<0.05 compared to HF, §p<0.05 compared to HFS, ‡p<0.05 compared to CAP, †p<0.05 compared to CAPS.

Descriptive characteristics				*95% Confidence interval*		*Captopril*	*Salt*	*Captopril * Salt*
	Treatment Group	Mean	Standard Error (±)	Lower Bound	Upper Bound	*p*-value	*p*-value	*p*-value
Baseline bodyweight (g)	HF	47.23	1.069	45.06	49.41	0.88	0.37	0.073
	HFS	46.26	1.014	44.20	48.32			
	CAP	45.47 [a]†	1.069	43.29	47.64			
	CAPS	48.35 ‡	1.014	46.29	50.41			
Final bodyweight (g)	HF	48.98§‡	1.396	46.14	51.82	0.014	0.15	6.1E-5
	HFS	44.76*	1.325	42.07	47.45			
	CAP	39.21*†[a]	1.396	36.37	42.05			
	CAPS	47.45‡	1.325	44.76	50.14			
Bodyweight difference (g)	HF	1.74§‡	0.955	-0.20	3.69	3.5E-4	0.27	5.4E-5
	HFS	-1.50*	0.906	-3.34	0.34			
	CAP	-6.26*†	0.955	-8.20	-4.31			
(baseline – final)	CAPS	-0.90‡	0.906	-2.74	0.94			
Bodyweight difference (%)	HF	3.63§‡						
	HFS	-3.30*						
	CAP	-14.78 *†						
	CAPS	-1.88 ‡						
Visceral fat (g)	HF	2.24§‡	0.102	2.04	2.45	0.00596	0.98	0.0012
	HFS	1.89*	0.097	1.69	2.09			
	CAP	1.60*†	0.102	1.39	1.81			
	CAPS	1.95‡	0.097	1.75	2.15			
Liver (g)	HF	4.56§‡	0.292	3.96	5.15	0.00181	0.39	1.24E-4
	HFS	3.57*	0.277	3.01	4.13			
	CAP	2.36*†	0.292	1.76	2.95			
	CAPS	3.84 ‡	0.277	3.28	4.40			

Kidney (g)	HF	0.48‡	0.018	0.44	0.52	0.323	0.10	0.040
	HFS	0.47	0.017	0.44	0.51			
	CAP	0.42*†	0.018	0.39	0.46			
	CAPS	0.49‡	0.017	0.46	0.53			
Visceral fat (g/100g bodyweight)	HF	4.61‡	0.208	4.19	5.03	0.0974	0.47	0.26
	HFS	4.23	0.197	3.83	4.63			
	CAP	4.04*	0.208	3.61	4.46			
	CAPS	4.12	0.197	3.72	4.52			
Liver (g/100g bodyweight)	HF	9.25§	0.50	8.24	10.26	0.00140	0.306	8.16E-4
	HFS	7.98*	0.47	7.03	8.93			
	CAP	5.80*†	0.50	4.79	6.81			
	CAPS	8.07‡	0.47	7.12	9.03			
Kidney (g/100g bodyweight)	HF	0.97§‡	0.034	0.90	1.04	0.15	0.74	0.049
	HFS	1.05*	0.032	0.99	1.12			
	CAP	1.09*	0.034	1.02	1.16			
	CAPS	1.03	0.032	0.97	1.10			

Table 2 Baseline and post-mortem characteristics: body, visceral fat, liver and kidney masses; main and interaction effects. Results are expressed as mean ± SEM. Statistical significances indicated by *p<0.05 compared to HF; § p<0.05 compared to HFS; ‡ p<0.05 compared to CAP; † p<0.05 compared to CAPS; [a] p<0.05 final bodyweight compared to respective pre-treatment (baseline) weight.

Feed Intake

Analysis of average daily feed intake (g day^{-1}) data by a Kruskal-Wallis test showed non-significant differences between groups (H(3)=4.251, p>0.05). Feed intake relative to 100 g bodyweight was also non-significant (H(3)=0.526, p>0.05). Mean rank for each group is displayed in table 3.

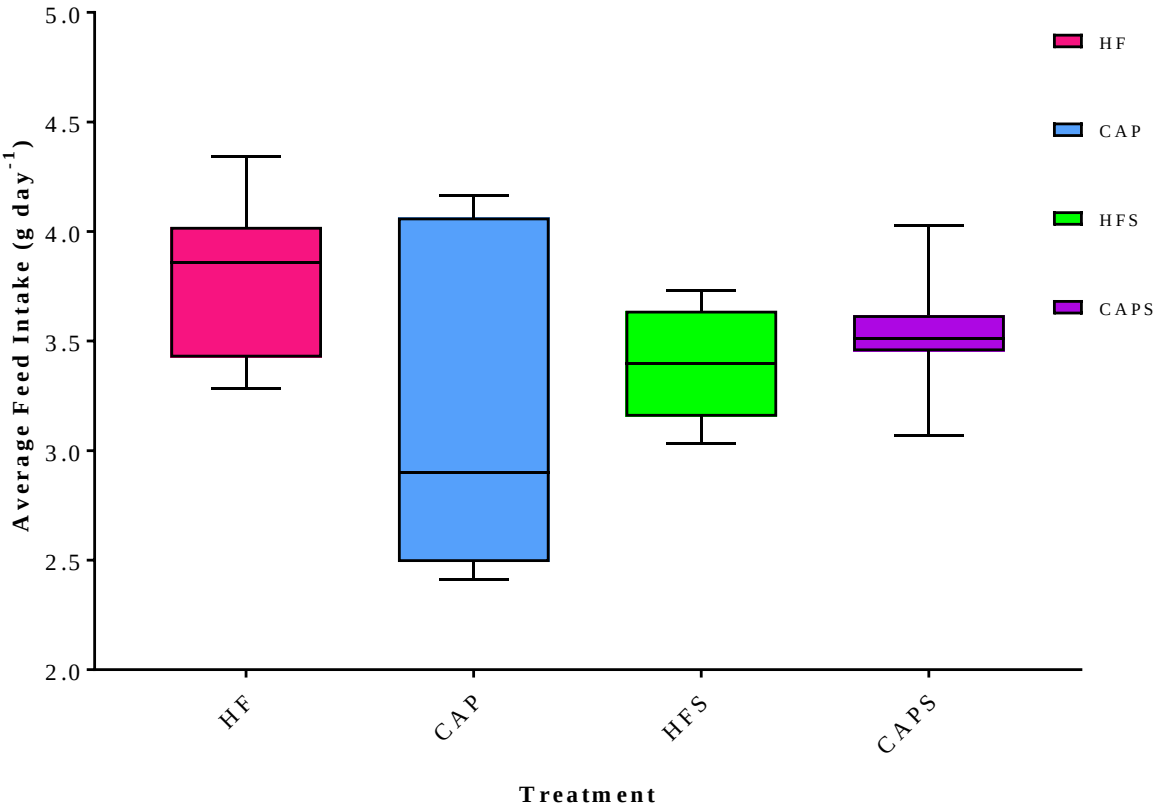

Figure 9. Effect of dietary salt and captopril on feed intake. Data are represented as individual value plots.

Average daily food intake	*Nonparametric Kruskal-Wallis test*					
	Treatment Group	Mean	Standard Dev. (±)	Energy (kcal)	Mean rank	n
Food intake (g day^{-1})	HF	3.79	0.35	17.55	25.78	9
	HFS	3.40	0.26	15.75	16.89	10
	CAP	3.23	0.80	14.96	28.56	9
	CAPS	3.54	0.25	16.41	19.50	10
	HF	7.785	0.60	36.10	21.22	9
	HFS	7.662	0.70	35.53	20.30	10

Food intake (g day^{-1}/100g bodyweight)	CAP	7.698	1.57	35.69	18.67	9
	CAPS	7.568	0.32	35.09	17.90	10

Table 3. Average daily food intake. Results are expressed as mean ± SD. A Kruskal-Wallis test by ranks was performed at an alpha level of 0.05.

Fluid Intake

Analysis of average daily fluid intake (ml day^{-1}) indicated a significant effect of captopril (F(3, 37)=21.764, p<0.05) and an interaction effect between captopril and salt (F(3,37)=4.24, p<0.05). There was a significant increase in fluid intake in the HFS and CAP treatment groups compared to the HF group (*p*<0.05). Fluid intake in the CAPS treatment group remained greater than its respective HFS control group (*p*<0.05).

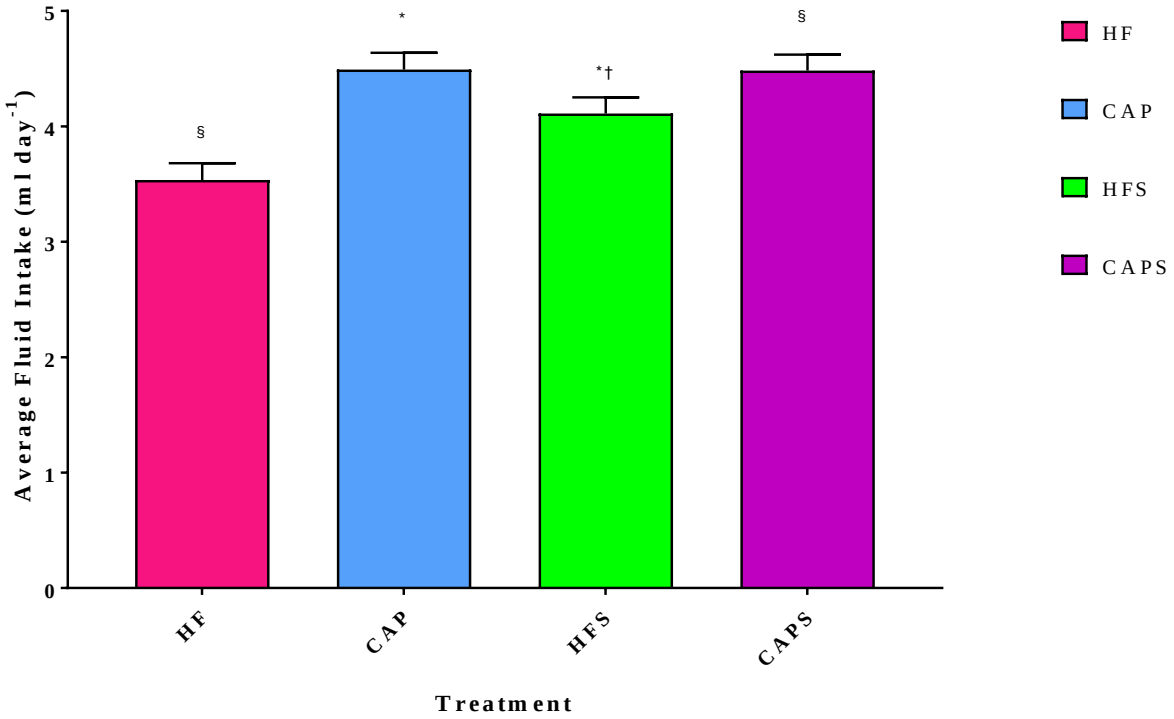

Figure 10. Effect of salt and captopril on average daily fluid intake. Data are represented as means ±SEM. *indicates individual treatment significantly different to CON, § to S, ‡ to CAP, and † to CAPS (p<0.05).

Average daily fluid intake				*95% Confidence interval*		*Captopril*	*Salt*	*Captopril * Salt*
	Treatment Group	Mean	Standard Error (±)	Lower Bound	Upper Bound	*p*-value	*p*-value	*p*-value
Fluid intake (ml day^{-1})	HF	3.54§	0.15	3.24	3.83	4.46E-5	0.054	0.047
	HFS	4.11*†	0.14	3.83	4.39			
	CAP	4.49*	0.15	4.20	4.79			
	CAPS	4.48§	0.14	4.20	4.76			

Table 4 Average daily fluid intake. Data are represented as means ±SEM. *indicates individual treatment significantly different to HF, § to HFS, ‡ to CAP, and † to CAPS (*p*<0.05).

Average daily Salt intake

Table 5 shows the average daily salt intake by each treatment group administered in drinking water taking in to consideration the average daily food intake. Significant differences in average daily salt intake were observed in salt administered groups, HFS and CAPS ($p<0.05$), whereas no differences were observed between salt un-administered groups, CON and CAP ($p>0.05$). Significant differences were observed between salt administered and un-administered treatment groups, HF and CAP versus HFS and CAPS respectively ($p<0.05$). There was no effect of captopril $F(3,37)=1.472$, $p>0.05$) or an interaction effect between captopril and salt ($F(3, 37)=3.134$, $p>0.05$) on the level of salt intake.

Average daily Captopril dosage

Table 5 shows the average daily dose of captopril administered in drinking water taking in to account the average daily fluid intake. Average daily captopril dose did not differ between CAP and CAPS treatment groups ($p>0.05$), and nor did salt intake effect average daily captopril dose. The daily dose of captopril (mg) per body weight (kg) equated to 4.64-5.97mg kg^{-1} and 4.10-4.47mg kg^{-1} per day for CAP and CAPS treatment groups respectively.

Daily averages				*95% Confidence interval*		*Captopril*	*Salt*	*Captopril * Salt*
	Treatment Group	Mean	Standard Error (±)	Lower Bound	Upper Bound	*p*-value	*p*-value	*p*-value
Salt intake (mg day^{-1})	HF	9.84§	2.68	4.40	15.28	0.23	-	0.086
	HFS	91.07*†	2.54	85.91	96.23			
	CAP	8.39†	2.68	2.95	13.83			
	CAPS	98.86§‡	2.54	93.70	104.02			
Captopril dosage (mg day^{-1})	HF	0.00	-	-	-	-	0.97	-
	HFS	0.00	-	-	-			
	CAP	0.23	0.0076	0.21	0.24			
	CAPS	0.22	0.0072	0.21	0.24			

Table 5 Average daily salt intake and captopril dose. Results are expressed as mean ± SEM. Statistical significances indicated by *p<0.05 compared to HF, §p<0.05 compared to HFS, ‡p<0.05 compared to CAP, †p<0.05 compared to CAPS, ns p>0.05.

CAP group mice fed a normal salt WD supplemented with 0.05 mg ml^{-1} of captopril in drinking water received between 4.939-5.728 mg kg^{-1} of captopril per day. Intake of 98.858 mg day^{-1} of salt combined with 4.636-4.724mg kg^{-1} captopril was not conducive to weight loss, as observed in

CAPS group mice. This level of salt intake was significantly higher than that of the HFS group mice displaying an average intake of 91.07mg day^{-1}.

A higher salt intake of 91.07mg day^{-1} curbed bodyweight gains in the HFS in comparison to HF group. No statistically relevant difference in the daily averages for feed intake was observed. The administration of salt and captopril increased fluid intake to where CAP and CAPS group averages were no different, and there appeared to be an additive influence of captopril on fluid intake in the CAPS group accounting for significant increase in dietary salt consumed against the HFS group.

Non-targeted metabolic profiling of plasma

Table 6 Discovery set: descriptive statistics of a two-way ANOVA assessing the interaction effect between captopril and dietary salt on semi-quantitative metabolite level

Metabolite				*95% Confidence interval*		*Captopril * Salt*
Sugars & sugar phosphates	Treatment Group	Mean	Standard Error (±)	Lower Bound	Upper Bound	*p*-value
Arabitol	HF	0.13	0.024	0.080	0.18	0.22
	HFS	0.10	0.024	0.053	0.15	
	CAP	0.10	0.024	0.047	0.14	
	CAPS	0.13	0.023	0.081	0.17	
Erythritol	HF	0.020‡	0.0039	0.0118	0.028	9.37E-4
	HFS	0.019	0.0039	0.0113	0.027	
	CAP	0.044*†	0.0039	0.0365	0.051	
log $transformed$	CAPS	0.020‡	0.0037	0.0123	0.027	
Fructose	HF	0.67‡	0.19	0.21	1.14	0.033
	HFS	0.86	0.19	0.39	1.32	
	CAP	1.51*†	0.19	1.30	2.18	
log $transformed$	CAPS	0.79‡	0.18	0.35	1.23	
6-phospho-gluconate	HF	0.0023	0.0011	6.9E-5	0.0046	0.087
	HFS	0.0014†	0.0011	-8.2E-4	0.0037	
	CAP	0.0038	0.0011	0.0015	0.0060	

log *transformed*	CAPS	0.0027§	0.0011	5.5E-4	0.0048	*FDR>0.20*
Glucose	HF	10.58	0.84	8.87	12.29	0.97
	HFS	10.66	0.84	8.95	12.37	
	CAP	10.48	0.84	8.77	12.19	
	CAPS	10.49	0.80	8.86	12.11	
Glucose-6-phosphate	HF	0.081	0.013	0.054	0.11	0.36
	HFS	0.073	0.013	0.046	0.10	
	CAP	0.080	0.013	0.053	0.11	
	CAPS	0.097	0.013	0.071	0.12	
Inositol	HF	0.082‡	0.018	0.0465	0.12	0.19
	HFS	0078	0.018	0.0427	0.11	
	CAP	0.20*†	0.018	0.169	0.24	
log *transformed*	CAPS	0.095‡	0.017	0.0608	0.13	
myo-Inositol-2-phosphate	HF	0.0067	0.0015	0.0036	0.0097	0.61
	HFS	0.0054	0.0015	0.0024	0.0085	
	CAP	0.0059	0.0015	0.0028	0.0090	
	CAPS	0.0062	0.0014	0.0033	0.0091	
Maltose/ Trehalose	HF	0.16	0.022	0.12	0.21	0.18
	HFS	0.18	0.022	0.13	0.22	
	CAP	0.13†	0.022	0.08	0.17	
	CAPS	0.20‡	0.021	0.16	0.25	
Ribitol	HF	0.011	0.0081	-0.0056	0.027	0.21
	HFS	0.010	0.0081	-0.0063	0.027	
	CAP	0.0065†	0.0081	-0.010	0.023	
	CAPS	0.024 ‡	0.0077	0.0079	0.039	*FDR>0.20*
Ribose	HF	0.032	0.0064	0.019	0.045	0.049
	HFS	0.026†	0.0064	0.013	0.039	
	CAP	0.024†	0.0064	0.011	0.037	

	CAPS	0.044§‡	0.0061	0.032	0.057	
Unknown sugar_2	HF	0.0026	0.00070	0.0011	0.0040	0.048
	HFS	0.0013†	0.00070	-0.00018	0.0027	
	CAP	0.0017†	0.00067	0.00031	0.0030	
log $\boldsymbol{transformed}$	CAPS	0.0032§‡	0.00067	0.0018	0.0046	
Sucrose	HF	0.044‡	0.068	-0.096	0.18	0.066
	HFS	0.054	0.068	-0.087	0.19	
	CAP	0.40*†	0.068	0.23	0.50	
log $\boldsymbol{transformed}$	CAPS	0.066‡	0.065	-0.066	0.20	

Organic acids				*95% Confidence interval*		*Captopril * Salt*
	Treatment Group	Mean	Standard Error (±)	Lower Bound	Upper Bound	*p*-value
2-keto-gluconate	HF	0.017‡	0.0037	0.0096	0.024	0.46
	HFS	0.018	0.0037	0.010	0.025	
	CAP	0.031*†	0.0035	0.024	0.038	
log $\boldsymbol{transformed}$	CAPS	0.018‡	0.0035	0.011	0.025	
Citrate	HF	0.064‡	0.0064	0.051	0.077	0.31
	HFS	0.051†	0.0064	0.038	0.064	
	CAP	0.097*†	0.0064	0.084	0.11	
	CAPS	0.071§‡	0.0061	0.059	0.084	
Erythronate	HF	0.16‡	0.024	0.11	0.21	0.17
	HFS	0.16	0.024	0.11	0.21	
	CAP	0.23*†	0.024	0.18	0.27	
log $\boldsymbol{transformed}$	CAPS	0.16‡	0.023	0.11	0.20	*FDR>0.20*
Fumarate	HF	0.077‡	0.014	0.048	0.11	0.045
	HFS	0.059	0.014	0.031	0.088	
	CAP	0.046*†	0.014	0.018	0.075	

	CAPS	0.086‡	0.0133	0.059	0.11	*FDR>0.20*
Gluconate	HF	0.022	0.0033	0.015	0.029	0.66
	HFS	0.016	0.0033	0.0094	0.023	
	CAP	0.022	0.0033	0.016	0.029	
	CAPS	0.019	0.0032	0.013	0.026	
Gluconate-1, 4-lactone	HF	0.013 ‡	0.0015	0.010	0.016	0.036
	HFS	0.010	0.0015	0.0073	0.014	
	CAP	0.0084*†	0.0015	0.0053	0.012	
	CAPS	0.012‡	0.0015	0.0094	0.015	*FDR>0.20*
Glutarate	HF	0.038§‡	0.00979	0.018	0.058	0.0036
	HFS	0.091*	0.00979	0.071	0.11	
	CAP	0.092*	0.00929	0.073	0.11	
log ***transformed***	CAPS	0.10	0.00929	0.085	0.12	
Glycerate	HF	0.10‡	0.020	0.061	0.14	0.094
	HFS	0.082	0.020	0.043	0.12	
	CAP	0.16*†	0.020	0.13	0.20	
log ***transformed***	CAPS	0.083‡	0.019	0.046	0.12	
Glycerate-3-phosphate	HF	0.011§	0.0017	0.0072	0.014	0.050
	HFS	0.0043*†	0.0017	0.00096	0.0077	
	CAP	0.0085	0.0016	0.0053	0.012	
	CAPS	0.0094§	0.0016	0.0062	0.013	
Glycolate	HF	0.031	0.0027	0.025	0.036	0.66
	HFS	0.028	0.0027	0.022	0.033	
	CAP	0.030	0.0027	0.025	0.036	
	CAPS	0.030	0.0025	0.025	0.035	
Lactate	HF	2.21	0.10	2.01	2.42	0.50
	HFS	2.17	0.10	1.96	2.38	
	CAP	2.10	0.10	1.89	2.30	

	CAPS	2.19	0.10	2.00	2.39	
Malate	HF	0.16§	0.023	0.11	0.21	0.38
	HFS	0.13*†	0.023	0.078	0.17	
	CAP	0.18	0.023	0.132	0.23	
	CAPS	0.19§	0.022	0.140	0.23	*FDR>0.20*
Oxalate	HF	0.0034‡	0.00046	0.0025	0.0044	0.72
	HFS	0.0027	0.00046	0.0018	0.0036	
	CAP	0.0045*†	0.00046	0.0035	0.0054	
	CAPS	0.0034‡	0.00044	0.0025	0.0043	*FDR>0.20*
Phosphate	HF	5.26§	0.52	4.20	6.33	0.40
	HFS	3.67*†	0.52	2.61	4.74	
	CAP	6.00†	0.52	4.94	7.07	
	CAPS	4.99§‡	0.50	3.98	6.00	*FDR>0.20*
Pyro-phosphate	HF	0.44	0.11	0.22	0.66	0.96
	HFS	0.27	0.11	0.047	0.49	
	CAP	0.53	0.11	0.30	0.75	
	CAPS	0.37	0.10	0.16	0.58	*FDR>0.20*
Pyruvate	HF	0.024	0.005	0.013	0.034	0.068
	HFS	0.020	0.005	0.0094	0.030	
	CAP	0.015†	0.005	0.0043	0.025	
	CAPS	0.030‡	0.005	0.020	0.040	
Ribonic acid	HF	0.025	0.0033	0.018	0.031	0.81
	HFS	0.029	0.0033	0.023	0.036	
	CAP	0.026	0.0033	0.020	0.033	
	CAPS	0.029	0.0031	0.023	0.036	
Succinate	HF	0.56‡	0.053	0.46	0.67	0.037
	HFS	0.54	0.053	0.43	0.65	
	CAP	0.42*†	0.053	0.31	0.53	

	CAPS	0.63‡	0.051	0.52	0.73	
Urea	HF	0.57	0.18	0.20	0.95	0.251
	HFS	0.67	0.18	0.29	1.04	
	CAP	0.93†	0.18	0.56	1.31	
log ***transformed***	CAPS	0.56‡	0.18	0.20	0.91	
Uric acid	HF	0.63‡	0.063	0.50	0.75	0.0259
	HFS	0.53†	0.063	0.40	0.65	
	CAP	0.49*†	0.063	0.36	0.62	
	CAPS	0.69§‡	0.060	0.56	0.81	

Amino acids (anaplerotic conversion product)				*95% interval*	*Confidence*	*Captopril * Salt*
	Treatment Group	Mean	Standard Error (±)	Lower Bound	Upper Bound	*p*-value
Alanine	HF	0.69	0.21	0.26	1.123	0.095
	HFS	0.66†	0.21	0.23	1.09	
(pyruvate)	CAP	0.43†	0.21	0.003	0.86	
	CAPS	1.12§‡	0.21	0.71	1.53	
Glutamate	HF	0.0062‡	0.00123	0.0037	0.0087	0.080
	HFS	0.0044	0.00123	0.0020	0.0069	
(α-ketoglutarate)	CAP	0.0037*†	0.00123	0.0013	0.0063	
	CAPS	0.0061‡	0.00117	0.0037	0.0085	
Glutamine	HF	0.33‡	0.078	0.17	0.49	0.0079
	HFS	0.29†	0.078	0.14	0.45	
(α-ketoglutarate)	CAP	0.12*†	0.078	-0.035	0.28	
	CAPS	0.53§‡	0.074	0.38	0.68	
Glycine	HF	0.30	0.089	0.12	0.48	0.033
	HFS	0.27†	0.089	0.088	0.45	
(pyruvate)	CAP	0.12*†	0.089	-0.059	0.30	

	CAPS	0.48§‡	0.084	0.31	0.65	
Isoleucine	HF	0.34	0.10	0.13	0.56	0.059
	HFS	0.35†	0.10	0.14	0.57	
(acetyl-CoA)	CAP	0.15†	0.10	-0.065	0.36	
	CAPS	0.56§‡	0.099	0.36	0.76	
Leucine	HF	0.31	0.099	0.11	0.51	0.076
	HFS	0.35†	0.099	0.15	0.55	
(acetyl-CoA)	CAP	0.18†	0.099	-0.023	0.38	
	CAPS	0.57§‡	0.094	0.38	0.76	
Methionine	HF	0.23	0.066	0.096	0.37	0.069
	HFS	0.18†	0.066	0.043	0.31	
(succinyl-CoA)	CAP	0.13†	0.066	-0.005	0.27	
	CAPS	0.32§‡	0.063	0.195	0.45	
Phenylalanine	HF	0.20	0.019	0.16	0.24	0.86
(fumarate/acetoacyl-CoA)	HFS	0.18	0.019	0.14	0.21	
	CAP	0.22	0.019	0.18	0.26	
	CAPS	0.19	0.018	0.15	0.23	
Proline	HF	0.042	0.012	0.018	0.065	0.76
	HFS	0.057	0.012	0.034	0.081	
(α-ketoglutarate)	CAP	0.039†	0.012	0.015	0.062	
	CAPS	0.061‡	0.011	0.039	0.084	
Serine	HF	0.15‡	0.035	0.083	0.22	0.41
	HFS	0.13	0.035	0.061	0.20	
(pyruvate)	CAP	0.25*†	0.035	0.18	0.32	
	CAPS	0.17‡	0.033	0.10	0.24	
Threonine	HF	0.076	0.024	0.028	0.13	0.93
	HFS	0.076	0.024	0.028	0.13	
	CAP	0.077	0.024	0.029	0.13	

(pyruvate, succinyl-CoA)	CAPS	0.073	0.023	0.026	0.12	
Tyrosine	HF	0.95	0.093	0.76	1.14	0.37
	HFS	0.92	0.093	0.73	1.11	
(fumarate/acetoacyl CoA)	CAP	0.92	0.093	0.73	1.11	
	CAPS	1.05	0.088	0.87	1.23	
Valine	HF	0.53	0.15	0.22	0.83	0.12
	HFS	0.57	0.15	0.26	0.87	
(Succinyl-CoA)	CAP	0.30†	0.15	-0.007	0.60	
	CAPS	0.81‡	0.14	0.53	1.10	
Fatty acids & sterols						
Glycerol	HF	0.40	0.023	0.36	0.45	0.16
	HFS	0.36	0.023	0.31	0.41	
	CAP	0.38	0.023	0.33	0.43	
	CAPS	0.40	0.021	0.36	0.44	
Glyerol-2-phosphate	HF	0.013	0.0027	0.0077	0.019	0.72
	HFS	0.018	0.0027	0.012	0.023	
	CAP	0.019	0.0027	0.014	0.025	
	CAPS	0.022	0.0026	0.016	0.027	
Glycerol-3-phosphate	HF	0.28	0.056	0.17	0.40	0.76
	HFS	0.36	0.056	0.25	0.48	
	CAP	0.35	0.056	0.23	0.46	
	CAPS	0.40	0.053	0.29	0.50	

Untargeted GC-MS was used in semi-quantitative identification of plasma metabolites post-treatment. Results of a 2-way ANOVA are expressed as means, ± SEM, 95% CI and interaction effect of captopril and salt (captopril*salt) on metabolite levels (AU). Statistical significances indicated by *p<0.05 compared to CON, §p<0.05 compared to S, ‡p<0.05 compared to CAP, †p<0.05 compared to CAPS.

Comparison across plasma samples of the total number of metabolites that were significantly altered between each treatment group shows differential responses to captopril and salt. In plasma, more metabolites were altered relative to the CAP group compared to respective HF and CAPS treatment groups. This means that the effect of captopril was more pronounced when administered in conjunction with a normal salt diet, and under these conditions ~29.45% of total metabolites detected in plasma were affected in contrast to its respective test groups. The number of biochemical differences were most pronounced between captopril administered groups.

Table 7. Validation set: discriminating metabolites after correcting for multiple testing (FDR)

Treatment group		*Erythritol*		*Fructose*		*Inositol*	
		p-values	*FDR*	*p-values*	*FDR*	*p-values*	*FDR*
HF	HFS	0.90	1.00	0.46	0.97	0.71	1.00
	CAP	5.0E-6*	2.97E-5◊	0.0022*	0.013◊	4.99E-6◊	2.99E-5◊
	CAPS	0.87	1.00	0.36	0.92	0.32	0.89
HFS	HF	0.90	1.00	0.46	0.97	0.71	1.00
	CAP	3.41E-6*	2.04E-5◊	0.016*	0.088◊	1.59E-6*	9.51E-6
	CAPS	0.77	1.00	0.87	1.00	0.18	0.67
CAP	HF	5.0E-6*	2.97E-5◊	0.0022*	0.013◊	4.99E-6*	2.99E-5◊
	HFS	3.41E-6*	2.04E-5◊	0.016*	0.088◊	1.59E-6*	9.51E-6◊
	CAPS	5.28E-6*	3.16E-5◊	0.020*	0.11◊	6.87E-5*	7.87E-4◊
CAPS	HF	0.87	1.00	0.36	0.92	0.32	0.89
	HFS	0.77	1.00	0.87	1.00	0.18	0.67
	CAP	5.28E-6*	3.16E-5◊	0.020*	0.11◊	6.87E-5*	7.87E-4◊
		Sucrose		***Ribose***		***Maltose/Trehalose***	
HF	HFS	0.98	1.00	0.58	0.99	0.57	0.99
	CAP	0.0040*	0.023◊	0.38	0.94	0.27	0.83
	CAPS	0.67	1.00	0.16	0.62	0.18	0.67
HFS	CON	0.98	1.00	0.58	0.99	0.57	0.99

	CAP	0.0043*	0.025◊	0.75	1.00	0.096	0.44
	CAPS	0.69	1.00	0.051	0.26	0.44	0.96
CAP	HF	0.0040*	0.023◊	0.38	0.94	0.27	0.83
	HFS	0.0043*	0.025◊	0.75	1.00	0.096	0.44
	CAPS	0.0098*	0.056◊	0.025*	0.13◊	0.016*	0.088◊
CAPS	CON	0.67	1.00	0.16	0.62	0.18	0.67
	S	0.69	1.00	0.051	0.26	0.44	0.96
	CAP	0.0098*	0.056	0.025*	0.13	0.016*	0.088
		Alanine		***iso-Leucine***		***Leucine***	
		p-value	*FDR*	*p-value*	*FDR*	*p-value*	*FDR*
HF	HFS	0.91	1.00	0.94	1.00	0.81	1.00
	CAP	0.39	0.94	0.20	0.71	0.34	0.91
	CAPS	0.15	0.61	0.14	0.56	0.069	0.33
HFS	HF	0.91	1.00	0.94	1.00	0.81	1.00
	CAP	0.45	0.97	0.17	0.66	0.24	0.79
	CAPS	0.13	0.53	0.16	0.62	0.11	0.49
CAP	HF	0.39	0.94	0.20	0.71	0.34	0.91
	HFS	0.45	0.67	0.17	0.66	0.24	0.79
	CAPS	0.025*	0.14◊	0.0069*	0.04◊	0.0071*	0.041◊
CAPS	HF	0.15	0.61	0.14	0.56	0.069	0.33
	HFS	0.13	0.53	0.16	0.62	0.11	0.49
	CAP	0.025*	0.14◊	0.0069*	0.04◊	0.0071*	0.041◊
		Glycine		***Glutamine***		***Homoserine***	
HF	HFS	0.82	1.00	0.77	1.00	0.73	1.00
	CAP	0.17	0.66	0.075	0.36	0.15	0.61
	CAPS	0.14	0.58	0.071	0.34	0.43	0.96
HFS	HF	0.82	1.00	0.77	1.00	0.73	1.00

	CAP	0.25	0.81	0.13	0.55	0.27	0.84
	CAPS	0.090	0.42	0.038*	0.20◊	0.28	0.82
CAP	HF	0.17	0.66	0.075	0.36	0.15	0.61
	HFS	0.25	0.81	0.13	0.55	0.27	0.84
	CAPS	0.0058*	0.034◊	6.76E-4*	0.004◊	0.028*	0.15◊
CAPS	HF	0.14	0.58	0.071	0.34	0.43	0.96
	HFS	0.090	0.42	0.038*	0.20◊	0.28	0.82
	CAP	0.0058*	0.034◊	6.76E-4*	0.004◊	0.028*	0.15◊
		Valine					
HF	HFS	0.85	1.00				
	CAP	0.29	0.86				
	CAPS	0.17	0.66				
HFS	HF	0.85	1.00				
	CAP	0.22	0.75				
	CAPS	0.36	0.79				
CAP	HF	0.29	0.86				
	HFS	0.22	0.75				
	CAPS	0.018*	0.098◊				
CAPS	HF	0.17	0.66				
	HFS	0.36	0.79				
	CAP	0.018*	0.098◊				
		2-ketogluconate		***Citrate***		***Erythronate***	
		p-value	*FDR*	*p-value*	*FDR*	*p-value*	*FDR*
HF	HFS	0.92	1.00	0.17	0.66	0.92	1.00
	CAP	0.012*	0.066◊	8.33E-4*	0.0049◊	0.055	0.28
	CAPS	0.82	1.00	0.39	0.94	0.95	1.00
HFS	HF	0.92	1.00	0.17	0.66	0.92	1.00

	CAP	0.015	0.085	1.52E-5	9.07E-5	0.068	0.33
	CAPS	0.90	1.00	0.028*	0.15◊	0.87	1.00
CAP	HF	0.012*	0.066◊	8.33E-4*	0.0049◊	0.055	0.28
	HFS	0.015	0.085	1.52E-5	9.07E-5	0.068	0.33
	CAPS	0.017*	0.097◊	0.0067*	0.039◊	0.043*	0.22
CAPS	HF	0.82	1.00	0.39	0.94	0.95	1.00
	HFS	0.90	1.00	0.028*	0.15◊	0.87	1.00
	CAP	0.017*	0.097◊	0.0067*	0.039◊	0.043*	0.22
		Fumarate		***Glycerate***		***Pyruvate***	
HF	HFS	0.39	0.94	0.19	0.69	0.60	1.00
	CAP	0.13	0.56	0.016*	0.090◊	0.23	0.77
	CAPS	0.62	1.00	0.21	0.73	0.38	0.93
HFS	HF	0.39	0.94	0.19	0.69	0.60	1.00
	CAP	0.51	0.98	4.13E-4*	0.0025◊	0.49	0.98
	CAPS	0.17	0.66	0.93	1.00	0.16	0.63
CAP	HF	0.13	0.56	0.016*	0.090◊	0.23	0.77
	HFS	0.51	0.98	4.13E-4*	0.0025◊	0.49	0.98
	CAPS	0.045*	0.23	4.01E-4*	0.0024◊	0.038*	0.20◊
CAPS	HF	0.62	1.00	0.21	0.73	0.38	0.93
	HFS	0.17	0.66	0.93	1.00	0.16	0.63
	CAP	0.045*	0.23	4.01E-4*	0.0024◊	0.038*	0.20◊
		Succinate		***Urea***		***Uric acid***	
HF	HFS	0.78	1.00	0.44	0.97	0.27	0.84
	CAP	0.061	0.30	0.047*	0.24	0.15	0.61
	CAPS	0.41	0.95	0.86	1.00	0.50	0.98
HFS	HF	0.78	1.00	0.44	0.97	0.27	0.84
	CAP	0.11	0.48	0.21	0.73	0.73	1.00

	CAPS	0.27	0.83	0.34	0.91	0.076	0.36
CAP	HF	0.061	0.30	0.047*	0.24	0.15	0.61
	HFS	0.11	0.48	0.21	0.73	0.73	1.00
	CAPS	0.0079*	0.045◊	0.028*	0.15◊	0.035*	0.19◊
CAPS	HF	0.41	0.95	0.86	1.00	0.50	0.98
	HFS	0.27	0.83	0.34	0.91	0.076	0.36
	CAP	0.0079*	0.045◊	0.028*	0.15◊	0.035*	0.19◊

Nominal *p*-values (LSD) and FDR-values (BH) are compared by using MANOVA: Statistical significance is indicated by *$p<0.05$ to respective group and ◊FDR<0.20 to respective group.

Table 8 Metabolite relationship with bodyweight, epididymal adipose and liver masses.

	Final bodyweight	Epididymal fat mass	Liver mass
Final bodyweight		0.687**	0.831**
		0.588**	
Sugars & sugar phosphates			
Erythritol	-0.748**	-0.662**	-0.664**
Fructose	-0.408*	-0.313	-0.391*
Sucrose	-0.619**	-0.633**	-0.559**
Inositol	-0.754**	-0.604**	-0.585**
6-phosphogluconate	0.368*	0.361*	0.253
Organic acids			
Erythronate	-0.532**	-0.471**	-0.242
Glycerate	-0.468**	-0.399*	-0.221
Citrate	-0.537**	-0.506**	-0.520**
Oxalate	-0.338*	-0.228	-0.225
Pyruvate	0.383*	0.131	0.048
2-ketogluconate	-0.622**	-0.505**	-0.432**
Glutarate	-0.438**	-0.474**	-0.443**
Amino acids & Amines			
Butyric acid, 2-amino	0.325*	0.081	0.345*
Glutamine	0.390*	0.213	0.228
Glycine	0.403*	0.182	0.307

Isoleucine	0.444**	0.189	0.316
Leucine	0.422**	0.132	0.312
Methionine	0.355*	0.147	0.124
Putrescine	0.387*	0.205	0.304
Serine	-0.321	-0.357*	-0.401*
Valine	0.428**	0.177	0.358*
Alanine	0.418*	0.187	0.318
Uracil	0.360*	0.116	0.110

Pearson's correlation coefficients, *r*, of plasma metabolites as predictive biomarkers associated with final body weight and absolute epididymal fat and liver masses. *$p<0.05$, **$p<0.01$.

Metabolite markers associated with bodyweight and fat mass were calculated by Pearson's pairwise correlation coefficients.

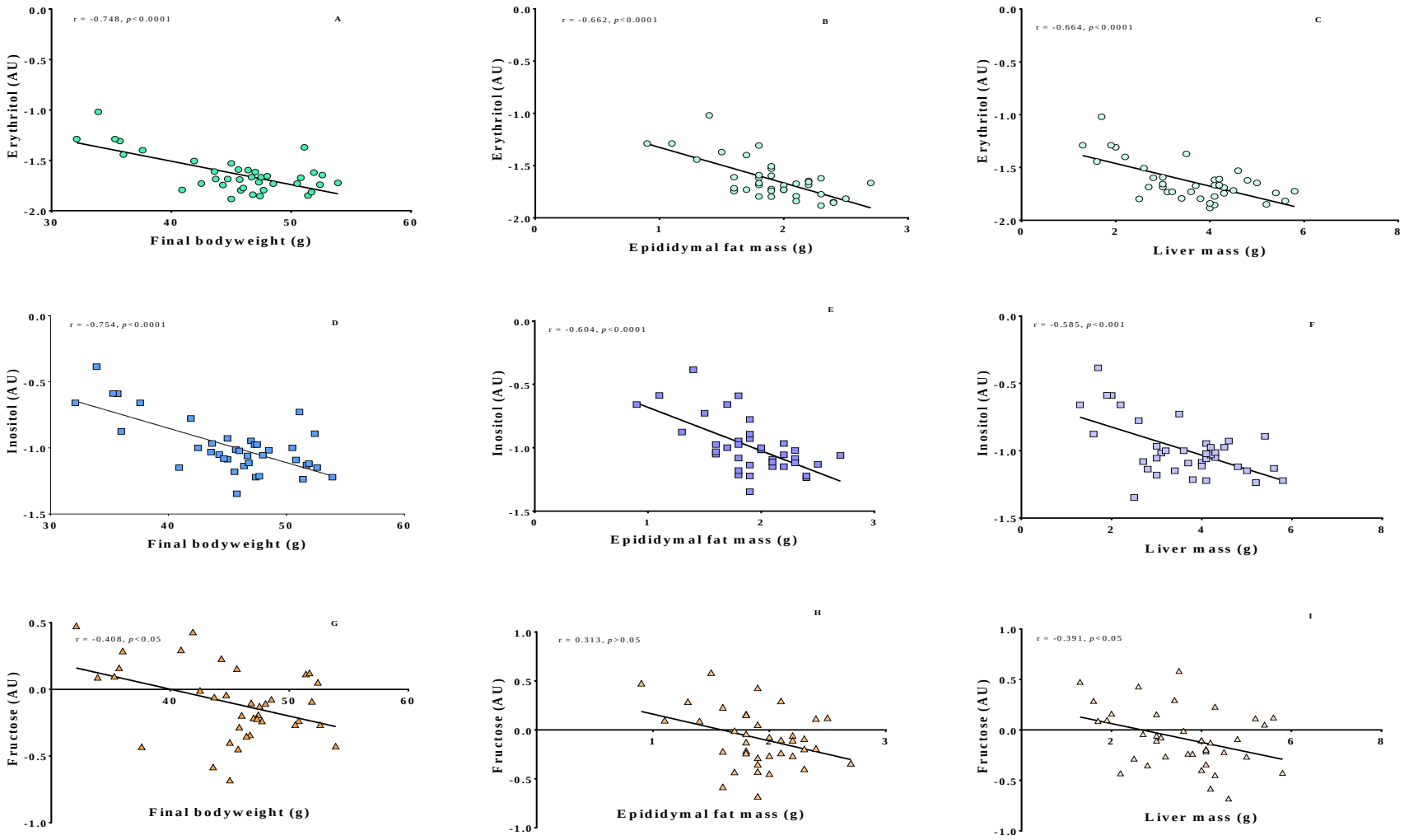

Figure 11. Correlation scatter plots modelling the relationship between plasma metabolite levels (AU) against biometric parameters of C57BL/6J mice with linear fit superimposed. Corresponding r- and *p*-value: (**A**) -0.748, *p*<0.0001; (**B**) -0.662, *p*<0.0001; (**C**) -0.664, *p*<0.0001; (**D**) -0.754, *p*<0.0001; (**E**) -0.604, *p*<0.0001; (**F**) -0.585, *p*<0.001; (**G**) -0.408, *p*<0.05; (**H**) -0.313, *p*>0.05; (**I**) -0.391, *p*<0.05.

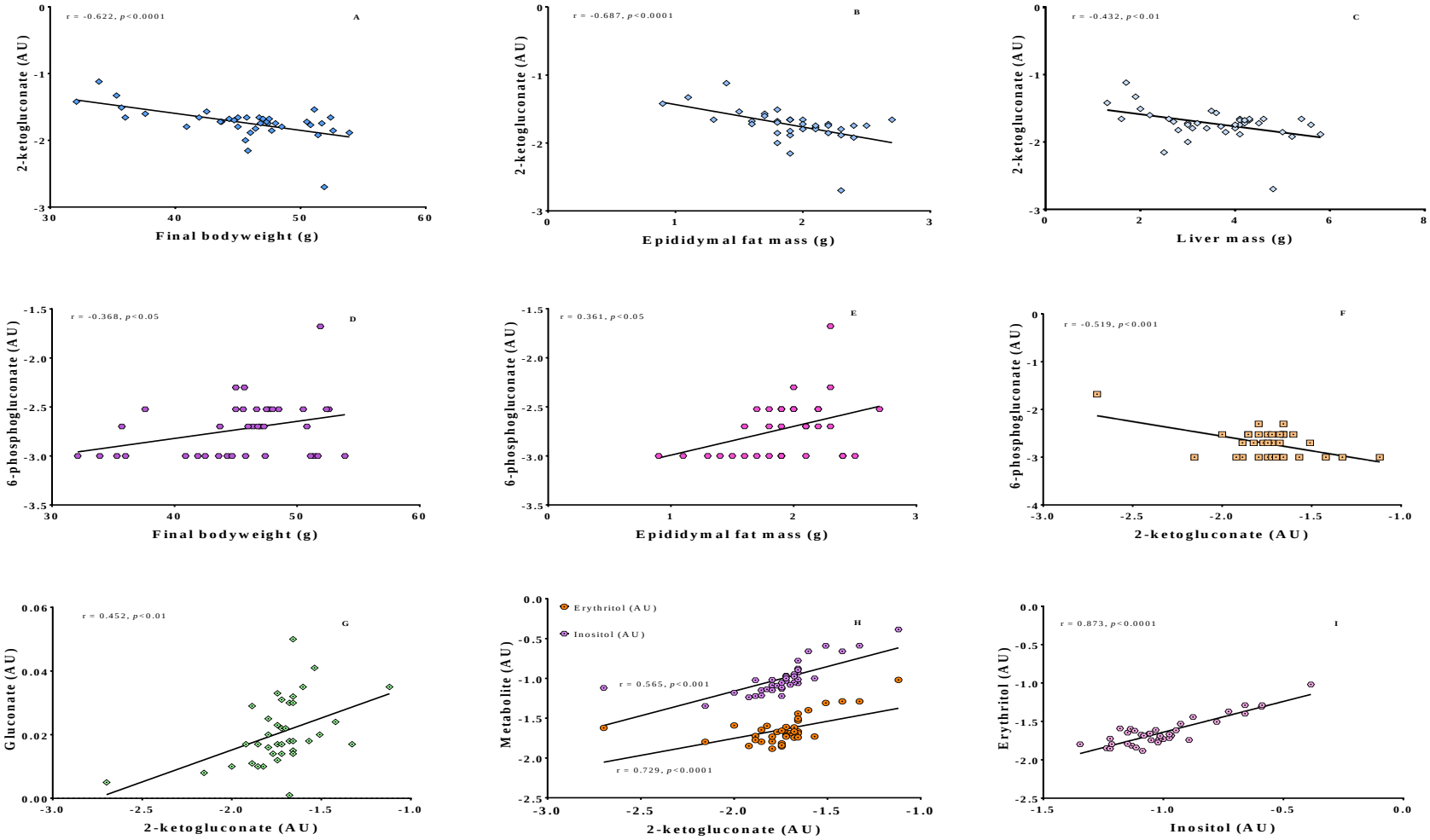

Figure 12. Correlation scatter plots modelling the relationship between plasma metabolite levels against (A-E) biometric parameters of C57BL/6J mice and (F-G) other metabolites identified in parallel pathways with linear fit superimposed. Corresponding r- and *p*-values: (**A**) -0.622, *p*<0.0001; (**B**) -0.687, *p*<0.0001; (**C**) -0.432, *p*<0.001; (**D**) -0.368, *p*<0.05; (**E**) 0.361, *p*<0.05; (**F**) 0.519, *p*<0.001; (**G**) 0.452, *p*<0.01; (**H**) Θ 0.729, *p*<0.0001, Θ 0.565, *p*<0.001; (**I**) 0.873, *p*<0.0001.

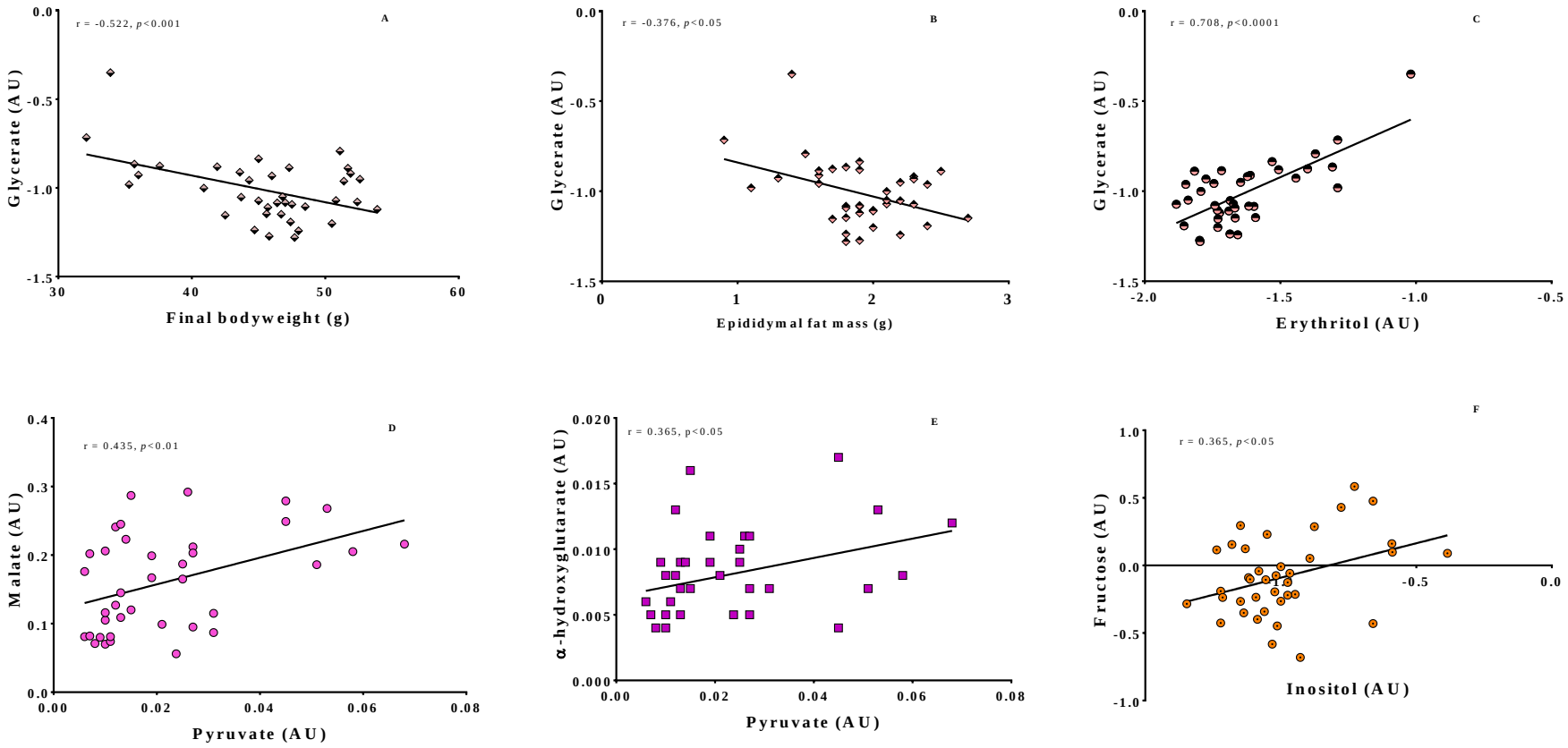

Figure 13. Correlation scatter plots modelling the relationship between plasma metabolite levels against (A-B) biometric parameters of C57BL/6J mice and (C-F) other metabolites identified in parallel pathways with linear fit superimposed. Corresponding r- and *p*-values: (**A**) -0.522, $p<0.001$; (**B**) -0.376, $p<0.05$; (**C**) 0.708, $p<0.0001$; (**D**) 0.435, $p<0.01$; (**E**) 0.365, $p<0.05$, (**F**) 0.365, $p<0.05$.

Discussion

The aim of this study was to investigate the effects of captopril on the plasma metabolite profiles of DIO C57BL/6J mice maintained on an obesogenic WD that was either considered to be 'normal' or 'high' in salt content (Martinez Steele et al., 2016; McMillan Price & Egger, 2017).

The effect of captopril and salt on bodyweight, organ mass, feed and water consumption

Prior to this study, the experimental outcomes of captopril and salt on bodyweight and body fat regulation has been reported concurrently with effects on food and water consumption in C57BL/6J mice (Premaratna et al., 2011; Radcliffe, 2013; Weisinger et al., 2009).

Previously, we showed doses of 3.69–6.78 mg kg^{-1} of captopril following a diet containing 6.10–86.0 mg day^{-1} of dietary salt to be conducive to captopril's weight loss effects in C57BL/6J mice (Premaratna et al., 2011; Radcliffe, 2013). Consistent with this, mice obtaining doses of 4.94–5.73 mg kg^{-1} day^{-1} of captopril combined with a daily intake of 8.39 mg salt were significantly lighter than their pre-treatment weights (-14.78%), whereas mice obtaining doses of 4.10-4.47mg kg^{-1} of captopril combined with 98.86 mg of salt per day were non-significantly different to their pre-treatment bodyweights (table 2). Moreover captopril treatment reduced the contribution of lipid accumulating tissues to overall bodyweight following a normal salt diet (table 2, figure 8), which too remains consistent with previously published data (Premaratna et al., 2011; Weisinger et al., 2009).

It is accepted that one of the major effects of captopril is an increase in the systemic levels of adiponectin (Premaratna et al., 2011; Radcliffe, 2013; Stanley, 2013; Tabbi-Anneni et al., 2008; Weisinger et al., 2009). It is suggested that the effects of adiponectin on energy homeostasis is, at least in part, mediated via peripheral activation of the LKB1–AMPK axis which may increase FA oxidation. This is thought to be a central mechanism whereby captopril elicits its protective effects against the development and progression of obesity and its symptoms (Masaki et al., 2003; Premaratna et al., 2011; Qi et al., 2004; Weisinger et al., 2009). The aforementioned mechanism of adiponectin will be a theme in various parts of this chapter.

The lack of reported weight loss in humans due to captopril may be explained by high dietary levels of salt (Radcliffe, 2013). To further understand the mechanism/s of interaction between captopril and salt, we characterised the plasma metabolomes of mice and discovered that metabolites belonging to various carbon (carbohydrate) metabolising pathways were most altered between treatment groups. These findings may help further elucidate the weight loss mechanism of action of captopril and the interaction mechanism with dietary salt.

We also showed that a high-salt diet may curtail excessive bodyweight and fat gain to that of HFD controls, albeit bodyweight change within groups did not differ from baseline. Similar effects have been described by Weidemann et al. (2015) and will discussed in latter parts of this thesis.

The effect of captopril and salt on the plasma metabolomes of C57BL6/J mice

Metabolites of carbohydrate origin were most strikingly altered by captopril and salt. Pathways that metabolise carbohydrates includes glycolysis, fructolysis, glycogenolysis, and the PP, inositol and gluconate pathways. As detected in plasma, distinct changes in carbohydrate profiles was apparent in mice treated with captopril in the presence or absence of a high-salt diet. At the end of the treatment period glycolytic and fructolytic pathways were identified by alterations in the levels of sucrose, maltose, fructose, uric acid (UA) and pyruvate. Alterations in 1, 4-gluconolactone (1, 4Gnl), ribose, ribitol, erythritol and erythronate indicated the PPP. Alterations in the levels of inositol and 2-ketogluconate indicated inositol and gluconate metabolising pathways, and the TCA cycle was identified with alterations in plasma levels of citrate, α-hydroxyglutarate, fumarate, succinate and glutamate.

Dietary disaccharides: Sucrose & Maltose

In the current study both sucrose and maltose were obtained from the implemented diet (see appendix for feed composition, SF00-219 Western style diet).

Metabolomics studies have identified urinary sucrose as a biomarker in positive association with BMI, WC, risk of weight gain and obesity (Campbell et al., 2017; Kuhnle et al., 2015). In the current study, metabolite analysis of plasma showed a marked elevation in circulating sucrose in captopril treated mice following a normal-salt diet. These effects were negated to that of untreated controls when captopril was administered in conjunction with a high-salt diet. High circulating levels of sucrose correlated negatively with increasing bodyweight, epididymal fat and liver masses (table 8), and this may indicate that the interaction between captopril and salt diet involves sucrose hydrolysis. Whilst our results may appear to be inconsistent with that of Campbell et al. (2017) and Kuhnle et al. (2015), disparities may be explained by differences in experimental aims, where we sought to determine the association of sucrose with subsequent weight loss and Campbell et al. (2017) and Kuhnle et al. (2015) sought to define associations with indicators of bodyweight gain and obesity. In support of the current finding, we identified two dietary intervention studies using metabolomics to assess the association of plasma sucrose with subsequent weight loss, however we could not identify a study investigating the effect of a high-salt intake on plasma levels of sucrose. In line with our finding, Khakimov et al. (2016) identified a positive association between fasting plasma sucrose and bodyweight loss that was endured by centrally obese individuals. Similarly, following a 12-week medium-fat diet, DIO rats that lost weight exhibited increased urinary excretion of sucrose compared to DIO rats maintained on a HFD (Chen et al., 2018). These studies however have been unable to elucidate the mechanisms underlying such association between weight gain and sucrose bioavailability (Chen et al., 2018; Khakimov et al., 2016). We propose captopril's actions may extend in to the gastrointestinal tract before its absorption in to the circulation, potentially interfering with the action of a α-glycosidases or -amylases to impede sucrose and starch hydrolysis respectively (Hamdan, Afifi, & Taha, 2004). Further studies are needed to determine the

influence of captopril and salt on nutrient absorption as well as their effects on gastrointestinal enzymes such as α–glycosidases and –amylases as well as sucrase and other enzymes alike.

Analysis of human blood derived from T2D patients showed higher circulating maltose to that of non-diabetic controls, and this was reversed following rosiglitazone treatment (Bao et al., 2009). Moreover, hepatic maltose concentrations were shown to be higher in DIO mice concurrent with systemic IR and hepatic steatosis, thus maltose is regarded a marker of impaired glucose tolerance in hepatic and extra-hepatic tissues (Holvoet et al., 2015; Kim et al., 2011; H. M. Park et al., 2017; Qiu & Zhang, 2019). In this study, captopril treatment reduced plasma maltose levels following a normal salt diet while the reverse was true in the presence of a high-salt diet. Hepatic TG accumulation caused by obesity accompanies an increase in liver mass, and weight loss is shown to reduce hepatic TGs and liver mass (Liu et al., 2013; Otten et al., 2018). There is also evidence showing that a high-salt diet promotes both IR and hepatic TG accretion, the onset and severity of which may be exacerbated when combined with an obesogenic WD (Lanaspa et al., 2018; Ogihara et al., 2001). In addition to improving glucose tolerance and insulin sensitivity, we and others have reported an overall increase in hepatic FA oxidation and a subsequent reduction in liver TG content and mass in DIO animals treated with captopril (Bitkin et al., 2013; Premaratna et al., 2011; Tabbi-Anneni et al., 2008). Therefore, as indicated by a reduction in plasma maltose levels, our observations may further support a role for captopril in whole-animal glucose tolerance and hepatic FA oxidation, and a role for salt in deregulating and diminishing these properties of captopril.

Glycolysis

Metabolic studies conducted in obese subjects has uncovered alterations to metabolites associated with pathways involving the action of insulin, including glycolysis (Park, Sadanala, & Kim, 2015). Several of these alterations included positive association between circulating levels of glucose, G6P, pyruvate, lactate and other glycolytic intermediates with BMI, weight gain and obesity (Zhao et al., 2016). As reviewed earlier intermediates of glycolysis may facilitate DNL. During glycolysis, glucose is catabolised to pyruvate which under aerobic conditions is converted to acetyl-coenzyme A (acetyl-CoA), the entry point in to either the TCA cycle or the DNL pathway, whereas under anaerobic conditions pyruvate can reduce to lactate (Butterworth, 2005b). Here we show captopril treatment following a normal salt intake to cause a reduction in the metabolite end-product of glycolysis, pyruvate, without altering lactate, glucose, G6P or glycerate-3-phosphate. These findings may indicate a reduction in glucose metabolism through lower glycolysis, *i.e.* metabolites downstream of enzyme GAPDH, a response akin to that reported by Jauch et al. (1987) who showed reduced muscular release of pyruvate and lactate in to the circulation following captopril treatment of diabetic patients. Moreover reductions in circulating pyruvate caused by captopril is in line with the weight loss effects, given pyruvate is an important intermediary in the conversion of carbohydrates to acetyl-CoA and FAs (Butterworth, 2005b). In contrast, a high-salt diet appears to preserve lower glycolysis (metabolites upstream of enzyme GAPDH) by countering captopril's

repression of plasma pyruvate, and such effect has also been observed in the renal and cardiac tissues of Dahl rats fed a high-salt diet versus low-salt fed controls (Fillmore et al., 2018; Wang, Liu, Zhang, & Wang, 2018). This may indicate another point of interaction between captopril and salt, whereby high-salt feeding counters weight loss induced by captopril via increasing energy metabolism through glycolysis, yielding pyruvate for entry in to TCA or DNL pathways (Butterworth, 2005b; Karl et al., 2017). Taken together, metabolic repression of glycolysis by captopril may be important for causing bodyweight and fat loss. Refer to figure 14 for glycolytic alterations caused by captopril following a normal salt intake versus a high salt intake.

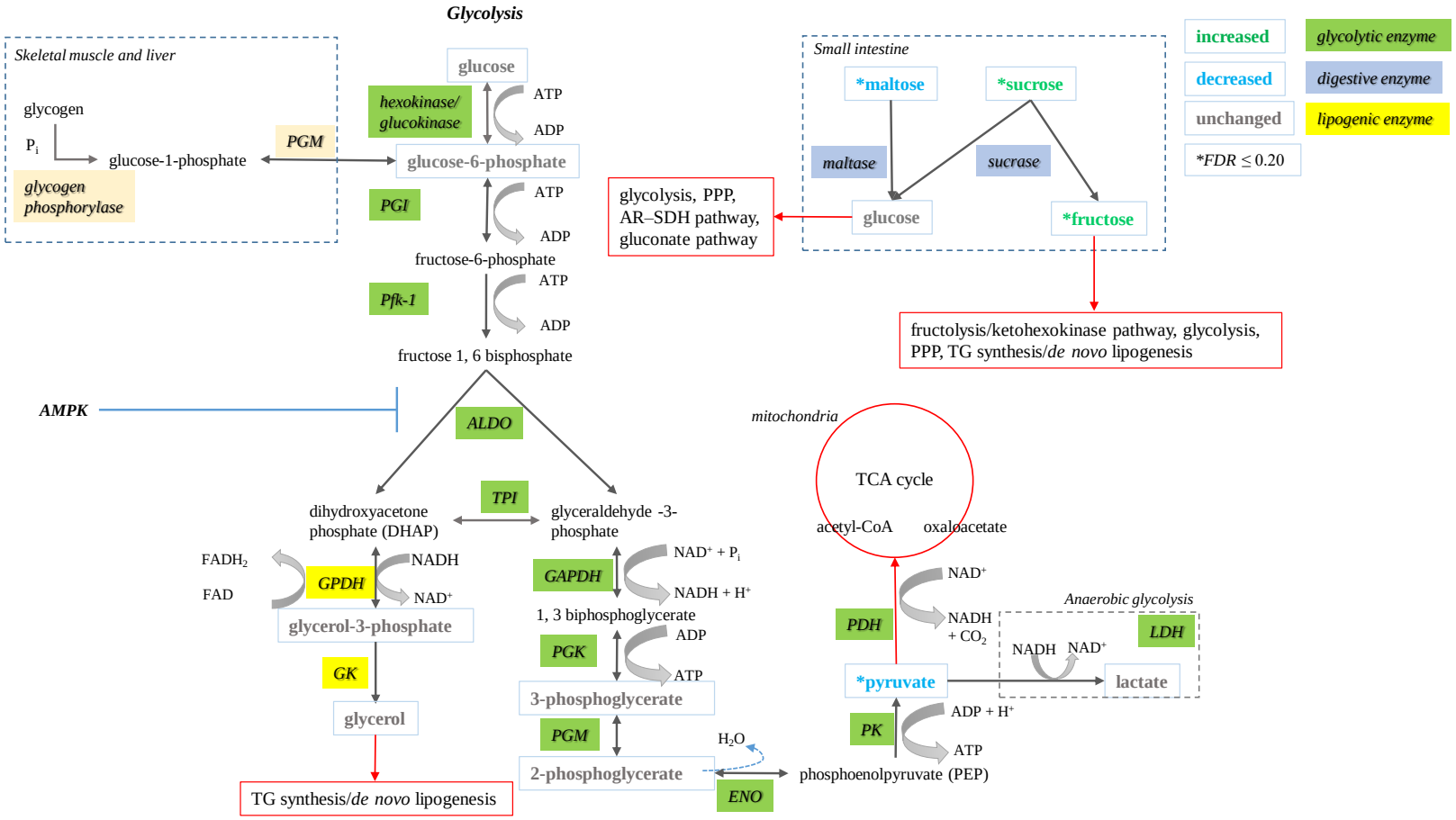

Figure 14. Glycolytic alterations detected in the plasma of C57BL6/J mice treated with captopril in response to a normal salt diet versus a high-salt diet. Intermediates and metabolites in **green** increased, **blue** decreased, **grey** remained stable, and black were unmeasured. **Red** lines describe pathways in which metabolites may participate. Enzymes include: phosphoglucose isomerase (PGI), phosphofructokinase (PFK-1), aldolase isoform A/C (ALDO), triose phosphate isomerase (TPI), glyceraldehyde phosphate dehydrogenase (GAPDH), phosphoglycerate kinase (PGK), phosphoglycerate mutase (PGM), enolase (ENO), pyruvate kinase (PK), pyruvate dehydrogenase (PDH), lactate dehydrogenase (LDH), glyceraldehyde phosphate dehydrogenase (GPDH), glycerol kinase (GK).

Tricarboxylic acid (TCA) cycle

In addition to a heightened rate of glycolysis, obesity is characterised by increased TCA cycle turnover due to increased energy demands. These increases may also induce anaploretic formation of glutamate from α-ketoglutarate, which was recently shown to interfere with adiponectin secretion and insulin sensitivity (Nagao et al., 2017). Metabolite studies have associated obesity with increased blood levels of succinate, fumarate, malate and acetate whereas reductions in lactate, citrate and α-ketoglutarate is only observed among IR humans and rodents (Baker et al., 2015; Cupisti et al., 2007; Gooda Sahib Jambocus et al., 2016). Dahl salt-sensitive rats also exhibit heightened TCA turnover due to increased glycolytic activity which could be exacerbated when exposed to a high-salt diet (Wang et al., 2014; Wang, Liu, et al., 2018).

The oxidation of FAs leads to the generation of NADH and H^+ which interferes with the action of TCA enzymes that are dependent on NAD^+ and $NADP^+$, such as IDH, ODGH and MDH (figure 15). This ultimately inhibits NADH/NADPH and ATP generation via OXPHOS (Butterworth, 2005b). Moreover, accumulated citrate that is generated from acetyl-CoA, and glycerate generated from FA oxidation, can negatively regulate glycolysis via repression of *Pfk*, which also has the capacity to negate glucose carbon metabolism through the TCA cycle (Nagao et al., 2017; Shearer et al., 2008). In contrast to a high-salt diet, captopril treatment of mice following a normal salt diet lead to an increase in plasma citrate and glycerate following a decrease in TCA metabolites including succinate, α-hydroxyglutarate, glutamate, glutamine and fumarate. This could indicate that a reduction in body fat may have occurred due to (1) an increase in FA-oxidation that may in turn negate TCA turnover (Karl et al., 2017), or (2) a reduction in glycolytic input. Although we did not identify differences in circulating levels of malate between groups, pyruvate levels correlated with malate and α-hydroxyglutarate levels to support the hypothesis that repression of glycolytic activity by captopril may hamper the TCA cycle (Janzer et al., 2014; Shearer et al., 2008).

Moreover, glutamine flux may also fuel the TCA cycle on anaploretic conversion to α-ketoglutarate from glutamate (Butterworth, 2005b; Nagao et al., 2017). Given we observed a significant reduction in glutamine and glutamate, captopril treatment may decrease TCA input by inhibiting precursors generated by nitrogen metabolism, as well as glucose metabolism (pyruvate), leading to a reduction in TCA cycle derived ATP and anabolic precursors that are necessary for DNL and adipogenesis. Therefore a high-salt diet may counter these effects by enhancing glucose-derived carbon input through the TCA cycle, supplying substrates, NADPH (from IDH, ODGH and MDH) and other factors that facilitates DNL (Wang et al., 2014). Taken together, metabolic reduction of the TCA cycle by captopril may be important for bodyweight and body fat reduction. This may indicate that the interaction between captopril and a high-salt diet may involve TCA cycle regulation and metabolite turnover (possibly due to differences in FA oxidation which as mentioned, can repress the cycle by generating NADH and H^+). Refer to figure 15 for TCA cycle alterations caused by captopril when dietary salt intake is normal versus when dietary salt is high.

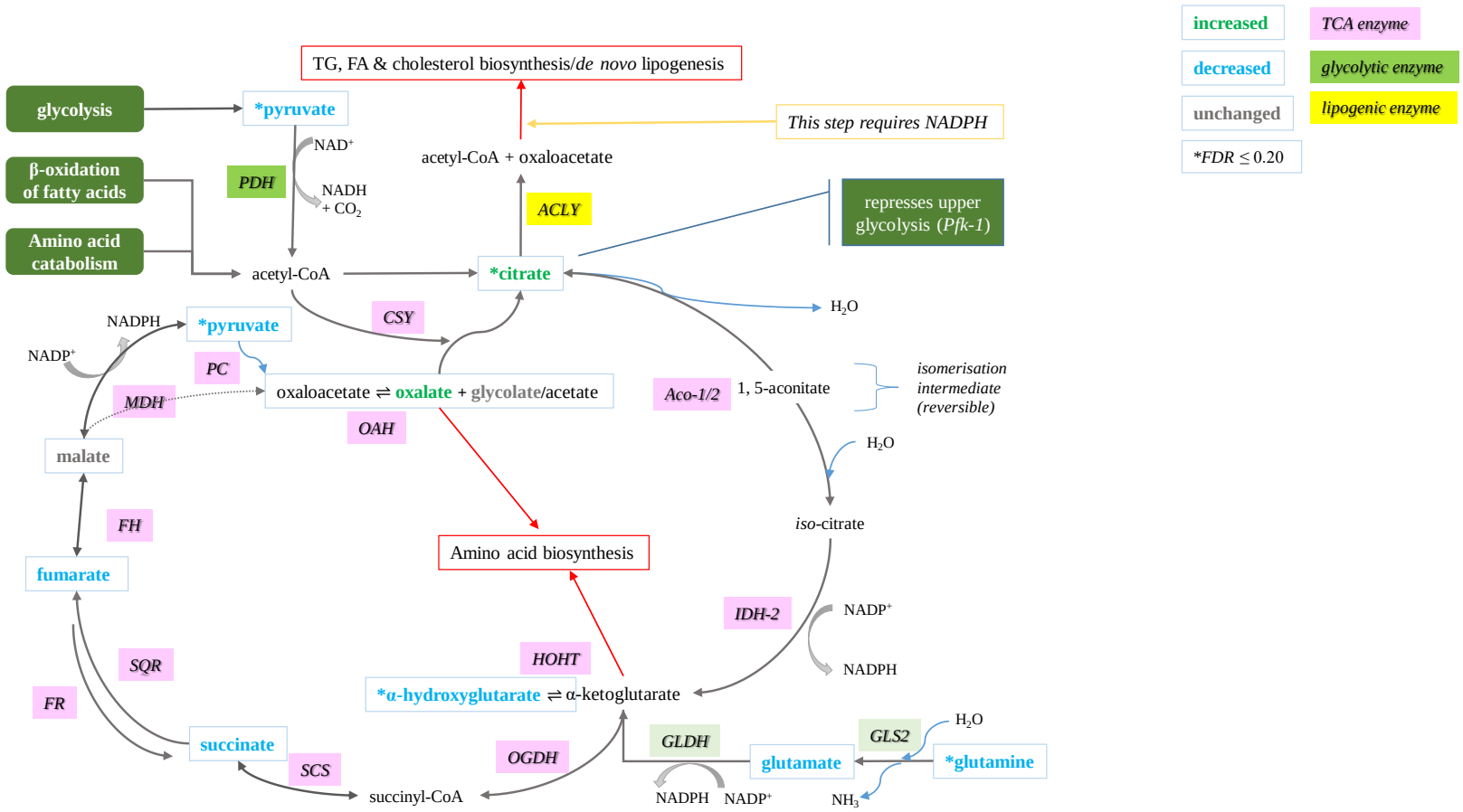

Figure 15. TCA cycle alterations detected in the plasma of C57BL6/J mice treated with captopril in response to a normal salt diet versus a high-salt diet. Intermediates and metabolites in **green** increased, **blue** decreased, **grey** remained stable, and black were unmeasured. **Red** lines describe pathways in which metabolites may participate. Enzymes include: citrate synthase (CSY), ATP citrate lyase (ACLY), aconitase 1 or 2 (Aco-1/2), *iso*-citrate dehydrogenase 2 (IDH-2), α-ketoglutarate dehydrogenase (OGDH), glutamate dehydrogenase (GLDH), glutaminase (GLS2), succinyl CoA synthetase (SCS), succinate dehydrogenase (SQR), fumarate reductase (FR), fumarase (FH), oxaloacetase acetylhyrolase (OAH), malate dehydrogenase MDH), pyruvate carboxylase (PC), hydroxyacid-oxoacid transhyrdrogenase (HOTH), pyruvate dehydrogenase (PDH).

Fructose metabolism / Aldose Reductase–Sorbitol Dehydrogenase (AR–SDH) pathway

Unlike glucose, hepatic metabolism of fructose increases DNL by its uninhibited entry in to the glycolytic pathway via the actions of the liver-specific enzymes ketohexokinase (KHK) and aldolase B (ALDOB), ultimately yielding carbon precursors for *de novo* FA synthesis (Khitan & Kim, 2013). Moreover, circulating uric acid (UA) is directly related to fructose metabolism and is a metabolite marker capable of predicting risk of developing obesity, T2D and hypertension and (Osgood, Krakoff, & Thearle, 2013).

Hyperglycaemia triggers the metabolism of glucose via the aldose reductase (AR)–sorbitol dehydrogenase (SDH) pathway leading to fructose biosynthesis (from sorbitol), and recently long-term dietary salt overloading was shown to promote the same pathway in mice resulting in significant bodyweight and fat gain, hyperuricemia, hepatic steatosis and other features of the MetS (Lanaspa et al., 2013; Lanaspa et al., 2018). In the case with a high-salt feeding, the aforementioned effects were shown to be accelerated when combined with a high-energy WD (Lanaspa et al., 2018). As reported in table 6, plasma fructose levels were significantly elevated in captopril treated mice subjected to a normal-salt diet and this effect was countered when treatment was administered in conjunction with a high-salt diet. Similar metabolite trends were also described subsequent to feeding of high-glucose and high-salt diets to AR and KHK deficient mice, where an inability to metabolise fructose resulted in its accumulation *in vivo* (Lanaspa et al., 2013; Lanaspa et al., 2018). In 2009 Ronal and colleagues showed that unlike controls, high-fructose fed mice treated with captopril opposed bodyweight and visceral fat gain. In this study we provide additional evidence to support an inverse association between plasma fructose with bodyweight and liver mass (table 8, figure 11G-I). Together with the findings of Roncal et al. (2009) and Lanaspa et al. (2013) (2018), we speculate that captopril may modulate the AR–SDH (polyol) or KHK–ALDOB (ketohexokinase) pathways to translate as either a reduction in the hepatic biosynthesis or uptake of fructose respectively, manifesting bodyweight and fat loss when dietary salt levels are below our founded salt range of 86.0 mg day^{-1}. In contrast, a high-salt diet may intervene with captopril's metabolically repressive properties by boosting the AR–SDH or KHK–ALDOB pathways to induce glycolytic and TCA cycle turnover, generating precursors that facilitates DNL, fat accumulation and bodyweight gain. This may suggest that the interaction between captopril and dietary salt may also involve the endogenous synthesis and/or metabolism of fructose.

Subsequent to hepatic fructose metabolism, UA is generated as a result of purine degradation (ATP depletion), and there is evidence that UA positively regulates hepatic AR and KHK mRNA and protein expression (Johnson et al., 2013; Lanaspa et al., 2012; Sanchez-Lozada et al., 2019). Here we showed captopril treatment of mice to cause a marked decline in plasma UA levels following a normal salt diet, whereas combined with a high-salt diet this effect was abolished and generated even higher levels of UA to that of respective controls (table 8). A surge in UA is not unseen in hypotensive animals and is thought to be an evolutionary advantage opposing environmental

pressures that may have led to a lowering of BP (Wang, Chu, et al., 2018), therefore with reference to the current findings, the added surge in UA (CAPS versus HFS mice) may be an additive consequence of the anti-hypertensive effects of captopril. Nonetheless, the metabolic relationship between plasma UA and fructose further aligns with our hypothesis that metabolic reduction of fructose metabolism and UA generation that is instigated by captopril may be important for bodyweight and body fat loss. These metabolites responded in the opposite direction when captopril was administered in conjunction with a dietary salt level that exceeded 86.0 mg day^{-1}, and is thus presumed to be proportional to the rate of fructose metabolism which can facilitate a positive feedback loop with UA to upregulate AR and KHK expression and activity, thus interfering with the aforementioned mode of action of captopril (Lanaspa et al., 2018; Lanaspa et al., 2012). This indicates that the interaction between captopril and salt may involve UA that is derived from the metabolism of fructose. Refer to figure 16 for AR–SDH and KHK–ALDOB pathway alterations caused by captopril when dietary salt intake is normal versus when dietary salt intake is high.

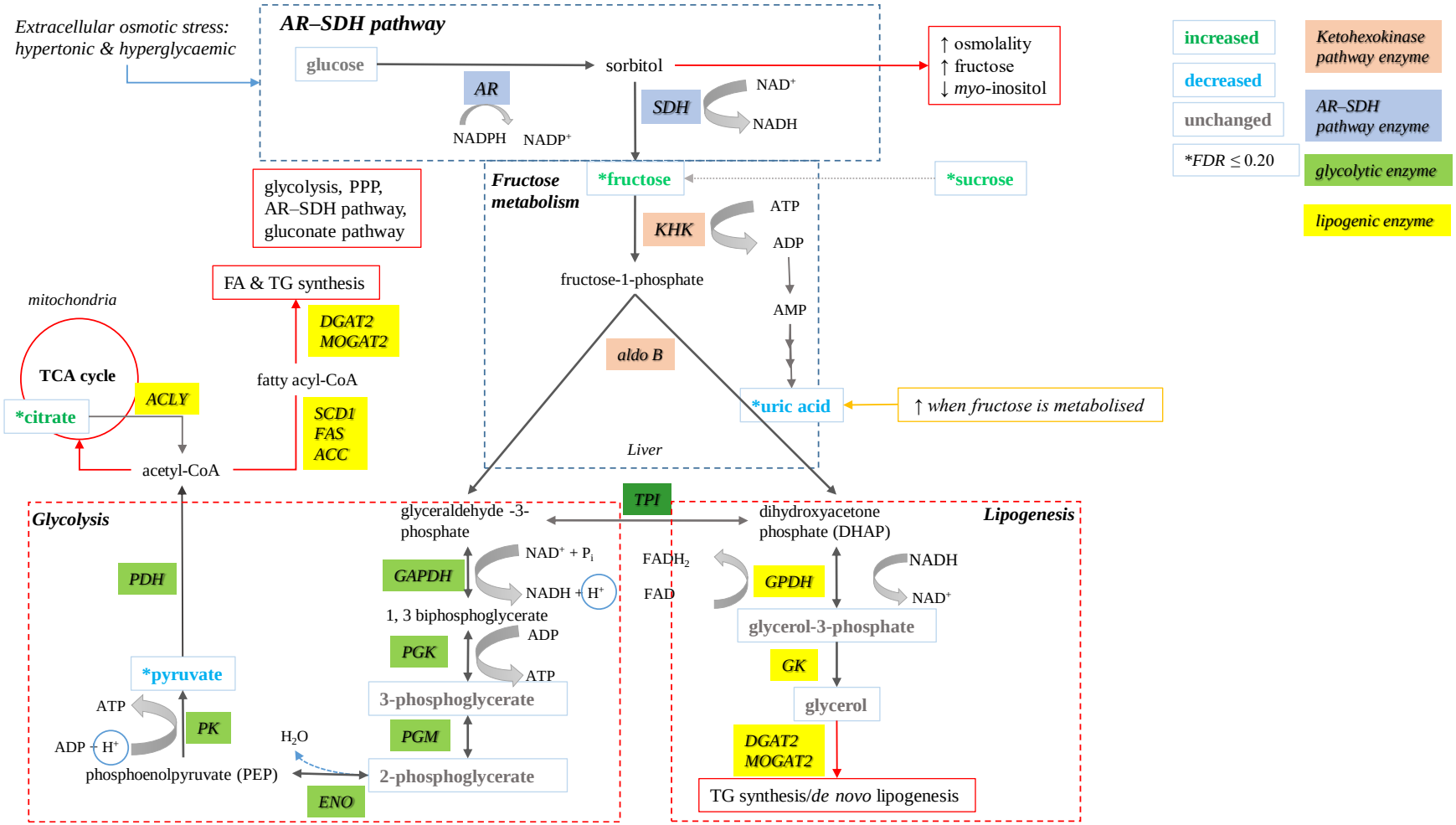

Figure 16. Fructose metabolising pathway alterations detected in the plasma of C57BL6/J mice treated with captopril in response to a normal-salt diet versus a high-salt diet. Intermediates and metabolites in **green** increased, **blue** decreased, **grey** remained stable, and black were unmeasured. **Red** lines describe pathways in which metabolites may participate. Enzymes include: ketohexokinase (KHK), aldolase B (aldo B), aldose reductase (AR), sorbitol dehydrogenase (SDH), ATP citrate lyase (ACLY), acetyl-CoA carboxylase (ACC), fatty acid synthase (FASN), stearoyl-CoA desaturase 1 (SCD1), diacylglycerol O-acyltransferase 2 (DGAT2), monoacylglycerol O-acyltransferase 2 (MOGAT2).

Inositol metabolism

Synthesised *de novo* from G6P or derived from the breakdown of PI and/or IP intermediates, *myo*-inositol is a major attenuated metabolite in obesity and defective epimerisation to its D-*chiro* stereoisomer is hallmark of IR and MetS (Eisenberg & Parthasarathy, 1987; Yunbae et al., 1998). This depletion appears to be related to abnormally high inositol excretion due to its competitive affinity with glucose for SGLT-1 and -2 mediated intracellular transport (Greene & Lattimer, 1982). Whilst inositol and inositol-related metabolites are recognised as measures of insulin sensitivity, cardioprotective effects are also apparent as elevations in blood adiponectin concentrations have been observed subsequent to *myo*-inositol supplementation (Santamaria et al., 2012).

In the current study we identified a significant elevation in plasma inositol levels in captopril treated mice following a normal-salt diet which may not be explained by dietary composition alone (*i.e.* 55 mg kg^{-1}, see SF0019 feed composition). Captopril treatment in conjunction with a high-salt diet reversed metabolite levels in mice to match that of untreated controls (table 6). A reduction in bodyweight and body fat correlated with an increase in plasma inositol levels (table 8, figure 11D-E), a finding which is in alignment with that of Croze, Géloën, and Soulage (2015) who described declines in bodyweight gain, VAT mass and adipocyte diameter subsequent to intravenous *myo*-inositol administration in DIO mice. Moreover, *myo*-inositol 2-phosphate (IP_2) and pyrophosphate remained unaltered between groups suggesting the improbability that endogenous inositol was derived from cellular fatty acyl modifications over *de novo* pathways and/or via improved cellular uptake and/or retention (Bevilacqua & Bizzarri, 2018; Eisenberg & Parthasarathy, 1987; Kim, Ahn, Kim, Lee, & Kim, 2017; Morine et al., 2011). This hypothesis is further supported by the finding that IPs may activate inositol polyphosphate multikinase (IPMK) to repress the LKB1–AMPK signaling axis (Bang et al., 2012), thus degradation of inositol-polyphosphates, such as IP_2, may theoretically impede captopril's weight loss efficacy via adiponectin-receptor mediated AMPK activation (Tabbi-Anneni et al., 2008). Though plasma adiponectin was not measured in the present study, recent experiments conducted in our laboratory showed a significant effect of captopril on plasma adiponectin in mice, independent of the level of dietary salt (Radcliffe, 2013 PhD Thesis).

A recent DASH trial showed an association between dietary-salt moderation and *myo*-inositol metabolite changes yet the direction of this relationship was not reported (Derkach, Sampson, Joseph, Playdon, & Stolzenberg-Solomon, 2017). As described, plasma inositol was depleted following captopril treatment when dietary salt content was high and was matched to the levels of that of respective controls. Depletion of *myo*-inositol and a concomitant accumulation of sorbitol has consistently been observed in obese and hyperglycaemic rats (Greene, Lattimer, & Sima, 1987; McCaleb & Sredy, 1992) and the reverse occured when AR was inhibited (Chang, 2011). Given it was recently established that a high-salt diet induces sorbitol biosynthesis to generate fructose via AR–SDH pathway activation (Lanaspa et al., 2018), a reduction in inositol may further support the hypothesis that AR–SDH pathway stimulation plays a pivotal part in countering the metabolic

effects of captopril; this is represented in figure 13F, as an inverse correlation between plasma inositol and fructose. Moreover, catabolism of *myo*-inositol via the glucoronate–xylulose pathway in the kidneys may lead to xylulose-5-phosphate, a substrate of the PPP (Croze & Soulage, 2013), to suggest inositol biosynthesis may also be in negative association with PPP activation. To support this hypothesis, we observed a striking correlation between plasma inositol, erythritol and 2-ketogluconate (figure 12G-I), assuming these metabolites are representative of a repressed PPP. Therefore, a high-salt diet may counteract these effects via boosting the AR–SDH and glucoronate–xylulose pathways, metabolising glucose to fructose (from sorbitol) and inositol to xylulose-5-phosphate respectively.

Taken together, the metabolic reduction of the AR–SDH pathway instigated by captopril may be important for the endogenous synthesis of inositol, and inositol may be regarded as an important marker in frequent association with bodyweight and fat loss. Further studies are needed to clarify these proposed relationships. Refer to figure 17 for inositol pathway alterations by captopril in response to a normal versus high dietary salt levels.

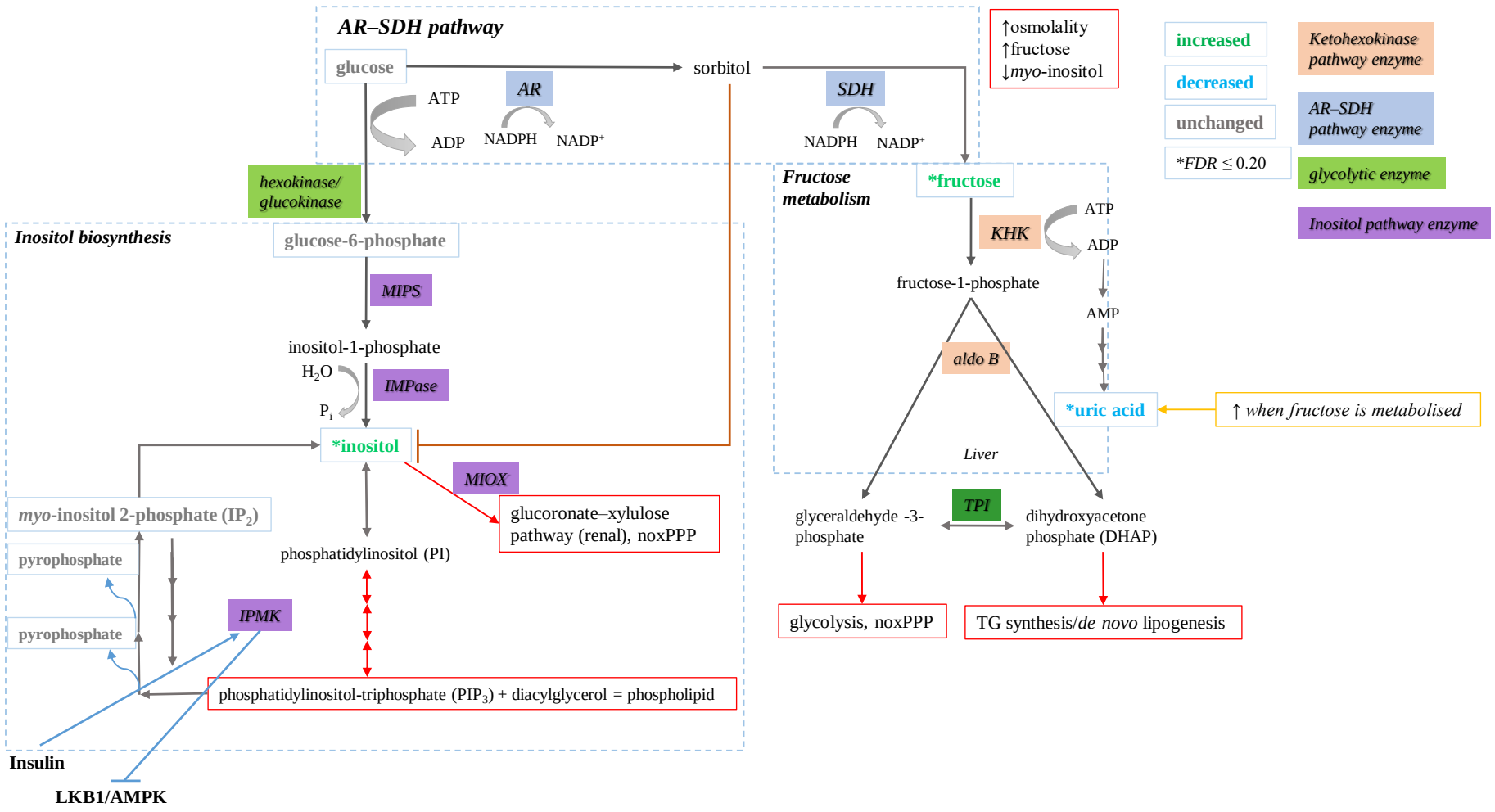

Figure 17. Inositol alterations detected in the plasma of C57BL6/J mice treated with captopril in response to a normal salt diet versus a high-salt diet. Intermediates and metabolites in **green** increased, **blue** decreased, **grey** remained stable, and black were unmeasured. **Red** lines describe pathways in which metabolites may participate. Enzymes include: *myo*-inositol-1-phosphate synthase (MIPS), inositol monophosphate phosphatase (IMPase), *myo*-inositol oxygenase (MIOX), inositol polyphosphate multikinase (IPMK).

Pentose phosphate pathway

Oxidative and non-oxidative pentose phosphate pathway (PPP)

The pentose phosphate pathway (PPP) is not fully understood and very few regulatory mechanisms have been identified. Metabolically active tissues of obese and diabetic subjects display enhanced glucose metabolism through the PPP, and similarly dietary salt-overloading in Dahl rats had the same effect (Fonseca-Alaniz et al., 2007; Kato et al., 2012; Park et al., 2005; T. Takamura et al., 2008; Wang, Liu, et al., 2018). These outcomes are largely under the influence of insulin and systemic stress, as demonstrated by rapid increases in the cellular concentration of pentose-phosphayes (PPs) and their metabolites, NADPH to $NADP^+$ ratios, NOX and ROS (Krycer et al., 2017; Wang, Liu, et al., 2018).

As reviewed, the mechanism of action of captopril entails a rise in plasma adiponectin followed by cytosolic translocation and phosphorylation of LKB1 and AMPK respectively (Chen et al., 2013; Kohlstedt et al., 2009; Ruan & Dong, 2016). In skeletal muscle tissues of DIO mice, adiponectin supplementation was shown to generally oppose several Ru5P derived diastereomer disturbances in accordance with a reduction in acetyl-CoA, leading to adipocyte hypotrophy (Liu et al., 2013). Comparison to mice subjected to a high-salt diet, captopril treatment of mice in the current study caused a significant decline in the level of oxidative PP metabolites, including 1, 4-Gnl and ribitol, (where ribitol derives from Ru5P, see figure 18 below). Given we have also shown captopril treatment of mice to increase plasma adiponectin and reduce adipocyte cell size to 40-45% that of untreated controls (Weisinger et al., 2009), combined, results are similar to the findings of Liu and colleagues (2013) who show adiponectin to promote a reduction in adipocyte size which appeared to be concurrent with reducing glucose flow in to the oxidative PPP. This agrees with captopril's mode of action via adiponectin.

Captopril arbitrates AMPK, and enzyme 6PGDH of the oxidative branch (for which 6PGn is a substrate) was shown to inhibit LKB1–AMPK signaling together with increased Ru5P and NADPH dependent *de novo* FA (and RNA) biosynthesis *in vitro* (Lin et al., 2015). Moreover, AMPK activation was shown to impair NADPH generation via the PPP (Jeon, Chandel, & Hay, 2012), suggesting an inverse association between the AMPK signaling cascade PPP activity. Although in the present study 6PGn remained indistinguishable between captopril treated groups, 6PGn correlated directionally with the bodyweights and the epididymal adipose masses of mice (figure 12D-E), which is consistent with the afore discussed relationship between 6PGDH and *de novo* FA biosynthesis (Lin et al., 2015; Patra & Hay, 2014). Although we did not measure NADPH status, according to significant reductions in plasma levels of ribitol and 1, 4-Gnl (from which 6PGn may derive), we suspect NADPH generated from the dehydrogenation of 6PGn may have declined in response to captopril treatment. According to metabolite levels in the reverse direction, high dietary salt intake may oppose captopril's weight loss effects by upholding 6PGn and its derivatives including. Ru5P and NADPH, to serve in DNL and cell growth (Lin et al., 2015). Together there is

indication of an interaction between captopril and salt on the ability to regulate glucose metabolism through the oxidative route of the PPP (as 1, 4-Gnl).

Ribose may be generated in the final steps of the oxidative branch via the isomerisation of Ru5P by the RPI enzyme in to R5P, which may then be dephosphorylated to liberate ribose (Huck et al., 2004). The non-oxidative branch is involved to a lesser extent given the broad substrate specificities of enzymes (Sprenger, Schorken, Sprenger, & Sahm, 1995), albeit reactions between PPs catalysed mainly by TKT may redeliver ribose (Berg, Tymoczko, & Stryer, 2002; Wamelink, Struys, & Jakobs, 2008). As a component of nucleotides and cellular intermediates, which includes RNA, DNA, ATP and CoA, ribose plays a role in adipocyte cell growth and proliferation (Butterworth, 2005b; Wamelink et al., 2008).

The current study shows that in contrast to high-salt conditions, captopril treatment of mice decreased plasma ribose when following a normal-salt diet. Subsequent to the ribitol, 1, 4-Gnl and 6PGn findings discussed above, captopril appears to reduce the production of oxidative intermediates thus a reduction in ribose levels is not unanticipated. Whilst we know little of PPP regulation, molecular inhibition of G6PDH, the first enzyme of the oxidative branch for which G6P is a substrate, was shown to abolish both NADPH and ribose synthesis to block cancer cell growth and proliferation (Tsouko et al., 2014). Moreover the urinary and blood characteristics of RPI deficient patients are shown to exhibit low levels of R5P, from which ribose derives (Huck et al., 2004). This could suggest carbon metabolism via the oxidative route may be critical for the synthesis of ribose and NADPH-mediated cellular growth, to support the hypothesis that metabolic reduction of the oxidative PPP instigated by captopril may be conducive to ribose metabolite depletion, and that this may lead to a reduction in PPP derived ribonucleotides, NADPH, and other anabolic factors that are required for DNL and adipocyte proliferation.

A high-energy diet is frequently associated with systemic oxidative stress and similarly high-salt (and fructose) feeding is shown to exacerbate this environment *in vivo* by upholding glucose metabolism through the PPP (Dornas et al., 2017; Dornas et al., 2013; Feng et al., 2012). This is supported by experiments conducted in Dahl rats where subsequent to dietary salt overloading, renal ROS, G6PDH and 6PGDH activity and expression, and R5P and 6PGn metabolite levels were augmented (Kitiyakara et al., 2003; Wang, Liu, et al., 2018). Therefore, a high-salt diet may counter ribose modulation (by captopril) by redirecting glycolytic substrates (probably from fructose derived G3P) in to the non-oxidative branch as a response to systemic stress, thereby facilitating the generation of ribonucleotides and NADPH. Consequently, this may uphold an environment that favours DNL and weight gain. Together there is indication of an interaction between captopril and salt on their ability to regulate the oxidative and non-oxidative branches of the PPP. Further studies are needed to explore all of the other known PPP derived intermediates as well as the NADPH-to-$NADP^+$ status of animals.

Erythritol, a putative pentose–phosphate pathway metabolite

Erythritol is a widely used sugar substitute recommended for diabetic patients for its lack of effect on blood glucose and insulin, additional being an antioxidant that provides protection against hyperglycaemia-induced oxidative damage to endothelium (den Hartog et al., 2010; Livesey, 2003). Assumed to be xenobiotic, Hootman et al. (2017) recently showed the endogenous metabolism of glucose to erythritol, presumably from the pentose sugar phosphate erythrose-4-phoshpate (E4P), which then oxidised to erythronate. An inability to distinguish between *in vivo* and dietary contributions to the endogenous "erythritol pool" renders clinical data uninterpretable (Hiele, Ghoos, Rutgeerts, & Vantrappen, 1993; Hootman et al., 2017; Khakimov et al., 2016). Here, we confirm no dietary influence of erythritol to levels that are detected in the plasma of mice. Refer to appendix for SF00-219 composition.

We showed differential regulation of erythritol and erythronate amongst treatment groups to support the finding that erythritol is endogenously synthesised and metabolised (Hootman et al., 2017). Captopril treatment of mice following a normal salt diet caused a substantial increase in plasma erythritol and erythronate levels (table 6), although the latter metabolite remained just above the FDR-threshold (table 7). Amongst remaining groups, erythritol levels were statistically non-differentiable. Moreover we identified an inverse correlation between erythritol and the final bodyweights of mice (figure 11A), and similarly a recent intervention trial identified a rise in plasma erythritol in accordance with weight loss in centrally obese subjects, however this change was thought to be due to dietary re-composition (Khakimov et al., 2016). Conversely Hootman et al. (2017) described a positive association between blood erythritol concentration and the incidence of central adiposity gain, in addition to noting that subjects with the lowest central adiposity change exhibited the highest concentration of erythritol in blood. We corroborated the latter finding by identifying a strong inverse relationship between plasma erythritol and fat mass, where mice with greater epididymal fat and liver masses exhibited lower levels of erythritol (figure 11B-C). Therefore in contrast to Hootman et al. (2017), we suggest plasma erythritol relates inversely to the direction of change of bodyweight and fat mass and is a putative endogenous marker in negative association with adiposity and PPP activation.

Inborn errors of pentose metabolism has been characterised by an accumulation of polyols and their metabolic by-products, including erythritol and erythronate in bodily fluids such as plasma and urine, albeit mechanisms have not been further investigated (Boyle et al., 2016; Engelke et al., 2010; Verhoeven et al., 2001). Reaction of TALDO and TKT may generate E4P, and recently E4P was identified as a substrate for GAPDH deriving erythronate-4-phosphate, and was identified as a potent repressor of 6PGDH. These repressive effects were shown to reduce cellular capacity to synthesise NADPH, in turn slowing cell growth (Collard et al., 2016). In parallel with the observation that captopril may reduce the availability of glycolytic intermediates that are required to replenish the non-oxidative branch (discussed earlier), it is possible that in the absence of a high-

salt diet, captopril facilitates the accumulation of E4P and its chemical products that may further repress 6PGDH and PP synthesis (Collard et al., 2016). This aligns with the ribitol and ribose findings above, given they may only be synthesised by 6PGDH when TKT and TALDO is absent (Boyle et al., 2016). Therefore captopril may have a secondary mechanism whereby an overall reduction in glucose metabolism via the PPP may be further compounded by (putative) E4P derived metabolites, erythritol and erythronate, which may further downregulate the PPP by repressing 6PGDH activities (and NADPH generation) to promote bodyweight and fat loss. Further studies are needed to assess this hypothesis.

A high-salt intake has been reported to enhance carbon metabolism via the PP (and glycolytic) pathways (Wang, Liu, et al., 2018), making it possible for glycolytic substrates to re-enter the PPP. This may encourage an overall repletion of the oxidative and non-oxidative arms to thereby favouring (reverse) reactions of E4P. This might explain the reduction in plasma erythritol and erythronate levels in high-salt fed mice, albeit due to lack of understanding of the dynamics of the PPP, it is difficult to discern sequences of events. Based on studies showing a high levels of erythritol excretion in patients with congenital PPP enzyme defects (Boyle et al., 2016; Huck et al., 2004; Verhoeven et al., 2001), plasma erythritol and erythronate may be negatively associated with PPP activity, and a reduction in these metabolites in response to salt may be due to PP substrate consumption, yielding NADPH and other precursors that can facilitate DNL and other metabolic processes. Taken together, there is indication of an interaction between captopril and salt on erythritol biosynthesis. Moreover, repression of the PPP by captopril may be important for erythritol and erythronate generation, and erythritol and erythronate biosynthesis may be regarded as novel marker in frequent association with reduced adiposity and fat loss. Refer to figure 18 for PPP alterations instigated by captopril when dietary salt intake is normal versus when dietary salt intake is high.

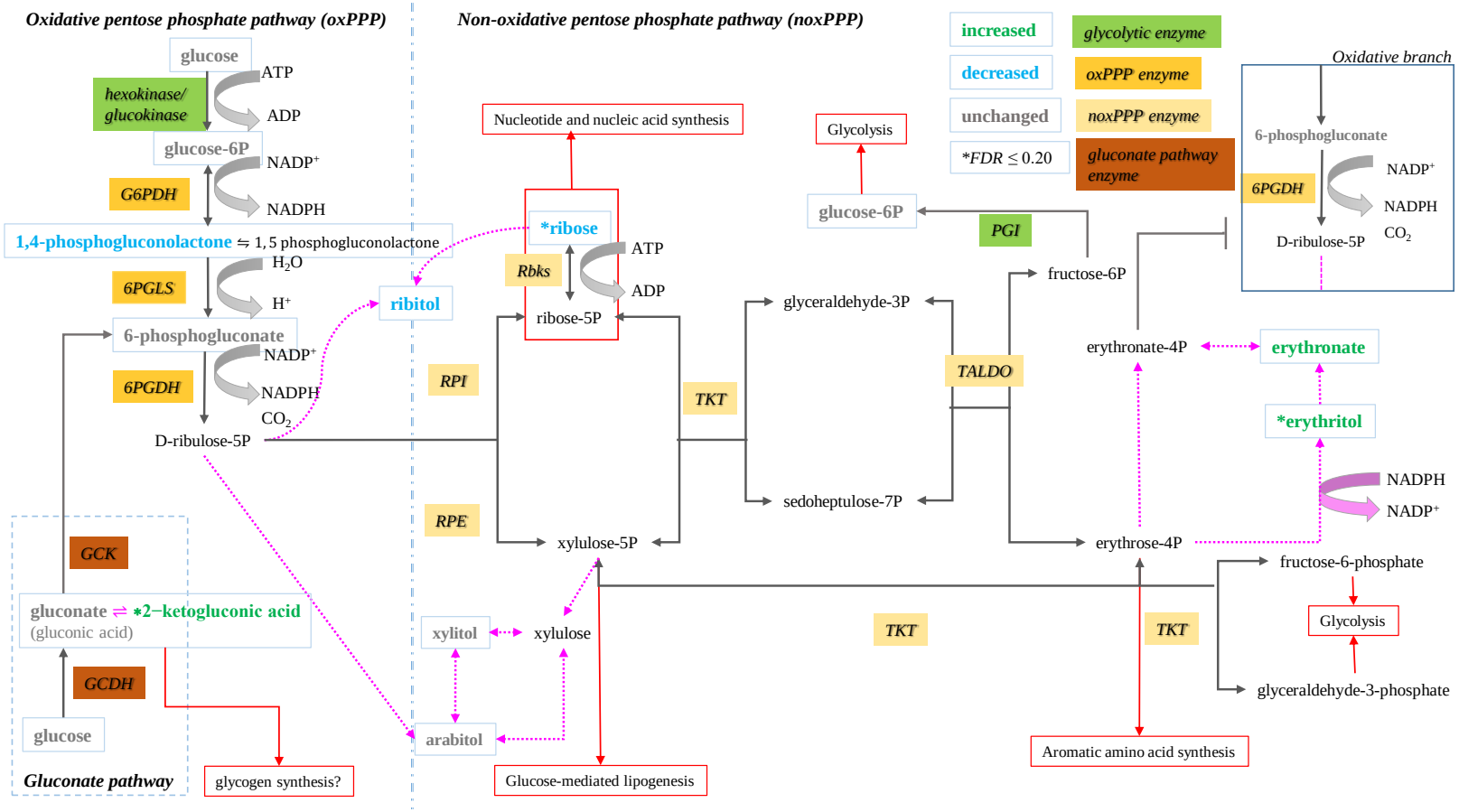

Figure 18 Detected pentose phosphate pathway (PPP) and gluconate pathway alterations in the sera of C57BL6/J mice treated with captopril in response to a medium-salt diet versus a high-salt diet. Intermediates and metabolites in **green** increased, **blue** decreased, **grey** remained stable, and black were unmeasured. **Pink** lines represent putative conversion of substrates and **red** lines describe pathways in which intermediates may participate. Enzymes include: glucose-6-phosphate dehydrogenase (G6PDH), 6-phosphogluconolactonase (6PGLS), 6-phosphogluconate dehydrogenase (6PGDH), D-ribulose-5-phosphate isomerase/empirase (RPI)/(RPE), transketolase (TKT), transaldolase (TALDO), ribokinase (Rbks), glucose dehydrogenase (GCDH), gluconate kinase (GCK).

Gluconate pathway (gluconate shunt)

Our current understanding of the gluconate pathway in higher animals is that G6P is not an intermediate, where glucose is directly oxidised to gluconate by glucose dehydrogenase (GCDH). Gluconate is then phosphorylated by gluconate kinase (GCK) to produce 6PGn, creating an alternative channel for glucose to enter the PPP without reliance on G6PDH (Rohatgi et al., 2014). Moreover, gluconate is shown to be metabolised differently to glucose in rat tissues, contributing to the production of glycogen and CO_2 (Bloom & Stetten, 1955; Stetten & Topper, 1953). On the other hand, microorganisms can oxidise gluconate to 2-ketogluconate, which may then be phosphorylated and converted from 2-keto-6PGn to 6PGn (Lockwood, Tabenkin, & Ward, 1941; Sun et al., 2018). Although the latter reactions have not been described in higher animals, alterations in 2-ketogluconate amongst T2D patients with renal failure underscores its relevance in human disease (Ng et al., 2012).

In the current study captopril treatment of mice caused a significant increase in plasma 2-ketogluconate levels following a normal salt intake without change in gluconate. Moreover, 2-ketogluconate was negatively (figure 12A-B) associated with bodyweight and epididymal fat mass and 6PGn was positively associated (figure 12D-E). We also identified a strong positive correlation between plasma gluconate and 2-ketogluconate (figure 12G), suggesting that as in microorganisms, these metabolites may also be chemical counterparts in higher organisms (Lockwood et al., 1941; Sun et al., 2018). To the best of our knowledge there have been no prior reports of such association. Captopril treatment in conjunction with a high-salt intake reduced 2-ketogluconate metabolite levels to resemble that of respective controls. With the knowledge that 2-ketogluconate may be derived from gluconate in an oxidation reaction, it is possible that the accumulation of 2-ketogluconate reflects an alternative shunt that occurs when 6PGDH is compromised and 6PGn cannot be synthesis from gluconate. This hypothesis may be supported by studies conducted in glial cells, where the inhibition of 6PGDH (with 6-aminonicotinamide) accumulated gluconate, concomitant with a rise in glycogen content, albeit 6PGn levels remained steady (Keller, Kolbe, Herken, & Lange, 1976). Prior studies have shown captopril treatment of rats to enhance (non-oxidative) glucose incorporation in to muscle glycogen whereas salt loading has been shown to reduce muscle and hepatic glycogen content (Cahová, Vavrinková, Tutterova, Meschisvilli, & Kazdova, 2003; Kitada et al., 2017). Though we do not provide data to support this hypothesis, we speculate that captopril treated mice following a normal salt diet accumulated 2-ketogluconate under circumstances of surplus glycogen and repressed 6PGDH activity via the gluconate pathway, thus comprising an alternative shunt. Such effects were countered by a high-salt intake according to 2-ketogluconate levels in the reverse direction, possibly reflecting redirection of glucose metabolites away from the alternative gluconate pathway towards PP synthesis. Further studies are needed to determine endogenous regulators of 2-ketogluconate and its potential association with PP and glycogeneic pathways in higher animals. Refer to figure 18 for a putative representation of the

gluconate pathway that may be instigated by captopril when dietary salt content is normal versus when dietary salt content is high. Taken together, metabolic reduction of the gluconate pathway by captopril may be important for reducing bodyweight and body fat in mice.

Conclusions

The aim of the current study was to validate the interaction effect between dietary salt and captopril on bodyweight and fat loss in DIO C57BL/6J mice, and to further uncover the effect of this interaction on the plasma metabolite profiles of mice. This study provides novel data and support for the reported anti-lipogenic, anti-anabolic, anti-inflammatory and anti-oxidant properties of captopril when combined with a normal salt intake (<86.0 mg day^{-1}), and offers insights in to captopril's effect on the metabolic state of C57BL/6J mice. Our findings indicate that captopril's impact on the plasma metabolome is affected by a high-salt intake in addition to impairing its weight loss properties. Metabolite differences suggest that the interaction between captopril and salt involves metabolic pathways that run in parallel to glycolysis. GC-MS data showed the weight loss properties of captopril following a normal salt diet involved striking alterations to carbohydrate metabolism through phosphorylative routes, and in particular, fructose breakdown and glucose metabolising pathways were affected in such a way as to upregulate processes of FA oxidation (citrate ↑, glycerate ↑). When dietary salt intake was normal, captopril altered metabolites involved in sucrose hydrolysis (sucrose ↑), glycolysis (pyruvate ↓, maltose ↓), the TCA cycle (succinate ↓, α-hydroxyglutarate ↓, glutamate ↓, glutamine ↓, citrate ↑, oxalate ↑), fructose metabolism (fructose ↑, uric acid ↓, inositol ↑), and oxidative and non-oxidative metabolism of glucose via the PPP (ribose ↓, 1, 4-Gnl ↓, ribitol ↓, erythritol ↑, 2-ketogluconate ↑), and a high-salt diet reversed these effects according to metabolite levels in the opposite direction. Moreover, static levels of lipolytic end-products (IP_2, PP_i, glycerol, glycerol-2-phosphate) and increased FA oxidation end-products and/or lipogenic precursors (citrate ↑, glycerate ↑) suggested the weight loss mechanism of action of captopril may suppress lipogenic pathways. One other possible weight loss mechanism of action of captopril involves the diversion/shunt of available dietary glucose away from intracellular phosphorylative pathways toward extracellular pathways that generate inert polyols and metabolites, such as erythritol, inositol and 2-ketogluconate, and in this way maintaining glucose homeostasis. In contrast, a high-salt diet may oppose these effects by inducing systemic and/or peripheral oxidative stress and a rise in extracellular osmolality. The latter effect may result in the upregulation of the AR–SDH pathway, whereby available glucose is synthesised to fructose thus opposing erythritol and inositol. Through the action of hepatic KHK and aldolase B, fructose may be metabolised to yield substrates that can be initiated in to glycolysis and the PPP to facilitate the generation of precursors that are required for *de novo* FA biosynthesis and adipogenesis. This may potentially manifest body fat gain and obesity. There may also be an independent role for oxidative stress in the progression of obesity and its symptoms, whereby a high-salt diet may exacerbate an oxidative environment, especially in combination with high-energy feeding, in effect upregulating

NADPH yielding pathways that also supports DNL, adipocyte cell growth and proliferation. This hypothesis requires further investigation.

Limitations

It should be noted that the metabolite levels measured at the end of the study may not reflect changes occurring at early stages of treatment, hence sampling at different time points during the treatment period would better clarify the effects of captopril on the plasma metabolome. Moreover, metabolite accumulations can indicate an increase in production or a decrease in utilisation, whilst static metabolite levels are generally thought to represent balance between production and consumption and therefore do not always reflect changes in the rate of flux. Metabolite levels may also indicate alterations in enzyme activity or their expression rate, and therefore changes in metabolite ratios does not give a correct representation of physiology. Measurements of metabolite flux, enzyme activity and expression studies in different tissues would be necessary to clarify whole-body interactions and effects of captopril and salt on metabolism.

Chapter 4

High dietary salt consumption impedes the weight loss efficacy of captopril in C57BL/6J mice maintained on a high-fat diet: liver and adipose tissue transcriptomics

Abstract

It was recently revealed that a high salt diet is a risk factor for the onset of obesity, independent of over-nutrition. Liver and adipose tissue microenvironment modifications in response to nutrient stress (high-fat, high-sugar and high-salt feeding) may be recognised as key in the development of obesity and progression of associated morbidities. We previously described an ostensible level of resistance to the weight loss efficacy of captopril treatment in mice with a high level of dietary salt intake, *i.e.* in excess of 86.0 mg day^{-1}, where a negligible outcome on the reversal of obesity and reduction of body fat mass was observed. In chapter 3 we reported on the systemic action of captopril, where at the metabolite level, there was strong indication of a diversion of available glucose-derived substrates are away from intracellular phosphorylative pathways towards other less defined pathways, *e.g.* the gluconate shunt and sugar-alcohol biosynthesis, which was influenced in the opposite direction when the consumption of dietary salt exceeded 86.0 mg day^{-1}. At present, the interaction effect of captopril with salt on the liver and adipose tissue transcriptome remains undefined, thus the aim of this experiment was to investigate the molecular mode(s) of action of these changes to identify key molecular pathways which may be involved. To this end, we analysed the transcriptomic profiles of liver and adipose tissue derived from mice maintained on a high-fat diet treated with or without captopril in the absence or presence of a high-salt diet for 4-weeks, by means of high-throughput RNA sequencing (n = 3 animals per treatment). We report that the molecular interaction between captopril and salt on liver and adipose transcriptome profiles may be characterised by common denominator genes, including *Agt*, *Gnb1* and *Gnb5*. In the liver, phosphorylative pathways of carbon metabolism, TCA cycle, cell cycle and p53 signaling were significantly modulated by captopril and reversely regulated by salt. In adipose tissue, the peroxisomal pathways of oxidative metabolism were significantly upregulated by captopril and reversely regulated by salt. Collectively, the findings of the present study highlighted key genes and pathways that may contribute to the interaction effect between captopril and salt on bodyweight and body fat regulation in C57BL/6J mice maintained on a high-fat diet. These may provide a basis for further investigation in to the underlying mechanism by which captopril may elicit anti-obesity effects.

Introduction

Earlier, we reported an interaction between captopril and salt on bodyweight and body fat mass, where a high level of dietary salt intake, *i.e.* >86.0 mg day^{-1}, caused ostensive resistance to the weight loss effect of captopril in C57BL/6J mice maintained on a HFD (Radcliffe, 2013). In chapter 3, we reported the interaction effect between captopril and salt to contribute to changes in the plasma metabolite profiles of lean and obese mice, where we noticed differences predominantly in the partitioning of glucose between pathways of glycolysis, PPP, TCA cycle and other less defined alternative routes of carbon metabolism.

The effect of salt on body fat regulation is currently under debate (Cui et al., 2017; DeClercq, Goldsby, McMurray, & Chapkin, 2016; Fonseca-Alaniz et al., 2007; Kitada et al., 2017; Lanaspa et al., 2018; Weidemann et al., 2015), and there is indication that dietary salt itself may regulate intracellular Ang-II production independent of the systemic RAS (Crestani et al., 2014; Devarajan et al., 2015; Lee et al., 2019; Tamura et al., 1999; Weidemann et al., 2015). Salt intake in Western societies generally exceeds 10 grams day^{-1}, an amount far beyond the recommendations of the WHO (Brown et al., 2009), and therefore local Ang-II production due to salt may be a factor in the lack of weight loss observed not just in mice within this study, but also in humans undertaking captopril therapy.

As the major bioactive peptide of the RAS, Ang-II is involved in various cardiovascular functions and diseases, the physiological effects of which is mediated through Ang-II type 1 and type 2 receptors (AT_1 and AT_2). AT_1 activation couples to G_q family of proteins to induce phospholipase C which cleaves PIP_2 in to IP_3 and 1,2-diacylglycerol (DAG). IP_3 increases cytosolic calcium concentration whereas DAG activates protein kinase C, triggering a plethora of molecular and intracellular pathways, such as FASN expression and mitogen-activated protein kinase (MAPK) signaling, leading to *de novo* lipogenesis (DNL), adipocyte hypertrophy, and oxidative inflammation (Forrester et al., 2018; Zorad et al., 2006; Zorad, Fickova, Zelezna, Macho, & Kral, 1995).

Interestingly, the AT_2 gene (*Agtr2*) has also been identified as a genetic marker strongly associated with low-carbohydrate dieting for fat loss (Seip et al., 2008). The AT_2 receptor may be activated by Ang(1-7), which is synthesised from Ang-I or -II, and couples to G_i proteins to stimulate PPAR-γ expression, AMPK signaling and the production of anti-inflammatory adipokines in adipose tissue (Gallo-Payet et al., 2012; Than et al., 2017). Through these mechanisms and others, Ang(1-7) has ameliorating effects on IR, fatty liver, obesity and adipogenic differentiation in rats receiving a high-fructose diet (Giani et al., 2009; Marcus et al., 2013). On the other hand, the main receptor for Ang(1-7) is the orphan G-protein coupled Mas receptor, and when activated facilitates lipolysis, glucose homeostasis and reduces adipose tissue inflammation through the induction of GLUT4/GLUT4 and HSL, and repression of leptin and transforming growth factor (TGF)-β

expression (Cao, Yang, Xin, Xie, & Yang, 2014; Oh et al., 2012; Santos et al., 2003; S. H. Santos et al., 2008). It has been reported that the Ang(1-7)–Mas–HSL axis is at least in part involved in the weight loss mechanism of captopril (Oh et al., 2012). Conversely a high-salt diet may reduce systemic Ang(1-7) levels (Shimoura et al., 2017) and presumably AT_2 and Mas receptor activation, albeit further studies are required to corroborate this.

Given the mechanism(s) of interaction between captopril and salt remains largely unknown, the aim of the current study was to further investigate this interaction on a molecular level in liver and visceral adipose tissues (VAT) of mice maintained on a HFD using transcriptomics analyses. These two tissues were selected as they are the major sites of *de novo* lipogenesis and FA synthesis (Hellerstein et al., 1996). In order to determine whether Ang-II and/or Ang(1-7) may be a factor in the interaction between the two factors, we begin with assessing classically known molecular markers of the Ang-II and Ang(1-7) signaling pathways within both tissues. We also aim to further identify novel molecular mechanisms of action underlying the interaction effect of captopril and dietary salt on bodyweight and body fat. We hypothesise that the liver and VAT transcriptomes of mice treated with captopril to reflect a gene expression profile that is altered in the opposite direction when treatment is administered alongside a diet that exceeds 86.0mg day^{-1} of salt, abolishing the bodyweight and fat loss efficacy of captopril.

Methods

Isolation of total RNA, library construction and RNA sequencing

Total RNA was extracted from liver tissues (n=3 per tissue per treatment group) using RNeasy Mini Kit (Qiagen GmbH, Hilden, Germany) according to manufacturer's protocol. Approximately 100mg of tissue samples were homogenized in 1ml of lysing buffer with 10µl β-mercaptethanol (Sigma Aldrich, USA) using the Precellys 24 homogeniser (Peqlab, Erlangen, Germany) and ceramic beads (1.4mm diameter). Extracts were then purified using the RNeasy MinElute Cleanup Kit (Qiagen GmbH, Hilden, Germany). RNA quality and concentration was determined using a microchip electrophoresis system (MCE-202 MultiNA, Shimadzu Corporation) with the RNA reagent kit (Shimadzu Corporation) according to manufacturer's protocol. The quantified samples with an RNA integrity number (RIN) greater than 8.0 were used and shipped to AgriBio (Bundoora, AUS) for RNAseq library construction.

A total of 12 separate sequencing libraries were constructed with the TruSeq Stranded mRNA Library Preparation Kit (Illumina, San Diego, CA, USA) according to manufacturer's protocol. Library quality was determined using the Qubit dsDNA HS Assay kit (ThermoScientific) on the Qubit® 3.0 Flurometer (Life Technologies). The average fragment size for each library was approximately 250bp. Prior to sequencing, 12 individually indexed libraries were pooled in equimolar quantities and sequenced using 150bp pair-end sequencing on one lane of an Illumina NextSeq500, generating approximately x-y million 150bp paired-end reads per tissue per treatment.

RNAseq data analysis

The quality of raw RNA-sequencing data was evaluated by using FastQC v.0.11.7 (http://www.bioinformatics.bbsrc.ac.uk/projects/fastqc). The paired end reads were trimmed by 10 on the 5' end and 2 on the 3' and mapped to GRCm38 using HISAT2 version 2.0.4. HISAT: a fast spliced aligner with low memory requirements. Mapped BAM files were used as inputs into featureCount version 1.6.3 and gene-level read counts were produced with annotation GENCODE version 12. featureCounts: an efficient general purpose program for assigning sequence reads to genomic features. Standard differential expression analysis was performed using a Bonferroni *p*-value of <0.05.

Gene ontology

Identified DEGs were investigated further using the DAVID (https://david.ncifcrf.gov/) and PANTHER (http://pantherdb.org/) gene ontology (GO) enrichment analysis tool to identify GO terms for significantly enriched biological processes, and functional annotation charts were generated via the Kyoto Encyclopaedia of Genes and Genomes (KEGG) database. DEGs in hepatic and visceral adipose tissues (VATs) were separated in to those that are up- and downregulated in the weight loss responsive CAP group relative to weight loss unresponsive groups, HF and CAPS, and ranked according to increasing *p*-value. GO analysis of DEGs was divided in to three functional

groups, including biological process, molecular function, and cellular component using the PANTHER tool. Genes were also correlated with the biometric traits of animals, gene × trait relationship, and gene × gene relationship using SPSS, and R>0.5 was accepted.

STRING v11 (https://string-db.org/) was used to identify protein-protein interaction (PPI) networks to evaluate the interactive relationship among DEGs (Szklarczyk et al., 2019).

Results

Transcriptome analyses of mouse livers

Differential gene expression in the livers of HF, HFS, CAP and CAPS mice.

As shown in figure 19, RNAseq analysis revealed 1,420 DEGs when comparing hepatic profiles from CAP and HF mice. Among these, 247 were upregulated whilst 1,173 were downregulated. 1,656 DEGs were found in the hepatocytes of CAP compared to CAPS mice, 216 of which were upregulated and 1,440 downregulated, highlighting distinctive transcriptional behaviour of hepatocytes under conditions of a normal-salt and a high-salt HFD. Relative expression patterns of genes were also compared pairwise on the basis of z-score and the highest z-score in CAP relative to HF and CAPS corroborated an upregulation of DEGs involved in rRNA transcription, and the lowest z-score in the CAP group relative to HF and CAPS corroborated a downregulation of DEGs involved in cellular (GO:0044763) and metabolic processes (GO:0008152). Heat maps and the complete list of GO terms are available in supplementary table S1 and figures S1**.** Comparison of DEGs of the CAP group with that of HF and CAPS revealed that the majority of DEGs were modulated by captopril. From a total of 1,440 hepatic DEGs between CAP and HF, 765 were uniquely expressed whereas of the 1,173 DEGs between CAP and CAPS, 1,001 were uniquely expressed, showing that the combination of captopril with a high-salt diet is associated with a unique hepatic profile to that of captopril and a normal-salt diet. To further delineate the influence of captopril and salt on changes of hepatocyte transcriptional programs, Venn diagrams were used to assess the number of DEGs and their overlap among experimental groups of CAP (lean mice), HF, HFS and CAPS (DIO mice). The comparison of transcriptomes of the CAP and HF group with that of the CAP and CAPS groups showed that 97 of the upregulated genes and 558 downregulated genes were associated with the weight loss phenotype since shared between the two comparisons (*i.e.* CAP/CAPS vs CAP/HF). Herein, these DEGs will be referred to as “weight-loss (WL)-related genes”. To delineate the functional relevance of these WL-related genes, we performed GO (table 9; figure 21-22) and KEGG Pathway (figure 23) enrichment analyses. Annotated GO terms of significantly enriched biological processes are listed in table 9. The comparison of transcriptomes of the HF and HFS group with that of CAP and CAPS showed that 3 of the downregulated genes in the CAP group were upregulated by a high-salt diet.

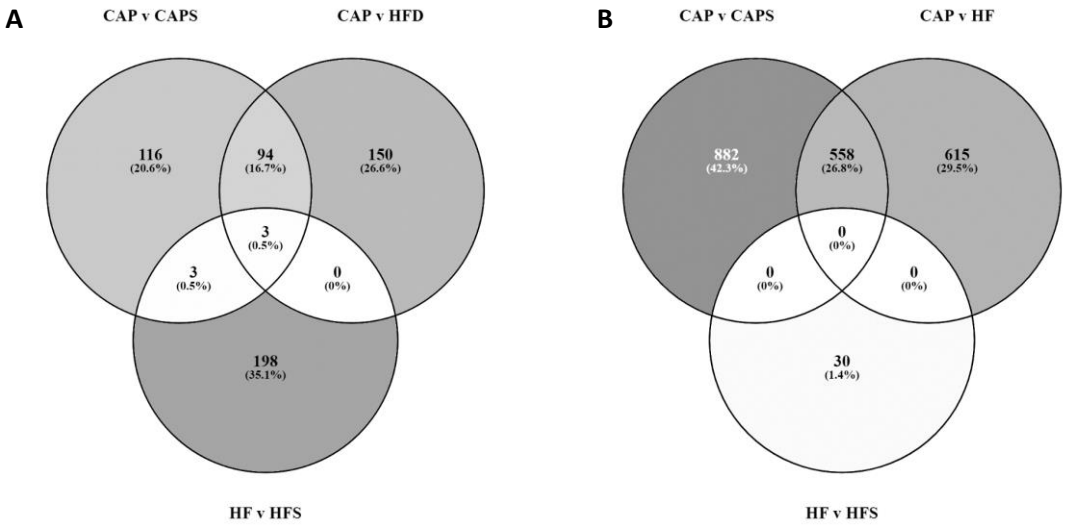

Figure 19. Venn diagram showing the number of DEGs between HF, HFS, CAP and CAPS livers. (A) A total of 366 genes were upregulated and (B) 2, 055 genes were downregulated in the livers of CAP mice relative to HF and CAPS mice. Of the downregulated genes, 3 were specifically upregulated by a high-salt diet and 3 were commonly upregulated by a high-fat diet.

Gene ontology and KEGG pathway enrichment analysis of "weight loss-related" DEGs.

As mentioned, the 97+558 overlapping DEGs identified (figure 19A-B) may be important for the weight loss efficacy of captopril. Based on the hypothesis that a high-salt intake may counteract the molecular effects of captopril to favour DIO, we explored biological processes, molecular functions, cellular components (figure 21-22) and pathways (figure 23) that are significantly enriched ($p<0.05$) focusing on those most relevant to weight loss. To this aim, GO term enrichment and KEGG pathway analysis of WL-specific genes was performed using the DAVID bioinformatics tool.

Table 9. The top-20 biological process GO terms of downregulated WL-related DEGs that are significantly enriched in the livers of lean CAP mice relative to respective DIO-mice.

GO term	Description of biological process	Gene count	*p*-value
Upregulated genes – no significant enrichment of 97 DEGs			
Downregulated genes – 558 DEGs			
GO:0055114	Oxidation-reduction process	46	5.00E-08
GO:0006099	Tricarboxylic acid cycle	9	8.32E-07
GO:0051301	Cell division	29	1.98E-06

GO:0007049	Cell cycle	39	3.26E-06
GO:0015031	Protein transport	36	2.14E-05
GO:0007067	Mitotic nuclear division	21	9.49E-05
GO:0010824	Regulation of centrosome duplication	5	0.00130
GO:0006974	Cellular response to DNA damage stimulus	24	0.00153
GO:0006606	Protein import into nucleus	8	0.00172
GO:0048146	Positive regulation of fibroblast proliferation	8	0.00207
GO:0006098	Pentose-phosphate shunt	4	0.00218
GO:0048280	Vesicle fusion with Golgi apparatus	4	0.00218
GO:0007080	Mitotic metaphase plate congression	6	0.00227
GO:0008340	Determination of adult lifespan	5	0.00238
GO:0008152	Metabolic process	25	0.00251
GO:0006997	Nucleus organization	5	0.00284
GO:0043123	Positive regulation of I-κB kinase/NF-κB signaling	12	0.00291
GO:0034976	Response to endoplasmic reticulum stress	8	0.00501
GO:0045740	Positive regulation of DNA replication	6	0.00642
GO:0098609	Cell-cell adhesion	13	0.00646

GO terms for HFD-related genes that are upregulated in response to a high-fat diet are listed in supplementary table S4; reference figure 19A. PPI network analysis did not identify interactions between HFD-related genes.

GO terms for genes that are reversely regulated by salt (otherwise upregulated by captopril) are listed in supplementary table S4. PPI network analysis did not identify interactions between aforementioned genes.

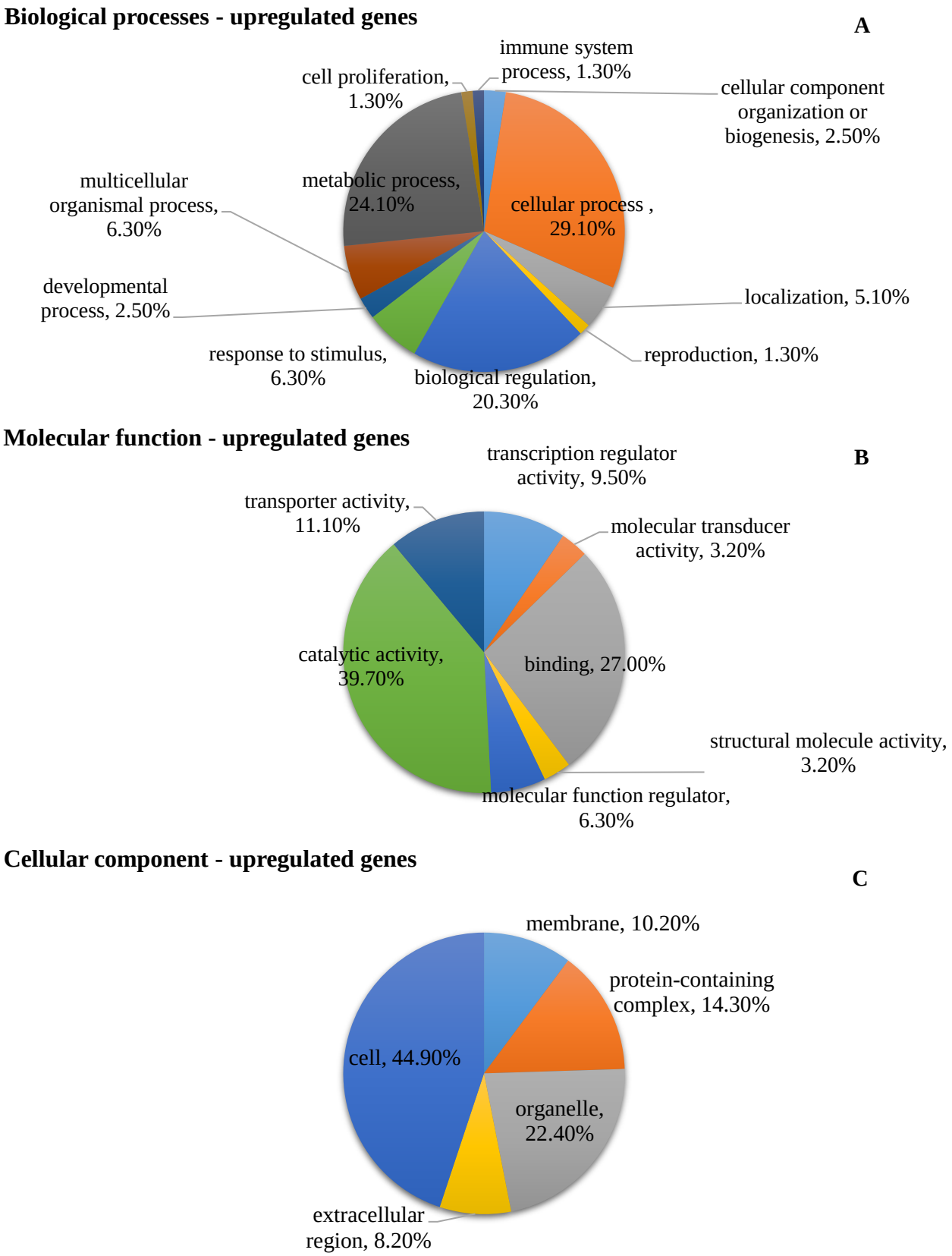

Figure 20. Gene ontology enrichment analysis of **upregulated** WL-related DEGs in liver tissues divided in to three functional groups: (A) biological processes, (B) molecular function, and (C) cellular component.

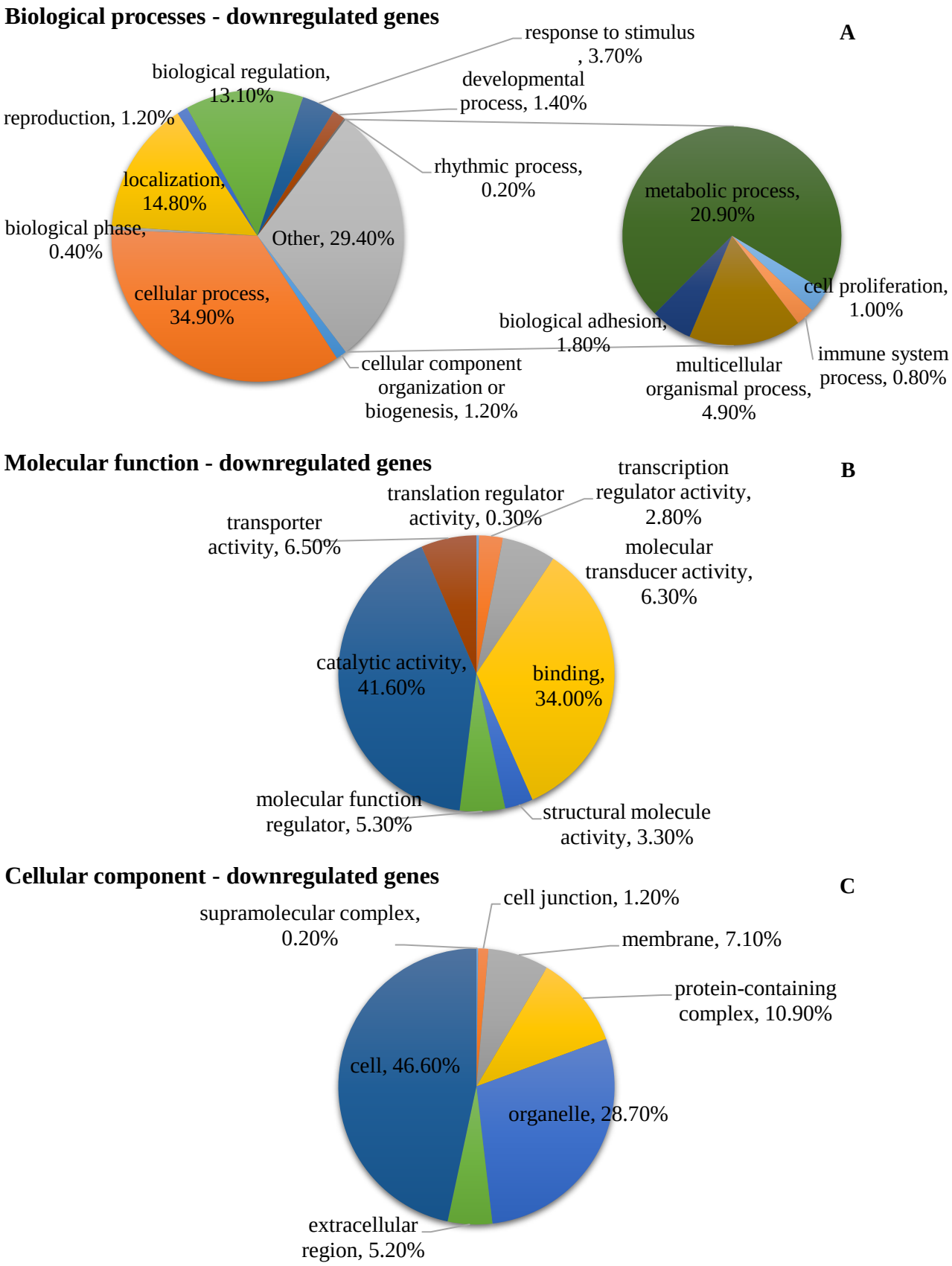

Figure 21 Gene ontology enrichment analysis of downregulated WL-related DEGs in liver tissues divided in to three functional groups: (A) biological processes, (B) molecular function, and (C) cellular component.

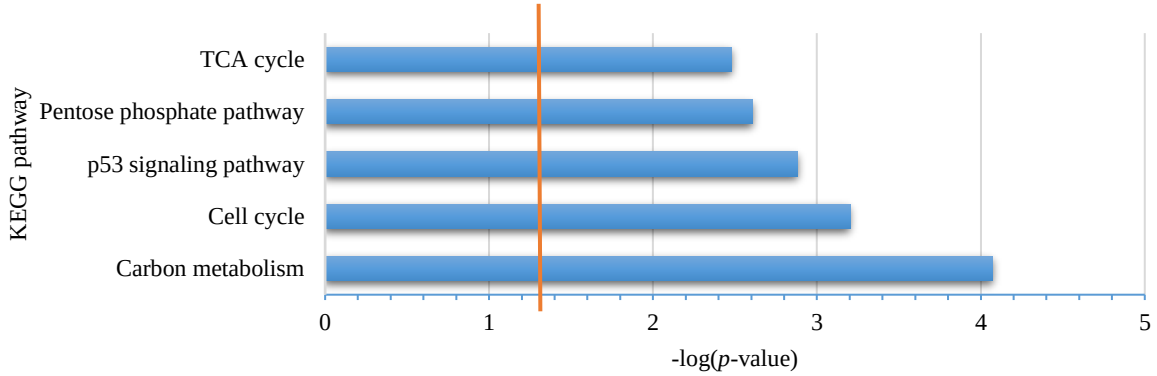

Figure 22. KEGG pathway enrichment analysis of the top-5 WL-related DEGs that are downregulated in the livers of CAP mice against that of DIO phenotypes of HF and CAPS mice. Log *p*-values have been reported on the x-axis and orange lines in panels represent the threshold significance for enrichment, $p<0.05$.

Histograms represent significant genes (*p*-value <0.05). As shown in figure 20, 21 and 22, the most enriched pathways WL-related DEGs were associated with included that of cellular processes (GO:0009987) and metabolic processes (GO:0008152), reflecting modulation of genes encoding enzymes involved in cell cycle regulation, p53 signaling, carbon metabolism, the pentose phosphate pathway and TCA cycle.

Differentially expressed genes in liver tissues

Table 10. Differentially expressed genes of liver ACE–Ang-II–AT_{1A} receptor and Ang(1-7)–ACE2–Mas receptor–HSL signaling axes and their interaction effects. Pathway associated genes described by Forrester et al. (2018), Murphy, Wong, and Bezuhly (2015), Oh et al. (2012), Taskin and Guven (2017).

Gene Symbol	Gene name	mRNA expression (FPKM)				CAP/HF	CAP/CAPS	*p*-value
		HF	**HFS**	**CAP**	**CAPS**	**log_2FC**	**log_2FC**	
Ace	Angiotensin-converting enzyme	0.49	0.22	0.34	0.40	0.49	0.22	0.15
Ace2	Angiotensin-converting enzyme2	0.11	0.13	0.16	0.054	0.60	1.60	0.33
Agt	Angiotensinogen	406.54‡	315.76	645.49*†	356.56‡	0.67	0.86	0.17
Agtr1a	Angiotensin II, receptor type 1a	21.74	14.47	13.10	19.99	-0.73	-0.61	0.13
Atp6ap2	Pro-renin receptor	11.76‡	7.08	3.16*	11.23	-1.90	-1.83	0.023
Calm1	Calmodulin 1	81.50‡	62.36	56.02*†	81.94‡	-0.54	-0.55	0.020
Ccnb1	Cyclin B1	0.39§‡	0.11*	0.010*†	0.24‡	-5.33	-4.62	0.0015
Cdc42	Cell division control protein 42 homolog	76.89‡	49.60	31.53*†	68.03‡	-1.29	-1.11	0.011
Col1a1	Collagen type l α 1 chain	9.84‡	3.80	1.64*†	4.53‡	-2.59	-1.47	0.059
Csnk1a1	Casein kinase 1α	14.33‡	11.77	9.79*†	15.17‡	-0.55	-0.63	0.0069
Dusp16	Dual specificity phosphatase 16	6.79‡	5.20	4.27*†	6.88‡	-0.67	-0.69	0.037
Egfr	Epidermal growth factor receptor	9.77‡	15.23	29.73*†	12.83‡	1.61	1.21	0.010

Egr2	Early growth response protein 2	0.51	0.082	0.076†	0.44‡	-2.75	-2.52	0.0069
Erc1	ELKS/RAB6-interacting/CAST family member 1	1.61‡	1.47	1.27*†	1.79‡	-0.33	-0.49	0.056
Fosl1	Fos-like antigen 1	0.64‡	0.067	0.047*†	0.53‡	-3.75	-3.49	0.0023
Fkbp1a	FK506 binding protein 1a	58.63‡	43.26	30.93*†	59.16‡	-0.92	-0.94	0.018
Gnai1	Guanine nucleotide binding protein, α inhibiting 1	5.36‡	4.36	1.85*†	4.97‡	-1.54	-1.43	0.078
Gnb1	Guanine nucleotide-binding protein subunit β-1	0.80‡	0.77	0.62*†	0.80‡	-0.36	-0.37	0.020
Gnb5	Guanine nucleotide-binding protein subunit β-5	0.59‡	0.40	0.30*†	0.41‡	-0.97	-0.46	0.028
Gngt1	Guanine nucleotide binding protein, γ transducing activity	2.21‡	1.75	0.77*†	2.19‡	-1.53	-1.52	0.027
Itgav	Integrin α V	2.01‡	1.16	0.85*†	1.78‡	-1.25	-1.07	0.0067
Ikbkg	Inhibitor of κB kinase γ	13.76‡	10.16	10.08*†	14.23‡	-0.45	-0.50	0.028
Itpr2	Inositol triphosphate	1.99‡	2.40	4.07*†	2.55‡	1.03	0.68	0.0042
Jun	Jun proto-oncogene	25.664	17.63	7.13*†	20.38‡	-1.85	-1.51	0.048
Klk1b4	Kallikrein 1-related pepidase b4	11.97‡	8.34	3.61*†	8.68‡	-1.73	-1.27	0.031
Lamb3	Laminin, β 3	2.77‡	2.31	1.62*†	2.81‡	-0.77	-0.79	0.033
Lipe	Lipase, hormone sensitive (HSL)	5.56	5.43	5.65	5.40	0.023	0.067	0.95
Lpar1	Lysophosphatidic acid receptor 1	2.13‡	2.09	1.01*†	2.54‡	-1.08	-1.34	0.070
Mapk1	mitogen-activated protein kinase 9 (ERK2)	9.13‡	6.68	4.02*†	8.54‡	-1.18	-1.09	0.066

Mapk8	Mitogen-activated protein kinase 8 / c-Jun terminal kinase (JNK)	3.15‡	2.58	2.16*†	3.61‡	-0.55	-0.74	0.026
Mapk9	Mitogen-activated protein kinase 9	11.86‡	8.72	6.64*†	12.01‡	-0.84	-0.86	0.037
Mas1	Ang(1-7) Mas receptor	0.75	0.40	0.24	0.50	-1.68	-1.10	0.078
Mme	Neprilysin	5.23‡	3.77	2.82*†	5.19‡	-0.89	-0.88	0.045
Nln	Neurolysin	9.65	7.28	4.59†	7.86‡	-1.07	-0.78	0.16
Pdgfra	Platelet derived growth factor receptor, α	1.31‡	0.87	0.65*†	0.99‡	-1.02	-0.61	0.025
Pdgfa	Platelet derived growth factor, α	11.14‡	7.12	5.52*†	8.90‡	-1.01	-0.69	0.031
Phlpp1	PH domain and leucine rich repeat protein phosphatase1	2.99‡	2.02	1.44*†	2.77‡	-1.05	-0.94	0.010
Plcb1	Phospholipase C	1.033‡	0.699	0.499*†	1.186‡	-1.049	-1.249	0.033
Ppp2ca	Protein phosphatase 2, catalytic subunit, α	27.93‡	21.23	14.31*†	28.25‡	-0.97	-0.98	0.018
Prkca	Protein kinase C, α	2.25‡	1.63	0.99*	2.67	-1.184	-1.43	0.038
Prkcb	Protein kinase C, β	0.84	0.57	0.42†	0.94‡	-1.01	-1.17	0.053
Prkci	Protein kinase C, ι	3.53‡	3.23	2.23*†	3.82‡	-0.66	-0.78	0.062
Rhoq	Ras homolog family member Q	4.35‡	2.51	1.60*†	3.72‡	-1.45	-1.22	0.015
Rock2	Rho associated coiled-coil containing protein kinase 2	6.26‡	5.07	4.16*†	6.01‡	-0.59	-0.53	0.11
Ralbp1	RalA binding protein 1	12.66‡	8.29	6.540*†	11.12‡	-0.95	-0.77	0.035

Rap1b	Ras related protein 1b	43.44‡	30.43	23.20*†	41.03‡	-0.91	-0.82	0.010
Rasa2	Ras p21 protein activator 2	0.24‡	0.14	0.10*†	0.18‡	-1.22	-0.83	0.026
Skp1a	S-phase kinase-associated protein 1A	147.98‡	105.26	76.48*†	150.77‡	-0.95	-0.98	0.033
Smad2	SMAD family member 2	2.16‡	1.58	0.76*†	2.10‡	-2.16	-1.58	0.051
Stradb	STE20-related kinase adapter protein β	9.477‡	5.758	2.962*†	8.691‡	-1.678	-1.553	0.024
Tgif1	TGFβ-induced factor homeobox 1	9.37‡	6.64	5.88*†	8.09‡	-0.67	-0.46	0.093
Ube2n	Ubiquitin-conjugating enzyme E2N	16.85‡	14.13	9.47*†	17.59‡	-0.83	-0.89	0.031
Wnt5a	Wingless-type MMTV integration site family, member 5A	0.59‡	0.22	0.13*†	0.37‡	-2.18	-1.49	0.010
Ywhab	14-3-3 protein β/α	65.15‡	48.66	36.45*†	66.22‡	-0.84	-0.86	0.017
Ywhag	14-3-3 protein γ	29.82‡	23.31	15.26*†	30.39‡	-0.97	-0.99	0.017
Ywhah	14-3-3 protein η	37.99‡	23.76	14.60*†	35.01‡	-1.38	-1.26	0.0026

Fold change (FC)

p-value<0.05; * vs. HF, § vs. HFS, ‡ vs. CAP, † vs. CAPS.

Table 11. Differentially expressed genes of carbon metabolism, TCA cycle and their interaction effect in liver tissues.

Gene symbol	Gene name	mRNA expression (FPKM)				CAP/HF	CAP/CAPS	*p*-value
		HF	**HFS**	**CAP**	**CAPS**	**log_2FC**	**log_2FC**	
Glycolysis								
Hk2	Hexokinase 2	3.38‡	1.849	0.71*†	2.16‡	-2.24	-1.59	0.010
Pfkm	Phosphofructokinase	5.21‡	3.914	2.19*†	4.39‡	-1.25	-1.01	0.037
Aldob	Aldolase B, liver type	3920.90‡	2623.67	2107.53*	2907.62	-0.90	-0.464	0.091
Tpi1	Triose phosphate isomerase 1	227.66	195.76	186.31	231.34	-0.29	-0.312	0.15
Gapdh	Glyceraldehyde-3-phosphate dehydrogenase	199.28	130.43	142.10	149.38	-0.49	-0.072	0.29
Gpd2	Glycerol-3-phosphate dehydrogenase 2	10.88‡	6.55	5.13*†	9.06‡	-1.09	-0.821	0.037
Pgk1	Phosphoglycerate kinase	5.21	4.30	2.78	5.59	-0.91	-1.011	0.14
Pgam1	Phosphoglycerate-mutase	240.88‡	189.95	161.44*†	239.81‡	-0.58	-0.57	0.044
Pklr	Pyruvate kinase	57.14	32.26	16.93	38.81	-1.76	-1.20	0.19
Ldha	Lactate dehydrogenase	182.30‡	125.70	75.40*†	187.08‡	-1.27	-1.31	0.041
Glucogenesis								
G6pc	Glucose-6-phosphatase	136.47	110.11	88.59	123.08	-0.62	-0.47	0.44
Fbp1	Fructose 1,6-bisphosphatase	269.42	186.39	100.50	225.65	-1.42	-1.17	0.11

Tpi1	Triose phosphate isomerase 1	227.66	195.76	186.31	231.34	-0.29	-0.31	0.15
Pgam1	Phosphoglycerate-mutase	240.88‡	189.95	161.44*†	239.81‡	-0.58	-0.57	0.044
Pcx	Pyruvate carboxylase	201.90	153.56	155.48	183.40	-0.38	-0.24	0.23
Pck1	Phosphoenolpyruvate carboxykinase 1	393.87	340.97	243.58	341.37	-0.69	-0.49	0.47
Pyruvate dehydrogenase (PDH) complex								
Pdhx	Pyruvate dehydrogenase complex, X	11.21‡	8.82	6.63*	10.03	-0.76	-0.60	0.086
Pdha1	Pyruvate dehydrogenase E1 α1	35.38	29.45	25.77	36.04	-0.46	-0.48	0.15
Pdp1	Pyruvate dehydrogenase phosphatase 1	0.20‡	0.059	0.051*†	0.16‡	-1.20	-1.63	0.017
Pdk4	Pyruvate dehydrogenase kinase, isozyme 4	11.05‡	9.31	2.40*†	9.90‡	-2.21	-2.05	0.11
Pklr	Pyruvate kinase	57.14	32.26	16.93	38.81	-1.76	-1.20	0.19
Glycogen metabolism								
Pgm1	Phosphoglycero-mutase	92.94	80.56	69.39	95.35	-0.42	-0.46	0.22
Ugp2	Uridine diphosphoglucose pytophosphorylase	196.37‡	118.29	91.54*	163.61	-1.10	-0.84	0.051
Gys2	Glycogen synthase	54.69	45.98	32.13	51.29	-0.77	-0.68	0.25
Pygl	Liver glycogen phosphorylase	193.19‡	147.84	139.16*	181.73	-0.47	-0.39	0.050
Pentose phosphate pathway								
Hk2	Hexokinase	3.38‡	1.85	0.71*†	2.16‡	-2.24	-1.59	0.010

G6pdx	Glucose-6-phosphate dehydrogenase	2.96	1.63	2.41	2.18	-0.30	0.14	0.32
Pgls	Phospho-6-gluconolactonase	43.88	37.27	56.25	44.73	0.36	0.33	0.76
Pgd	Phospho-6-gluconate dehydrogenase	24.92‡	16.48	12.30*†	20.66‡	-1.02	-0.75	0.029
Rpia	Ribose-5-phosphate isomerase	5.02‡	3.81	3.21*†	4.38‡	-0.645	-0.45	9.6E-5
Rpe	Ribulose-5-phosphate 3-epimerase	6.32	3.63	2.94	6.56	-1.11	-1.16	0.12
Tkt	Transketolase	72.97‡	52.97	36.05*†	62.86‡	-1.02	-0.80	0.032
Taldo1	Transaldolase	170.98‡	137.65	108.53*†	177.82‡	-0.66	-0.71	0.037
Prps2	Phosphoribosyl pyrophosphate synthetase 2	6.50‡	4.56	3.09*†	5.58‡	-1.072	-0.85	0.030
Polyol pathway								
Sord	Sorbitol dehydrogenase	997.99	927.76	815.81†	1155.98‡	-0.29	-0.50	0.13
Gluconate shunt (incompletely elucidated)								
Idnk	Gluconate kinase	34.49	34.48	40.45	38.08	0.23	0.087	0.77
Inositol biosynthesis (incompletely elucidated)								
Isyna1	Inositol-3-phosphate synthase	4.13	3.040	3.66	3.79	-0.18	-0.052	0.53
Impa1	Inositol monophosphatase	17.69	12.95	10.24	19.27	-0.788	-0.91	0.062
Fructose metabolism (liver)								
Aldob	Aldolase B, liver-type	3920.90‡	2623.67	2107.53*	2907.63	-0.90	-0.46	0.091

Khk	Ketohexokinase	917.12	733.33	865.44	778.87	-0.08	0.15	0.70
Tricarboxylic acid cycle								
Aco1	Aconitase 1	57.91‡	48.35	34.23*†	66.51‡	-0.76	-0.96	0.038
Acly	ATP citrate lyase	75.40	46.34	34.48	48.48	-1.13	-0.49	0.32
Cs	Citrate synthase	145.15‡	112.15	95.49*†	148.29‡	-0.60	-0.64	0.0162
Dlst	Dihydrolipoyllysine- succinyltransferase component	80.61‡	63.42	42.16*†	77.06‡	-0.94	-0.87	0.050
Fh1	Fumarate hydratase 1	81.60	62.46	75.023	68.21	-0.121	0.14	0.68
Idh2	Isocitrate dehydrogenase ($NADP^+$)	62.81‡	46.60	28.84*†	55.34‡	-1.12	-0.94	0.098
Mdh1	Malate dehydrogenase 1	274.99‡	209.33	144.48*	269.32	-0.93	-0.90	0.13
Me1	Malic enzyme	135.76‡	89.67	33.83*†	116.79‡	-2.01	-1.79	0.22
Ogdh	Oxoglutarate dehydrogenase	47.73‡	37.92	33.19*†	49.57‡	-0.52	-0.58	0.070
Sdha	Succinate dehydrogenase complex, subunit A	94.11‡	81.43	61.32*†	101.49‡	-0.62	-0.73	0.055
Sdhd	Succinate dehydrogenase complex, subunit D	246.26‡	169.05	76.18*†	203.80‡	-1.69	-1.42	0.033
Sucla2	Succinate-Coenzyme A ligase	27.91‡	21.31	12.21*†	27.41‡	-1.19	-1.17	0.044
Sucnr1	Succinate receptor 1	19.77§‡	10.46*	4.48*†	17.52‡	-2.14	-1.97	0.15
Anaplerotic metabolism								
Glud1	Glutamate dehydrogenase	329.10	236.00	283.22	347.71	-0.22	-0.30	0.048

Glul	Glutamine synthetase	582.71	605.48	648.47	844.18	0.15	-0.38	0.18
Mut	Methylmalonyl-CoA mutase	30.50	21.90	17.63	30.33	-0.79	-0.78	0.097
Got1	Glutamic-oxaloacetic transaminase, 1	41.68	39.29	41.60	42.71	-0.003	-0.038	0.86
Adsl	Adenylosuccinate lyase	3.39	2.63	2.85	2.60	-0.25	0.13	0.72
Other								
Slc2a2	Glucose transporter type 2 (GLUT2)	46.25‡	23.66	17.16*	38.52	-1.43	-1.17	0.58

Fold change (FC)

p-value<0.05: * vs. HF, § vs. HFS, ‡ vs. CAP, † vs. CAPS.

Table 12. Differentially expressed genes of cell cycle regulation and p53 signaling, and their interaction effect in liver tissue.

Gene symbol	Gene name	mRNA expression (FPKM)				CAP/HF	CAP/CAPS	*p*-value
		HF	**HFS**	**CAP**	**CAPS**	**log_2FC**	**log_2FC**	
Cell cycle								
Ccnb1	Cyclin B1	0.39‡	0.11	0.010*†	0.24‡	-5.33	-4.62	0.0015
Cdk1	Cyclin dependent kinase 1	2.55‡	1.41	0.44*†	2.12‡	-2.52	-2.26	0.010
Chek1	Checkpoint kinase 1	0.21‡	0.24	0.038*†	0.35‡	-2.47	-3.19	0.0029
Cdc25c	M-phase inducer phosphatase 3	0.12‡	0.046	0.021*†	0.13‡	-2.51	-2.65	0.0028

Skp1a	S-phase kinase-associated protein 1A (SCF)	147.98‡	105.26	76.48*†	150.77‡	-0.95	-0.98	0.033
Mad2l1	MAD2 mitotic arrest deficient-like 1	1.33‡	0.82	0.32*†	1.02‡	-2.05	-1.67	0.040
Mcm2	Minichromosome maintenance complex component 2	3.29‡	2.39	1.08*†	3.29‡	-1.60	-1.60	0.014
Mcm3	Minichromosome maintenance complex component 3	3.37‡	2.54	1.054*†	3.29‡	-1.68	-1.64	0.037
Mcm5	Minichromosome maintenance complex component 5	1.59‡	1.09	0.26*†	1.18‡	-2.62	-2.19	0.066
Mcm6	Minichromosome maintenance complex component 6	2.84‡	1.34	0.53*†	1.92‡	-2.43	-1.86	0.019
Ywhab	14-3-3 protein β/α	65.15‡	48.66	36.45*†	66.22‡	-0.84	-0.86	0.017
Ywhag	14-3-3 protein γ	29.82‡	23.31	15.26*†	30.39‡	-0.97	-0.99	0.017
Ywhah	14-3-3 protein η	37.99‡	23.76	14.60*†	35.01‡	-1.38	-1.26	0.0026
p53 signaling pathway								
Bbc3	Bcl-2-binding component 3 (PUMA)	8.89‡	6.77	5.01*†	7.45‡	-0.83	-0.57	0.11
Ccnb1	Cyclin B1	0.39‡	0.11	0.010*†	0.24‡	-5.33	-4.62	0.0015
Ccng1	Cyclin G1	16.66‡	10.63	7.87*†	17.32‡	-1.08	-1.14	0.0080
Cdk1	Cyclin dependent kinase 1 (Cdc2)	2.55‡	1.41	0.44*†	2.12‡	-2.52	-2.26	0.010
Chek1	Checkpoint kinase 1	0.21‡	0.24	0.038*†	0.35‡	-2.47	-3.19	0.0029
Cycs	Cytochrome c, somatic (Cycts)	29.95‡	17.51	8.47*†	25.29‡	-1.82	-1.58	0.0086
Perp	p53 apoptosis effector	128.44‡	87.90	53.73*†	128.62‡	-1.26	-1.26	0.013

Sesn3	Sestrin-3	2.53‡	1.87	0.84*†	2.68‡	-1.60	-1.68	0.014
Zmat3	Zinc finger matrin-type protein 3 (PAG608)	1.28‡	0.85	0.64*†	1.30‡	-0.99	-1.021	0.017
Other genes of interest								
Pparg	Peroxisome proliferator activated receptor γ	12.00‡	8.73	3.65*†	10.63‡	-1.72	-1.54	0.11
Mdm2	Transformed mouse 3T3 cell double minute 2	6.08	5.21	5.05†	7.21‡	-0.27	-0.51	0.083
Myc	Myelocytomatosis oncogene	4.24‡	2.31	1.69*	3.43	-1.33	-1.019	0.11
Trp53	Transformation related protein 53	4.42	3.49	3.87	3.69	-0.19	0.069	0.70
Trp53bp2	Tumor protein p53 binding protein 2	3.88‡	2.88	2.15*†	3.68‡	-0.85	-0.78	0.073
Trp53inp1	Transformation related protein 53 inducible nuclear protein 1	11.63‡	6.85	4.36*†	10.02‡	-1.42	-1.20	0.040
Stk11	Liver kinase B	31.05‡	31.38	41.86*	34.29	0.43	0.29	0.33

Fold change (FC)

p-value<0.05: * vs. HF, § vs. HFS, ‡ vs. CAP, † vs. CAPS.

Protein–protein interaction (PPI) network analysis.

Nodes represent genes, lines represent the interaction of proteins between genes, and line thickness indicates the strength of data support. Filled nodes represent the structure of proteins.

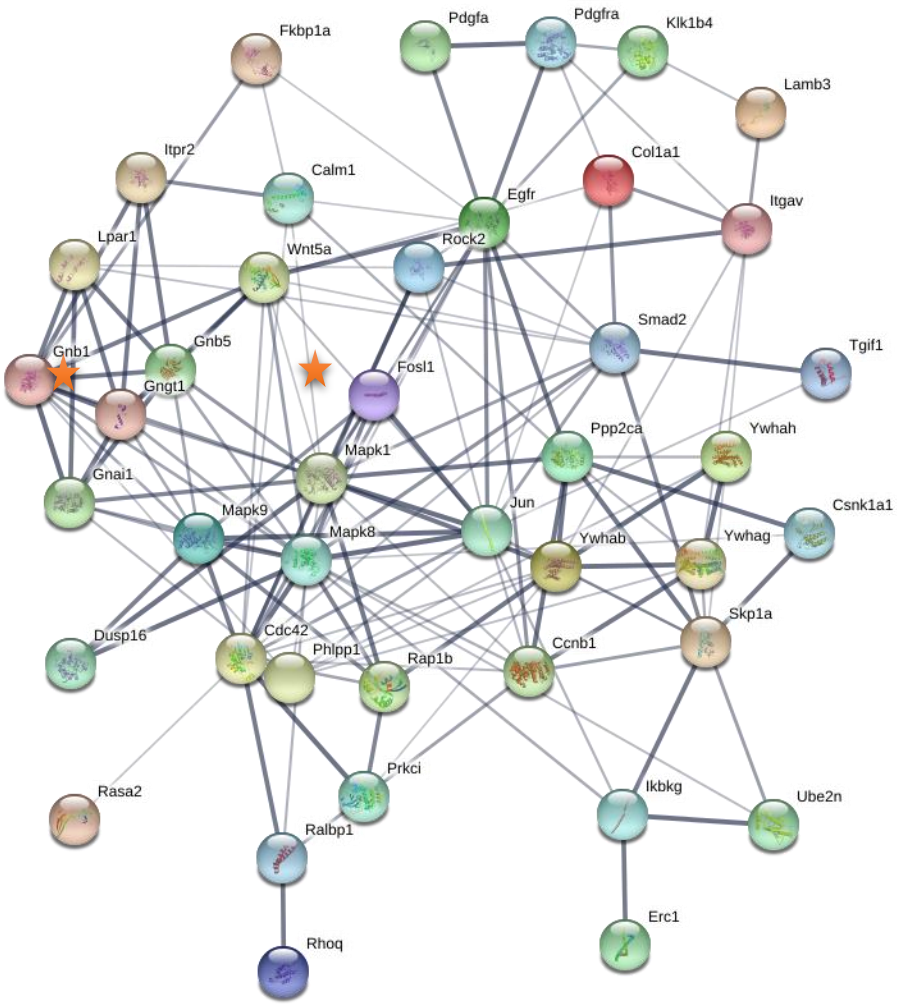

Figure 23. Liver PPI network of the Ang-II–AT_1-receptor interacting G-protein cascade that is significantly modulated by captopril and deregulated when combined with a high-salt diet. *Gnb1* and *Gnb5* are marked by orange stars. Genes and their expression levels are listed in 10. PPI enrichment score: p<1.0E-16.

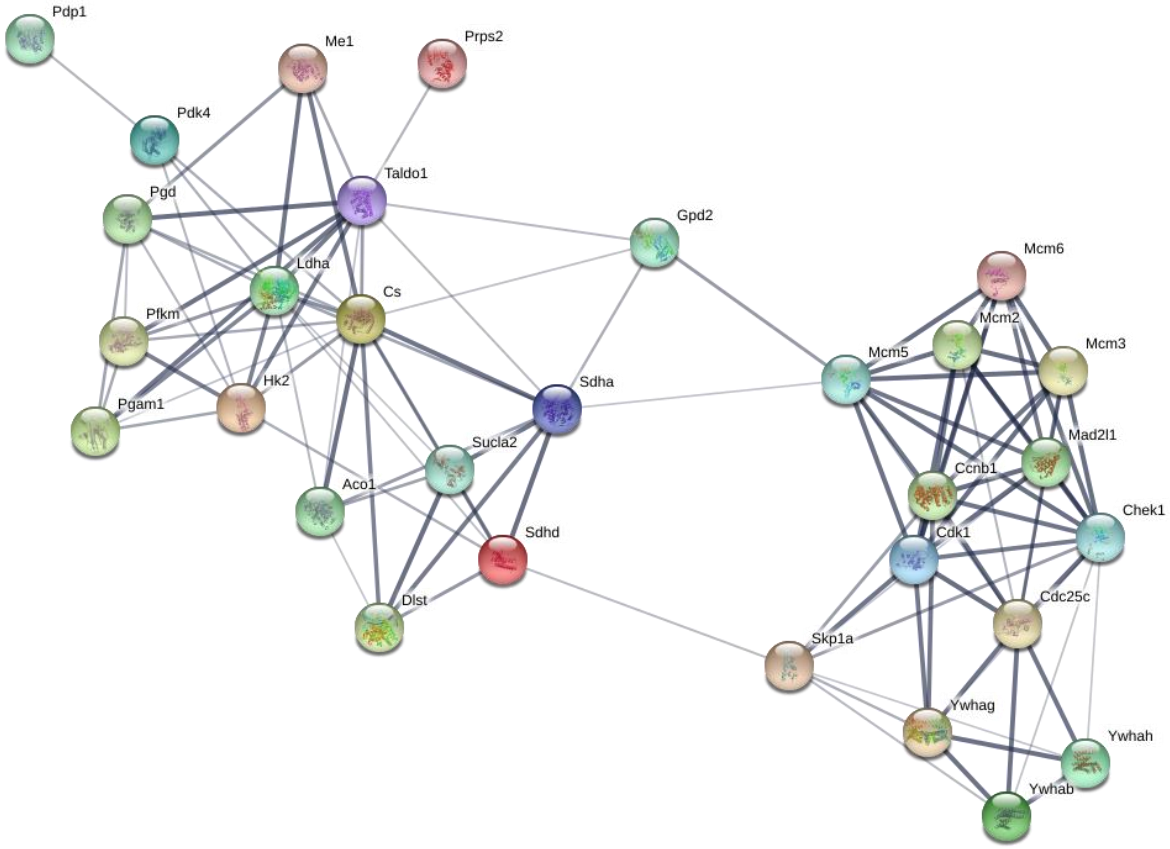

Figure 24. Liver PPI network of DEGs involved in glucose carbon metabolism and cell cycle regulation that is significantly modulated by captopril and deregulated by salt. This figure highlights the relationship between cellular metabolism and cell cycle machinery. Genes and their expression levels are listed in table 11. PPI enrichment score: p<1.0E-16.

Transcriptome analyses of mouse adipose tissues

Differential gene expression in the adipose tissues of HF, HFS, CAP and CAPS mice.

As shown in figure 25, RNAseq analysis revealed 971 DEGs when comparing adipose tissue (AT) profiles from CAP and HF mice. Among these, 719 were upregulated and 252 were downregulated. 2,038 DEGs were found in the ATs of CAP compared to CAPS mice, 1,103 of which were upregulated and 935 downregulated, highlighting distinctive transcriptional behaviour of ATs under conditions of a normal-salt and a high-salt HFD. Unlike liver tissue, comparison of AT DEGs of the CAP group with that of HF and CAPS revealed that the majority of DEGs were upregulated by captopril. From a total of 971 AT DEGs between CAP and HF, 536 were uniquely expressed whereas of the 2,038 DEGs between CAP and CAPS, 1,558 were uniquely expressed, showing that the combination of captopril with a high-salt diet is associated with a unique hepatic profile to that of captopril and a normal-salt diet. To further delineate the influence of captopril and salt on changes of AT transcriptional programs, Venn diagrams were used to assess the number of DEGs and their overlap among experimental groups of CAP (lean mice), HF, HFS and CAPS (DIO mice). As depicted, the comparison of transcriptomes of the CAP and HF group with that of the CAP and CAPS groups showed that 335 of the upregulated genes and 99 downregulated genes were associated with the weight loss phenotype since shared between the two comparisons (CAP/CAPS vs CAP/HF), *i.e.* “weight-loss (WL)-related genes”. To delineate the functional relevance of these WL-related genes in AT samples, we performed GO (figure 28 and 29) and KEGG Pathway (figure 30) enrichment analyses. Annotated GO terms of significantly enriched biological processes are listed in table 13. The comparison of transcriptomes of the HF and HFS group with that of CAP and CAPS showed that 22 of the downregulated genes in the CAP group were upregulated and 27 of the upregulated genes were downregulated in response to a high-salt diet.

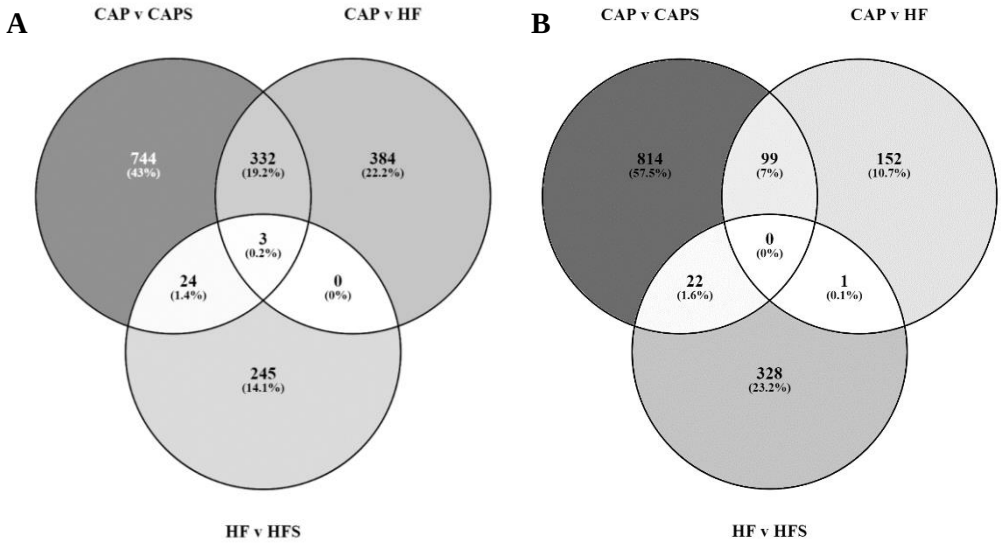

Figure 25. Venn diagram showing the number of DEGs between HF, HFS, CAP and CAPS adipose tissues. (A) A total of 1,487 genes were upregulated and (B) 1,088 genes were downregulated in the livers of CAP mice relative to HF and CAPS mice. Of the up- and down-regulated genes in CAP mice, 24 were specifically downregulated and 22 specifically upregulated by a high-salt diet respectively. Of the upregulated genes, 3 DEGs were downregulated by a high-fat diet.

Gene ontology and KEGG pathway enrichment analysis of "weight loss-related" DEGs.

As mentioned, the 99+335 overlapping DEGs identified in ATs (figure 25A-B) may be important for the weight loss efficacy of captopril. Based on the hypothesis that a high-salt intake may counteract the molecular effects of captopril to favour DIO, we explored biological processes, molecular functions, cellular components (figure 29 and 30) and pathways (figure 31) that are significantly enriched ($p<0.05$) focusing on those relevant to weight loss. To this aim, GO term enrichment and KEGG pathway analysis of WL-related genes was performed using the DAVID bioinformatics tool.

Table 13. Biological process GO terms of upregulated WL-related genes that are significantly enriched in the adipose tissues of lean CAP mice relative to respective DIO-mice.

GO term	Description of biological process	Gene count	*p*-value
Upregulated genes – 335 DEGs			
GO:0008380	RNA splicing	13	4.77E-04
GO:0006397	mRNA processing	15	6.45E-04
GO:0006974	Cellular response to DNA damage stimulus	17	0.00112
GO:0000184	Nuclear-transcribed mRNA catabolic process, nonsense-mediated decay	5	0.00138

GO:0007049	Cell cycle	19	0.00915
GO:0007067	Mitotic nuclear division	11	0.0131
GO:0006351	Transcription, DNA-templated	43	0.0142
GO:0042407	Cristae formation	3	0.0173
GO:0006355	Regulation of transcription, DNA-templated	49	0.0229
GO:0042326	Negative regulation of phosphorylation	3	0.0323
GO:0000398	mRNA splicing, via spliceosome	6	0.0327
GO:0033539	Fatty acid β-oxidation using acyl-CoA dehydrogenase	3	0.0357
GO:0051301	Cell division	12	0.0365
GO:0030968	Endoplasmic reticulum unfolded protein response	4	0.0402
GO:0090292	Nuclear matrix anchoring at nuclear membrane	2	0.0467
GO:0006368	Transcription elongation from RNA polymerase II promoter	3	0.0468
GO:0030308	Negative regulation of cell growth	6	0.0486

Downregulated genes – no significant enrichment of 99 DEGs

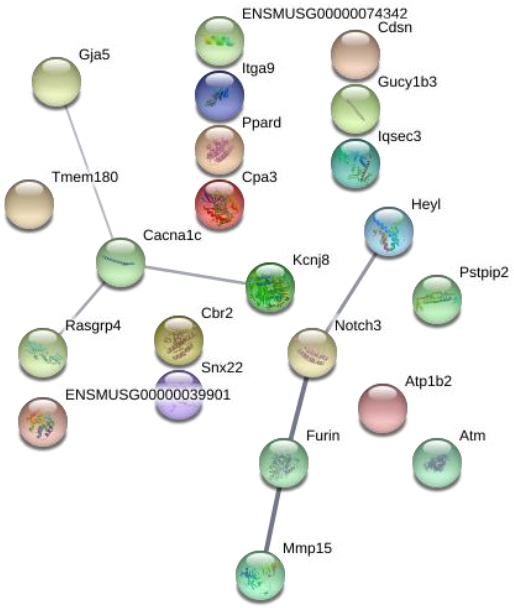

Figure 26. Genes that are reversely regulated by salt in epididymal adipose tissues that is otherwise downregulated by captopril. No significant pathway enrichment was observed. See supplementary table S4 for GO terms of individual DEGs.

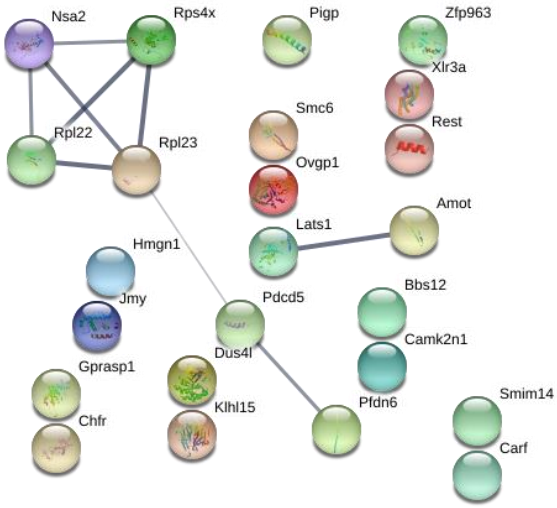

Figure 27. Genes that are reversely regulated by salt in epididymal adipose tissue that is otherwise upregulated by captopril. No significant pathway enrichment was observed. See supplementary table S4 for GO terms of individual DEGs. Note: DEGs that are common amongst all groups (high-fat diet responsive genes) are marked by *.

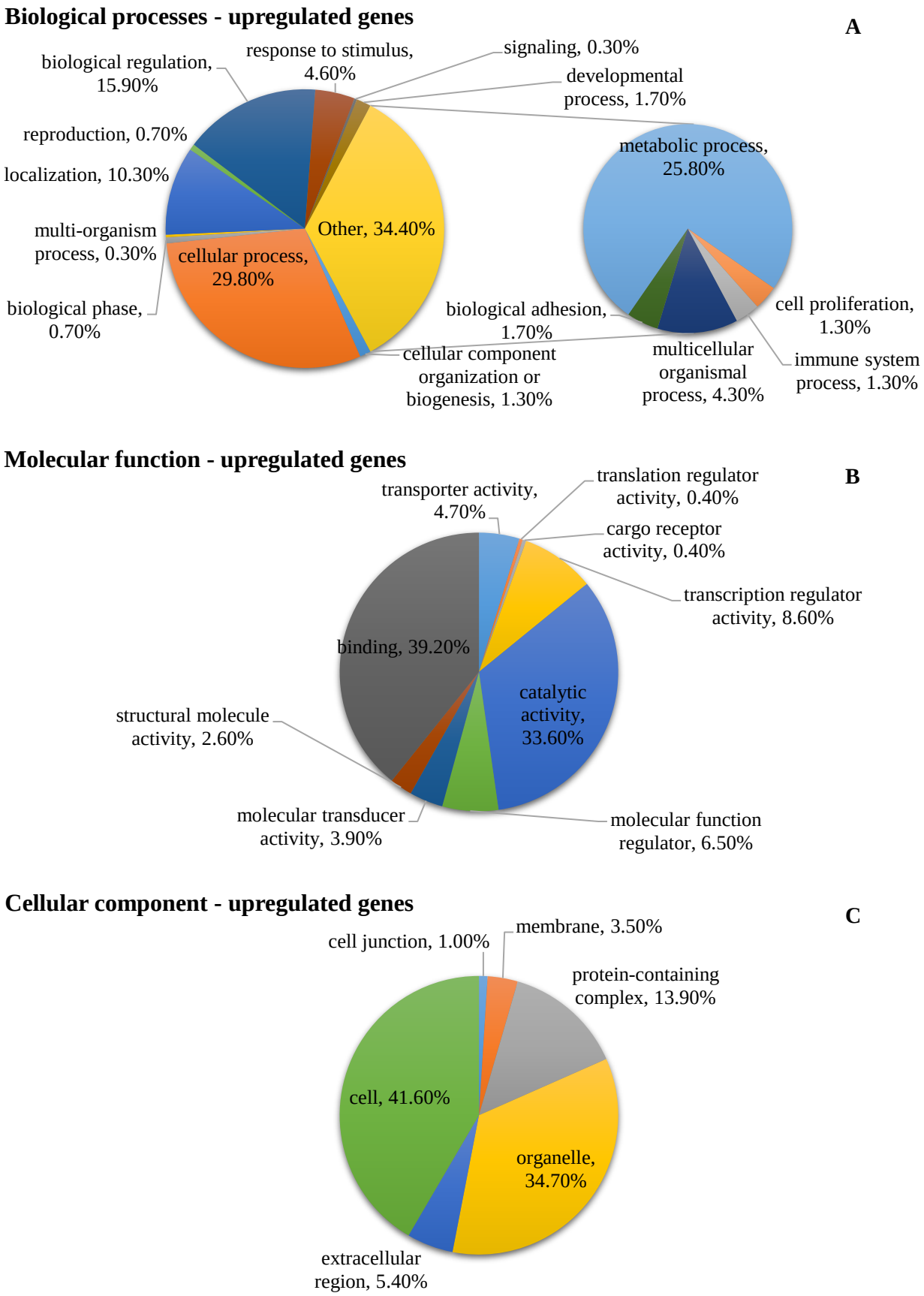

Figure 28. Gene ontology enrichment analysis of upregulated WL-related DEGs in adipose tissue divided in to three functional groups (A) biological processes, (B) molecular function, and (C) cellular component.

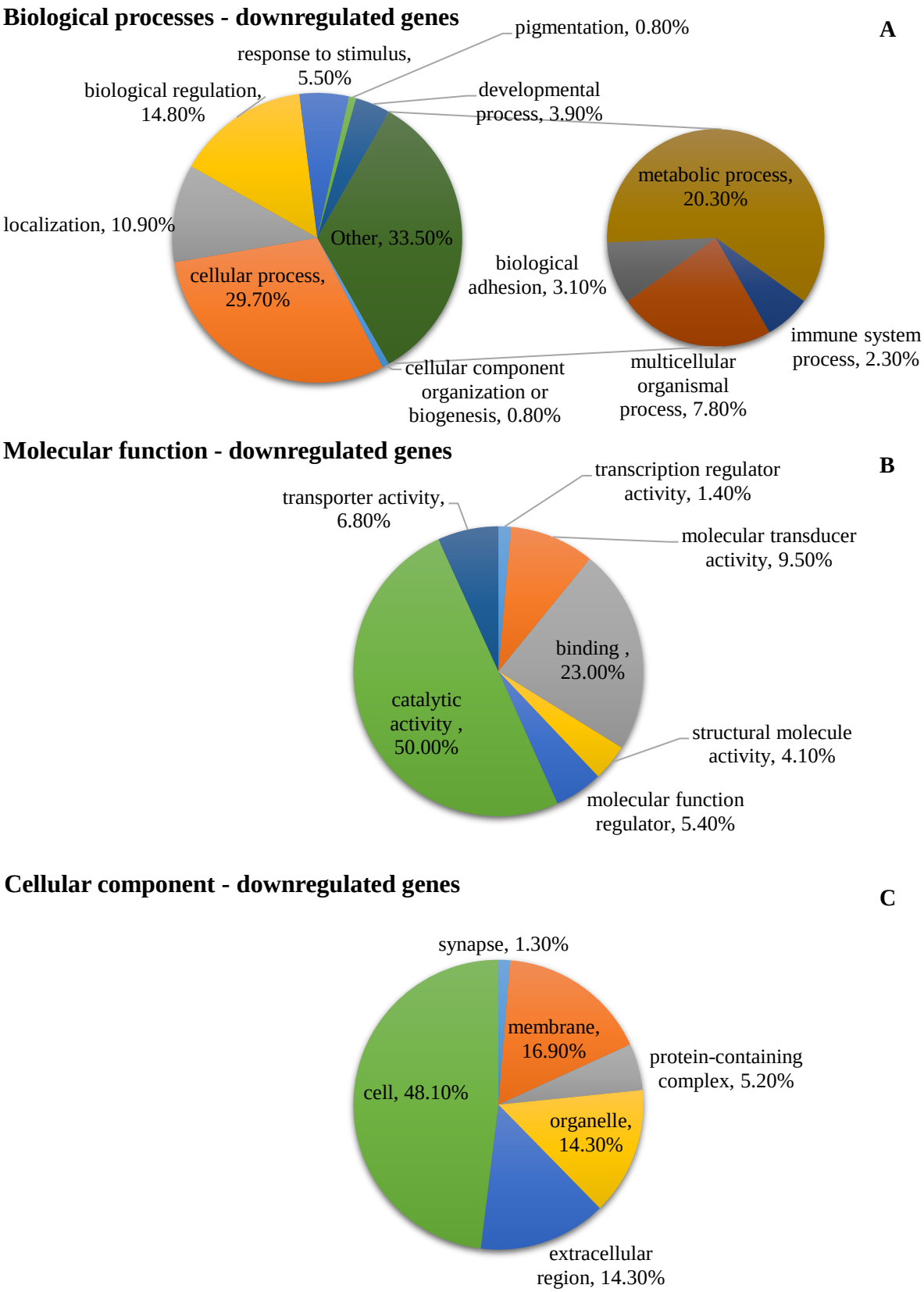

Figure 29. Gene ontology enrichment analysis of downregulated WL-related DEGs in adipose tissue divided in to three functional groups (A) biological processes, (B) molecular function, and (C) cellular component.

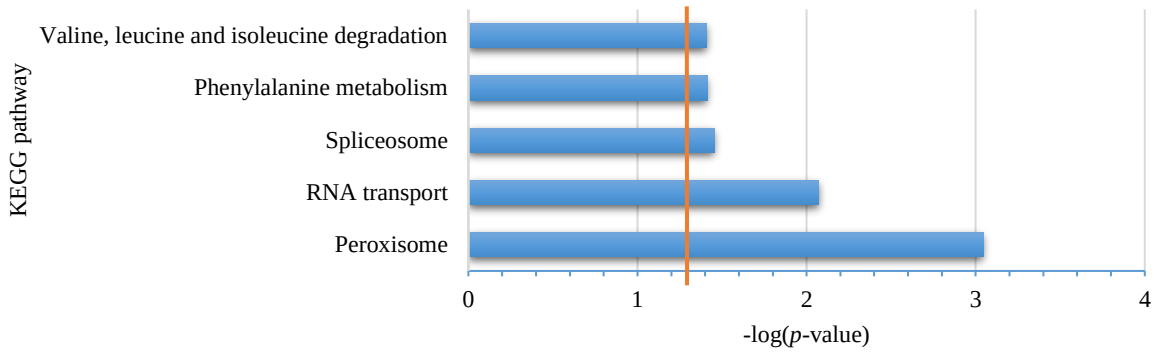

Figure 30. KEGG pathway enrichment analysis of WL-related DEGs that are upregulated in the adipose tissues of CAP mice against DIO phenotypes of HF and CAPS mice. Log *p*-values have been reported on the x-axis and orange lines in panels represent the threshold significance for enrichment, $p<0.05$.

Histograms (figure 30) represent significant genes (*p*-value <0.05). As shown in figures 28-29, the most enriched pathways involving WL-related DEGs in adipose tissues were associated with cellular processes (GO:0009987) and metabolic processes (GO:0008152), reflecting an upregulation of genes encoding enzymes involved in peroxisomal processes, RNA transport, spliceosome components, and phenylalanine and BCAA metabolism. KEGG analyses did not identify significant enrichment of biological pathways for the downregulated DEGs in adipose tissues.

Differentially expressed genes in Adipose Tissue

Table 14. Differentially expressed genes of the adipose tissue ACE–Ang-II–AT_1-receptor and ACE2–Mas receptor–HSL signaling axes and their interaction effects. Pathway associated genes are described by Carroll et al. (2013), Forrester et al. (2018), Oh et al. (2012), Nehme et al. (2019), Slamkova, Zorad, and Krskova (2016) and Y. Zhang et al. (2018).

Gene symbol	Gene name	mRNA expression (FPKM)				CAP/HF	CAP/CAPS	*p*-value
		HF	**HFS**	**CAP**	**CAPS**	**log_2FC**	**log_2FC**	
Ace	Angiotensin converting enzyme	132.23	124.13	177.06	120.94	0.42	0.55	0.55
Ace2	Angiotensin converting enzyme 2	0.91‡	0.31	0.17*	0.29	-2.38	-0.73	0.29
Agt	Angiotensinogen	88.13‡	114.61	152.24*†	96.37‡	0.79	0.66	0.052
Agtr1a	Angiotensin II, receptor type 1a	17.26	26.25	28.74	22.42	0.74	0.36	0.052
Agtr2	Angiotensin II receptor type 2	0.16	0.037	0.16	0.00	0.014	0.00	0.86
Angptl1	Angiopoiten-like protein 1	7.13	8.54	5.57†	9.47‡	-0.36	-0.77	0.59
Gnb5	Guanine nucleotide-binding protein subunit β-5	44.36‡	47.36	33.80*†	46.21‡	-0.39	-0.45	0.18
Irs1	Insulin receptor substrate 1	0.93‡	1.92	2.17*†	1.24‡	1.22	0.81	0.014
Lamb3	Laminin, β 3	5.28‡	6.99	3.63*†	6.98‡	-0.54	-0.94	0.14
Plcb1	Phospholipase C	6.22‡	6.95	4.23*†	6.40‡	-0.56	-0.60	0.025
Prkci	Protein kinase C, ι	23.29‡	23.59	27.52*†	20.56‡	0.24	0.42	0.017
Prkaa1	AMP-activated protein kinase, α1	29.58‡	33.63	36.21*†	27.88‡	0.29	0.38	0.015

Prkag2	AMP-activated protein kinase, γ2	22.03‡	24.10	29.85*†	20.87‡	0.44	0.52	0.016
Lipe	Lipase, hormone sensitive (HSL)	504.28§‡	803.54*	736.52*	695.87	0.55	0.082	0.081
Mas1	Ang(1-7) receptor	0.21‡	0.24	4.24*†	0.42‡	4.36	3.33	0.17
Mme	Neprilysin	27.617‡	23.65	16.35*	19.98	-0.76	-0.29	0.31
Nod1	Nucleotide-binding oligomerization domain-containing protein 1	37.98	44.26	37.34†	42.06‡	-0.02	-0.17	0.87
Nos1ap	Nitric oxide synthase 1 adaptor protein	0.87	1.38	0.55†	1.35‡	-0.70	-1.36	0.52
Nos2	Nitric oxide synthase 2	10.68	15.02	11.05†	13.54‡	0.050	-0.29	0.46
Saa3	Serum amyloid A3	22.94‡	13.63	2.67*†	34.28‡	-3.10	-3.68	6.4E-3
Stat1	Signal transducer and activator of transcription 1	35.78‡	31.58	21.39*	31.04	-0.74	-0.54	0.25
Ren1	Renin	0.16	0.08	0.14	0.09	-0.16	0.59	0.87
Thop1	Thimet oligoprptidase 1	8.88‡	12.10	24.59*†	12.47	1.47‡	0.98	0.070
Tnfrsf21	TNF receptor superfamily member 21	38.28‡	36.81	25.708*†	39.25‡	-0.57	-0.61	0.018
Trp53bp2	Tumor protein p53 binding protein 2	14.27‡	14.46	17.93*†	13.45‡	0.33	0.41	0.015
Wnt8b	Wingless-type MMTV integration site family, member 8B	2.59‡	2.37	0.75*†	2.84‡	-1.79	-1.92	0.019
Other								
Cma1	Chymase	17.35	28.58	23.82†	38.53‡	0.46	-0.69	0.76

Ctsd	Cathepsin D	2137.95	2260.71	1698.69†	2910.76‡	-0.33	-0.78	0.13
Ctsg	Cathepsin G	0.20	0.64	0.12†	0.49‡	-0.67	-1.99	0.81
Ctsl	Cathepsin L	1726.51	1679.52	1334.76†	2143.15‡	-0.37	-0.68	0.14
Gpx1	Glutathione oxidase 1	863.31‡	1286.21	1696.28*†	1309.40‡	0.97	0.37	0.034
Slc2a4	Glucose transporter type 4 (GLUT4)	96.57‡	145.60	180.29*†	104.98‡	0.90	0.78	0.0037
Sod1	Superoxide dismutase 1	1063.96‡	1214.97	1491.20*†	1224.29‡	0.49	0.29	0.0068

Fold change (FC)

p-value < 0.05**;** * vs. HF, § vs. HFS, ‡ vs. CAP, † vs. CAPS

Table 15. Differentially expressed genes involved in DNL, adipogenesis, obesity and body composition as described by Sall et al. (2017), Song et al. (2018), Yang, Kelly, and He (2007), and Zhu, Cheng, Zhu, and Guan (2015).

Gene symbol	Gene name	mRNA expression (FPKM)				CAP/HF	CAP/CAPS	*p*-value
		HF	**HFS**	**CAP**	**CAPS**	**log_2FC**	**log_2FC**	
Adipogenic/ lipogenic genes								
Acaca	Acetyl-CoA carboxylase	64.22§	89.92*	53.27†	73.56‡	-0.27	-0.47	0.40
Acly	ATP-citrate lyase	316.61‡	399.22	240.82*	354.84	-0.40	-0.56	0.82
Acsl3	Acyl-CoA Synthase long-chain family member 3	36.88‡	48.03	18.37*†	48.41‡	-0.44	-1.40	0.092
Adpgk	ADP-dependent glucokinase	11.22	12.60	9.73†	12.54‡	-0.21	-0.37	0.37
Aldoa	Aldolase A	850.22	1034.85	810.57†	1038.18‡	-0.07	-0.36	0.29

C1qtnf6	C1q and TNF related 6	38.92‡	37.58	21.89*†	47.36‡	-0.83	-1.11	0.030
Cnr1	Cannabinoid receptor 1	3.12‡	3.01	1.59*†	3.07‡	-0.97	-0.95	0.028
Dgat2	Diacylglycerol O-acyltransferase 2	1979.13§	2796.77*	1202.09†	2573.63‡	-0.72	-1.10	0.45
Elovl6	ELOVL fatty acid elongase 6	37.63‡	29.42	14.01*†	33.95‡	-1.43	-1.28	0.0086
G6pdx	Glucose-6-phosphate dehydrogenase X-linked	330.33§	430.45*	306.03†	418.03‡	-0.11	-0.45	0.20
Igf2	Insulin-like growth factor 2	5.48‡	5.19	3.83*†	6.28‡	-0.52	-0.71	0.23
Lep	Leptin	2780.76§‡	3010.25*	1333.31*†	2862.98‡	-1.06	-1.10	0.22
Lpl	Lipoprotein lipase	2035.95	2171.14	1450.04†	2251.36‡	-0.49	-0.64	0.28
Mogat2	Monoacylglycerol O-acyltransferase 2	16.46	23.81	6.29	19.76	-1.39	-1.65	0.40
Me1	Malic enzyme	809.52‡	940.58	357.08*†	870.55‡	-1.18	-1.29	0.19
Fads3	Fatty acid desaturase 3	545.58§	795.12*	523.11†	774.86‡	-0.06	-0.57	0.99
Fasn	Fatty acid synthase	750.41§	1481.74*	466.26†	1268.82‡	-0.69	-1.44	0.86
Gpd1	Glycerol-3-phosphate dehydrogenase 1	751.33	991.05	738.75†	1070.89‡	-0.02	-0.54	0.16
Gys2	Glycogen synthase 2	26.19‡	30.70	11.29*†	28.97‡	-1.21	-1.36	0.070
Insig1	Insulin-induced gene 2	701.81‡	736.11	251.63*†	780.32‡	-1.48	-1.63	0.018
Pgd	Phosphogluconate dehydrogenase	244.06‡	313.98	158.41*†	307.14‡	-0.62	-0.96	0.24
Pnpla3	Adiponutrin	306.77‡	382.76	110.54*†	350.28‡	-1.47	-1.66	0.097

Rxra	Retnoid X receptor, α	95.30	134.81	98.01†	120.04‡	0.040	-0.29	0.43
Scarb1	Scavenger receptor class B1	59.50	78.37	64.54†	84.95‡	0.12	-0.40	0.91
Scd2	Stearoyl-CoA desaturase 2	1079.89‡	1082.90	312.62*†	1059.74‡	-1.79	-1.76	0.035
Serpine1	Serine proteinase inhibitor, clad E1(PAI-1)	203.84‡	133.83	83.66*†	190.28‡	-1.29	-1.19	0.13
Serpine2	Serine proteinase inhibitor, clad E2 (PAI-2)	44.36	42.02	31.41†	44.68‡	-0.50	-0.51	0.28
Sfrp1	Secreted frizzled-related protein 1	30.17	35.79	23.71†	39.01‡	-0.35	-0.72	0.35
Sorl1	Sortilin-related receptor, LDLR class A repeats-containing	14.35‡	17.86	6.79*†	18.69‡	-1.08	-1.46	0.081
Taldo1	Taldolase	483.45	560.95	406.01†	553.51‡	-0.25	-0.45	0.35
Tpi1	Triosephosphate isomerase	519.32	598.93	404.52†	627.28‡	-0.36	-0.63	0.23
Tph2	Tryptophan hydroxylase 2	158.45‡	109.60	7.00*†	157.46‡	-4.50	-4.49	0.021
Anti-obesogenic / β-oxidation genes								
Acad10	Acyl-COA dehydrogenase, member 10	5.43‡	6.90	8.17*†	5.55‡	0.59	0.56	0.0035
Acad12	Acyl-CoA dehydrogenase, member 12	9.97‡	12.56	17.17*†	9.94‡	0.78	0.79	0.0036
Acot7	Acyl-coenzyme A thioesterase 7	48.712‡	50.863	109.498*†	57.561‡	1.169	0.928	0.019
Adipoq	Adiponectin	4261.14§‡	6425.63*	6063.97*	5520.15	0.51	0.14	0.063
Adrb3	Adrenergic, β-3, receptor	182.79‡	384.46	451.79*†	276.95‡	1.31	0.71	3.7E-5

Cfd	Complement factor D	2703.69‡	4256.45	7144.82*†	3966.40‡	1.40	0.85	0.011
Cpt1c	Carnitine palmitoyltransferase 1C	4.13‡	4.48	7.40*†	4.54‡	0.84	0.70	0.14
Enho	Adropin	9.63§‡	15.39*	14.24*†	11.43§‡	0.57	0.32	0.0025
Fabp3	Fatty acid binding protein 3	8.51‡	0.64	17.37*†	2.37‡	1.03	2.87	0.37
Hsbp11	Heat shock protein, β-11	7.20‡§	9.05*	10.20*†	7.57§‡	0.50	0.43	6.6E-4
Hsbp6	Heat shock protein, β-6	37.42‡	47.73	50.38*	44.65	0.43	0.17	0.018
Irs1	Insulin-receptor substrate 1	0.93‡	1.92	2.17*†	1.24‡	1.22	0.81	0.014
Mrps9	Mitochondrial ribosomal protein S9	14.285‡	15.634	16.272*	14.593	0.188	0.157	0.087
Prkci	Protein kinase C, ι	23.29‡	23.59	27.52*†	20.56‡	0.24	0.42	0.017
Prkaa1	AMP-activated protein kinase, α1	29.58‡	33.63	36.21*†	27.88‡	0.29	0.38	0.015
Prkag2	AMP-activated protein kinase, γ2	22.03‡	24.10	29.85*†	20.87‡	0.44	0.52	0.016
Rorc	Retnoid-related orphan receptor C	5.74‡	4.97	10.69*†	3.76‡	0.90	1.51	0.035
Sik3	Salt-inducible kinase 3	13.708‡	17.404	20.946*†	16.207‡	0.612	0.370	0.011
Sirt3	Sirtuin 3	4.285‡	5.56	6.514*†	4.68‡	0.60	0.48	5.1E-3
Stk40	Serine/threonine kinase 40	40.275§‡	51.502*	59.402*†	49.886‡	0.561	0.252	0.010

Fold change (FC)

p-value < 0.05; * vs. HF, § vs. HFS, ‡ vs. CAP, † vs. CAPS.

Table 16. Differentially expressed genes involved in peroxisome, RNA transport, Spliceosome, Phenylalanine and BCAA metabolism.

Gene symbol	Gene name	mRNA expression (FPKM)				CAP/HF	CAP/CAPS	*p*-value
		HF	HFS	CAP	CAPS	log_2FC	log_2FC	
Peroxisome								
Abcd2	ATP-binding cassette 2	180.99§‡	255.49*†	213.55*†	187.69§‡	0.24	0.19	0.19
Crat	Carnitine O-acetyltransferase	129.46§‡	183.03*	234.55*†	170.54‡	0.86	0.46	0.0020
Dhrs4	Dehydrogenase/ reductase SDR family member 4	101.95§‡	123.40*	130.99*†	110.92‡	0.36	0.24	0.015
Ephx2	Epoxide hydrolase 2, cytoplasmic	325.21§‡	489.33*	604.31*†	367.12‡	0.89	0.72	0.0063
Mlycd	Malonyl-CoA decarboxylase	32.70§‡	44.91*	50.34*†	41.48‡	0.62	0.28	0.0053
Pex5	Peroxisomal biogenesis factor 5	55.33§‡	68.96*	73.17*†	59.50‡	0.40	0.50	0.0080
Pex6	Peroxisomal biogenesis factor 6	30.37§‡	42.47*	54.01*†	39.05‡	0.83	0.47	9.0E-4
Pex12	Peroxisomal biogenesis factor 12	11.86‡	13.06	15.83*†	10.51§‡	0.42	0.59	0.0031
Pxmp2	Peroxisomal membrane protein 2	29.89§‡	45.38*	59.12*†	34.10‡	0.98	0.79	0.0033
Sod1	Superoxide dismutase 1, soluble	1063.96‡	1214.97	1491.20*†	1224.29‡	0.49	0.29	0.0068
RNA transport								
Casc3	Cancer susceptibility candidate 3 (Mln51)	29.25§‡	35.32*	38.41*†	33.12‡	0.39	0.21	0.011
Eif3g	Eukaryotic translation initiation factor 3, subunit G	98.02‡	96.02	123.77*†	94.80‡	0.34	0.39	0.031
Eif3h	Eukaryotic translation initiation factor 3, subunit H	327.29‡	323.55	389.57*†	329.45‡	0.25	0.24	0.0039
Eif4a3	Eukaryotic translation initiation factor 4A3	61.37‡	61.59	75.12*†	65.37‡	0.29	0.20	0.062
Eif4b	Eukaryotic translation initiation factor 4B	181.82‡	180.50	214.37*†	176.21‡	0.24	0.28	0.048
Fxr2	Fragile X mental retardation, autosomal homolog 2 (Fmrp)	61.83‡	69.36	74.21*†	63.79‡	0.26	0.22	0.0094

Pabpc1	Poly(A) binding protein, cytoplasmic 1	229.22‡	212.49	318.12*†	213.28‡	0.47	0.58	0.024
Rnps1	Ribonucleic acid binding protein S1	57.41‡	58.17	70.07*†	61.40‡	0.29	0.19	0.0020
Spliceosome								
Cdc40	Cell division cycle 40	0.54‡	0.28	4.65*†	0.48‡	3.10	3.29	0.121
Cdc5l	Cell division cycle 5-like	36.47‡	36.83	42.87*†	36.42‡	0.23	0.24	0.029
Eif4a3	Eukaryotic translation initiation factor 4A3	61.37‡	61.59	75.12*†	65.37‡	0.29	0.20	0.062
Prpf40b	Pre-mRNA processing factor 40B	16.33‡	18.41	22.74*†	16.92‡	0.48	0.43	0.0084
Snrnp40	Small nuclear ribonucleoprotein 40 (U5)	15.60§‡	13.54*	18.32*†	14.43‡	0.23	0.35	0.077
Srsf7	Serine/arginine-rich splicing factor 7	66.58‡	66.60	77.64*†	62.05‡	0.22	0.32	0.011
Phenylalanine metabolism								
Aoc2	Amine oxidase, copper containing 2	2.33§‡	3.18*	4.15*†	2.64‡	0.83	0.65	0.0011
Il4i1	Interleukin 4 induced 1	0.068‡	0.047	0.28*†	0.04‡	2.04	2.77	0.023
Mif	Macrophage migration inhibitory factor	44.29‡	41.36	74.12*†	61.57‡	0.74	0.27	0.24
Valine, leucine and isoleucine degradation								
Bcat2	Branched chain aminotransferase 2, mitochondrial	60.90§‡	90.00*	101.29*†	75.85‡	0.73	0.42	0.013
Hadha	Hydroxyacyl-Coenzyme A dehydrogenase	77.93§‡	98.00*	104.66*†	90.19‡	0.43	0.22	0.0044
Il4i1	Interleukin 4 induced 1	0.068‡	0.047	0.28*†	0.041‡	2.04	2.77	0.023
Ivd	Isovaleryl coenzyme A dehydrogenase	82.28§‡	111.73*†	124.36*†	84.45§‡	0.60	0.56	0.0041
Other genes of interest								
Aldh1a1	Aldehyde dehydrogenase 1, member A1	486.23†	303.93	406.59*†	239.69‡	0.26	0.76	0.021
Eif1b	Eukaryotic translation initiation factor 1B	95.94‡	88.22	119.58*	97.58	0.32	0.29	0.45
Eif4a2	Eukaryotic translation initiation factor 4A2	178.05	170.94	190.54†	137.80‡	0.10	0.47	0.017

Eif2b5	Eukaryotic translation initiation factor 2B subunit ε	55.10	62.65†	63.87†	55.50§‡	0.21	0.20	0.022
Eif2s3x	Eukaryotic translation initiation factor 2, subunit 3, structural gene X-linked	78.78	77.50†	73.92†	69.43§‡	-0.09	0.09	0.45
Pex1	Peroxisomal biogenesis factor 1	5.44‡	5.18	4.13*	4.82	-0.40	-0.22	0.13
Pex7	Peroxisomal biogenesis factor 7	9.62‡	9.14†	8.36*	8.26§	-0.20	-0.02	0.040
Pex14	Peroxisomal biogenesis factor 14	10.49§‡	14.83*	14.80*	16.35	0.18	-0.14	0.26
Pex26	Peroxisomal biogenesis factor 26	7.32	7.99	8.01†	7.13‡	0.3	0.17	0.067
Ppargc1a	Peroxisome proliferator-activated receptor-γ, coactivator 1 α (PGC-1α)	1.49	1.70†	1.66†	1.15§‡	-0.01	0.53	0.062

Fold change (FC)

p-value <0.05; * vs. HF, § vs. HFS, ‡ vs. CAP, † vs. CAPS.

Discussion

Liver tissue transcriptomics

The local hepatic RAS is under-defined yet there is evidence that it is perturbed in obesity and in instances of liver pathology (Simões, Miranda, Rocha, & Teixeira, 2017). While there is also evidence that bodyweight regulates local RAS and *vice versa* (Takeshita et al., 2008; Winkler et al., 2016), in the context of obesity, the contribution of hepatic RAS to whole-body metabolism and adiposity remains under-defined. One hypothesis is the existence of cross-talk between liver-derived AGT with peripheral tissues possessing a local RAS, *e.g.* WAT, thus activation of the RAS in virtually any organ may have implications beyond its origin (Gentile et al., 2015). In addition to being the primary site for AGT synthesis, the liver is also the primary site for glucose and fructose uptake and metabolism, DNL, lipolysis and FA-oxidation (de Kloet, Krause, & Woods, 2010). Captopril has been shown to regulate DNL and glucose utilisation in hepatocytes by suppressing gluconeogenesis in response to insulin infusion (Torlone et al., 1991), whereas Ang-II infusion has been shown to impair hepatic glucose utilisation to stimulate DNL, increase blood TG content and promote IR (Ran, Hirano, & Adachi, 2004).

A high-salt diet counteracted captopril's repression of early downstream Ang-II–AT_1-receptor interacting G-proteins and classical intracellular signal transduction pathways in the liver

As mentioned, the role of hepatic RAS in bodyweight regulation is incompletely understood. Research suggests hepatic *Agt* mRNA expression, circulating Ang-II and ACE activity is elevated in obese, T2D and hypertensive animals and humans (Harp et al., 2002; Saiki et al., 2009; Takeshita et al., 2008). In lean rats, two-weeks of salt loading showed the level of salt intake to relate inversely with hepatic expression of *Agt* and AT_{1A} as well as plasma Ang-II (Sechi et al., 1996), and six-weeks showed a similar trend except an increase in ACE activity was observed when the salt content of feed exceeded 4% (Crestani et al., 2014). Interestingly, Ang-II levels in DIO mice fed a HFD with high-salt content did not differ from that of controls, yet mice experienced no further weight gain unlike lower salt counterparts (Weidemann et al., 2015). We similarly observed suppression of bodyweight gain following a diet high in salt and fat (chapter 3) and in this chapter we showed hepatic expression of *Ace*, *Agt*, and *Agtr1a* mRNA to remain akin to that of HF controls. This may imply that the functionality of the local Ang-II–AT_{1A} signaling axis among normal- and high-salt HFD fed mice may be alike, underscoring a similar molecular/micro-environment whereby deregulation of tissue RAS and possibly Ang-II generation may be of influence to a similar capacity.

Plasma Ang-II, ACE activity, and liver *Agt* mRNA levels were reported as unchanged following captopril therapy compared to untreated controls (Hu, Chen, Chen, Jin, & Wang, 1996; Jonsson, Frewin, & Head, 1994). In the current study, captopril treatment of mice significantly increased liver *Agt* mRNA expression to that of respective groups whereas *Ace* mRNA was unchanged, and while the former observation remains inconsistent with that of Hu et al. (1996) and Jonsson et al.

(1994), HFD-induced local (hepatic) RAS overactivation was not a factor in either study. We propose that an increase in *Agt* mRNA may be an essential response to counter the sustained hypotensive effects of chronic ACE-inhibition with captopril, albeit further analyses are required to corroborate this hypothesis. Angiotensin-II receptor type 1a (*Agtr1a*) expression tended to be lower following captopril treatment without statistical significance, a likely reflection of the variability within group samples. The addition of salt however counteracted captopril's repression of neprilysin (*Mme*) which is an identified non-AT_{1A} (and -AT_2) binding site with consistent K_m for Ang-I (Bricca et al., 2015), the activity and tissue expression of which is demonstrated to correlate with BMI, obesity and IR (Standeven et al., 2011). Moreover a high-salt diet reversed captopril's repression of genes encoding AT_1-receptor interacting G-proteins, *Gnb1* and *Gnb5*, that are central in downstream signal transduction pathways of Ang-II (Shenoy & Lefkowitz, 2005). Despite reporting no differences in expression of *Agtr1a* amongst animals, a reduction in *Gnb1* and *Gnb5* mRNA following captopril may reflect a reduction in Ang-II signaling and subsequent desensitisation of cells to Ang-II stimulation (Bhatnagar et al., 2013). Several classically known downstream targets of G-proteins are reported (figure 3 and 6) and those which are significantly altered by captopril are listed in table 10. With this, PPI network analysis was conducted (figure 23) which included KEGG identified pathways in which *Gnb1* and *Gnb5* was represented alongside several of their early downstream target genes. This analysis showed *Gnb1* and *Gnb5* to interact with *Wnt5a*, *Egfr*, *Gnai1*, *Itpr2*, *Gngt* and *Gnai1*, and these were closely related to *Mapk1*, *Mapk8 (Jnk)*, *Mapk9*, *Fosl1*, *Rock2* and *Jun*, creating an interaction of sub-networks involved in cyclic AMP, MAPK, PI3K–Akt, TGF-β, TLR and Ras signaling, as well as fibrogenesis (*Col1a1*) and angiogenesis (*Mapk8*). These pathways are consistently reported as being overrepresented following Ang-II–AT_1-receptor activation as well as in obesity and NAFLD (Forrester et al., 2018; Higuchi et al., 2007; Loza et al., 2007; Murphy et al., 2015; Shenoy & Lefkowitz, 2005; Taskin & Guven, 2017). This suggests that captopril's repression of *Gnb1* and *Gnb5* expression may be important for weight loss (Jonsson et al., 2001), and high-salt mediated revival of G-protein mRNA transcription may be implicated in the deregulation of these therapeutic effects of captopril. Together, the molecular interaction between dietary salt and captopril on bodyweight and fat regulation may involve liver AT_{1A}-coupled G-protein signal transduction, suggesting ACE-independent pathways of Ang-II generation may be at play (as alluded to in the previous section). Further analysis of blood and liver biochemistry is required to ascertain whether Ang-II may be a factor in captopril and salt treated animals.

A high-salt diet counteracted captopril's repression of genes involved in energy metabolism

Whilst many of the effects of Ang-II (or tissue RAS) is mediated through systemic stimulation of specific membrane receptors, *in vitro* studies conducted in cardiac myocytes identified chronic glucose exposure as a potent stimulus for intracellular Ang-II generation (Singh, Le, Bhat, Baker, & Kumar, 2007). Interestingly, cultured proximal tubules transfected with an intracellular Ang-II

fusion protein enhanced mitochondrial respiration, glycolytic response, as well as G-protein coupled receptor signaling via stimulation of 'mitochondrial AT_1-receptors' (Li & Zhuo, 2015; Li & Zhuo, 2017). Ang-II infusion of mice was also shown to reduce the content of oxidative (type I) skeletal muscle fibres and increase fast glycolytic (type IIb) fibres (Kadoguchi et al., 2015), and this compositional switch is characteristic of muscle biopsies derived from obese patients (Tanner et al., 2002). The emerging picture is that Ang-II plays a major role in whole-body metabolism, causing a series of metabolic alterations in tissues that may facilitate the generation of carbon skeleton and reducing equivalents required for DNL and cellular growth. Given a high-salt diet appears to counteract captopril's repression of hepatic Ang-II responsive genes, including *Gnb1* and *Gnb5*, it is plausible to assume captopril may suppress genes involved in respiration and energy metabolism (due to reduction of Ang-II synthesis), which may also be counteracted by salt (due to likely induction of Ang-II synthesis). Accordingly, KEGG pathway analysis of the 558 interacting genes related to the weight loss phenotype (CAP group) revealed the majority of captopril modulated genes were involved in carbon metabolism and metabolic pathways running in parallel to glycolysis, *i.e.* the pentose-phosphate pathway (PPP), as well as downstream to glycolysis, *i.e.* the TCA cycle (table 11).

In vivo, hepatic uptake of glucose activates HK which in turn activates the rate-limiting enzyme of glycolysis, PFK, allowing glucose to be promptly oxidise to pyruvate (Butterworth, 2005a). It has been reported that the expression of glycolytic genes is upregulated in the livers of obese and T2D humans and rodents (Kirchner et al., 2016; Zhang et al., 2013). Moreover, the rate of glycolysis is also reported to increase in the metabolically active tissues of mice exposed to salt overload (Fillmore et al., 2018; Wang, Liu, et al., 2018) alongside an increase in the rate of *de novo* glucose incorporation in to lipids (Fonseca-Alaniz et al., 2007). Here, we report captopril treatment downregulated the mRNA expression of key glycolytic genes including *Hk2* and *Pfkm*, and this effect was counteracted following a high-salt diet to resemble that of DIO mice (table 11). This observation is in further support of the reported association between hepatic glycolytic gene expression and obesity (Kirchner et al., 2016; Zhang et al., 2013), and links salt with gene modifications that are akin to Ang-II-induced metabolic alterations and those observed in obesity. This data suggests the molecular interaction between salt and captopril on bodyweight loss may involve regulation of glycogenic gene expression and glycolysis.

A distinctive function of the hepatocytes of mice exposed to a high-salt diet was recently reported to involve the endogenous generation of fructose via the induction of the polyol (AR–SDH) pathway (Lanaspa et al., 2018). The metabolism of fructose favours DNL more strongly than a HFD through the efficient and uninhibited action of *Khk* and *Aldob*, from which intermediates may be incorporated in to the glycolytic pathway yielding substrates that fulfil the biosynthetic requirements of cellular hypertrophy and hyperplasia (Herman & Samuel, 2016). In the current study, *Khk* expression was consistent amongst animals whilst *Aldob* was significantly

downregulated following weight loss in response to captopril against that of HFD controls. Moreover *Ar* mRNA expression was enhanced in whilst *Sord* mRNA expression was suppressed in lean captopril treated mice to that of HFD and high-salt administered mice, respectively. Given these changes appear to be treatment specific, there is indication that captopril and salt may alter molecular components of the polyol pathway differently, and this could be one defining metabolic switch whereby a high-salt diet may resist captopril's molecular efficacy toward weight loss. Findings are similar to that of Lanaspa et al. (2018) who showed mice lacking the ability to metabolise fructose (via *Khk*) had increased hepatic *Ar* mRNA expression and sorbitol content, and this genotype was inversely associated with excess bodyweight gain.

Though KEGG pathway analyses did not identify 'pyruvate metabolism' as an enriched pathway, pyruvate dehydrogenase kinase 4 (*Pdk4*) mRNA expression was one of the top most differentially expressed genes between lean (CAP) and obese (HF and CAPS) mice. *Pdk4* is a key regulator of the PDH complex linking glycolysis to the TCA cycle, DNL and OXPHOS through pyruvate, acetyl-CoA and citrate (Zhang, Hulver, McMillan, Cline, & Gilbert, 2014). Increasing evidence suggests that the upregulation of *Pdk4* expression is closely associated with obesity and IR, indicative of reduced *Pdk4* sensitivity (Rosa et al., 2003). *Pdk4* deficient mice given a HFD were shown to exhibit bodyweight loss and reduced lipogenesis, manifested by diminished hepatic steatosis through the induction of AMPK and negative regulation of mTOR signaling (Hwang, Jeoung, & Harris, 2009; Zhang, Zhao, Li, & Wang, 2018). A high-salt diet was also shown to induce *Pdk4* mRNA expression and this was proposed as being reflective of improved carbohydrate utilisation (Cui et al., 2017). It is important to note that the metabolic state of an animal (or microenvironment of tissues) may influence PDH activity differently through posttranslational regulation; normal nutritional cues in which the action of insulin is not compromised will suppress *Pdk4* to enable glucose oxidation through activation of the PDH complex (Zhang et al., 2014), and over-expression of *Pdk4* is enough to establish a metabolic profile similar to that seen in obesity, *i.e.* increased β-oxidation and reduced glucose utilisation (Rosa et al., 2003; Zhang et al., 2014). For this reason, the suppositions of Cui and colleagues (2017) may be somewhat misguided. Here we showed that in contrast to DIO animals, *Pdk4* was downregulated following captopril treatment of mice, and treatment in conjunction with a high-salt diet resisted these effects to resemble that of DIO groups (table 11). This suggests the interaction between captopril and salt on bodyweight may involve molecular regulation of the hepatic PDH complex, and that modulation of *Pdk4* mRNA expression may be important for the weight loss efficacy of captopril during long-term HFD consumption.

As a branch of glucose metabolism, the oxidative pentose phosphate pathway (PPP) supplies NADPH and H^+ for antioxidant machinery and FA and cholesterol biosynthesis. The non-oxidative PPP supplies R5P for nucleic acid and sugar phosphate precursors required for amino acid synthesis, and depending on cellular demands, may supply glycolysis with intermediates of R5P and *vice*

versa (Stincone et al., 2015). The relationship between the PPP and RAS is understudied, however there is evidence that Ang-II-induces NADPH oxidase expression, hypertension and smooth muscle hypertrophy in mice via G6PDH dependent mechanisms *i.e.* via derivation of NADPH (Matsui et al., 2005). It is reported that PPP genes are upregulated in the livers of obese and T2D patients and animals (Jin, Lee, Murphy, & Malloy, 2018; Toshinari Takamura et al., 2008). The significance of the PPP in its facilitation of DIO has been generally studied, and there are reports of attenuated weight gain and preferential reductions in adipogenesis in *G6pdx*-deficient and *Tkt*-haploinsufficient mice respectively, and this is thought to be due to low NADPH levels (Hecker et al., 2012; Xu, Wawrousek, & Piatigorsky, 2002). In *C. elegans*, downregulation of the *tald-1* (*Taldo1*) gene by means of RNAi caused dramatic reductions in intestinal fat levels via a fasting-like response involving *atgl-1* induced lipolysis (Bennett et al., 2017; Vrablik, Petyuk, Larson, Smith, & Watts, 2015), and genetically obese *Ob*/*Ob* mice have increased bioavailability of hepatic phosphoribosyl pyrophosphate derived from *Prps* (Kunjara, Sochor, Greenbaum, & McLean, 1993). A high-salt diet is also shown to cause upregulation of the PPP specifically through the activity of *G6pdx* and *Pgd* in renocytes, and increased [NADPH]/[$NADP^+$], NADPH oxidase activity and ROS supported the hypothesis that oxidative stress caused by salt overload induced PPP alterations (Wang, Liu, et al., 2018). In staying with the premise that Ang-II signaling may be stimulated by salt overload, through KEGG analysis the present study identified the PPP as a significantly enriched pathway that was modulated in lean mice subsequent to captopril therapy (figure), and high-salt feeding favoured these molecular components in the opposite direction to resemble DIO. With the exception of *G6pdx*, *Pgls* and *Rpe*, the remaining set of genes encoding PPP enzymes were modulated by captopril (table 11). Since Ang-II (and salt) is reported to elicit many of its functions through G6PDH (Matsui et al., 2005), one would expect *G6pdx* mRNA to respond accordingly, albeit Fonseca-Alaniz et al. (2007) described enhanced G6PDH activity without change in mRNA levels following salt overload in rats, which may also translate to the current study. We also report that *Taldo1*, which normally metabolises the products of *Tkt* reaction, was one of the top most differentially expressed genes among lean and obese animals and this may ascribe *Taldo1* to a major role in the determination of proneness of animals towards weight loss and/or weight gain. We propose the hepatic genes responsible for the generation of anabolic PPP precursors and metabolites may be mediated by ACE (through Ang-II), and that suppression of this response may be important for the weight loss efficacy of captopril. Together, there is indication that the interaction between captopril and salt involves molecular regulation of the hepatic PPP, and that *Taldo1* in particular may play an important role in bodyweight and fat regulation.

The TCA cycle is a central route for mitochondrial OXPHOS in cells and fulfils anabolic and catabolic requirements via its main substrate, acetyl-CoA, produced from the breakdown of carbohydrates, protein and lipids. It has been reported that TCA genes are co-ordinately upregulated alongside other glucose metabolising pathways in the hepatocytes of obese compared to non-obese

humans and rodents (Satapati et al., 2012; Toshinari Takamura et al., 2008). While a high-salt diet is shown to increase the abundance and suppress the activities of hepatic TCA enzymes in salt-sensitive rats, higher circulating levels of TCA metabolites was described (Wang et al., 2014; Wang, Liu, et al., 2018). Of note, several TCA cycle intermediates are reported to act out of their cycle, and succinate has been shown to increase in response to high glucose to act as a ligand for the G-protein coupled receptor *Sucnr1* (GPR91), triggering RAS to cause hypertension in mice. Captopril attenuated succinate-induced hypertension, suggesting ACE may mediate this response (He et al., 2004). In the current study, *Sucnr1* expression levels tended to be lower in captopril treated mice and higher when captopril was administered in conjunction with a high-salt diet, albeit differences did not reach significance (table 11). KEGG analyses on the other hand identified the TCA cycle as an enriched molecular pathway that was modulated by captopril, and of the 8 DEGs, 6 DEGs encoded enzymes that either derived or metabolised succinate. Based on the classically known functions of the TCA cycle, there is indication that captopril may cause a reduction in mitochondrial oxidative metabolism by modulating carbohydrate (carbon) breakdown (figure 32). With respect to other identified signaling functions of TCA intermediates, there appears to be a role for the TCA cycle in the regulation of local and intracellular RAS and *vice versa*, further aligning with the hypothesis that Ang-II signaling may be restored by a high-salt intake. This suggests that the interaction between captopril and salt on bodyweight may involve differential regulation of genes encoding TCA cycle enzymes, and that modulation of TCA genes in hepatocytes may be important for the efficacy of captopril in weight loss.

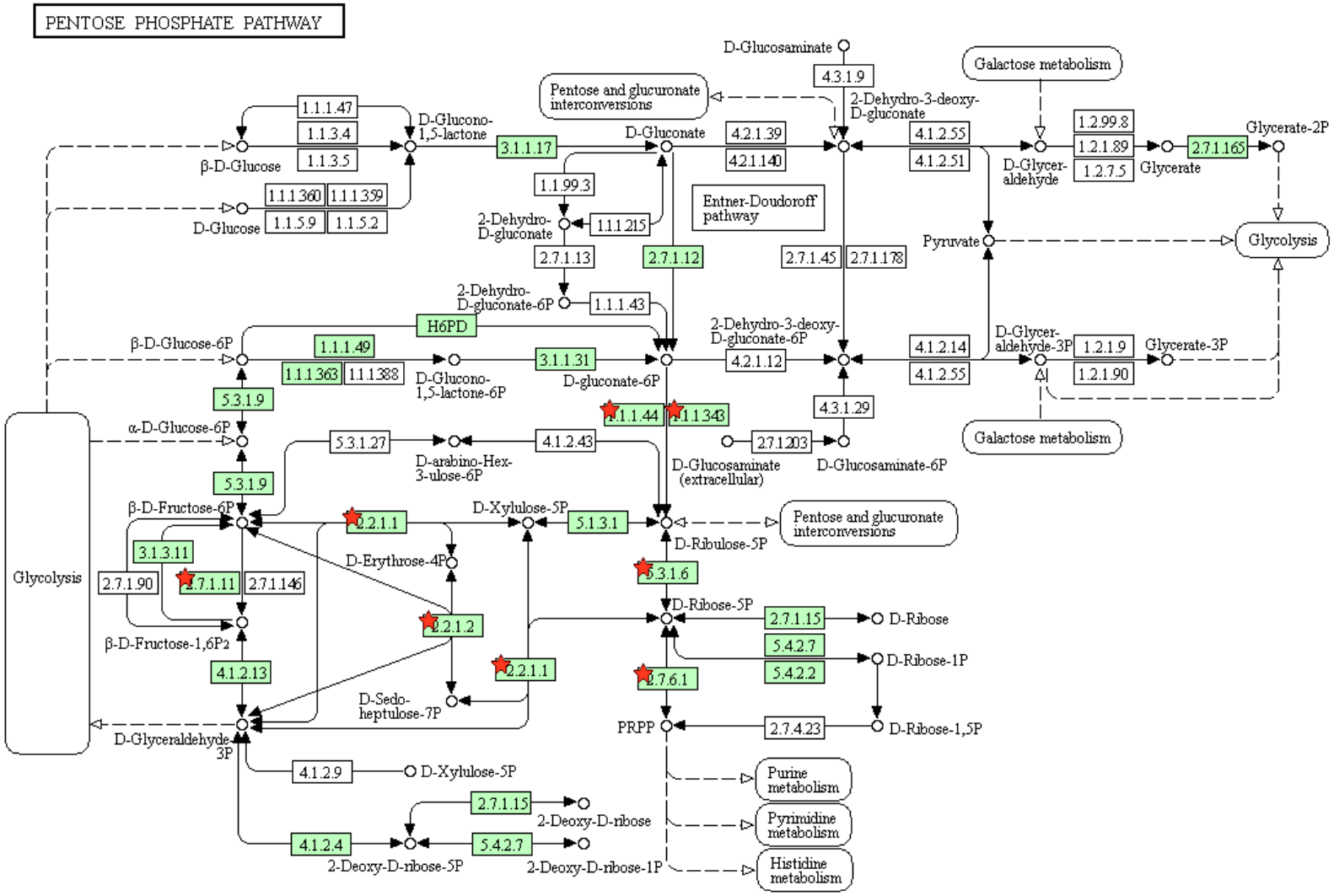

Figure 31. KEGG pathway analysis identified glycolysis and the PPP for DEGs (red stars) as important pathways involved in the interaction effect between captopril and salt in liver tissues. KEGG ID – *gene symbol*: 2.7.1.11, *Pfkm*; 2.2.1.1 – *Tkt*; 2.2.1.2 – *Taldo1*; 2.7.6.1 – *Prps2*; 5.3.1.6 – *Rpia*; 1.1.1.44/1.1.1.343 – *Pdg*. See table 12 for the names of listed gene symbols.

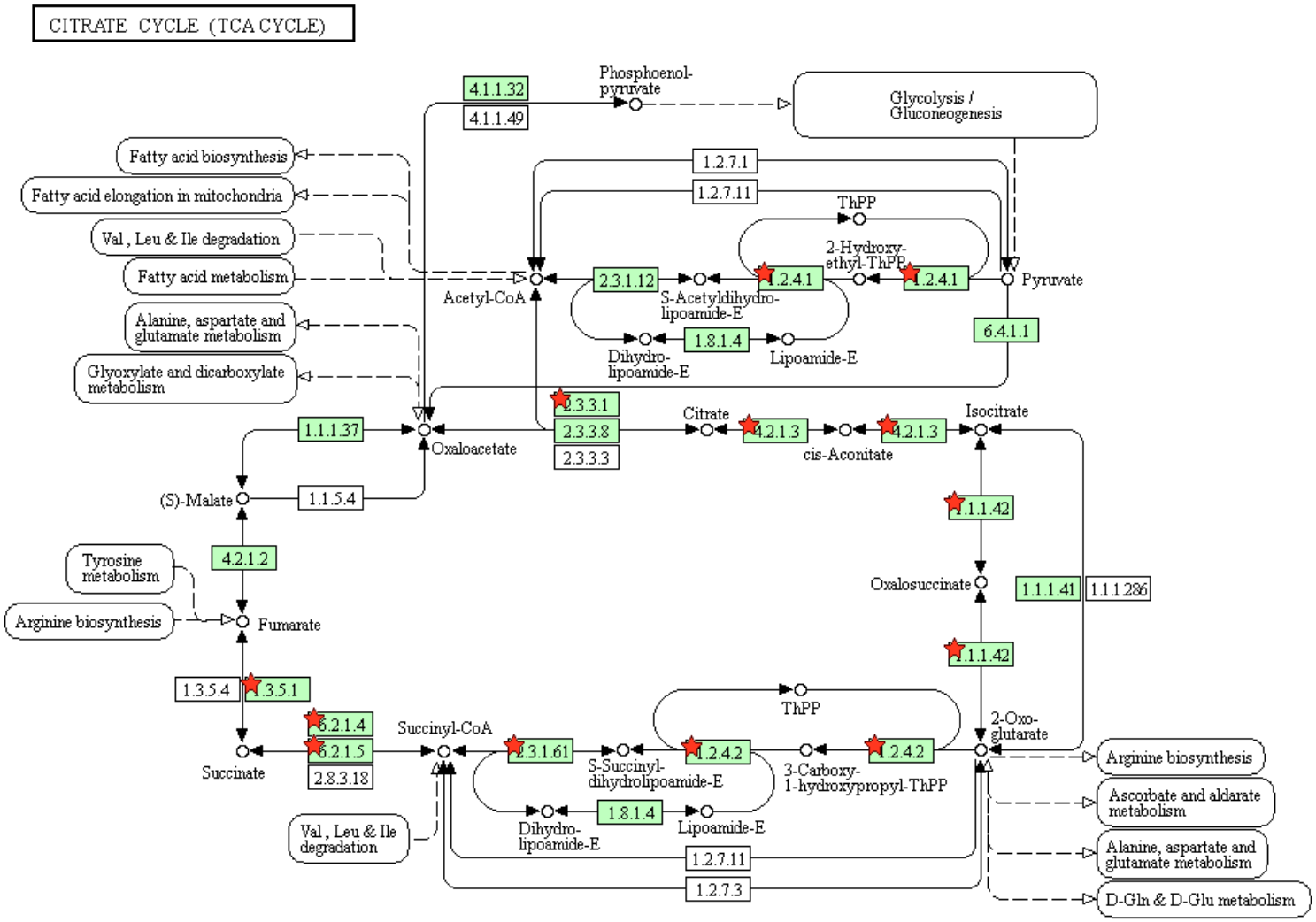

Figure 32. KEGG pathway analysis identified the TCA cycle for DEGs (red stars) as an important pathway that is involved in the interaction effect between captopril and salt in liver tissues. KEGG ID – *gene symbol*: 1.3.5.1 – *Sdha/Sdhd*; 6.2.1.4/6.2.1.5 – *Sucla2*; 2.3.1.61 – *Dlst*; 1.2.4.2 – *Oghd*; 1.1.1.42 – *Idh2*; 2.3.3.1 – *Cs*; 4.2.1.3 – *Aco1*; 1.2.4.1 – *Pdha1*. See table 12 for the names of listed gene symbols.

A high-salt diet counteracted captopril's repression of genes involved in cell cycle regulation

In the present study, KEGG analysis identified 'cell cycle' as an enriched pathway what was significantly modulated in the livers of lean captopril treated mice to that of DIO mice (HF and CAPS). The 'cell cycle' describes the process by which the genetic material within a cell is duplicated and segregated in to two separate components, triggered through an increase in the amount of cyclin family member proteins and cyclin-dependent kinases (CDK). This is the driving force for cellular hyperplasia or biomass accretion *i.e.* proliferative cellular growth, cellular differentiation and decreased apoptosis, a common feature of hepatic (and adipose) tissues derived from obese humans and animals (Loyer, Corlu, & Desdouets, 2012; Lindsey A. Muir et al., 2016; Yang, Lin, Hwang, Chacko, & Diehl, 2001). The glycolytic intermediate fructose 2,6-bisphosphate, an allosteric activator of PFK-1, was shown to positively regulate CDK1 activity coupling glucose metabolism with cell proliferation (Yalcin et al., 2014). Interestingly, a newly discovered role for CDKs also includes the coordination of carbon metabolism throughout specific phases of the cell cycle. Lopez-Mejia et al. (2017) showed that CDK inhibits AMPK to promote glycolysis and prevent FA-oxidation, and CDK knockout mice exhibited increased oxidative metabolism and exercise capacity in an AMPK-dependent manner (Lopez-Mejia et al., 2017). Though the impact of CDK-mediated regulation of AMPK on cell cycle and growth is not clear, the relationship between cellular metabolism and cell cycle appears to be bidirectional. Apart from vasoconstriction, Ang-II treatment of vascular smooth muscle cells (VSMC) also results in the inactivation of AMPK (Duan, Song, Ding, & Zou, 2017), and Ang-II has been assigned pro-mitotic properties in several cell lines in association with checkpoint kinase, cyclin and CDK-dependent mechanisms that stimulates cellular hyperplasia, hypertrophy, senescence and fibrillation (Braun-Dullaeus, Mann, Ziegler, von der Leyen, & Dzau, 1999; Guillemot, Levy, Raymondjean, & Rothhut, 2001; Li et al., 2016; Sai et al., 2019; Watanabe et al., 1996; Wolf & Wenzel, 2004; Yoshiji et al., 2001). Indeed, Ang-II is reported to enhance DNA synthesis and cell proliferation in hepatic stellate cells through AT_{1A} receptors, suggesting the pro-mitotic activities of Ang-II may also expand in to the liver which could be of pathophysiological relevance (Bataller et al., 2000).

Here, we showed *Chek1, Cdk1, Ccnb1, Mcm2-6* and *14-3-3* mRNA levels were among the top most differentially expressed genes between lean and DIO animals, all of which were downregulated following weight loss due to captopril treatment and reversed when treatment was administered alongside a high-salt diet (table 12). *Chek1* and *14-3-3* proteins may negatively regulate *Cdc25c in vivo,* which is an important DNA damage response required for the prevention of replication of damaged cells (Chen, Ryan, & Piwnica-Worms, 2003). *Cdc25c* is one of three cell cycle regulators that removes inhibitory phosphorylation of *Cdk1* to allow its complexation with *Ccnb1*, enabling mitosis at the G_2/M transition (Schmitt et al., 2006; Takizawa & Morgan, 2000; Timofeev, Cizmecioglu, Settele, Kempf, & Hoffmann, 2010). The minichromosome maintenance complex (MCM) is essential for DNA replication, the activity of which is also regulated by CDKs during the

G_1/S transition and late S to M phases, resulting in the recruitment of DNA polymerase and the dissolution of the MCM respectively. Ang-II was has too been shown to positively regulate the expression of MCM components (Leung et al., 2013) in addition to causing cell cycle progression from the G_1 in to S phase in VSMCs (Jahan, Kobayashi, Nishimura, & Kanaide, 1996). Moreover, we identified one study addressing high-salt induced activation of S phase in cardiac cells, and such alteration was associated with Ang-II mediated cell cycle changes, *i.e.* increased $AT_{1A/B}$ expression and myocardium Ang-II concentration (Ding et al., 2010). This suggests that the effects of captopril goes far beyond the treatment of hypertension, and supports a role for captopril in the suppression of mitosis whilst a high-salt diet may reverse such effect to uphold mitotic activity (Ding et al., 2010; Hixon et al., 2000; Reddy, Baskaran, & Molteni, 1995). Thus, modulation of *Chek1*, *Cdk1*, *Ccnb1*, *Mcm* and *14-3-3* mRNA expression may be important for bodyweight and hepatic biomass loss in response to captopril during long-term HFD feeding of mice, and the re-introduction of these genes in response to high-salt feeding may be important for the observed resistance to weight loss effects of captopril. With respect to metabolic regulation of cell cycle machinery, we propose that the molecular modifications associated with captopril and salt on genes of glycolysis, TCA cycle, PPP and amino acid metabolism may directly influence cell cycle progression (see PPI network, figure 25). Of course, further studies are required to test this hypothesis. Together, there is indication that the interaction between captopril and salt may involve molecular regulation of hepatic cell cycle genes, possibly a downstream effect of mRNA expression of genes encoding enzymes of carbon metabolising pathways and the TCA cycle.

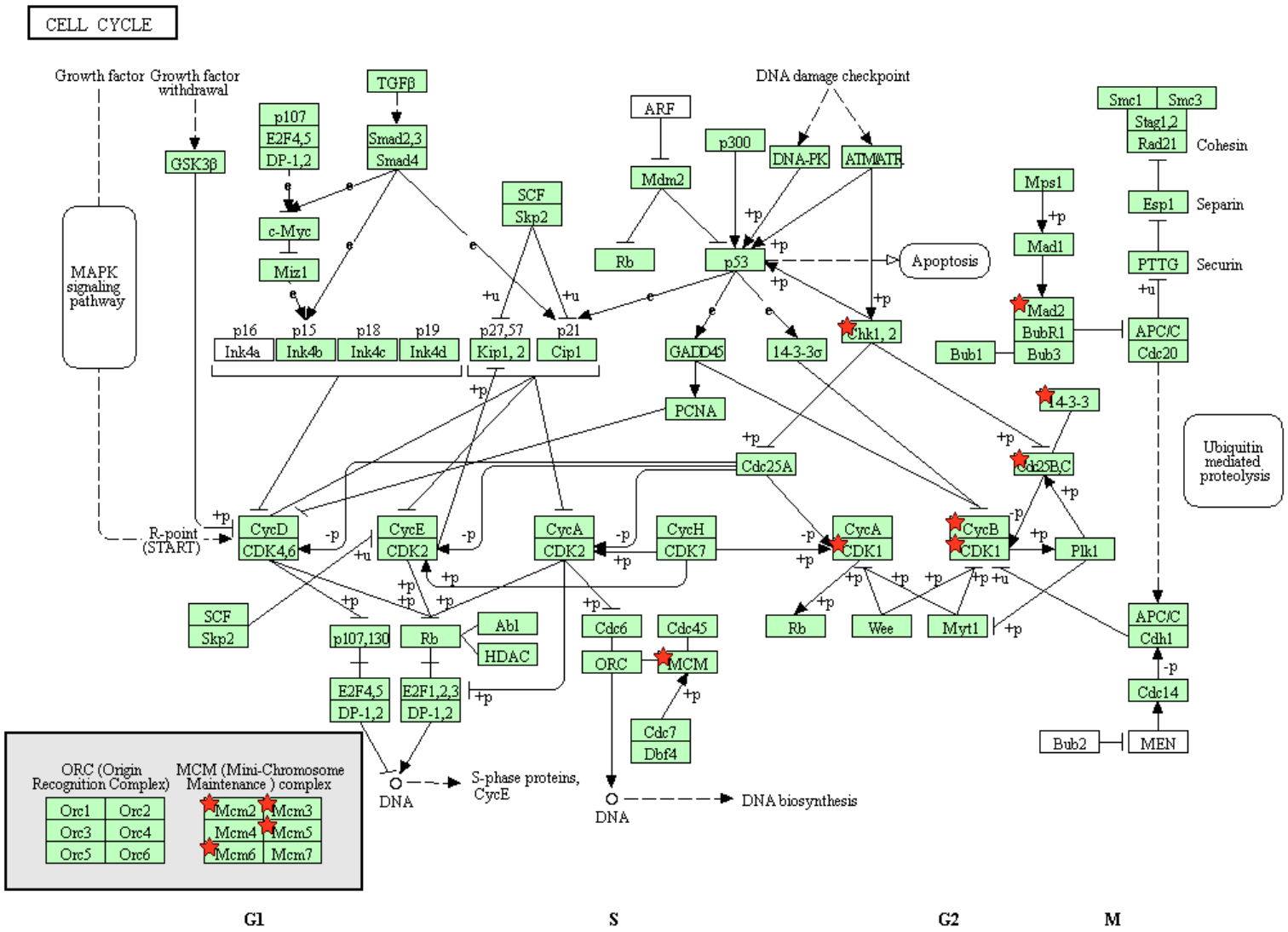

Figure 33. KEGG pathway analysis identified the cell cycle for DEGs (red stars) as an important pathway that is involved in the interaction effect between captopril and salt in liver tissues. See table 12 for the names of listed gene symbols.

A high-salt diet counteracted captopril's molecular repression of genes involved in p53 signaling

According to KEGG pathway analyses, the 'p53 signaling pathway' was significantly enriched in the livers of lean captopril treated mice to that of DIO animals (HF and CAPS). The p53 transcription factor itself is best known for its role in cell cycle arrest, senescence and apoptosis, yet increasing evidence suggests that p53 plays a vital role in normal and pathological lipid metabolism (Krstic, Galhuber, Schulz, Schupp, & Prokesch, 2018). Generally considered a negative regulator of lipid synthesis, chronic activation of p53 has been observed in obesity (Sabir et al., 2019; Yahagi et al., 2004), albeit the mechanistic association between p53 and fat accumulation is still largely undetermined. Whilst p53 knockout strains tend to accumulate liver fat, adopting a pharmacological approach using the p53-inhibitor, pifithrin-α, attenuated HFD-induced bodyweight gain and hepatic steatosis without influencing food intake (Derdak et al., 2013). One recent study showed genetic ablation of upstream activators of p53 (including *Mdm2*) increased energy expenditure and decreased fat accumulation in mice fed a HFD (Liu, Kim, Franklin, & Zhang, 2017). Because hyperglycaemia is also reported to activate p53 (Fiordaliso et al., 2001; Itahana & Itahana, 2018), it is likely that the dysregulation of the p53 signaling cascade caused by nutrient stress may be of relevance to the progression of obesity.

There also appears to be a role for p53 in the regulation of local RAS and *vice versa*. Activation of p53 was shown to increase *Agt* and AT_{1A} expression alongside Ang-II levels in myocytes, an effect which was prevented when p53 was inhibited (Leri et al., 1998; Leri et al., 2000). Ang-II was also shown to activate the p53 pathway (Liu et al., 2009) and therefore a positive feedback loop between the RAS and the p53 signaling cascades may also be of relevance to DIO. Moreover, a recent study revealed that a high-salt intake may enhance the expression of p53 in breast cancer cells (Xu et al., 2018), and we can only speculate that in the context of long-term high-salt feeding, chronic activation of p53 may be problematic *i.e.* induce nutrient stress.

Here, whilst *Trp53* itself remained consistent amongst animals, *Trp53bp2* (also known as ASPP2) was significantly suppressed by captopril in response to normal-salt but not high-salt feeding (table 12). *Trp53bp2* is one of three binding partners of p53 shown to enhance apoptosis and inhibit autophagy, hence it is likely that modulation of *Trp53bp2* by captopril may mitigate p53-mediated apoptotic processes and target gene transcription (Samuels-Lev et al., 2001). Accordingly, *Trp53bp2* was strongly correlated with *Agtr1a*, *Gnb1* and *Gnb5* mRNA expression (figure S2) to support strong transcriptional association between hepatic Ang-II and p53 related pathways that may be mediated by *Trp53bp2*. To the best of our knowledge, this is the first study to define such relationship. Whilst *in vitro* and *in vivo* overexpression of *Trp53bp2* attenuated hepatic TG accretion through a reduction in autophagy (Xie et al., 2015), the relationship between autophagy and liver fat accumulation remains controversial (Fukuo et al., 2014). We previously measured autophagy flux in the hepatocytes of captopril and salt treated mice without identifying significant changes in LC3II and LC3I ratios *i.e.* no difference in autophagy flux between treatments

(Radcliffe, 2013). These results combined may therefore suggest that indifferences in of autophagy flux following captopril treatment may be independent of *Trp53bp2*-mediated mechanisms. Here, *Trp53bp2* mRNA levels were positively associated with the bodyweight and liver masses of mice to suggest hepatic expression of *Trp53bp2* may be deregulated with ongoing HFD and salt feeding.

Several downstream gene targets of the p53 cascade were also highly correlated with *Trp53bp2* mRNA and significantly downregulated following weight loss in response to captopril treatment; these genes included *Bbc3*, *Ccng1*, *Cycs*, *Perp*, *Sesn3*, *Zmat3* (as well as *Ccnb1* and *Cdk1* which has already been discussed). It is well accepted that all of the aforementioned genes have a role in stress induced apoptosis induction, yet little is known about their function in different biological processes and diseases. Increased expression of *Bbc3*, *Cycs* and *Sesn3* has been observed in the livers of HFD-fed mice to facilitate lipoapoptosis (Cazanave et al., 2010; Kimball, Ravi, Gordon, Dennis, & Jefferson, 2015; Lebeau et al., 2019; Wang, Lv, Yao, Yin, & Shang, 2015; Wang et al., 2017), and this can be of detriment due to tissue specific functional deficits (Unger & Orci, 2002). Furthermore, gene expression profiles of liver samples derived from obese humans showed *Ccng1* and *Zmat3* as two overexpressed genes associated with hepatic steatosis (Wang, Wang, & Zhuang, 2016), and HFD induced liver overexpression of *Perp* has been associated with systemic inflammatory diseases, atherosclerosis in particular (Recinos et al., 2004). Our data demonstrates that captopril can prevent p53 signaling in hepatic tissues, possibly via suppression of *Trp53bp2* mRNA expression. Whilst further studies are needed to determine whether *Trp53bp2* is indeed a key regulator of p53 (and Ang-II) signaling, there is indication that salt interferes with captopril's modulatory effect on hepatic *Bbc3*, *Ccng1*, *Cycs*, *Perp*, *Sesn3* and *Zmat3* mRNA expression which could uphold the apoptotic cascade. Thus downregulation of these genes may be important for bodyweight loss in response to captopril therapy during HFD feeding, and resistance of such gene modifications in response to high-salt feeding may be important for the lack of reversal of obesity in mice treated with captopril. Thus, we propose that the interaction between captopril and salt may involve molecular regulation of the hepatic p53 signaling pathway, and that the molecular modifications associated with captopril and salt on *Trp53bp2* may be of particular importance.

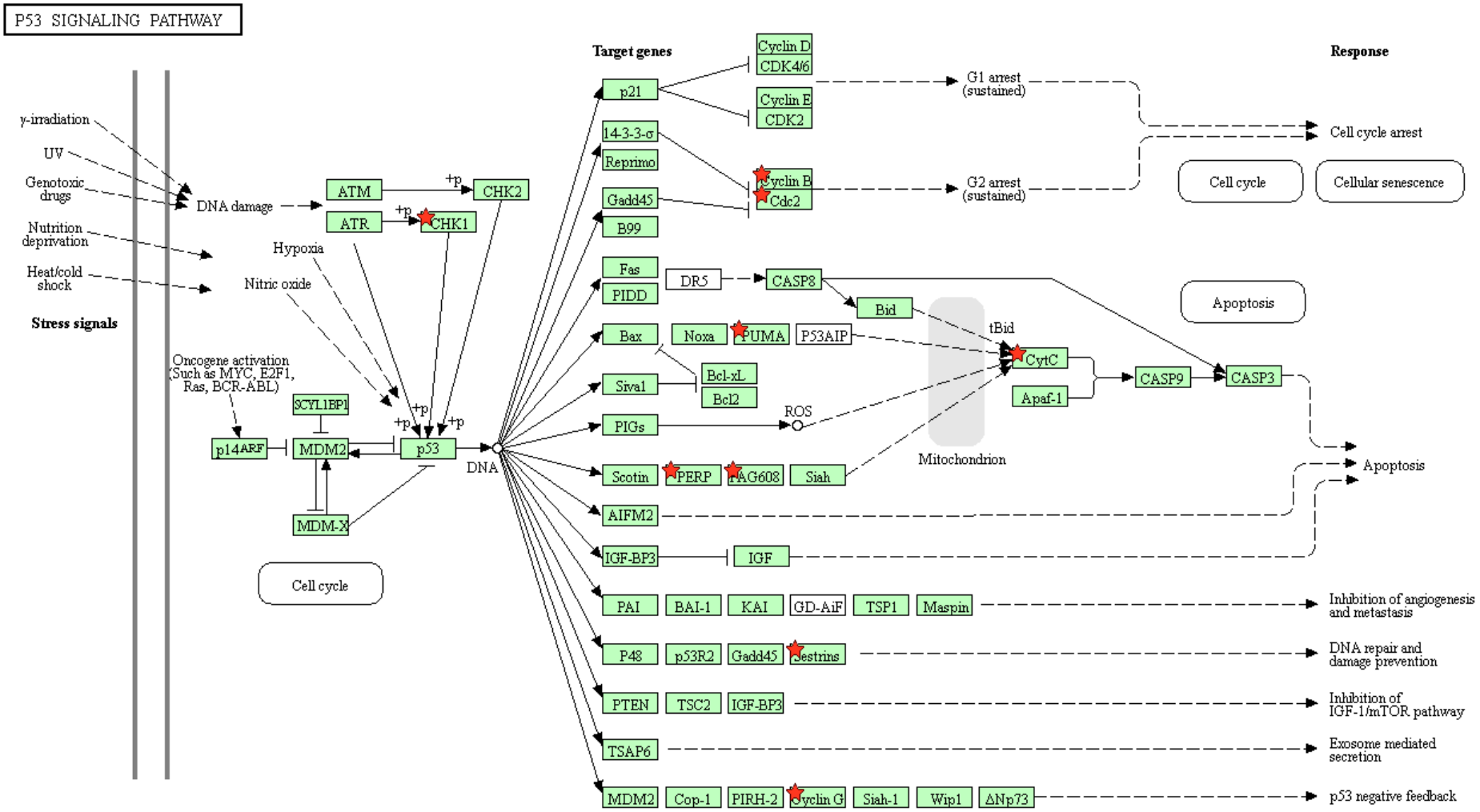

Figure 34. KEGG pathway analysis identified the p53 signaling cascade for DEGs (red stars) as an important pathway involved in the interaction effect between captopril and salt in liver tissues. See table 12 for the names of listed gene symbols.

Adipose tissue transcriptomics

Adipose tissue (AT) expresses all components of the RAS and heightened systemic levels of Ang-II (and Agt) is implicated in DNL, body fat accumulation and obesity (Jones et al., 1997; Saiki et al., 2009; Y. Zhang et al., 2018). Moreover, *in vivo* and *in vitro* Ang-II stimulation of adipose AT_1 receptors induces oxidative stress in a NADPH-oxidase dependent manner (ROS induction), to alleviate GLUT4 (*Slc2a4*) translocation and inhibit of IRS1 (*Irs1*) signaling causing systemic IR (Kalupahana et al., 2012; Menikdiwela et al., 2019). Genetic disruption of the RAS as well as preclusion of Ang-II formation and signaling by means of ACE-inhibitors or ARBs, respectively, is shown to promote thermogenicity of WATs thereby leading to a reduction in body fat and improved insulin sensitivity, possibly comprised of induction of the counter-regulatory arm of the RAS involving Ang(1-7), Mas (*Mas1*) receptor activation, and enhanced secretion of adipokines *e.g.* adiponectin (*Adipoq*) and apelin (Jayasooriya et al., 2008; Kalupahana et al., 2012; Kouyama et al., 2005; Premaratna et al., 2011; Than et al., 2017; Tsukuda et al., 2016; Weisinger et al., 2009). Accordingly, we and others have shown ACE-inhibition by captopril to cause profound decreases in AT mass in both visceral and subcutaneous compartments due to improved adiponectin release, FA-metabolism and lipolysis through the action of AMPK (*Prkaa1*, *Prkag2*) and Ang(1-7)–MAS–HSL (*Lipe*) axis respectively, in addition to improved detoxification mechanisms involving SOD (*Sod1*) and GSH (*Gpx1*) (de Kloet et al., 2009; Karimani, Mamashkhani, Moghadam Jafari, Akbarabadi, & Heidarpour, 2018; Oh et al., 2012; Premaratna et al., 2011; Radcliffe, 2013; Tabbi-Anneni et al., 2008; Weisinger et al., 2009). As reported in chapter 3, captopril treatment following standard HFD feeding in mice indeed reduced epididymal fat mass against that of respective groups, and here we report that as the case in liver tissue, adipose *Agt* mRNA expression was upregulated without change in *Ace*, *Ace2*, *Agtr1a* or *Agtr2*, whereas *Mas1*, *Lipe*, *Prkaa1*, *Prkag2*, *Irs1*, *Sod1*, *Gpx1* and *Slc2a4* mRNA expression was enhanced in mice exhibiting bodyweight and visceral fat loss. These findings combined further supports the probable involvement of AMPK and Ang(1-7)-mediated mechanisms of FA-oxidation and lipolysis respectively, and GLUT4, IRS1, SOD and GSH facilitated improvements in glucose utilisation and ROS detoxification in ATs. We propose that the increase in *Agt* mRNA expression may concomitantly reflect an increase in local angiotensinogen and Ang-I generation, and in the absence of ACE activity, may serve as a substrate for enzymes such as *Ace2* and *Thop1* to form Ang-(1-7) (Pereira et al., 2013; Tipnis et al., 2000).

A high-salt diet counteracted captopril's repression of adipose genes that are involved in Ang-II–AT_1-receptor signal transduction pathways

In addition to inducing oxidative stress and inflammatory pathways, enhanced Ang-II signaling in adipocytes by either *Agt* overexpression or direct Ang-II treatment of cells induces DNL alongside heightened activation of FASN and GPDH (*Gpd1*) (Jones et al., 1997; Menikdiwela et al., 2019). While systemic RAS components are mitigated in response to a high-salt intake in healthy subjects, local RAS seems to respond independently by increasing adipose *Ace* mRNA expression without

affecting *Agt*, *Ren* or *Agtr1a* expression (Engeli et al., 2006). Albeit the biological significance of these findings has not been proposed, however it was postulated that local RAS may be regulated by inflammation and metabolic factors (Engeli et al., 2006; Harte et al., 2005; Seok, Sohn, & Son, 2014; Sun et al., 2016). This hypothesis is supported by animal studies showing that high levels of dietary salt intake can promote AT inflammation, oxidative stress and exacerbate DNL by reducing adiponectin expression and AMPK activation, enhancing enzymatic activities of G6PDH (*G6pdx*) and ME (*Me1*), and upregulating the transcription of lipogenic genes such as *Fasn*, *Lep* and *Acaca* (Fonseca-Alaniz et al., 2007; Lanaspa et al., 2018; Lee et al., 2019; Uetake et al., 2015). Conversely, salt-restriction may largely oppose such effects (Hattori et al., 2014; Lee et al., 2019; Zhu et al., 2014). Lee et al. (2019) recently reported high-salt treatment of cultured adipocytes boosted Ang-II levels, and in line with this, research suggests salt overloading *in vivo* may potentiate local AT_1-receptor signaling though ACE-independent routes of Ang-II generation involving tissue-specific induction of stress and inflammation responsive enzymes, such as chymase (*Cma1*), cathepsin G (*Ctsg*) and cathepsin D (*Ctsd*) (Devarajan et al., 2015; Dostal & Baker, 1999; Karlsson et al., 1998; Mizunoe et al., 2017; Nehme et al., 2019; Starodub & Samokhina, 2013). Accordingly, here we showed increased expression of *Cma1*, *Ctsd* and *Ctsg* mRNA in response to a high-salt intake alongside *Gnb5* and other classical downstream molecular counterparts of the adipose Ang-II/G-protein signaling axis (table 14). This suggests the upregulation of *Cma1*, *Ctsd* and *Ctsg* mRNA may be important for the apparent opposition of the weight loss properties of captopril when dietary salt is high, and subsequent overexpression of *Gnb5* may further implicate Ang-II in the diminution of captopril's efficacy against bodyweight and visceral fat loss in mice. Moreover, salt overloading upregulated the expression of lipogenic genes (table 15) such as *Fasn*, *Me1*, *G6pdx*, *Acaca*, *Lpl*, *Lep*, *Dgat2* and *Mogat2*, and these observations are is in line with studies of Fonseca-Alaniz et al. (2007) and Lee et al. (2019), who also describe these salt-induced pathways in relation to adipogenesis and DNL. The crosstalk between Ang-II and inflammatory cytokines in adipocytes is also a characteristic of obesity, and here we showed that salt increased the expression of *Serpine1* (PAI-1), *Serpine2* (PAI-2), *Tnfrsf21, Nod1, Nos2, Saa3,* and *Angptl1,* all of which encode enzymes positively associated with high-salt and Ang-II mediated characteristics of hypertrophic ATs (Carroll et al., 2013; Forrester et al., 2018; Lee et al., 2019). We therefore propose salt-induced mechanisms of local Ang-II generation may mimic an adipose microenvironment that is characteristic during obesity, and that this may oppose the weight loss effects of captopril in an ACE-independent manner. Of course further studies are needed to ascertain whether Ang-II may be a factor in the differential expression of genes in response to captopril and salt administration in mice.

A high-salt diet counteracted captopril-mediated expression of genes involved in peroxisomal metabolic processes in adipose tissue

In the present study, KEGG analysis identified the 'peroxisome' as an enriched organelle/pathway that was overrepresented in the VATs of lean captopril treated mice against that of DIO animals (HF and CAPS). Besides scavenging ROS, oxidative breakdown of FAs is also compartmentalised in peroxisomes (Lazarow & De Duve, 1976) and until recently their function in adipocytes have not been appreciated. Peroxisomes may arise *de novo* or by fission via unknown mechanisms orchestrated by PGC-1α (*Ppargc1a*), and peroxisomal markers are downregulated in the adipocytes of genetically obese mice and upregulated in the adipocytes of obesity resistant mice (Huang et al., 2017; Liu, Lu, Shi, Klein, & Su, 2019; Xie et al., 2011; Zhou et al., 2018). Peroxisomal 'maturation' occurs by the action of specialised peroxisomal proteins, *i.e.* peroxins (*Pex*) that collectively govern matrix protein import. Among them, *Pex6* is anchored to the peroxisome membrane (by *Pex26*) and plays a vital role with *Pex1* in coordinating transport of the receptor-protein *Pex5* in to the cytosol (Nuttall, Motley, & Hettema, 2014). In the cytosol, *Pex5* recognises and interacts with peroxisomal targeting sequence type 1 (PTS1) containing proteins and associates in to a mobile receptor-cargo complex (Francisco et al., 2013; Pedrosa et al., 2018). It has been reported that *Pex5* receptor-cargo complex docks with the membrane bound *Pex14*, and it is assumed that this interaction constitutes a translocon allowing proteins to cross in to the peroxisomal matrix (Neuhaus et al., 2014). In yeast, *Pex12* is reported to facilitate the monoubiquitination of *Pex5* for new rounds of peroxisomal protein import (Léon, Goodman, & Subramani, 2006; Platta et al., 2009). Though we were unable to identify studies assessing the effects of captopril or high-salt feeding on peroxins, here we report upregulation of *Pex5*, *Pex6* and *Pex12* mRNA in the VATs of captopril treated mice exhibiting bodyweight and visceral fat loss, the expression of which was countered when combined with high-salt feeding to that of respective DIO groups (table 15). No statistically relevant differences in important interacting genes *i.e. Pex1*, *Pex14* and *Pex26*, were observed, and together our results identify a previously unknown relationship between captopril-induced weight loss and adipose peroxins. This suggests that in the absence of a high-salt intake, captopril may influence intraperoxisomal protein content and the interaction between the two factors may involve differential regulation of peroxin genes encoding peroxisomal membrane proteins, receptor-cargo proteins, and receptor recycling proteins.

The *Pxmp2* gene encodes another integral peroxisomal membrane porin, and mice lacking *Pxmp2* exhibited disturbances in FA metabolism in mammary fat pads, e.g. decreased myristic acid (a probable β-oxidation product) suggestive of a role in lipid homeostasis (Vapola et al., 2014). Here we showed the expression of *Pxmp2* increased in the ATs of captopril treated mice, and this aligns with the gene expression profile of adipocyte cultures in which *Agt* mRNA silencing upregulated *Pxmp2* mRNA, which lead to a reduction in Ang-II levels, lipid accumulation, and the expression of adipogenic, lipogenic and inflammatory genes (Carroll et al., 2013). We did not show change in

Pxmp2 mRNA expression in response to high-salt feeding with captopril treatment (to that of respective DIO animals), and a recent study conducted in rats showed high-salt induced cardiac hypertrophy accompanied reduced *Pxmp2* mRNA in left ventricular tissues to that of controls (Ono et al., 2017). The physiological significance of the *Pxmp2* gene in relation to these above mentioned outcomes has not been defined, and our study suggests the interaction between captopril and salt may involve differential regulation of *Pxmp2* that likely facilitates appropriate peroxisomal FA uptake and β-oxidation.

In the absence of a high-salt diet, there is indication that captopril upregulates the expression of PTS1 sequence containing genes in VATs. In the current research, captopril treatment following a standard HFD increased the expression of PTS1 containing genes involved in peroxisomal oxidative processes, including *Abcd2*, *Crat* and *Mlycd. Abcd2*, which encodes for one of three ATP-binding cassette transporters, is critically involved in the transport of CoA esters of VLCFAs in to the peroxisomal lumen, and its expression is upregulated during prolonged periods of fasting and downregulated during periods of HFD feeding (Fourcade et al., 2009; Nesteruk et al., 2014). We could not identify any published studies that used transcriptomics to study the association of RAS regulators and high-salt loading with *Abcd2* mRNA expression, albeit it is likely that *Abcd2* is a critical factor involved in captopril-induced weight loss and macro- and micronutrient-induced resistance to weight loss, as *Abcd2* deficient mice are reported to exhibited rapid onset of obesity, hepatic steatosis and IR upon being challenged with dietary FAs (Liu et al., 2012).

The *Crat* gene encodes a key member of the carnitine acyltransferase family (CrAT) that is reactive with short-chain acetyl-CoAs/acyl-CoAs, generating acetylcarnitine/acylcarnitine and CoA that are exported out of the peroxisome, via unknown mechanisms, and enters mitochondria through CPT1 comprising an essential step in the oxidation of FAs (Westin, Hunt, & Alexson, 2008). Whilst the role of CrAT in ATs is largely underexplored, evidence generated in muscle-specific knockout models suggests CrAT promotes glucose oxidation (Muoio et al., 2012). Interestingly, activity of CrAT is reduced during obesity leading to impaired glycemic control (Seiler et al., 2014), and CrAT-deficient myocytes accumulated long-chain acylcarnitines suggestive of incomplete β-oxidation (Muoio et al., 2012). Since captopril increased *Crat* mRNA expression in ATs and a high-salt intake counteracted this effect, there is indication that *Crat* is a potential mediator for insulin sensitivity, bodyweight and fat mass.

In peroxisomes, it has been proposed that the gene product of *Mlycd*, *i.e.* malonyl-CoA decarboxylase (MCD), degrades intraperoxisomal malonyl-CoA (to acetyl-CoA) produced from the β-oxidation of odd-chain length dicarboxy FAs (Sacksteder, Morrell, Wanders, Matalon, & Gould, 1999). Whilst little is known about intraperoxisomal oxidative processes, cytosolic malonyl-CoA is an immediate substrate for *Fasn* and facilitates DNL via its potent inhibition of CPT1 (Butterworth, 2005a). Active AMPK is shown to decrease malonyl-CoA formation via mechanisms

that induce MCD and suppress ACC (*Acaca*) (Saha et al., 2000). It has been reported that the overexpression of *Mlycd* in the livers of rats fed a HFD significantly decreased malonyl-CoA content whilst increasing FA-oxidation and improving whole-body IR (An et al., 2004), and similarly, the activity of AMPK and MCD increases in ATs of rats following exercise, the net effect of which would be to enhance FA oxidation (Park et al., 2002). In the current research, captopril treatment increased the expression of adipose *Mlycd* following a normal-salt diet, a response which was not seen when treatment was administered with a high-salt diet. The increased expression in AT could indicate that captopril treatment may upregulate the degradation of intraperoxisomal malonyl-CoA, which may assist in the disinhibition of mitochondrial CPT1 to promote FA β-oxidation, whilst decreased expression due to high-salt feeding may indicate the converse (Butterworth, 2005a). Therefore we propose captopril may increase β-oxidation of FAs and reduce DNL in VATs via the upregulation of peroxisomal *Mlycd* mRNA in a *Prkaa1*-dependent manner, and downregulation of *Fasn* and *Acaca* mRNA when in the absence of a high-salt diet (see table 7 and 8). Further studies are needed to test these suggested mechanisms.

In the absence of a high-salt diet, several other PTS1 expressing genes were upregulated in the ATs of captopril treated animals, including *Dhrs4*, *Ephx2* and *Sod1*. *Dhrs4* encodes an intraperoxisomal retinal reductase/retinol dehydrogenase that may be important in the synthesis of retinoid acid (RA) (Huang & Ichikawa, 1997). A recent study reported upregulation of cardiac *Dhrs4* mRNA following captopril treatment that was equally modulated in animal models of Ang-II and isoproterenol-induced cardiac hypertrophy; the physiological significance of this gene in the heart however remains obscure (Roussel, Drolet, Lavigne, Arsenault, & Couet, 2018). The role of *Dhrs4* in ATs has not been defined, yet peroxisomal *Dhrs4* protein derived from the liver has been assigned a role in retinoid metabolism or RA production (Lei, Chen, Zhang, & Napoli, 2003), and based on this we speculate a potential function of this gene in adipose RA synthesis. This aligns with the probable weight loss mechanism of captopril as not only have other ACE-inhibitors been reported to activate adipose RA receptors *in vitro* (Kohlstedt et al., 2009), but RA treatment of predipocytes is reported to prevent adipogenesis and promote FA-oxidation, and to reduce adiposity in DIO rats via BAT *Ucp1* mRNA upregulation and WAT *Lep* mRNA downregulation; see review by Jeyakumar and Vajreswari (2015).

Of all above mentioned PTS1 containing genes, *Ephx2* is perhaps better studied. Encoding the soluble epoxide hydrolase (sEH), *Ephx2* plays a major role in inflammation and BP regulation *in vivo* via sEH-mediated metabolism of epoxyeicosatruebiuc acids (EETs) to form the antipressor dihydroxyeicosatrienoic acid (Bettaieb et al., 2013; Jung et al., 2005; Schmelzer et al., 2005). Salt-sensitive models of hypertension are associated with an inability to increase EET when fed a high-salt diet, suggesting that decreased EET following high-salt feeding may potentiate antipressor effects (Imig et al., 2005). Ang-II is also reported to induce sEH in vascular endothelium leading to hypertension (Ai et al., 2007; Jung et al., 2005), and increased mRNA expression and enzyme

activity is detected in ATs derived from DIO mice and differentiating adipocytes, albeit the physiological significance of this has not been elucidated (De Taeye et al., 2010). In our study, it is not entirely clear why VAT-*Ephx2* expression was induced in lean captopril treated mice, and we speculate that maximal expression of *Ephx2* was stimulated in effort to metabolise EET to oppose sustained hypotensive effects of captopril. It may be beneficial to include lean chow-fed controls in order to determine whether *Ephx2* mRNA upregulation is a unique response to captopril treatment, and further studies are needed to determine the metabolic role of *Ephx2* in AT. Combined, there is indication that the interaction between captopril and salt on bodyweight and visceral fat mass may involve regulation of peroxisomal metabolic processes.

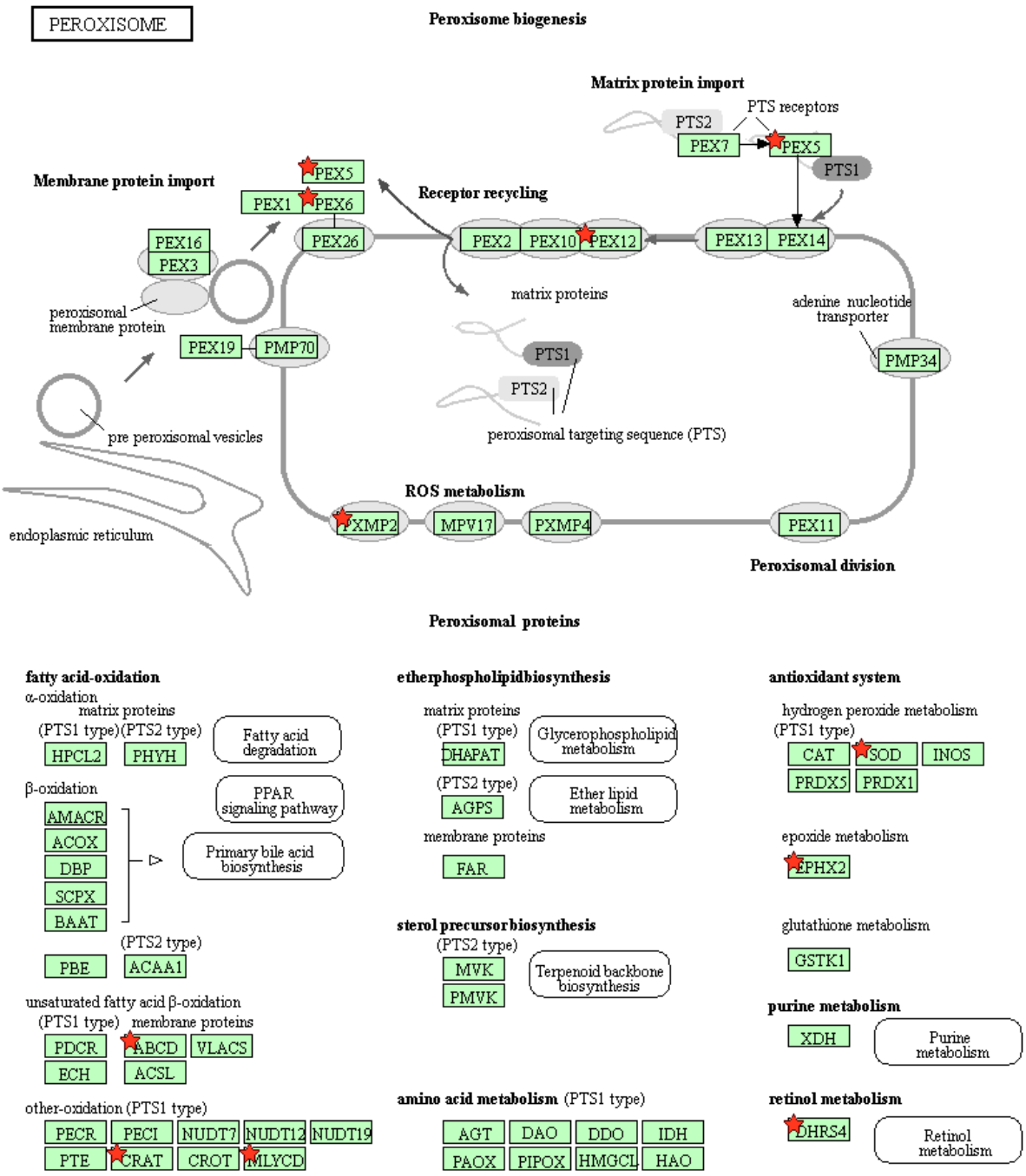

Figure 35. KEGG pathway analysis identified the peroxisome for DEGs (red stars) as an important organelle involved in the interaction effect between captopril and salt in adipose tissues. See table 16 for the names of listed gene symbols.

Conclusion

This study showed that salt interferes with the liver and VAT gene expression profiles of captopril, and upregulates the expression of genes involved in classical downstream Ang-II signal transduction pathways, such as *Gnb1* and *Gnb5*, which may have led to the resistance to bodyweight and fat loss in obese mice. Based on GO analyses, the majority of DEGs in the liver were downregulated by captopril treatment, a result which was reversed when treatment was administered in conjunction with a high-salt diet. Conversely in VATs, the majority of DEGs were upregulated by captopril treatment, and once again this effect was reversed when treatment was administered alongside a high-salt intake. This suggests the transcriptomic changes during captopril treatment and high-salt feeding in the liver and VAT of mice may orchestrate risk of and resistance to obesity.

Based on KEGG pathway enrichment analyses of DEGs in the liver, captopril treatment of mice maintained on a HFD suppressed carbon metabolism, phosphorylative metabolism (PPP), the TCA cycle, p53 signaling and the cell cycle when the level of dietary salt intake did not exceed 86.0 mg day^{-1}. In VATs, the peroxisome pathway was the most significant upregulated transcriptomic regulation KEGG pathway in response to captopril when dietary salt intake was maintained at a normal level, a result opposed when salt intake exceeded 86.0 mg day^{-1}. Other pathways influenced by captopril in VATs included RNA transport, spliceosome, phenylalanine and BCAA degradation. It is of importance to note that this study relied primarily on gene expression levels, and more thorough analyses are needed by way of validation by quantitative PCR and at the level of protein content, activity and localisation, before any definitive conclusions are drawn. Additionally, it would be of great value to investigate whether ACE-independent mechanisms of Ang-II generation were involved in the interaction between captopril and salt on gene expression and regulation of bodyweight, liver and VAT masses.

Acknowledgements

Initial bioinformatics analysis of the RNA sequencing data, *i.e.* fastqc, HISAT2 and GENCODE, was performed by Jing-Dong from Jackie Han's lab at the Shanghai Institute for Biological Sciences (SIBS), Chinese Academy of Sciences (CAS), P.R. China.

Supplementary Data – Transcriptomics

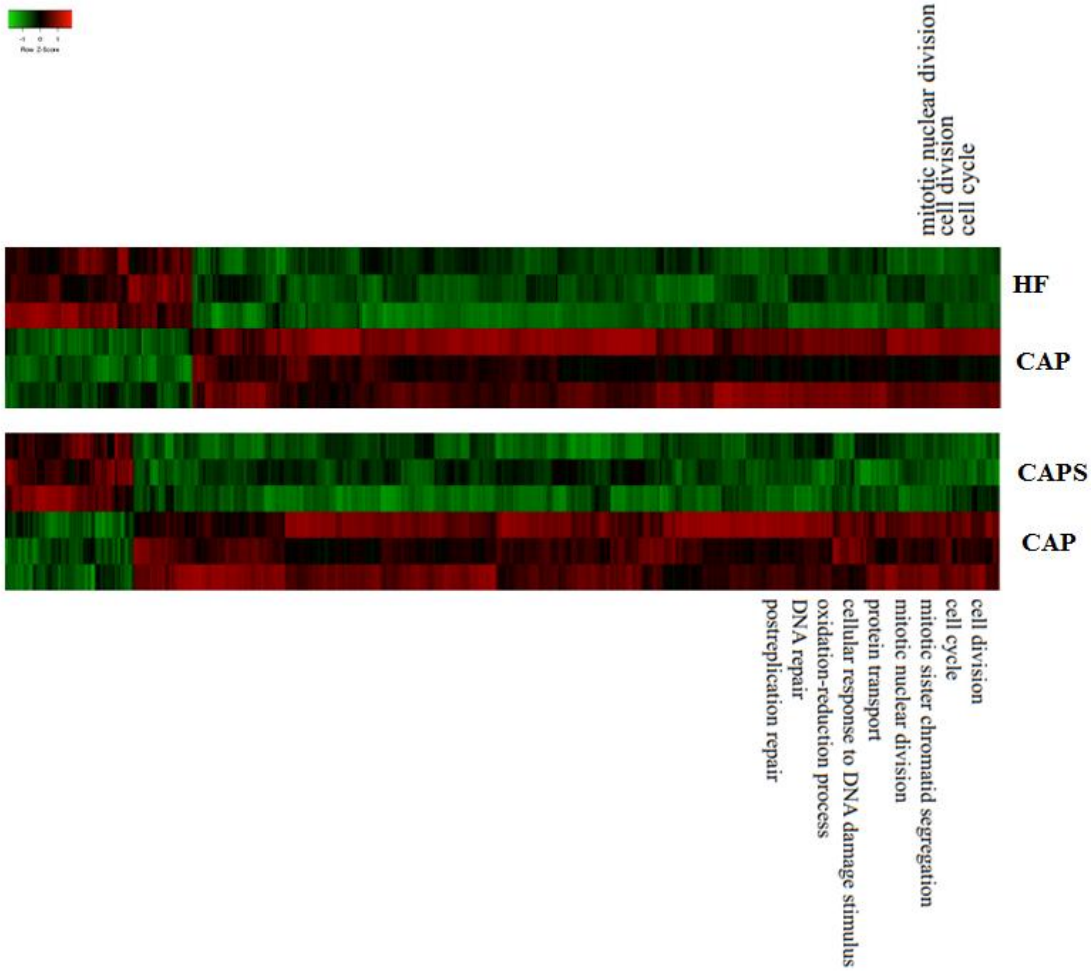

Figure S1. Heat map screened on the basis of z-score was used to assess the match between observed up- and downregulation patterns of genes. Red indicates that expression of gene is relatively downregulated, green indicates that the expression of genes is relatively upregulated, and black indicates no significant changes in gene expression.

Table S1. Biological process GO terms significantly enriched among downregulated genes in the livers of CAP mice

GO term	Description of biological process	Gene count	*p*-value
No significant enrichment of upregulated genes (CAP relative to HF and CAPS)			
Downregulated genes (CAP relative to HF and CAPS)			
GO:0007049	cell cycle	134	4.99E-19
GO:0051301	cell division	93	3.91E-17
GO:0007067	mitotic nuclear division	69	7.74E-13
GO:0000070	mitotic sister chromatid segregation	14	3.51E-08
GO:0006281	DNA repair	64	5.22E-08
GO:0006974	cellular response to DNA damage stimulus	78	5.83E-08
GO:0055114	oxidation-reduction process	110	1.47E-07
GO:0015031	protein transport	99	1.81E-07
GO:0006810	transport	242	5.75E-07
GO:0006301	postreplication repair	8	8.19E-06
GO:0006886	intracellular protein transport	45	1.62E-05

Unmapped genes: *Gm10110*, *Gm42791*, *Gm21967*, *Gm10762*

Table S2. Liver mRNA expression of FOXO genes (n.s.)

	mRNA expression (FPKM)					
Gene symbol	**HF**	**HFS**	**CAP**	**CAPS**	**log_2FC (CAP/HF)**	**log_2FC (CAP/CAPS)**
Foxo1	8.485958	8.96142	12.3606	10.16863	0.542599	0.281623
Foxo3	12.06333	13.80668	17.67376	14.26499	0.55098	0.30913
Foxo4	11.6373	10.47881	16.66565	12.92993	0.51812	0.366163
Foxo6	0.018284	0.038817	0.0769	0.031511	2.072354	1.287138

n.s. – not significant

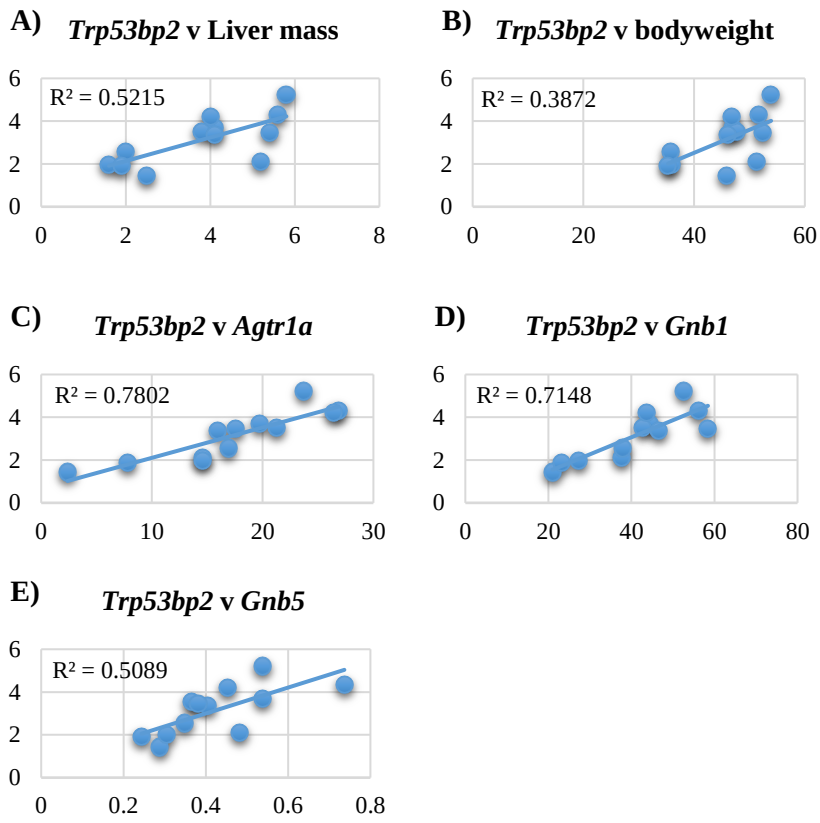

Figure S2. Correlation scatter plot of *Ttp53bp2* mRNA expression levels (FPKM) against (A-B) phenotype and (C-E) molecular expression levels of Ang-II signal transduction components.

Table S3. GO terms for: that are commonly upregulated in the livers of all groups in response to high-fat diet feeding (**HFD-related genes)**; genes that are reversely regulated by **salt** that are otherwise upregulated by captopril (reference figure 19A).

Gene symbol	*Gene name*	*Molecular function*	*Biological process*	*Cellular component*
HFD-related genes				
Amigo3	Amphoterin-induced protein 3	n/a	brain development	membrane
Ahdc1	AT-hook DNA-binding motif-containing protein 1	DNA binding	n/a	n/a
Zfp2	Zinc finger protein 2	metal ion binding	transcription regulation	nucleus
Reversely regulated by a high-salt diet				
Dand5	DAN domain family member 5	morphogen activity	atrial septum development	extracellular region or secreted
Fam189b	Protein FAM189B	WW domain binding	unknown	membrane
Sobp	Sine oculis-binding protein homolog	metal ion binding	cochlea development	nucleus

Table S4. Genes that are reversely regulated by salt in epididymal adipose tissue that is otherwise upregulated by captopril (reference figures25A & 27) or downregulated by captopril (reference figures 25B & 26).

	Gene name	*Molecular function*	*biological process*	*cellular component*
Upregulated by captopril, reversely regulated by salt (reference figure 26A & 28)				
Pdcd5	Programmed cell death protein 5	n/a	n/a	cell
Amot	Angiomotin	n/a	biological regulation, cellular process, localisation, multicellular organismal process	cell junction, organelle
*Trmt112 **	Multifunctional methyltransferase subunit TRM112-like protein	n/a	metabolic process	n/a
Rpl22	60S ribosomal protein L22	binding, structural molecule activity	n/a	n/a
Chfr	E3 ubiquitin-protein ligase CHFR	catalytic activity	biological regulation, cellular process, metabolic process	organelle
*Snrnp40 **	U5 small nuclear ribonucleoprotein 40 kDa protein	n/a	n/a	n/a
Dus4l	tRNA-dihydrouridine(20a/	catalytic activity	metabolic process	n/a

	20b) synthase [NAD(P)+]-like			
Carf	Calcium-responsive transcription factor	n/a	n/a	n/a
Jmy	Junction-mediating and -regulatory protein	binding	cellular process	cell
Hmgn1	Non-histone chromosomal protein HMG-14	binding	cellular process, metabolic process	n/a
Gprasp1	G-protein coupled receptor-associated sorting protein 1	n/a	n/a	n/a
Camk2n1	Calcium/calmodulin -dependent protein kinase II inhibitor 1	n/a	n/a	n/a
Klhl15	Kelch-like protein 15	n/a	n/a	n/a
Pigp	Phosphatidylinositol N-acetylglucosaminyltransferase subunit P	n/a	n/a	n/a
*Sac3d1 **	SAC3 domain-containing protein 1	n/a	cellular process, localisation	organelle, protein-containing complex
Pfdn6	Prefoldin subunit 6	binding	cellular process	cell, protein-containing complex
Zfp963	Zinc finger protein 963	n/a	n/a	n/a
Rps4x	40S ribosomal protein S4, X isoform	binding, structural molecule activity	metabolic process	cell
Bbs12	Bardet-Biedl syndrome 12 protein homolog	n/a	n/a	n/a
Xlr3a	X-linked lymphocyte-regulated protein 3A	n/a	reproduction	organelle
Ovgp1	Oviduct-specific glycoprotein	binding, catalytic activity	cellular process, metabolic process	cell
Carf	CDKN2A-interacting protein	n/a	n/a	n/a
Lats1	Serine/threonine-protein kinase LATS1	catalytic activity	biological regulation, cellular process, developmental process, multicellular organismal process	cell
Smc6	Structural maintenance of chromosomes protein 6	n/a	n/a	n/a

Rest	RE1-silencing transcription factor	binding	biological regulation, metabolic process	protein-containing complex
Smim14	Small integral membrane protein 14	n/a	n/a	n/a
Nsa2	Ribosome biogenesis protein NSA2 homolog	n/a	n/a	organelle, protein-containing complex
Rpl23	60S ribosomal protein L23	structural molecule activity	n/a	cell
Downregulated by captopril, reversely regulated by salt (reference figure 26B & 27)				
Kcnj8	ATP-sensitive inward rectifier potassium channel 8	transporter activity	localisation	n/a
Gja5	Gap junction alpha-5 protein	transporter activity	cellular process	cell
Heyl	Hairy/enhancer-of-split related with YRPW motif-like protein	binding, transcription regulator	biological regulation, cellular process, metabolic process, multicellular organismal process	organelle
Mmp15	Matrix metalloproteinase-15	catalytic activity	cellular process, metabolic process	extracellular region
Cpa3	Mast cell carboxypeptidase A	catalytic activity	n/a	extracellular region
Snx22	Sorting nexin 22	n/a	n/a	n/a
Rasgrp4	RAS guanyl-releasing protein 4	binding, molecular function regulator	cellular process	n/a
Cacna1c	Voltage-dependent L-type calcium channel subunit alpha-1C	transporter activity	n/a	n/a
Ppard	Peroxisome proliferator-activated receptor delta	binding, molecular transducer activity, transcription regulator	biological regulation, cellular process, localisation, metabolic process, multicellular organismal process, response to stimuli	organelle
Atp1b2	Sodium/potassium-transporting ATPase subunit beta-2	catalytic activity, molecular function regulator, transporter activity	biological regulation, localisation	protein-containing complex
Itga9	Integrin alpha-9	n/a	biological adhesion	n/a
Cbr2	Carbonyl reductase [NADPH] 2	catalytic activity	biological adhesion, metabolic process	n/a
Atm	Serine-protein kinase ATM	catalytic activity	biological regulation, cellular process	organelle

Iqsec3	IQ motif and SEC7 domain-containing protein 3	n/a	cellular process	n/a
Furin	Furin	catalytic activity	metabolic process	cell, organelle
Mfsd13a	Transmembrane protein 180	n/a	n/a	n/a
Cdsn	Corneodesmosin	binding	n/a	n/a
Gucy1b3	Guanylate cyclase soluble subunit beta-1	n/a	cellular process	cell
Pstpip2	Proline-serine-threonine phosphatase-interacting protein 2	binding	cellular process	cell, organelle
Notch3	Neurogenic locus notch homolog protein 3	n/a	n/a	n/a

n/a – GO terms not available

(*) marks genes that are upregulated across all treatment groups in the epididymal adipose tissues of mice in response to high-fat diet feeding.

Table 17. Pearson's correlation (r) of DEGs belonging to the ACE–Ang-II–AT_{1A} receptor and Ang(1-7)– ACE2– Mas receptor–HSL signaling axes in liver tissue and their relationships with phenotype (extension of table 10).

Gene	**Final bodyweight**	**Epididymal fat mass**	**Liver mass**
Ace	0.2424	0.5003	0.413
Ace2	-0.2327	-0.02764	-0.1706
Agt	-0.6712*	-0.506	-0.4551
Agtr1a	0.4652	0.4426	0.6095*
Atp6ap2	0.7117**	0.4817	0.7578**
Calm1	0.652*	0.3752	0.7593**
Ccnb1	0.8012**	0.7169**	0.902****
Col1a1	0.624*	0.5693	0.7098**
Csnk1a1	0.8046**	0.4475	0.8401***
Dusp16	0.6539*	0.5254	0.7978**
Egfr	-0.8454***	-0.7136**	-0.7383**
Egr2	0.6576*	0.566	0.7814**
Erc1	0.61*	0.3458	0.6986*
Fosl1	0.673*	0.7089**	0.7941**
Fkbp1a	0.7394**	0.5946*	0.861***
Gnai1	0.7876**	0.4399	0.8377***

Gnb1	0.7147**	0.5897*	0.8434***
Gnb5	0.668*	0.7058*	0.771**
Gngt1	0.8176**	0.4259	0.8057**
Itgav	0.783**	0.5496	0.8997****
Ikbkg	0.5861*	0.3451	0.7508**
Itpr2	-0.8623***	-0.7984**	-0.8065**
Jun	0.6997*	0.6768*	0.7878**
Klk1b4	0.778**	0.5149	0.8136**
Lamb3	0.6593*	0.4349	0.7088**
Lipe	0.04964	-0.1813	0.2038
Lpar1	0.6735*	0.6239*	0.7259**
Mapk1	0.6667*	0.423	0.7366**
Mapk8	0.6924*	0.3326	0.7636**
Mapk9	0.6515*	0.4328	0.7602**
Mas1	0.6118*	0.3861	0.7517**
Mme	0.6739*	0.3058	0.743**
Nln	0.6048*	0.3827	0.7072*
Pdgfra	0.7441**	0.5475	0.8247***
Pdgfa	0.7217**	0.4762	0.833***
Phlpp1	0.7639**	0.6173*	0.8702***
Plcb1	0.3937	0.2327	0.424
Ppp2ca	0.774**	0.4754	0.8391***
Prkca	0.7264**	0.345	0.7786**
Prkcb	0.5339	0.5091	0.6542*
Prkci	0.7297**	0.4343	0.8013**
Rhoq	0.7843**	0.5048	0.8769***
Rock2	0.5937*	0.4096	0.7396**
Ralbp1	0.6412*	0.4977	0.7471**
Rap1b	0.7764**	0.6053*	0.8965****
Rasa2	0.6638*	0.6488*	0.7878**
Skp1a	0.6583*	0.3811	0.7275**
Smad2	0.6838*	0.5206	0.7123**
Stradb	0.7281**	0.5119	0.8022**
Tgif1	0.5883*	0.4101	0.7519**
Ube2n	0.7561**	0.5512	0.8438***
Wnt5a	0.749**	0.4431	0.8084**
Ywhab	0.7254**	0.5206	0.8242***

Ywhag	0.7659**	0.499	0.8351***
Ywhah	0.8557***	0.61*	0.9389****

p<0.05*, *p*<0.01**, *p*<0.001***, *p*<0.0001****

Table 18. Pearson's correlation (r) of KEGG pathway identified DEGs in liver tissue and their relationships with phenotype (extension of tables 11-12).

	Final bodyweight	**Epididymal fat mass**	**Liver mass**
Carbon metabolism			
Glycolysis			
Hk2	0.8342***	0.6097*	0.9053****
Pfkm	0.7306**	0.62*	0.8076**
Aldob	0.6144*	0.3228	0.7176**
Tpi1	0.4952	0.1078	0.6271*
Gapdh	0.2688	0.199	0.4558
Gpd2	0.653*	0.3978	0.7605**
Pgk1	0.5381	0.3819	0.6068*
Pgam1	0.7231**	0.4102	0.828***
Pklr	0.5146	0.159	0.5535
Ldha	0.6624*	0.4559	0.7323**
Gluconeogenesis			
G6pc	0.2688	0.1696	0.322
Fbp1	0.6079*	0.3599	0.6486*
Tpi1	0.4952	0.1078	0.6271*
Pgam1	0.7231**	0.4102	0.828***
Pcx	0.3625	0.09234	0.5264
Pck1	0.3504	0.2776	0.4326
Pyruvate dehydrogenase (PDH) complex			
Pdhx	0.6368*	0.481	0.7526**
Pdha1	0.5292	0.1633	0.6647*
Pdp1	0.6604*	0.3538	0.6905*
Pdk4	0.762**	0.3717	0.7743**
Pklr	0.5146	0.159	0.5535
Glygogen metabolism			
Pgm1	0.425	0.432	0.5071
Ugp2	0.628*	0.3768	0.7357**
Gys2	0.4898	0.3084	0.5809*

Pygl	0.6126*	0.289	0.7162**
Pentose phosphate pathway			
Hk2	0.8342***	0.6097*	0.9053****
G6pdx	0.1214	0.3013	0.3382
Pgls	-0.3891	-0.3341	-0.1899
Pgd	0.7552**	0.3081	0.8441***
Rpia	0.9041****	0.7022*	0.9213****
Rpe	0.4274	0.2376	0.4655
Tkt	0.758**	0.5058	0.853***
Taldo1	0.6435*	0.4393	0.7567**
Prps2	0.7692**	0.3974	0.8636***
Polyol pathway			
Sord	0.4761	0.213	0.588*
Gluconate shunt (incompletely elucidated)			
Idnk	-0.2753	-0.2524	0.009622
Inositol biosynthesis (incompletely elucidated)			
Isyna1	0.06984	0.3627	0.2727
Impa1	0.5599	0.3308	0.6162*
Fructose metabolism (liver)			
Aldob	0.6144*	0.3228	0.7176**
Khk	0.02096	-0.2136	0.1976
Tricarboxylic acid cycle			
Aco1	0.6243*	0.4388	0.6818*
Acly	0.4546	0.04535	0.441
Cs	0.7136**	0.4773	0.8463***
Dlst	0.7331**	0.4319	0.8203**
Fh1	0.01296	-0.04255	0.1561
Idh2	0.6418*	0.4334	0.7427**
Mdh1	0.5324	0.3435	0.5999*
Me1	0.7453**	0.3333	0.7491**
Ogdh	0.5845*	0.4169	0.7427**
Sdha	0.6973*	0.4469	0.7488**
Sdhd	0.7833**	0.5047	0.8365***
Sucla2	0.7109**	0.4415	0.7502**
Sucnr1	0.472	0.265	0.4863
Anoplerotic metabolism			
Glud1	0.3222	0.2096	0.5284

Glul	0.04912	0.09444	0.2027
Mut	0.5412	0.2649	0.6003*
Got1	0.02991	-0.08669	0.06451
Adsl	0.1103	-0.02581	0.2463
Cell cycle			
Ccnb1	0.8012**	0.7169**	0.902****
Cdk1	0.7382**	0.6572*	0.8366***
Chek1	0.7328**	0.5214	0.6767*
Cdc25c	0.4519	0.6306*	0.5238
Skp1a	0.6583*	0.3811	0.7275**
Mad2l1	0.7439**	0.458	0.8185**
Mcm2	0.8183**	0.5819*	0.8927****
Mcm3	0.7224**	0.5734	0.786**
Mcm5	0.7157**	0.522	0.7663**
Mcm6	0.744**	0.531	0.8293***
Ywhab	0.7254**	0.5206	0.8242***
Ywhag	0.7659**	0.499	0.8351***
Ywhah	0.8557***	0.61*	0.9389****
P53 signaling pathway			
Bbc3	0.6523*	0.3194	0.7652**
Ccnb1	0.8012**	0.7169**	0.902****
Ccng1	0.7046*	0.5994*	0.8386***
Cdk1	0.7382**	0.6572*	0.8366***
Chek1	0.7328**	0.5214	0.6767*
Cycs	0.8046**	0.5424	0.8601***
Perp	0.7559**	0.5172	0.8392***
Sesn3	0.8174**	0.506	0.8626***
Zmat3	0.6728*	0.5616	0.7782**
Other			
Pparg	0.6192*	0.3922	0.6774*
Mdm2	0.4684	0.3591	0.6139*
Myc	0.5732	0.494	0.6675*
Slc2a2	0.4689	0.2659	0.5101
Trp53	0.07425	0.01945	0.2408
Trp53bp2	0.6223*	0.4127	0.7222**
Trp53inp1	0.6954*	0.3543	0.7599**
Stk11	-0.531	-0.2168	-0.3686

p<0.05*, *p*<0.01**, *p*<0.001***, *p*<0.0001****

Table 19. Pearson's correlation (r) of DEGs belonging to the ACE–Ang-II–AT_{1A} receptor and Ang(1-7)– ACE2– Mas receptor–HSL signaling axes in epididymal adipose tissue and their relationships with phenotype (extension of table 14).

	Final bodyweight	**Epididymal fat mass**	**Liver mass**
Ace	-0.3243	-0.2977	-0.3239
Ace2	0.3478	0.377	0.3058
Agt	-0.7353**	-0.5367	-0.7789**
Agtr1a	-0.5354	-0.4144	-0.5626
Agtr2	-0.1482	-0.09272	-0.1422
Angptl1	0.3705	0.1221	0.2199
Gnb5	0.6994*	0.3642	0.5372
Irs1	-0.5926*	-0.6204*	-0.7277**
Lamb3	0.5377	0.4421	0.4336
Plcb1	0.6128*	0.1957	0.4663
Prkci	-0.6672*	-0.6135*	-0.6977*
Prkaa1	-0.5732	-0.6592*	-0.573
Prkag2	0.1358	-0.04596	-0.09624
Lipe	-0.3277	-0.4524	-0.3818
Mas1	-0.6495*	-0.753*	-0.5577
Mme	0.5291	0.4464	0.396
Nod1	0.1944	-0.01488	0.1767
Nos1ap	0.5119	0.249	0.4596
Nos2	0.1916	-0.1295	0.08116
Saa3	0.5997*	0.5111	0.6182*
Stat1	0.5903*	0.2183	0.5557
Ren1	-0.05335	0.01828	-0.0173
Thop1	-0.7269**	-0.8062**	-0.6698*
Tnfrsf21	0.7444**	0.5457	0.7059*
Trp53bp2	-0.7078*	-0.6917*	-0.6718*
Wnt8b	0.7888**	0.6372*	0.7407**
Other			
Cma1	0.01154	0.118	0.05785
Ctsd	0.4208	0.3976	0.4499
Ctsg	0.2945	0.1795	0.217

Ctsl	0.4371	0.3559	0.5014
Gpx1	-0.7362**	-0.4492	-0.6816*
Slc2a4	-0.773**	-0.7376**	-0.8644***
Sod1	-0.8099**	-0.6524*	-0.7409**

p<0.05*, *p*<0.01**, *p*<0.001***, *p*<0.0001****

Table 20. Pearson's correlation (r) of epididymal adipose tissue DEGs involved in DNL, adipogenesis, obesity and body composition and their relationships with phenotype (extension of table 15).

	Final bodyweight	**Epididymal fat mass**	**Liver mass**
Adipogenic/ lipogenic genes			
Acaca	0.3904	-0.00733	0.1805
Acly	0.3321	0.1906	0.1034
Acsl3	0.5664	0.4094	0.3991
Adpgk	0.493	0.3189	0.407
Aldoa	0.28	0.2034	0.1061
C1qtnf6	0.6483*	0.5052	0.6692*
Cnr1	0.5983*	0.4769	0.4406
Dgat2	0.4904	0.2524	0.2842
Elovl6	0.7839**	0.6116*	0.69*
G6pdx	0.2713	0.2483	0.1929
Igf2	0.5233	0.2934	0.5914*
Lep	0.6008*	0.384	0.4592
Lpl	0.5189	0.3835	0.4274
Mogat2	0.5692	0.3296	0.3514
Me1	0.6526*	0.3787	0.4732
Fads3	0.2519	0.1162	0.1352
Fasn	0.3606	0.2448	0.1191
Gpd1	0.1806	0.04371	-0.00283
Gys2	0.588*	0.3688	0.388
Insig1	0.6586*	0.4773	0.5187
Pgd	0.5673	0.3437	0.4023
Pnpla3	0.6992*	0.4305	0.4942
Rxra	0.1606	-0.08586	0.008922
Scarb1	0.1032	0.05209	0.06895
Scd2	0.7774**	0.4806	0.6098*

Serpine1	0.5258	0.5007	0.6234*
Serpine2	0.5424	0.3268	0.5992*
Sfrp1	0.3571	0.3389	0.1396
Sorl1	0.6542*	0.4093	0.4918
Taldo1	0.5287	0.3523	0.3667
Tpi1	0.4846	0.3338	0.3392
Tph2	0.7584**	0.4881	0.7377**
Anti-obesogenic / β-oxidation genes			
Acad10	-0.7549**	-0.6999*	-0.681*
Acad12	-0.8243***	-0.643*	-0.8071**
Acot7	-0.8226**	-0.7991**	-0.6943*
Adipoq	-0.3515	-0.4638	-0.3995
Adrb3	-0.831***	-0.6985*	-0.8813***
Cfd	-0.8235***	-0.7762**	-0.7788**
Cpt1c	-0.6714*	-0.7187**	-0.6056*
Enho	-0.564	-0.4481	-0.6358*
Fabp3	-0.5638	-0.2574	-0.4459
Irs1	-0.5926*	-0.6204*	-0.7277**
Mrps9	-0.4421	-0.6133*	-0.4287
Prkci	-0.6672*	-0.6135*	-0.6977*
Prkaa1	-0.5732	-0.6592*	-0.573
Prkag2	-0.6846*	-0.8628***	-0.6439*
Rorc	-0.689*	-0.6265*	-0.5872*
Sik3	-0.7433**	-0.6857*	-0.6678*
Sirt3	-0.7349**	-0.6778*	-0.7686**
Stk40	-0.7926**	-0.7113**	-0.8153**

$p<0.05$*, $p<0.01$**, $p<0.001$***, $p<0.0001$****

Table 21. Pearson's correlation (r) of KEGG pathway identified DEGs enriched in epididymal adipose tissue and their relationships with phenotype (extension of table 16).

	Final bodyweight	Epididymal fat mass	Liver mass
Peroxisome pathway			
Abcd2	-0.1437	-0.3344	-0.2948
Crat	-0.8652***	-0.7797**	-0.8644***
Dhrs4	-0.6196*	-0.6114*	-0.6893*
Ephx2	-0.7658**	-0.6434*	-0.8776***
Mlycd	-0.737**	-0.6192*	-0.763**
Pex5	-0.6944*	-0.6769*	-0.798**
Pex6	-0.8816***	-0.6852*	-0.8475***
Pex12	-0.7878**	-0.7208**	-0.7594**
Pxmp2	-0.7923**	-0.7177**	-0.8524***
Sod1	-0.8099**	-0.6524*	-0.7409**
RNA transport			
Casc3	-0.7083**	-0.6828*	-0.7071*
Eif3g	-0.7459**	-0.7747**	-0.6123*
Eif3h	-0.8128**	-0.6265*	-0.6601*
Eif4a3	-0.7517**	-0.5453	-0.5501
Eif4b	-0.6659*	-0.6533*	-0.4968
Fxr2	-0.7159**	-0.7647**	-0.7003*
Pabpc1	-0.7539**	-0.7514**	-0.607*
Rnps1	-0.7875**	-0.6638*	-0.637*
Spliceosome			
Cdc40	-0.783**	-0.6204*	-0.7083**
Cdc5l	-0.81**	-0.72**	-0.6762*
Eif4a3	-0.7517**	-0.5453	-0.5501
Prpf40b	-0.8067**	-0.7921**	-0.7918**
Snrnp40	-0.6626*	-0.5262	-0.4604
Srsf7	-0.7491**	-0.5148	-0.6568*
Phenylalanine metabolism			
Aoc2	-0.8584***	-0.7311**	-0.856***
Il4i1	-0.7454**	-0.7861**	-0.6649*
Mif	-0.7332**	-0.3941	-0.5634
Valine, leucine and isoleucine degradation			

Bcat2	-0.7102**	-0.6167*	-0.8108**
Hadha	-0.7257**	-0.6241*	-0.7825**
Ivd	-0.6806*	-0.7676**	-0.7899**
Il4i1	-0.7454**	-0.7861**	-0.6649*

p<0.05*, *p*<0.01**, *p*<0.001***, *p*<0.0001****

Chapter 5

Captopril extends lifespan, reduces body fat and improves age-related deterioration and response to stress in *Caenorhabditis elegans*

Abstract

In rodents, captopril reduces blood pressure, induces bodyweight and fat loss, improves insulin-sensitivity, and exhibits anti-inflammatory properties. The mechanism of action of captopril with respect to these aforementioned effects is not fully understood. Inhibition of ACE by captopril is due to its binding to the zinc-containing active site of the enzyme. A homolog of ACE (*acn-1*) is expressed in *Caenohabditis elegans* (*C. elegans*) but lacks the zinc-containing active site. The aim of the current study was to investigate the physiological response to captopril on body fat composition and lifespan, stress and locomotive patterns in *C. elegans*.

Standard nematode growth medium was mixed with three levels of captopril (0.02%, 0.05% and 0.10%), gentamycin (and FuDR for lifespan analyses), and seeded with 10% (*w/v*) OP50 *Escherichia coli (E. coli)*. For lifespan analyses, 100-150 worms were manually transferred on to control and captopril-treated plates containing FuDR. Worms were scored for death every other day. Body fat composition was assessed by upright microscope on fixative Oil red O stained worms. For analysis of animal pharyngeal pumping rates and motility, worms were recorded at 10-fold magnification using a stereo microscope. Image analysis was conducted using ImageJ (1.48v) and motility analysis was conducted using MBF WormLab software version 4.1.

Our results show treatment of L4 and young adult stage *C. elegans* (excluding L1-L3) extends the average lifespan by up to 33%. The average survivability of worms to both heat-shock and paraquat stressors under 0.10% captopril increased 17% and 45% respectively. Oil red O microscopy showed a reduction of body fat by up to 30% in captopril-treated worms relative to controls. These effects were dependent on the *daf-16*/FOXO transcription factor. Video analysis of worms crawling on treatment plates revealed decreases in mobility, where a declines of 61% and 42% was observed in track length and average speed respectively.

In conclusion, captopril extends lifespan, decreases overall body fat, and improves age-related decline and stress response of *C. elegans*.

Introduction

Identifying compounds that regulate energy homeostasis have the potential to facilitate the prevention of obesity and associated complications. Currently several anti-obesity compounds are on the market however their efficacy remains marginal (Butsch, 2015). The development and application of novel compounds requires a thorough understanding of molecular and cellular networks, however ascertaining integrated *in vitro* and *in vivo* responses of these compounds is challenging due to the complexity of tissues and animals. Therefore *in vivo* work is vital for bridging the knowledge gap between development and application of anti-obesity therapeutics and whole animal response (Alabaster, 2002).

A powerful approach to understanding the pathology of obesity is the shared expression of analogous signaling networks between humans and other animal species. The selective persistence of peptides and genes between animals suggests particular networks arose early in evolution and remains vital to life. One such example of this is the insulin/IGF-1 signaling pathway (IIS) and conservation of its role in determining lifespan and regulating fat storage in mammals and invertebrates (Kenyon, Chang, Gensch, Rudner, & Tabtiang, 1993; Papatheodorou, Petrovs, & Thornton, 2014). Alterations to IIS particularly in *Caenorhabditis elegans* (*C. elegans*) has aided our understanding of fundamental functions of the molecular and cellular machinery and its impact on whole animal fat metabolism and energy expenditure mechanisms (Apfeld, O'Connor, McDonagh, DiStefano, & Curtis, 2004; Kenyon et al., 1993; Van Gilst, Hadjivassiliou, Jolly, & Yamamoto, 2005).

Rationale

As a major component of the renin-angiotensin system (RAS), angiotensin-converting enzyme (ACE) is widely thought to play its most pivotal role in the regulation of blood pressure (BP), yet recent studies reveal inhibition of ACE in animals also potentiates insulin sensitivity and regulates body fat and bodyweight (de Kloet et al., 2009; Premaratna et al., 2012; Weisinger et al., 2009). Captopril belongs to a subclass of drugs known as ACE-inhibitors which inactivates the metalloprotease ACE mitigating the conversion of Ang-I to the endothelial effector peptide Ang-II (Mann, 1984). Unlike second generation ACE-inhibitors which compete with Ang-I for two active sites of ACE i.e. C- and N-domains (making them more potent), captopril forms a strong ionic bond between its thiol moiety and the zinc-ion residing within the active site of ACE (Uehara et al., 1994).

The *C. elegans* has become an attractive model organism in medical research for it shares 35% gene homology with humans where 83% of its proteome has homologous human genes (Lai, Chou, Ch'ang, Liu, & Lin, 2000). More specific to our interests, *C. elegans* also contains a homologue of the mammalian ACE gene (*acn-1*) although the post-translational product lacks the zinc-containing catalytic residue (Brooks, Appleford, Murray, & Isaac, 2003; Turner & Hooper, 2002). A BLASTN

of *Homo sapiens* against *C. elegans* reveals no sequence similarities to the precursor to ang-I (AGT) or ang-II receptor types (AT_1 and AT_2), and despite the identification of sequence similarities with the mammalian (pro)renin-receptor (PRR), divergent functions have been substantiated (Bader, 2007). Therefore unlike mammalian ACE, the *C. elegans* ACN-1 is catalytically inactive and functionally independent of a RAS (Bader, 2007; Coates, 2003; Coates, Siviter, & Isaac, 2000; Isaac, Siviter, Stancombe, Coates, & Shirras, 2000; Turner & Hooper, 2002). We therefore investigated the effects of captopril in *C. elegans* in an effort to determine whether body fat, stress and locomotive patterns are comparable to that of captopril administered rodents, and whether these effects converge on to AMPK signaling pathways. We hypothesise that captopril will cause a reduction in body fat, increase health span, improve stress tolerance, and alter the locomotive patterns of *C. elegans* to a capacity that may be comparable to that of rodents treated with captopril.

Methods

Strains and maintenance

Wild-type *C. elegans* strain (N2) and mutant strain *daf-16* were acquired from CGC, *flcn-1* was supplied by Professor Arnim Pause (McGill University, Montreal Quebec), and *dhs-3::gfp* strain was supplied by Professor Ping Sheng Liu (Chinese Academy of Sciences, Beijing China), and maintained at 20ºC on NGM agar plates seeded with *E. coli* OP50 as food source.

Captopril treatment of agar plates

Captopril was obtained from Sigma Aldrich (St. Louis, MO, USA), and three levels of the drug, 0.02%, 0.05% and 0.10% (w/v), and mixed in freshly autoclaved and cooled (~55ºC) NGM solution, making up a final concentration of 0.92mM, 2.30mM and 4.60mM respectively.

Lifespan experiments

Lifespan studies were conducted as previously described (Sutphin & Kaeberlein, 2009). Experimental worms were grown at 20ºC for three generations without starving and L1 were hatched by standard hyperchlorite procedure (Porta-de-la-Riva, Fontrodona, Villanueva, & Ceron, 2012)). L4 larvae were transferred on to 30mm experimental plates (10 animals per plate).

All lifespan experiments were performed on NGM agar plates or NGM plates supplemented with the above mentioned concentrations of captopril mixed with gentamicin (Thermo Fisher, AU) and 2'-deoxy-5-fluoroudine (FuDR; Sigma Aldrich, USA), to a final concentration of 50mg/L and 100mg/L respectively. All plates were prepared with a 2% palmitic acid ring dissolved in absolute ethanol to prevent animals from escaping. Animals that did not move after repeated stimulus were considered dead. Animals that crawled away from plate or with burst vulva were excluded from the analysis. A total number of 50-100 animals were used for each condition and experiment. All lifespan experiments were performed three to five times. Maximum lifespan was defined as the

mean of 10% long lived animals. A *log*-rank *p*-value of less than 0.05 was used for establishing significance.

Preparation of worm homogenates and biochemical assays

Preparation of worm homogenates was performed as previously described (Palgunow, Klapper, & Döring, 2012). Briefly, wild-type nematodes were cultivated under regular NGM or NGM containing different levels of test compound with standard cholesterol concentration (12.5µM). L1 worms were hatched by standard hypochlorite procedure, and aliquoted on to a nitrocellulose filter (pore-size 0.1µm) to remove carcases. Worms were allowed to crawl off overnight, and filters were removed.

For each replicate, ~3000 L4 larvae were collected. Animals were homogenised in 100µl buffer (150 mM NaCl; 1 mM EDTA; 50 mM Tris-HCl, pH 7.5; 0.5% CHAPS) using Precellys 24 homogonizer (Bertin Technologies) and ceramic beads (1.4mm). Cell debris was removed by centrifugation at 21,000 *g* for 20 min. Homogenates were used in Indiko analyser (Thermo Fisher Scientific, AU) for colorimetric determination of the triglycerides and protein content. The TG content was determined using an enzymatic assay in accordance with the Indiko platform. The protein content was measured using Pierce® BCA protein assay kit (Thermo Fisher Scientific, AU) and adapted to the Indiko platform according to manufacturer's protocol, and bovine serum albumin (BSA) as protein standard.

Oil Red O preparation, *C. elegans* fixation, fat staining and analysis

Oil red O staining was conducted as previously reported (Wahlby et al., 2014). A 0.5% Oil red O (Sigma Aldrich, USA) stock solution was prepared in 100% isoptopanol (Sigma Aldrich, USA), allowed to rock for a day and filtered twice through a 0.45µm filter (Millipore, USA). The day before use, stock was diluted to 60% in distilled water and filtered again through a 0.45 µm filter just before use.

Wild-type and mutant strain *C. elegans* were harvested at L4 stage in to 1.5ml tubes, washed three times in M9 buffer and allowed to settle by gravity. Worms were fixed by resuspending in 500µl of 60% isopropanol, allowed to settle and the supernatant aspirated. 500µl of freshly filtered Oil red O working solution was added and worms were stained for 6-18 hours in a wet chamber. After staining, the supernatant was washed with M9 followed by the resuspension of animals in to 250µl of 0.01% Triton X-100 (Sigma Aldrich, USA) in S-basal. For image acquisition, 3% agar pads were prepared on slides, and 3µl of mounting medium (Vector Labs) was added on to 24 × 24 mm cover slips. 5µl of the worm suspension was transferred on to the cover slip, mixed with the mounting medium using the tip of a pipette, and flipped on to agar pads. Images per condition were acquired on the Nikon inverted microscope and analysed using Image J (v14.8v) software.

Determination of body length, pharyngeal pumping rate and motility

For analysis of body length, Oil red O stained animals were measured using Image J software and length measurements derived by the sum-total of a number of segmented lines of known length, down the centre of the worm. For analysis of animal pharyngeal pumping rate, 20 animals per treatment group were analysed at L4 larval stage on a Nikon inverted microscope. The pharynx was filmed for 60 seconds at 100-fold magnification using Nikon DS-Fi2 camera, and the pharyngeal pumping rate (pumps/min) was counted on slowed films. For analysis of animal motility, worms were recorded for 20 seconds at 8-fold magnification using Nikon upright microscope fitted with a Nikon camera, and MBF WormLab software version 4.1 was used for video analysis of worms exposed to different levels of captopril. Locomotion parameters selected from the analysis included track length (μm) [forward + reversal] and speed (μm/s) [tracklength per second].

Stress response assays

Wild-type *C. elegans* were cultivated at 20ºC under control or 0.10% captopril and transferred to stressful contirions and monitored for survival. Thermotolerance assays were performed as described (McColl et al., 2010); briefly, L4 larvae were transferred to 34ºC and scored the percentage of dead and live animals starting at 6 hours and continuing every hour until all animals died. To perform oxidative stress assays, a total of 10 L4 larvae were transferred to experimental NGM plates containing 40mM paraquat and scored for survival every hour. Experiments were performed three times.

Statistical Analysis

Data are represented as mean ± standard deviation (SD), unless otherwise stated. Numerical data was analysed by repeated measures ANOVA and unpaired t-test (two-tailed) using IBM Statistical Package for Social Science version 25.0 (SPSS, Chicago IL). For survival analyses, *p*-values were calculated by the log-rank test. Difference were considered statistically significant at $p<0.05$.

Results

The effect of captopril on lifespan of *C. elegans*

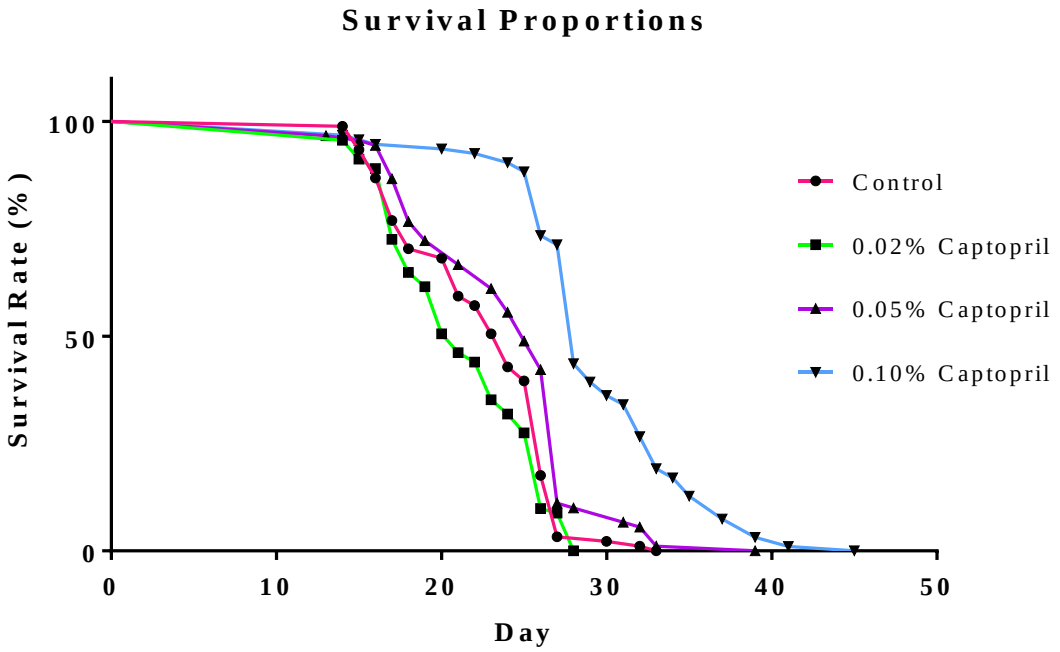

Figure 36. Survival curves were recorded for WT worms exposed from L4 stage to varying levels of captopril; control (0%), 0.02%, 0.05% and 0.10% was incorporated in to their growth medium. Survival is presented as survival rate % (Kaplan-Meyer curve) as mean of three different experiments with 30-50 worms each.

As shown in figure 38, doses of 0.05% and 0.10% captopril had a significant effect on the lifespans of *C. elegans.*

Survival				
	Control	**0.02% Captopril**	**0.05% Captopril**	**0.10% Captopril**
Mean (days)	21.1±4.7	21.3±4.3	23.9±5.2*†	29.3±5.7*†‡
Difference (%)		0.94±8.9	12.4±10.1	32.5±19.2
Minimum (days)	15.6±1.1	14.8±1.0	16.7±1.5	22.4±6.3*†‡
Maximum (days)	27.4±0.9	26±0	31.7±1.7*†	39±2.8*†‡

Table 22. The effect of captopril on the lifespan of *C. elegans*. Data are represented as mean lifespan ± SD from three independent experiments. *P*-values were calculated between all groups using one-way ANOVA. Statistical significances indicated by *p<0.05 vs control; †p<0.01, vs 0.02% captopril; ‡p<0.01vs 0.05% captopril. Percent difference represents percentage change of mean

lifespan of control group versus three independent treatments groups and maximum represents mean lifespan of the bottom 10th percentile.

Table 17 summarises the most notable lifespan outcomes of captopril administration in *C.elegans*. As tabulated, there was a significant increase of 12.4% and 32.5% in the mean lifespan of worms receiving 0.05% and 0.10% captopril from their medium in comparison to the two remaining groups. A significant lengthening of the average age of death of the upper 10th percentile (minimum) of worms administered a dose of 0.10% captopril (35.8%) and lower 10th percentile (maximum) of worms administered a dose of 0.05% and 0.10% captopril (14.6% and 35.4%, respectively) was also observed.

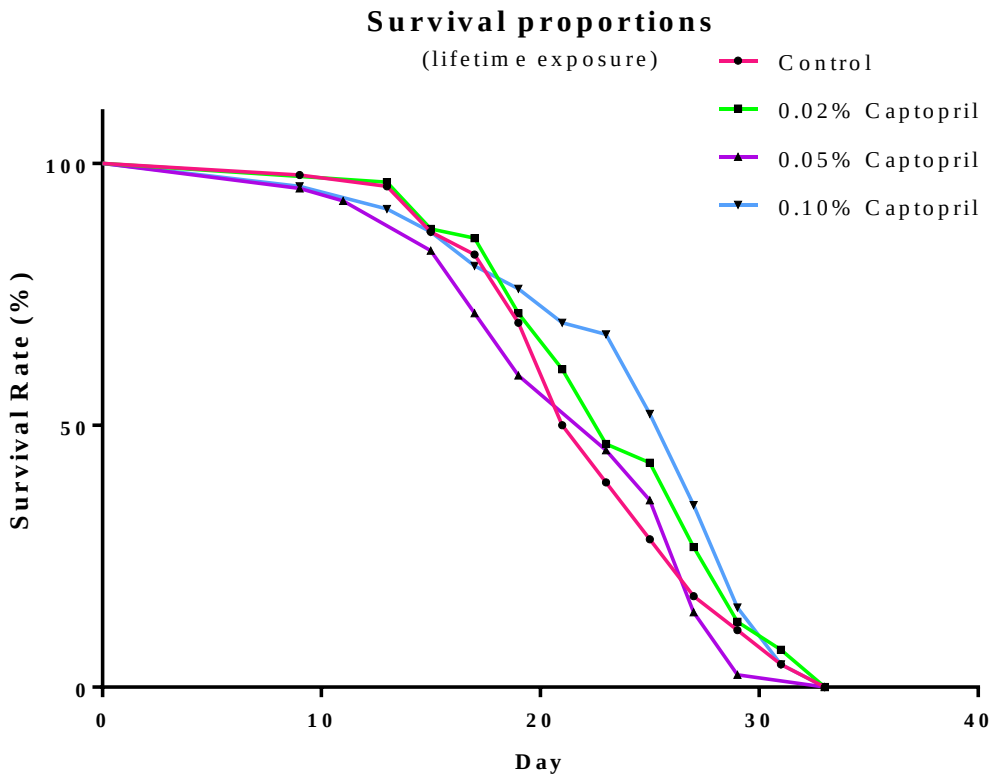

Figure 37. Survival curves were recorded for WT *C. elegans* with varying levels of captopril, control (0%), 0.02%, 0.05% and 0.10%, incorporated in to their growth medium from L1 stage of life. Survival is presented as survival rate % as mean of three different experiments with 15-20 worms each.

Figure 37 indicates that lifespan extension properties of captopril are undetectable when worms are exposed from L1 through to death.

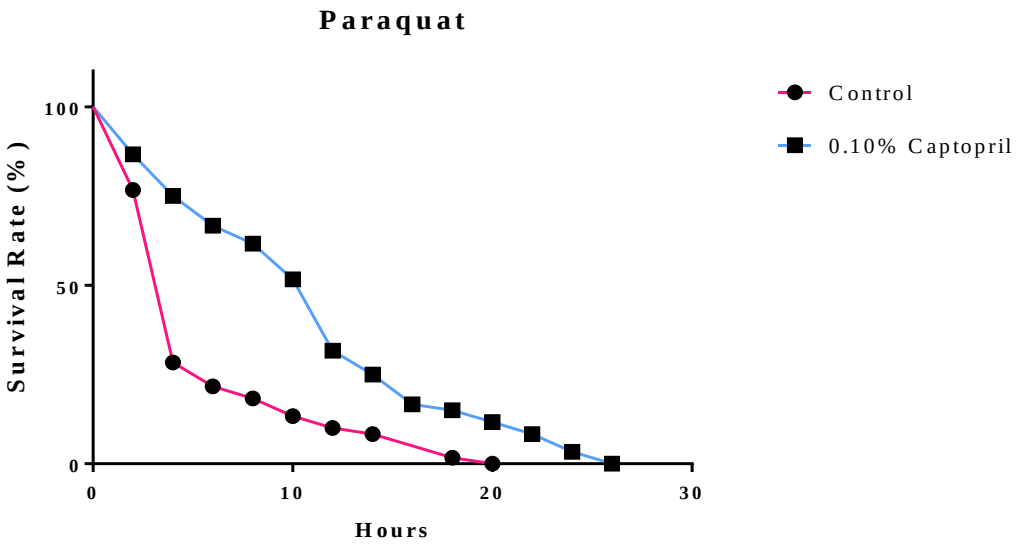

Figure 38. Survival curves were recorded for L4 WT worms exposed to 40mM of paraquat treated with or without 0.10% captopril. Survival is presented by survival rate (%) as mean of three different experiments with 30-50 worms each. At 30 hours, survival rates for positive controls (*C. elegans* unexposed to paraquat) is 100%.

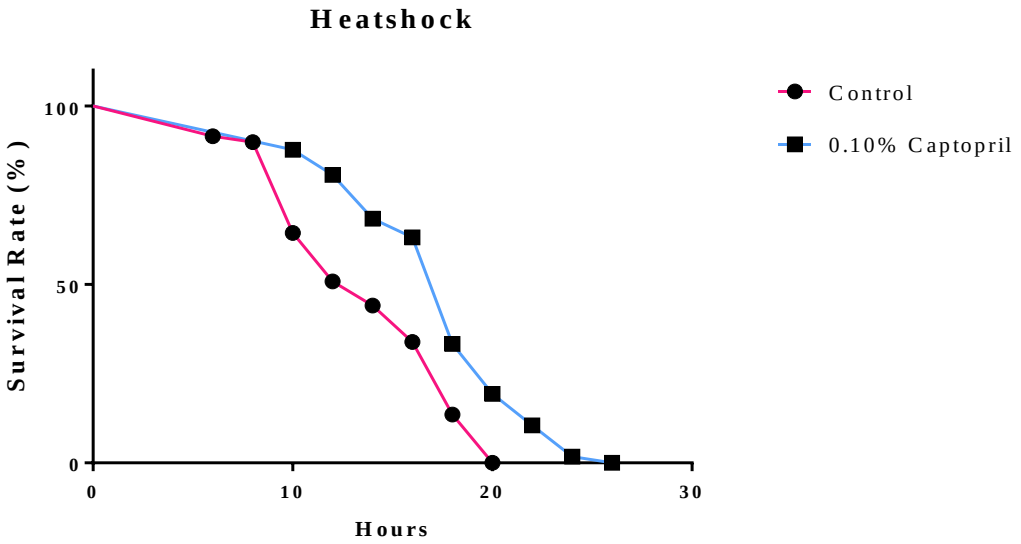

Figure 39. Survival curves were recorded for L4 WT worms exposed to continuous 34°C heat stress with or without 0.1% captopril. Survival is presented by survival rate (%) as mean of three different experiments with 30-50 worms each. At 30 hours, survival rates for positive controls (*C. elegans* unexposed to paraquat) is 100%.

As presented in figures 38 and 39, L4 *C. elegans* exposed to stressful conditions, including continuous 34°C heat and the oxidant paraquat (40mM), coped better in the presence of 0.10% captopril over their control counterparts. Refer to table 18 below for a summary of results.

Stressor				
Survival	*Paraquat (200mM)*		*Heat (34°C)*	
	Control	**0.10% Captopril**	**Control**	**0.10% Captopril**
Mean (hours)	5.7± 4.7	11.0± 6.8****	13.8± 4.4	17.3± 4.3****
%Difference	63.5±36.5		22.5±2.3	

Table 23. The effect of captopril on stress responses in *C. elegans*. Data are represented as mean lifespan ± SD from three independent experiments. *P*-values were calculated between all groups using unpaired t-test. Statistical significances indicated by **p*<0.05, ***p*<0.01, ****p*<0.001 *****p*<0.0001 vs control. Percent difference represents percentage change of mean lifespan of control group versus treatment groups.

Table 18 summarises the lifespan outcomes in captopril treated and non-treated *C. elegans*. Worms exposed to 0.10% captopril in the presence of 40mM paraquat on average lived 63.5% longer (11.0 hours) than their control counterparts (5.7 hours), and worms exposed to continuous heat in the presence of 0.10% captopril on average lived 22.5% longer (17.3 hours) than controls (13.8 hours).

The effect of captopril on fat storage in *C. elegans*

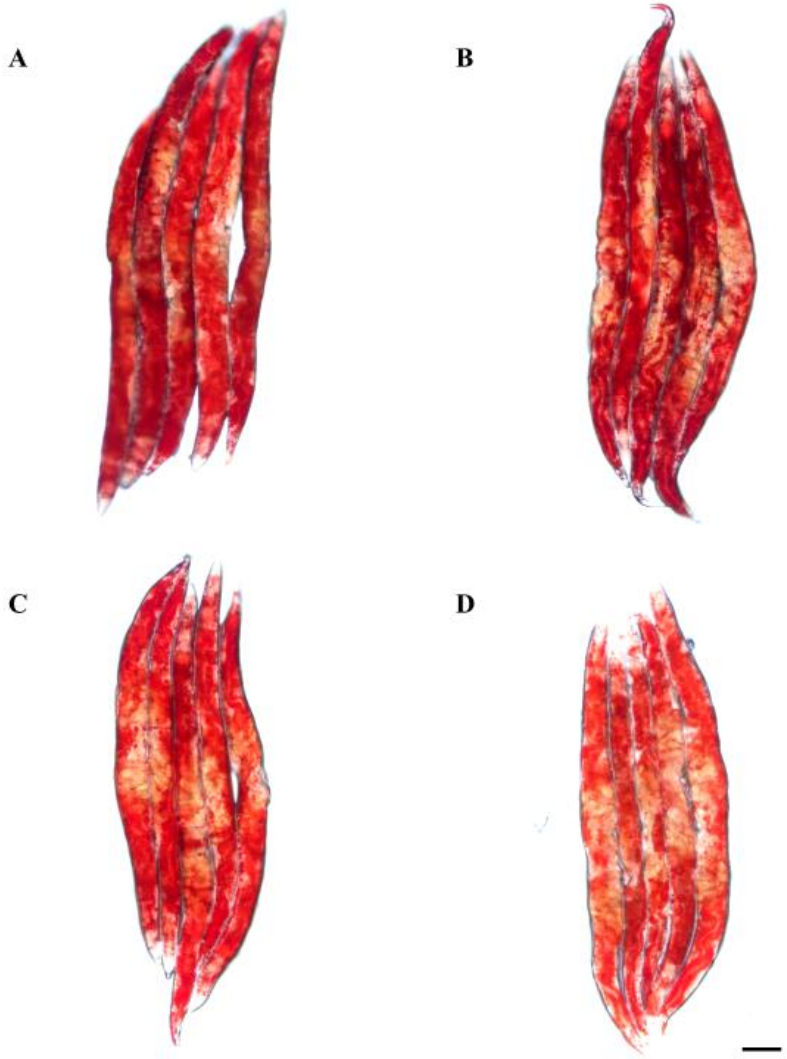

Figure 40. Bright field microscopy images of oil red O staining of (A) control, (B) 0.02%, (C) 0.05% and (D) 0.10% captopril administered WT *C. elegans*. Magnification 100×, scale bar 100μm.

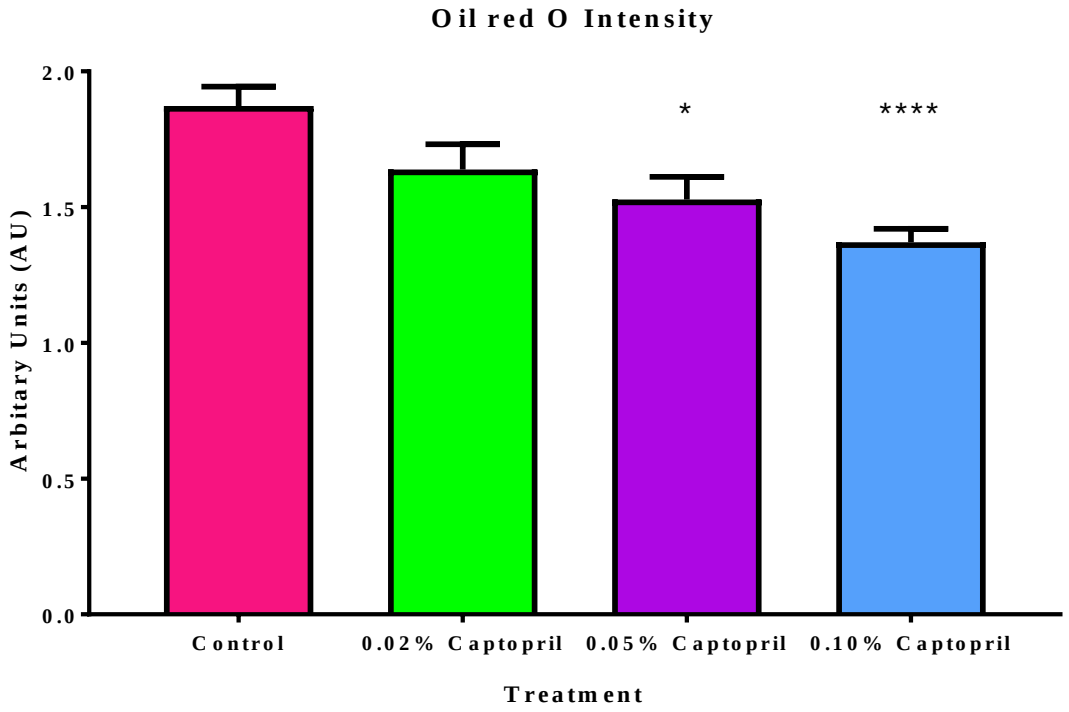

Figure 41. Influence of varying levels of captopril on TG content of WT L4 *C. elegans.* Worms were harvested at L4 stage and fixed with lipophilic stain oil red O. Results are represented as mean ± SEM of three independent experiments using 15-20 worms per treatment group. *P*-values were calculated using one-way ANOVA. Statistical significances indicated by *$p<0.05$, ****$p<0.0001$ vs control.

As presented in figure 41, *C. elegans* treated with 0.05% and 0.10% captopril showed a 20.25% and 30.90% reduction in oil red O staining in comparison to controls. No significant differences were observed between 0.02% captopril treated worms and controls, and no significant differences were observed between 0.05% and 0.10% captopril treated groups. Results are summarised in table 19 below.

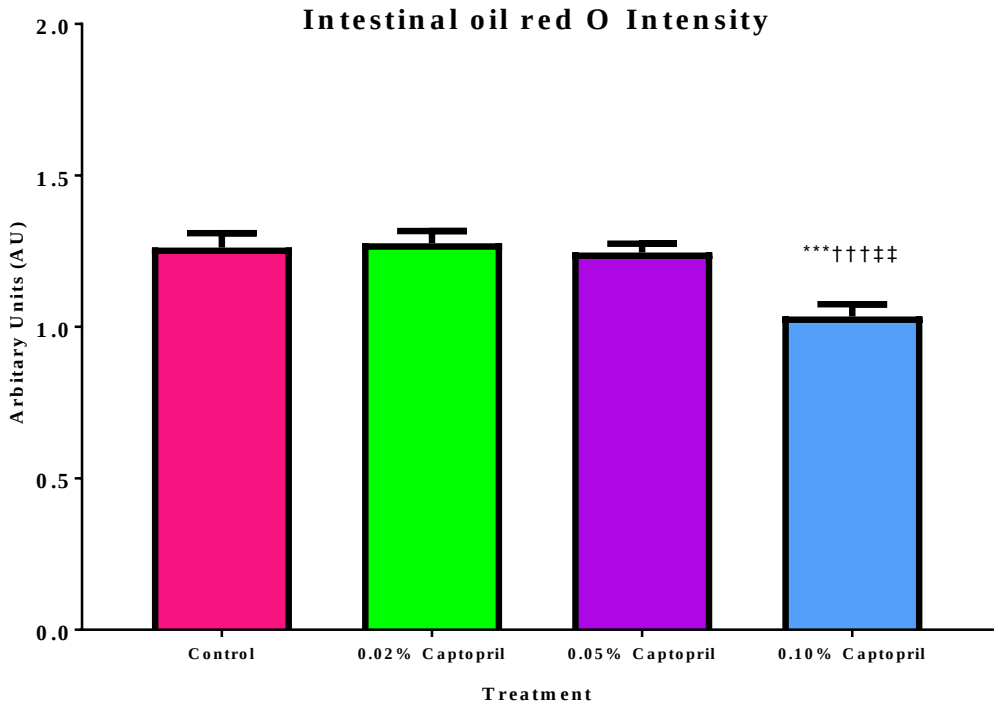

Figure 42. Influence of varying levels of captopril on TG content in intestinal regions of WT L4 *C. elegans*. Results are represented as mean ± SEM of three independent experiments using 15-20 worms per treatment group. *P*-values were calculated using one-way ANOVA. Statistical significances indicated by ***p<0.001 vs control, ††† p<0.001 vs 0.02% captopril and ‡‡ p<0.01vs 0.05% captopril.

Whole Body				
	Control	**0.02% Captopril**	**0.05% Captopril**	**0.10% Captopril**
Mean (AU)	1.87± 0.32	1.64± 0.42	1.53± 0.37*	1.37± 0.22****
%Difference		13.27±26.8	20.25±15.82	30.90±35.87
Intestinal Region				
Mean (AU)	1.26±0.20	1.28±0.16	1.25±0.12	1.04±0.17***††‡‡
%Difference		1.57±22.22	-0.8±50.0	19.13±16.22
Intestinal lipid droplets (dhs-3::gfp)				
Diameter (µm)	1.93±0.13	-	-	1.08±0.076***

Table 24. The effect of captopril on fat storage and LD diameter in *C. elegans*. Data are represented as mean extinction values (AU) ± SD from three independent experiments with 10-15 worms each. *P*-values were calculated between all groups using one-way ANOVA. Statistical significances indicated by *p<0.05, ***p<0.001 and ****p<0.0001 vs control; p<0.001 vs 0.02% captopril and ‡‡ p<0.01vs 0.05% captopril. Percent difference represents percentage change of mean of treatment groups to control.

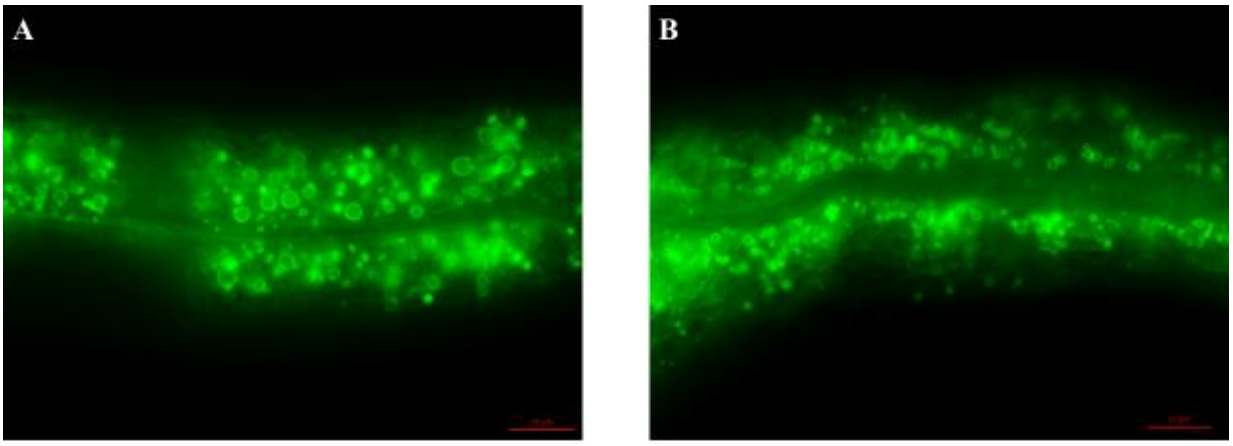

Figure 43. Fluorescent microscopy of intestinal lipid droplets of (A) control and (B) 0.10% captopril administered *dhs-3*::gfp *C. elegans* at L4 stage. Magnification of photographs 200×; scale bar, 10µm. See table 19 for a summary of results.

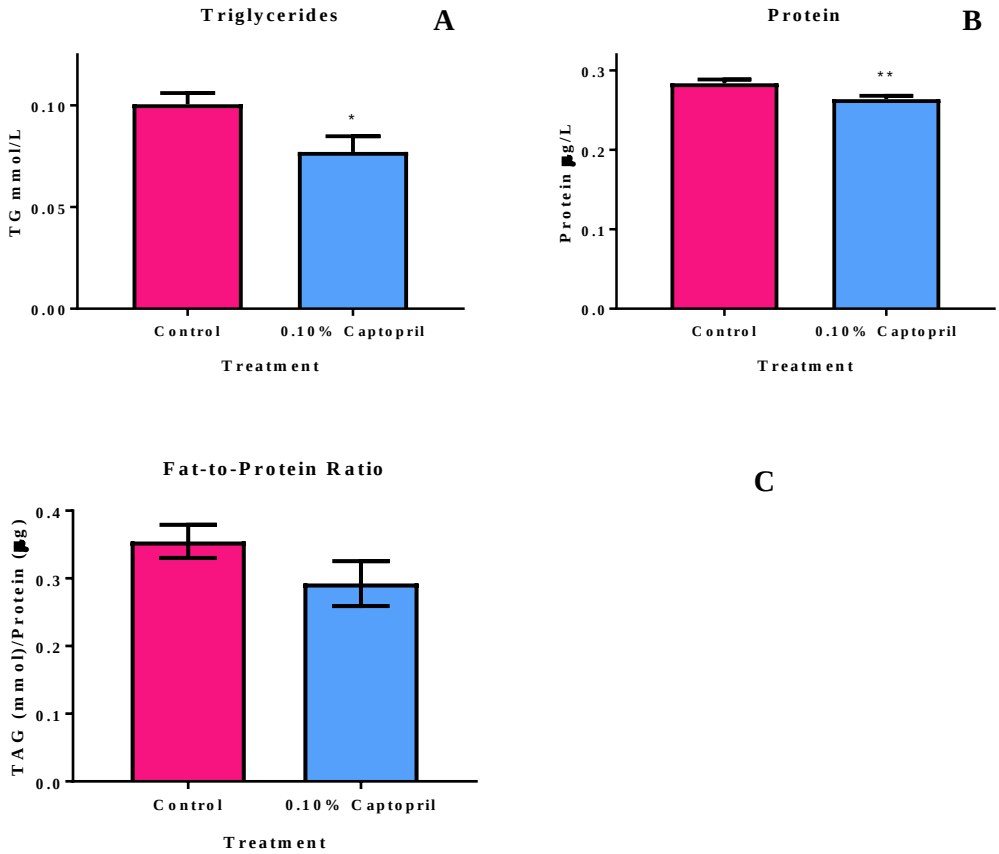

Figure 44. Triglyceride-to-protein ratio of pooled WT L4 *C. elegans* homogenates receiving either no treatment or 0.10% captopril. Results are represented as mean ± SEM from three independent experiments where *p<0.05, **p<0.01.

Figure 42 shows 0.10% captopril treated WT *C. elegans* had a 19% reduction in oil red O staining intensity within intestinal regions (or mid-third) in comparison to controls, 0.02% and 0.05% captopril treated groups. Figure 43 shows a 56% reduction in LD diameter in the intestinal regions

of *C. elegans* receiving 0.10% captopril from their growth medium. Figure 44A-B represents the body composition analysis carried out on 5000-6000 L4 stage worms using TG and protein measurements. TG content of worms treated with 0.10% captopril decreased along with protein content in comparison to untreated control counterparts. There was a relative decrease in TG-to-protein ratio in captopril treated worms (figure 44C) although this was not significant (p = 0.594). Results are summarised in table 19 above.

The effect of captopril on age-related functional change and satiety

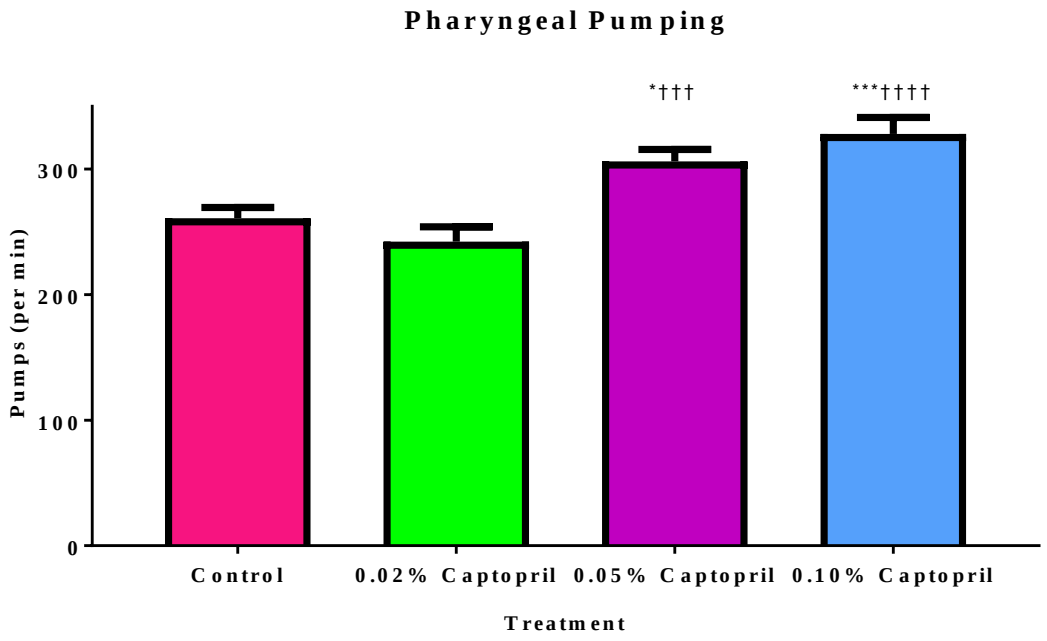

Figure 45. Mean pharyngeal pumping rate of WT L4 *C. elegans* receiving either no captopril or 0.02%, 0.05% and 0.10% captopril in their growth medium. Results are represented as means ± SD of three experiments with 10-15 worms each. Statistical significance was analysed using one-way ANOVA, where *p<0.05 & ***p<0.001 vs. control; †††p<0.001 & ††††p<0.0001 vs. 0.02%

Pharyngeal pumping rate is often positively correlated with ageing rates in *C. elegans* (Huang, Xiong, & Kornfeld, 2004). Exposure of L4 *C. elegans* to 0.05% and 0.10% captopril induced a significant increase in pharyngeal pumping relative to controls and 0.02% captopril treated worms (Figure 10, mean±SEM, control: 260.9±8.58 pumps min^{-1}, 0.02% captopril: 242.2±11.84 pumps min^{-1}; 0.05% captopril: 306.1±9.55 pumps min^{-1}; 0.10% captopril: 328.1.1±13.06 pumps min^{-1}).

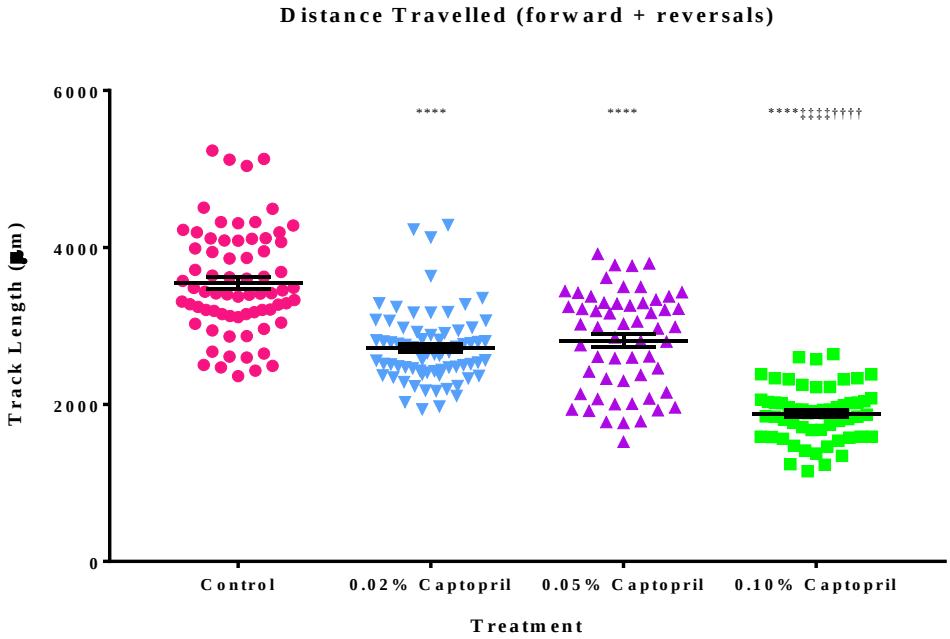

Figure 46. The distance travelled by captopril administered WT *C. elegans* was analysed using worm tracking software (refer to Materials and Methods). Nematodes were analysed at L4 stage. Results are represented as mean ± SEM of three experiments with 20-25 individual worms. Significant decreases in the track lengths of captopril administered worms is indicated by asterisks where ****p<0.0001 vs control, ††††p<0.0001 vs. 0.02% ‡p<0.05, ‡‡‡‡p<0.0001 vs. 0.05%.

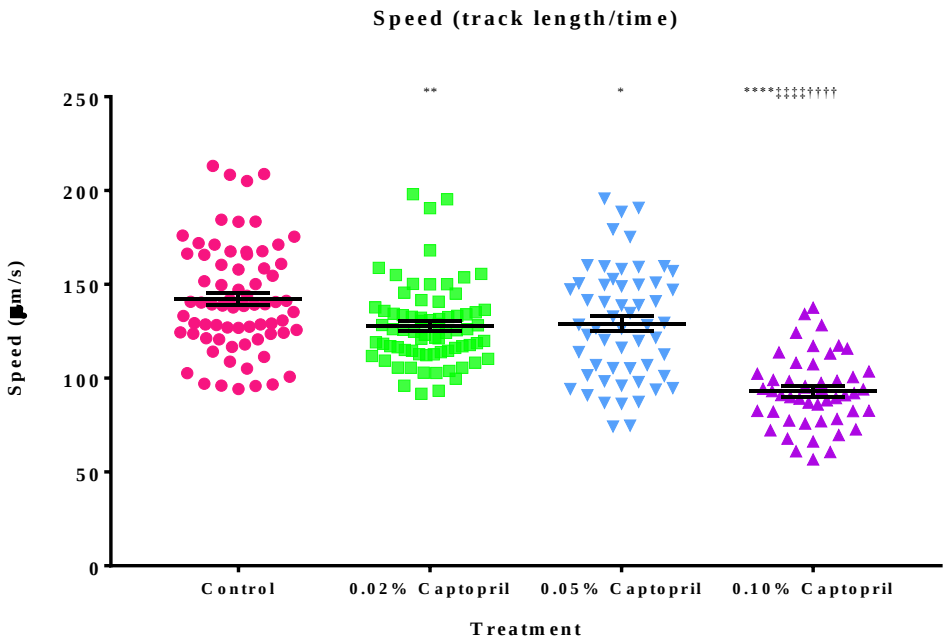

Figure 47. Speeds of movement of captopril administered L4 *C. elegans* were analysed using worm tracking. Results are represented as mean ± SEM of three experiments with 20-25 individual worms.

Significant decreases in captopril administered worms is indicated by asterisks where *p<0.05, **p<0.001, ****p<0.0001 vs control, ††††p<0.0001 vs. 0.02% ‡‡‡‡p<0.0001 vs. 0.05%.

	Control	**0.02% Captopril**	**0.05% Captopril**	**0.10% Captopril**
Body length (µm)	929.9±48.04	900.4±32.2	912.8±36.08	754.6±59.7
Pharyngeal pumping (pumps sec^{-1})	260.9±28.44	242.2±39.28	306.1±33.06	328.1±43.32**
Track length (µm)	3550±670.5	2719±467.1****	2184±786.2****	1884±344.8 ****††††‡‡‡‡
Speed (µm sec^{-1})	142.1±28.63	127.7±21.41**	124.5±28.11*	92.89±18.82 ****††††‡‡‡‡

Table 25. The effect of captopril on age-related functional changes and satiety in *C. elegans*. Results for length, feeding behaviour and motility [track length + speed] of WT L4 C. elegans grown in the presence of denoted captopril concentrations are summarised. Data derived from bright-field microscopy as images and 40-60 second videos. Results are presented as mean ± SD of three independent experiments. Differences are indicated on corresponding figures.

Note: Maximum speeds of *C. elegans* also followed the same trend where a steady decline with captopril treatment was observed (data not shown).

Muscular activity and locomotive behaviour in *C. elegans* can be influenced by their internal and external milieu. We quantified worm's pharyngeal contractions and motility including track length [forward + reversal µm] and speed (µm s^{-1}) using high magnification videos and worm tracking software respectively (refer to Materials and Methods). Administering 0.05% and 0.10% captopril in the growth medium lead to a 15.9% and 22.8% increase in muscular activity of the pharynx L4 *C. elegans* to that of controls. Captopril also resulted in significant changes in whole animal motility over un-administered controls by decreasing distances travelled and speeds of movement; results are summarised in table 20.

The effect of captopril on lifespan and fat accumulation in *daf-16* and *flcn-1* loss-of-function *(lf)* mutants

We next looked at possible candidate pathways captopril may influence that either facilitate or repress AMPK signaling pathways by administering our founded optimal dose of 0.10% to mutant *C. elegans* strains.

daf-16

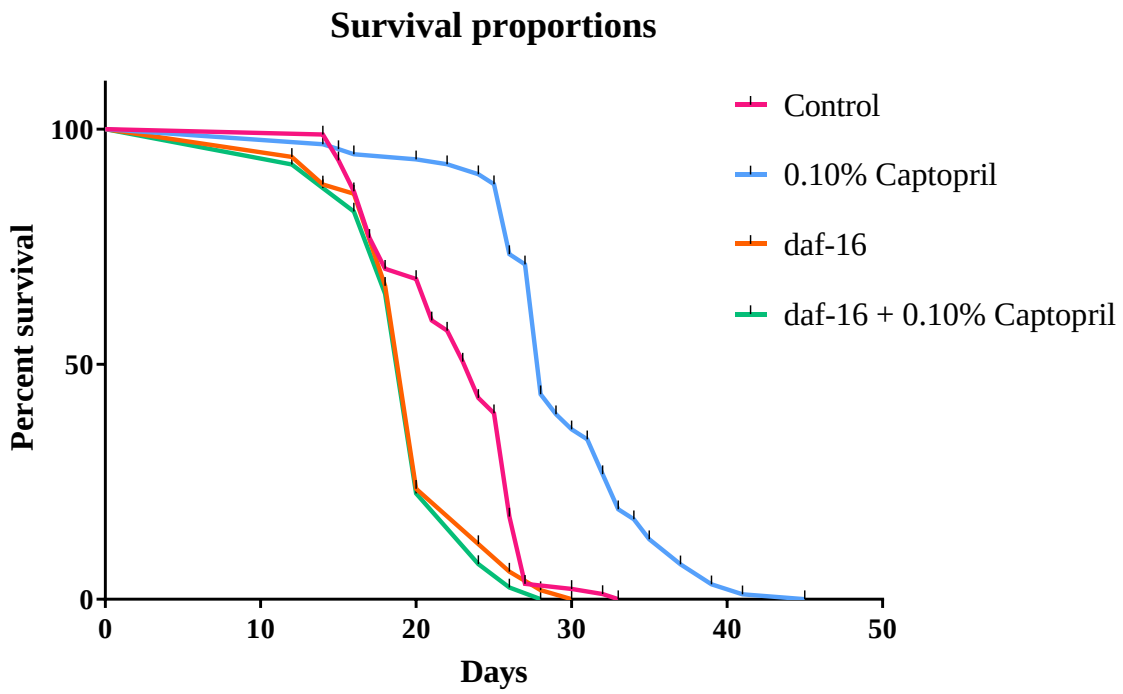

Figure 48. Survival curves were recorded for WT and *daf-16* worms with and without 0.10% captopril incorporated in to their growth medium. Survival is presented as survival rate % as mean of two different experiments with 30-50 worms each.

As shown in Figure 48, captopril did not extend the lifespan of *daf-16(lf)* worms. This suggests *daf-16*/FOXO transcription factor activity is required for the longevity effect of captopril. Captopril's ability to extend lifespan may therefore be regulated upstream of *daf-16*/FOXO.

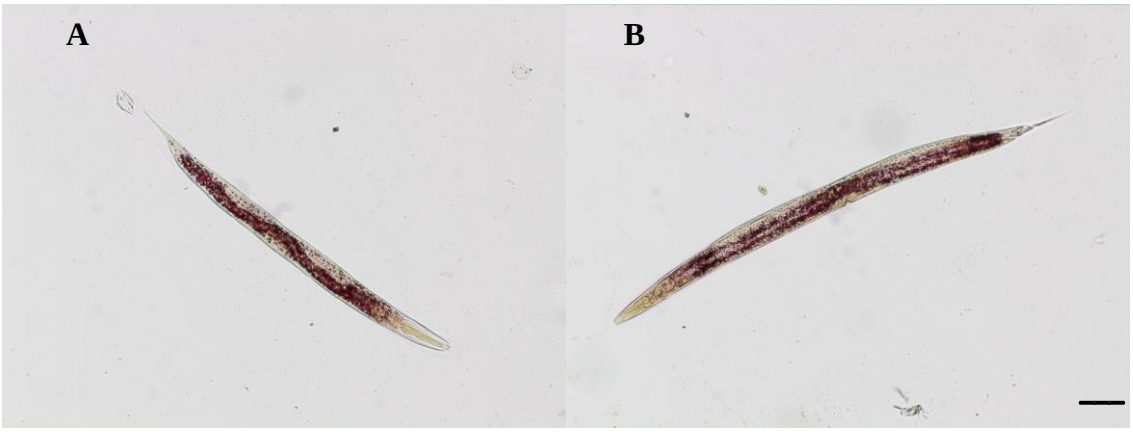

Figure 49. Bright field microscopy images of Oil red O stained (A) *daf-16* and (B) *daf-16* with 0.10% captopril added to their growth medium. Magnification of all photographs 100×, scale bar 100µm.

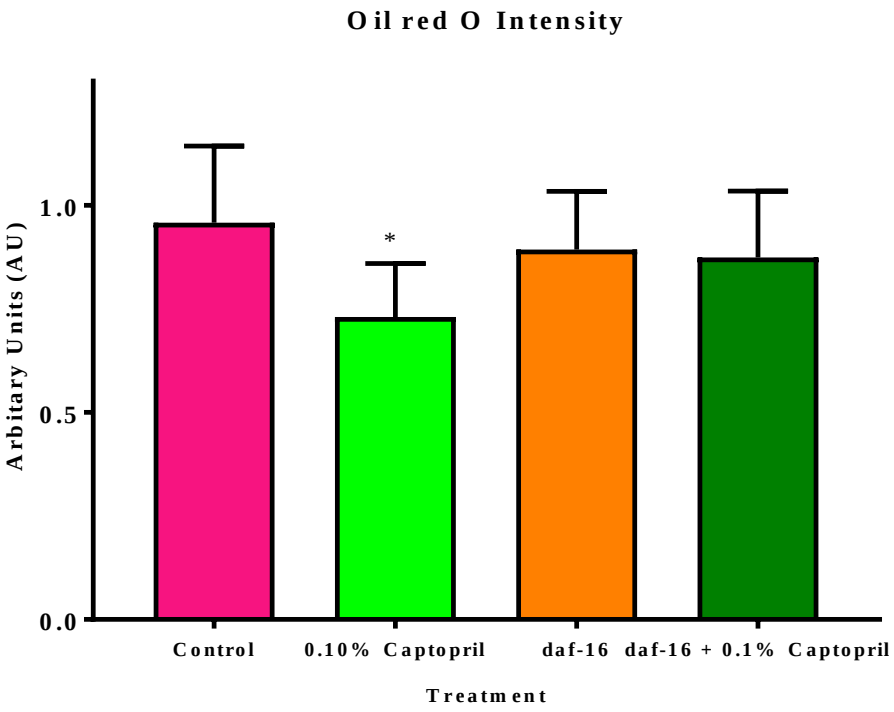

Figure 50. WT and daf-16 worms were harvested at L4 stage and fixed with oil red O. Results are represented as mean ± SEM of two independent experiments using 15-20 worms per treatment group. Captopril had no significant effect on oil red O intensity between treated and untreated daf-16 worms and untreated WT worms.

Figure 50 shows no difference in oil red O staining intensities between 0.10% captopril treated and untreated *daf-16*/FOXO mutant nematodes.

	Control (WT)	WT + 0.10% Captopril	*daf-16(mu)*	*daf-16(mu)* + 0.10% Captopril
Survival				
Mean (days)	20.8±6.5	23.8±3.7**	17.5±2.6**	17.6±2.7**††††
Difference (%)		13.45	-17.23	0.57

Table 26. The effect of captopril on the lifespan of *daf-16* loss-of-function mutants. Data are represented as mean lifespan ± SD from three independent experiments. *P*-values were calculated between all groups using one-way ANOVA. Statistical significances indicated by **p<0.01; ****p<0.0001 vs control; ††††p<0.0001 vs 0.10% captopril. Percent difference represents percentage change of mean lifespan of control group versus three independent treatments groups.

flcn-1

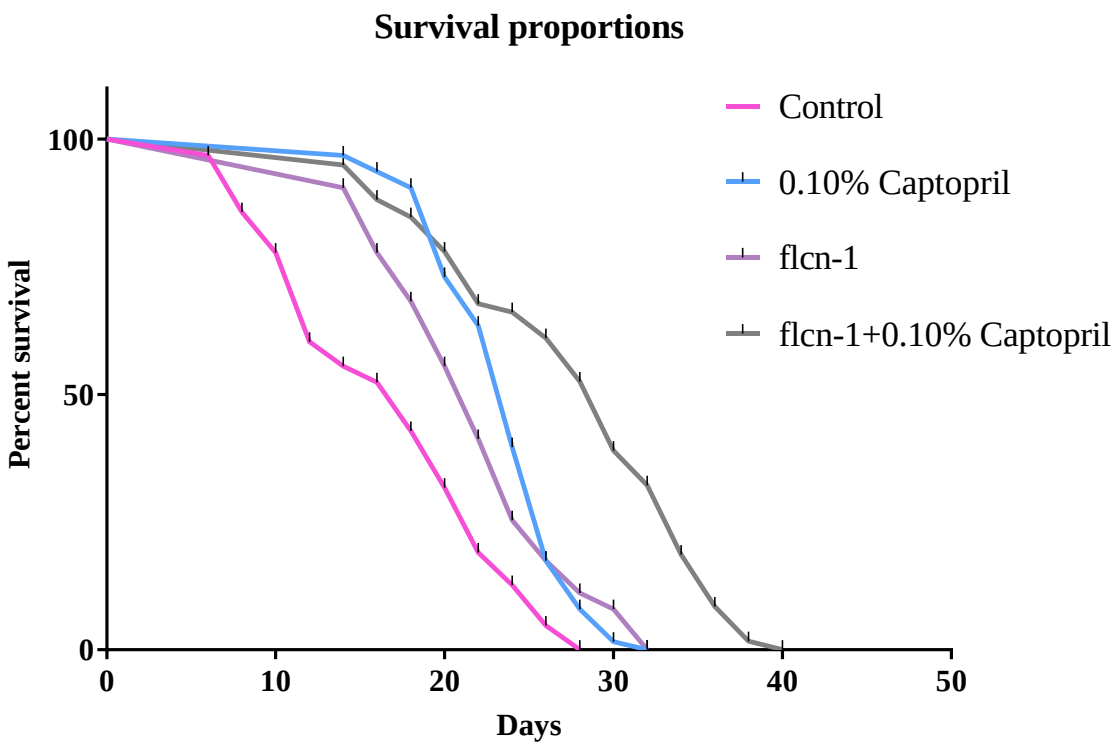

Figure 51. Survival curves were recorded for WT and *flcn-1(lf)* worms with and without 0.10% captopril incorporated in to their growth medium. Survival is presented as survival rate % as mean of two different experiments with 30-50 worms each.

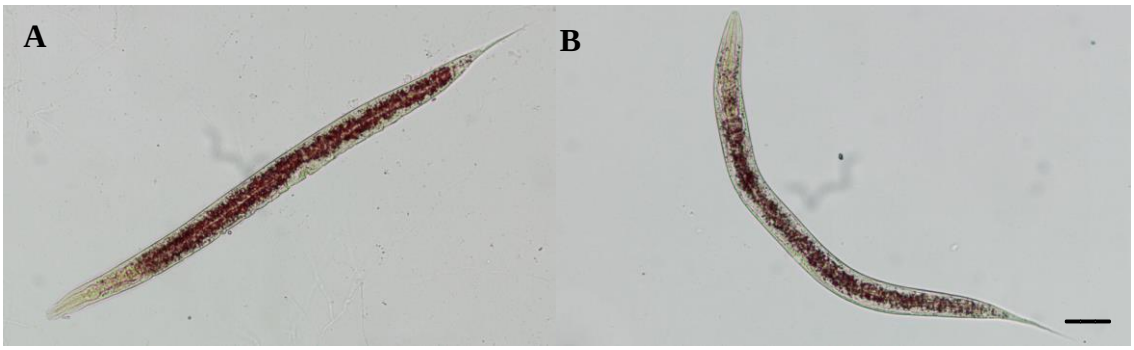

Figure 52. Bright field microscopy images of oil red O stained (A) *flcn-1* and (B) *flcn-1* + 0.10% captopril (B) added to their growth medium. Magnification of all photographs 100×, scale bar 100µm.

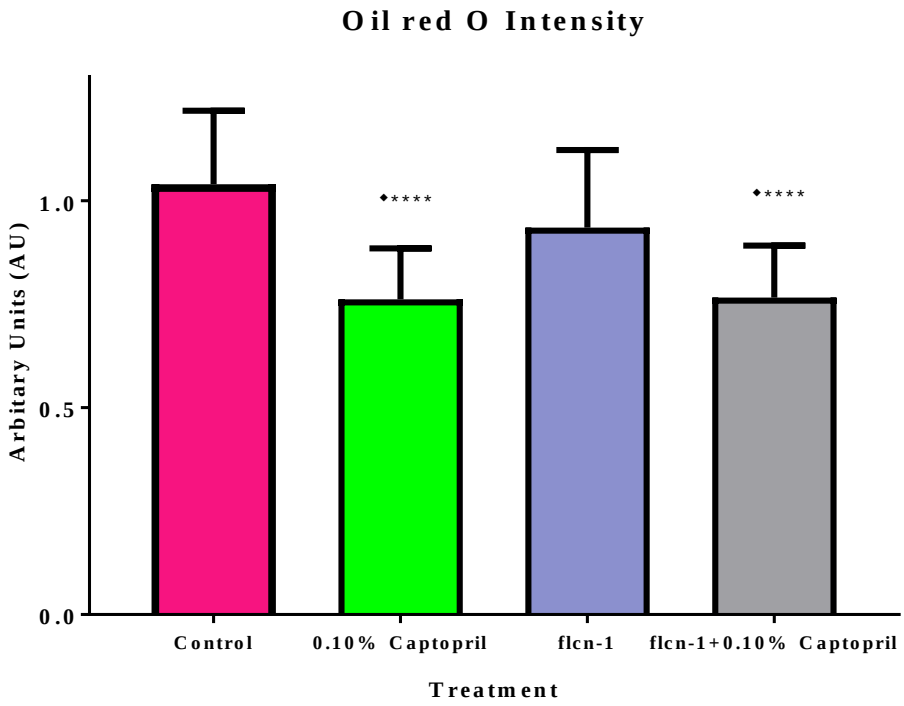

Figure 53. WT and *flcn-1* worms were harvested at L4 stage and fixed with oil Red O. Results are represented as mean ± SEM of two independent experiments using 15-20 worms per treatment group. Captopril reduced oil red O intensity between treated and untreated *flcn-1* and WT nematodes to the same degree.

Figure 52 shows oil red O staining pattern in untreated *flcn-1* versus 0.10% captopril treated *flcn-1* worms. Figure 53 shows 0.10% captopril treatment of WT and *flcn-1(lf)* nematodes reduces oil red O staining intensities to a similar extent. Results suggest that captopril's additive effect on *flcn-1* strain longevity is independent of the *flcn-1* protein, and captopril's negative effect on TG accumulation is also regulated independent of *flcn-1*. Fat content of *flcn-1* mutants and WT are alike as previously described in FLCN knockout rodents (Yan et al., 2016).

	Control (WT)	WT + 0.10% Captopril	*flcn-1(ok975)*	*flcn-1(ok975)* + 0.10% Captopril
Survival				
Mean (days)	17.2±6.3	23.7±4.0*	21.9±5.2*	27.9±7.4†
Difference (%)		31.8	24.0	47.5

Table 27. The effect of captopril on the lifespan of *flcn-1* loss-of-function mutants. Data are represented as mean lifespan ± SD from two independent experiments. P-values were calculated between all groups using one-way ANOVA. Statistical significances indicated by *p<0.05 vs control; †p<0.05 vs *flcn-1*; ‡p<0.05 vs 0.10% captopril. Percent difference represents percentage change of mean lifespan of control group versus treatments groups

Discussion

The effect of captopril on body fat storage and survival in *C. elegans*

Captopril reduced triglyceride content in wild-type C. elegans

In the present study we used TG specific oil red O staining protocol optimised by Wahlby et al., (2014) to visualise and assess the fat content of WT *C. elegans* treated with captopril. Our results indicate a dose dependent reduction in whole-body oil red O staining where 0.05% and 0.10% captopril administered worms showed a substantial 20% and 31% drop in red intensity respectively relative to controls. We next assessed whether fat reduction was region specific in *C. elegans*, to which end we ascertained that only the 0.10% captopril treated worms showed a substantial reduction of 19% in oil red O staining within their mid-third (intestinal) region to that of controls. Intestinal lipid droplets of *dhs-3::gfp C. elegans* also depicts a 56% decrease in LD diameter suggestive of a reduction in TG content of cells, which can further be corroborated by a 23% reductions in TG biochemistry of worm homogenates as per quantitative assaying (control: 0.1006±0.006 versus 0.10% captopril: 0.0771±0.008 mmol/ml). Observations are consistent with that of Weisinger et al. (2009) who described a marked decrease in the cell size of isolated epidydimal fat tissues of captopril treated mice. Although we did not observe a difference in the fat content of worms when triglyceride content was normalised to protein concentration (fat-to-protein ratio), variations may have likely been due to technical issues with the analysis given the platform is adapted to large animal biochemistry.

Captopril reduced triglyceride content in flcn-1, but not daf-16 mutants

We hypothesise captopril enhances AMPK phosphorylation of key metabolic pathways responsible for the catabolism of FAs and TGs, or inhibition of synthetic pathways to negatively influence body fat accumulation in *C. elegans*.

daf-16

Since AMPK has previously been described as acting directly via FOXO/*daf-16* transcription factor in both mammals and *C. elegans*, we next tested if captopril altered body fat accumulation in *daf-16(lf)* strains (Greer, Dowlatshahi, et al., 2007; Greer, Oskoui, et al., 2007). As shown in Figures 51-52, captopril had no influence on body fat in *daf-16* mutants when compared to treated WT and non-treated *daf-16* and WT strains. This suggests captopril reduces body fat in a *daf-16* dependent manner. *C. elegans* similarly stores fat in intestinal and hypodermal cells in the form of LDs resembling visceral and subcutaneous adipocyte in higher animals (Mak, 2012). Therefore it is still likely that upregulating *daf-16* prevents LD formation in a fashion similar to that of adipose tissue. In a study assessing the role of FOXO1 in adipocyte differentiation, Munekata and Sakamoto (2009) showed FOXO1-siRNA decreased LD formation in mouse 3T3-L1 adipocytes, as well as rigorously inhibiting adipocyte formation. Although the mechanism(s) by which FOXO influences body fat accumulation is not completely understood, FOXO1 appears to negatively regulate adipogenesis by suppression of PPAR-γ transcription factor (Armoni et al., 2006; Farmer, 2003; Nakae et al., 2003). A fixed homolog for PPAR-γ per se has not been classified in the *C. elegans* although *daf-16* and *daf-12* seem to resemble the interaction between FOXO1 and PPAR-γ (Dowell, Otto, Adi, & Lane, 2003). In a study specifically assessing lipid metabolism and larval development, *daf-12* null *C. elegans* showed suppression of excess fat storage in lipid accumulating strains (Ludewig et al., 2004). Taken together, captopril may curtail body fat accumulation via AMPK activation and subsequent FOXO/*daf-16* signaling to in turn downregulate PPAR-γ/daf-12 mediated LD formation.

flcn-1

It has been suggested that FLCN modulates the activities of AMPK and FOXO to influence various metabolic processes (Ghazi, 2010). Mouse studies have revealed that a hyperactive AMPK due to molecular ablation of FLCN can lead to browning of WAT resulting in resistance of animals to DIO (Ghazi, 2010; Possik et al., 2014). In order to determine whether captopril reduced body fat by mitigating the FLCN protein, we administered 0.10% captopril to WT and to *flcn-1* null *C. elegans.* We would imagine that if the FLCN protein were essential for captopril to stimulate reduction of fat storage, we would see no difference in oil red O staining intensities between WT and captopril treated and untreated *flcn-1* strains. Here, captopril reduced TG content in *flcn-1* loss of function worms to the same magnitude as captopril treated WT worms. This result demonstrates that captopril does not mitigate or require FLCN to negatively affect body fat accumulation.

In summary captopril reduced body fat and LD cell size in *C. elegans* in a dose dependent manner, observations which are also paralleled in rodent studies. Interestingly, the reduction in TG content was most prominent in the intestinal regions (visceral tissue) of the worms treated with 0.10% captopril. As previously alluded to in earlier parts of this discussion, region specific reductions in fat is akin to observations made in rodent models where the majority of fat is driven from

epidydymal fat pads. It appears that the mechanism(s) leading to an overall reduction in body fat in *C. elegans* is independent of FLCN/*flcn-1* regulation as reduction in TG content was observed in *flcn-1* null strains. The TG reducing capability of captopril was however diminished in *daf-16(lf)* strains therefore indicating a role for FOXO/*daf-16* transcription factor in captopril's efficacy towards FA metabolism and/or LD formation.

Captopril extended the lifespan of wild-type C. elegans

All lifespan experiments were carried out in the presence of FuDR to a final concentration of 100mg/L. Co-administering FuDR with captopril did not affect lifespan results when *C. elegans* were matched to their FuDR un-administered counterparts (data not shown).

In figure 38 we show that exposure of WT *C. elegans* to 0.05% [2.3mM] and 0.10% [4.6mM] captopril (from L4 stage onwards) results in 12% and 33% prolongation of mean survival respectively. Minimum and maximum life expectancy was calculated from the average age of onset of death of the 10th percentile of worms where a dose of 0.10% captopril resulted in a 36% increase in minimum life expectancy, and doses of 0.05% and 0.10% captopril resulted in increases of 15% and 36% in maximum life expectancy respectively. Next we tested whether exposure to captopril from L1 stage until end of life prolonged life to a similar extent as those exposed from L4 stage. The life prolongation effects of captopril appeared to be abrogated when administered from L1 stage as no substantial differences between control and treated groups were observed.

Concurrent lifespan prolongation effects of captopril and *acn-1* RNAi treatment of *C. elegans* has previously been reported. Although no lifetime data for captopril treatment was available, lifetime data pertaining to *acn-1* RNAi treatment of WT L1 *C. elegans* demonstrated substantial extension to mean and maximum lifespan (Kumar, Dietrich, & Kornfeld, 2016). Whilst our results may appear to oppose the proposed mode of action of captopril put forward by Kumar et al. (2016), differences may imply captopril's efficacy may be dependent on the timing or the duration of treatment as various longevity pathways have been shown to be induced by specific stimuli in middle-aged animals e.g. calorie restriction (Greer, Dowlatshahi, et al., 2007).

One notable observation by Kumar et al. (2016) is that lifespan extensions due to captopril treatment was additive in various long-lived mutant strains including *eat-2* (chronic caloric restriction/feeding defective mutant), *daf-2* (mammalian IRS-1 homologue) and *age-1* (mammalian PI3K homologue). Typically, the feeding defective strain *eat-2* displays an extensive lifespan via mechanisms that are dependent on FoxA/*pha-4* and independent of AMPK and FOXO/*daf-16* signaling, whereas *daf-2* and *age-1* mutant strains display longevity via mechanisms that are dependent on *daf-16* activation (Lakowski & Hekimi, 1998; Panowski, Wolff, Aguilaniu, Durieux, & Dillin, 2007). The most distinguished effect of *daf-2* signaling is the activation of *age-1* and subsequent recruitment of *akt-1* leading to inhibition and cytosolic sequestration of *daf-16* (Alam et al., 2010; Dorman, Albinder, Shroyer, & Kenyon, 1995; Henderson & Johnson, 2001; Kenyon et al., 1993; Lin, Hsin, Libina, & Kenyon, 2001; Narasimhan, Mukhopadhyay, & Tissenbaum, 2009). It should be noted that *daf-16* is also known to interact with other longevity inducing factors, such as JNK1 and SIR-2.1, hence is not exclusively targeted by IIS signals (Berdichevsky, Viswanathan, Horvitz, & Guarente, 2006; Oh et al., 2005). Despite Kumar et al. (2016) reporting captopril as shortening the lifespan of *daf-16* mutants (which will be discussed later), it appears captopril facilitates a "signal" representing an

input that converges downstream of *daf-2* and *age-1* signaling, and *eat-2* longevity suggests the mode of action of captopril may at least in part dependent on *daf-16* transcription factor.

Captopril increased the lifespan of flcn-1, but not daf-16 mutants

We hypothesise captopril suppresses and/or encourages pathways that activates AMPK phosphorylation, in turn facilitating nuclear translocation of FOXO/*daf-16* to increase transcription and translation of "protective target genes" involved in overall cell maintenance and metabolism.

daf-16

Greer, Dowlatshahi, et al. (2007) showed that AMPK can phosphorylate FOXO to influence *C. elegans* lifespan. AMPK mutant *C. elegans* appear to have a shorter lifespan than WT, and transgenic animals overexpressing AMPK live longer (Apfeld et al., 2004; Greer, Dowlatshahi, et al., 2007). *In vitro* assays have revealed AMPK phosphorylates all four FOXOs with a preference for FOXO3, and FOXO3 genotype has been associated with human longevity (Anselmi et al., 2009; Greer, Oskoui, et al., 2007; Willcox et al., 2008). We therefore wanted to investigate whether lifespan in *C. elegans* was also mediated by captopril through FOXO signaling in *daf-16(lf)* strains. Since we propose captopril regulates AMPK and FOXO appears to be a substrate for AMPK, we expect that AMPKs signal will not transduce in *daf-16* null mutants and no further extension to lifespan will be observed. Figure 13 shows mean lifespan was no different between captopril treated and untreated *daf-16* mutants, and *daf-16* mutants had a shorter lifespan in comparison to captopril treated and untreated WT worms.

In *C. elegans* loss of *daf-16* characteristically results in a short-lived phenotype and over expression of *daf-16* has been shown to slightly increase lifespan (Henderson & Johnson, 2001; Murphy et al., 2003). Numerous isoforms of AMPK exist in *C. elegans* all of which appear to have an ambiguous functional relationships with *daf-16* in different aging pathways (Apfeld et al., 2004; Curtis, O'Connor, & DiStefano, 2006; Greer & Brunet, 2009; Greer, Dowlatshahi, et al., 2007). Transgenic *C. elegans* with overactive AMPK-γ2 displayed longevity which was rescued when worms were treated with *daf-16* RNAi (Greer, Dowlatshahi, et al., 2007). When investigating regulation by *daf-16* of genes encoding AMPK, *daf-16* appeared to enhance the expression of *aakg-4* (AMPK-γ subunit homolog) in *C. elegans*. Treating *C. elegans* with *aakg-4* RNAi delayed expression of *daf-16* target genes as well as shortening the lifespan of long-lived *daf-2* mutants in a *daf-16* dependent manner (Tullet et al., 2014). In view of Kumar et al. (2016) reporting captopril and *acn-1* RNAi treatment of *C. elegans* as further extending the lifespan of *daf-2(lf)* and *age-1(lf)* strains, we propose captopril may prolong the lifespan of *C. elegans* by differentially enhancing AMPK activity, such as the *aakg-4*/ AMPK-γ, to accelerate the induction of *daf-16*/FOXO target genes involved in survival.

Conversely, Kumar et al. (2016) described captopril treatment as causing a 10% shortening of mean lifespan in *daf-16* mutants. Although difficult to discern, the discrepancy may be due to variations

in experimental protocol, or more specifically due to the antibacterial nature of captopril and consequent induction of starvation (Tejesvi, Kini, Prakash, Subbiah, & Shetty, 2008). Prolonged starvation of adult *daf-16* mutants has been reported to reduce lifespan (Henderson, Bonafe, & Johnson, 2006) and promote sequestration of *daf-16*::gfp within the cytoplasm (Weinkove, Halstead, Gems, & Divecha, 2006).

flcn-1

While the function(s) of FLCN are largely unknown, it has been identified as an AMPK binding protein that antagonises kinase activity (Baba et al., 2006; Possik et al., 2014). *flcn-1* null *C. elegans* characteristically have an extensive lifespan which can be rescued by *aak-2* (orthologue of mammalian AMPK-α2 catalytic subunit) but not *aak-1* mutations (Gharbi et al., 2013; Ghazi, 2010). Double mutant studies assessing the molecular interaction between *daf-2;flcn-1* and *daf-16;flcn-1* have further implicated FLCN as a component of IIS with a function that is downstream of *daf-2* and dependent on *aak-2* and *daf-16* (Ghazi, 2010). Since *flcn-1* appears to directly modulate the activity of *aak-2* and *daf-16*, we wanted to investigate whether captopril treatment influences the lifespan of *C. elegan*s in an *flcn-1* dependent manner. If captopril extends the lifespan of *C. elegans* by supressing *flcn-1* and thereby enhancing *aak-2*, then no further extension to lifespan is expected in *flcn-1* null strains. Figure 16 shows *flcn-1* nulls had an extensive lifespan to that of untreated WT and was like that of captopril treated WT. Treating *flcn-1* null mutants with 0.10% captopril further extended their lifespan suggesting captopril additively influenced lifespan in parallel to pathways modulated by *flcn-1* and captopril's effects were not *aak-2* dependent specifically.

In summary captopril extended the lifespan of *C. elegans* in a dose dependent manner which is in support of published data by Kumar et al. (2016). Mechanisms leading to an overall extension of lifespan with captopril treatment appeared to be dependent on FOXO/*daf-16* transcription factor as lifespan extension was abolished in *daf-16(lf)* strains. Interestingly captopril treatment of long-lived *flcn-1* mutants further prolonged life to suggest both captopril and *flcn-1* can regulate survival pathways in parallel to influence lifespan. Taken together we propose captopril stimulates a specific isoform of AMPK, possibly the AMPK-γ/*aakg-4* catalytic subunit, which subsequently promotes FOXO/*daf-16* transcription factor and downstream activation of target genes committed to survival.

Captopril improved tolerance of *C. elegans* to oxidative and heat stress

C. elegans with mutations in lifespan modulating genes such as *daf-2* and *age-1* show increased resistance to environmental stress, and conversely mutations in lifespan alleviating genes such as *daf-16* (and *mev-1*) are sensitive to such stress (Martin, Austad, & Johnson, 1996; Yanase, Yasuda, & Ishii, 2002). We therefore wanted to assess survivability of WT *C. elegans* exposed to continuous oxidative and thermal stress in the presence or absence of 0.10% captopril treated NGM. We reported a time dependent decrease in the lifespan of all animals exposed to paraquat (oxidative) and heat (35°C) stress.

The effect of captopril on oxidative stress resistance in C. elegans

When subjected to mitochondrial oxidative stress caused by 200mM paraquat, 0.10% captopril treated WT worms were more resistant to stress showing a 65.3% increase in mean survival (5.7 hours to 11 hours) over untreated WT. Although Kumar et al. (2016) did not test the effect of captopril on oxidative stress resistance in *C. elegans*, they showed that exposing WT treated with *acn-1* RNAi to 40mM paraquat improved survival by 21% over time. Albeit significant, the magnitude of variance between differing treatments suggests captopril and *acn-1* RNAi may (1) influence oxidative stress resistance pathways differently or to a different capacity, and/or (2) overall mechanism(s) of action are different. In line with our proposed mechanism of action of captopril, *i.e.* AMPK activation, Greer, Dowlatshahi, et al. (2007) described an 86% increase in resistance to 300mM paraquat of worms with constitutively active AMPK-γ2 in comparison to controls, an effect which was abolished when treated with *daf-16* RNAi. Moreover active AMPK-γ2 caused an increase in the expression of a *daf-16* target associated with stress resistance and longevity known as *sod-3* (homologue to mammalian SOD), and short-lived *aak-2* mutants showed downregulation of *sod-3* expression (Greer, Dowlatshahi, et al., 2007; Honda & Honda, 1999; Murphy et al., 2003). In addition to mitigating *daf-2* longevity, reducing *aakg-4*/AMPK-γ expression was also shown to downregulate various other *daf-16* target genes involved in stress resistance and longevity including *scl-1*, *nnt-1*, *cpr-2*, *dod-8* and *lys-7* (Tullet et al., 2014). Results presented are consistent with the observed extent of stress resistance and survival reported by Greer, Dowlatshahi, et al. (2007) and mechanisms presented by Tullet et al. (2014), *i.e. daf-16* binds to the promoter of various AMPK subunits (*aakg-4*, *aakg-5*, *aak-2*, *aakb-1*) to activate their expression and *daf-16* is also phospho-activated by AMPK operating in a positive feedback loop.

The effect of captopril on heat stress resistance in C. elegans

In Figure 4 we show that WT *C. elegans* exposed to continuous heat stress (35°C) and treated with 0.10% captopril increased survivability by 22% (13.8 hours to 17.3 hours) over untreated controls (Table 2). Kumar et al. (2016) reported continuous heat stress (34°C) in *rrf-3(pk1426) C. elegans* (a mutant strain hypersensitive to RNAi feeding) fed *acn-1* RNAi as causing a 12% increase in resistance over corresponding controls. Although differences may be attributed to differences in strains, chemical concentrations and methodologies employed, it appears *acn-1* RNAi effects survival to a lesser (albeit significant) capacity to 0.10% captopril treatment. This may suggest captopril treatment promotes heat stress resistance through different mechanism/s potentially by targeting a single or multiple survival inducing pathways not limited to *acn-1* mitigation.

Current literature shows that HSF-1 (heat-shock factor) and its subsequent gene targets (heat-shock proteins, *hsp*) is recruited in response to heat and other forms of stress and has been implicated in aging (Hsu, Murphy, & Kenyon, 2003). Transcriptomic analysis confirms that when exposing L4 *C. elegans* to 35°C heat for 0-12 hours, heat-shock response pathways are activated via *hsf-1* which eventually follows a transient decline and attenuation over time (Jovic et al., 2017). Consistent with

our proposed mode of action of captopril, *daf-16* and AMPK (*aak-2*) have also been implicated in heat-stress resistance by correlating with *hsf-1* activation in *C. elegans* (Apfeld et al., 2004; Hsu et al., 2003).

Taken together our results indicate captopril substantially improved *C. elegans* resistance to oxidative and thermal (heat) stress responses, possibly via differential pathways of AMPK activation and subsequent phospho-activation of *daf-16* to upregulate target gene networks involved in stress resistance, detoxification of ROS (such as *sod-3*) and damage repair pathways (such as *hsf-1* and *hsp*) promoting survival. Captopril's efficacy may be (at least partially) independent of *acn-1* mitigation.

The effect of captopril on age-related changes in C. elegans: pharyngeal pumping and motility

Captopril increased pharyngeal pumping rates in *C. elegans*

Pharyngeal pumping rate is one of two functional measures of aging in *C. elegans* (Herndon et al., 2002; You, Kim, Raizen, & Avery, 2008). The span of pharyngeal pumping and deterioration of pharyngeal muscles has previously been correlated with lifespan and age respectively and describes a proportional relationship (Huang et al., 2004; Zhao et al., 2017) .We monitored the pharyngeal pumping rate by directly observing the number of muscular contractions of the pharynx of WT L4 *C. elegans* over a 40-60 second period. Those treated with 0.05% (306±9.55 pumps min^{-1}) and 0.10% (328±13.06 pumps min^{-1}) captopril displayed significantly faster rates of pharyngeal pumping relative to 0.02% (242±11.84 pumps min^{-1}) and non-administered control (261±8.58 pumps min^{-1}) groups. Longitudinal observations made by Kumar et al. (2016) conversely showed WT *C. elegans* treated with captopril beginning from L4 stage did not display significant differences in pumping rates over time, whereas *acn-1* RNAi treated groups did from 12 to 20 days of adulthood. Despite the aforementioned differences in protocol and methods of data collection, where Kumar et al. (2016) observed pharyngeal contractions over 10 seconds (versus our 40-60 seconds), captopril's potential to indirectly induce DR may have resulted in the observed dissociation between pharyngeal pumping span and rate with lifespan which is typically observed in DR *C. elegans* (Mair, Panowski, Shaw, & Dillin, 2009; Palgunow et al., 2012). Despite not observing pharyngeal pumping longitudinally, fast pharyngeal pumping has been correlated with the lifespan of *C. elegans* (Huang et al., 2004). Taken together our results show captopril caused an increase in pharyngeal pumping speeds, suggestive of a deceleration of age-related deterioration of pharyngeal muscles consistent with respective survival spans.

Captopril reduced locomotor activity in *C. elegans*

In *C. elegans* locomotor activity can reflect age, fitness, satiety, quiescence and a variety of other states related to and influenced by their internal and external milieu. As in all animals, nutritional status can regulate behavioural states such that a hungry animal will display greater locomotor activity by increasing exploratory behaviours like roaming and dwelling to seek food; in contrast,

satiated or full animals will cease eating and reduce locomotor activity by decreasing exploratory behaviours and even enter a resting or sleep-like state known as quiescence (Antin, Gibbs, Holt, Young, & Smith, 1975; Shtonda & Avery, 2006; You & Avery, 2012; You et al., 2008). Our group showed daily administration of captopril in mice to induce effects akin to rapid satiation, that is (1) a suppression of appetite, (2) a reduction in food intake and (3) a decrease in overall motility resembling a behavioural state reminiscent of rest or quiescence (Premaratna et al., 2012; Stanley, 2013; Weisinger et al., 2009). We therefore hypothesise captopril treatment of WT *C. elegans* to take after behavioural sequences observed in captopril treated mice, causing a reduction in foraging and feeding behaviours quantified by observing track lengths and locomotive speeds travelled by worms.

Distance travelled by C. elegans declined with captopril

Feeding or foraging *C. elegans* typically increase roaming and dwelling behaviours and the distances travelled by individual worms reflects this proportionally. In contrast satiated *C. elegans* will reduce and confine displacement indicative of a resting or 'satiety-induced quiescence'-like behavioural state specified by reductions in the distances worms travel (Raizen et al., 2008; You et al., 2008). Accordingly, we investigated the influence of captopril on distances travelled in *C. elegans* on NGM-agar plates with an *E. coli* lawn, where 60 second video recordings of WT L4 worms were analysed using WormLab software and the mean track length [forward + reversals μm] of all groups determined. As shown reported, captopril treatment of *C. elegans* substantially reduced distances travelled over untreated controls. Worms treated with 0.10% captopril in particular travelled almost half the distance of that of controls (1.9cm vs 3.6cm respectively) and data ranges belonging to 0.10% treated worms reveals a confined range of displacement compared to the broader ranges displayed in the remaining. Taken together captopril treatment reduced displacement of worms through the *E. coli* lawn, *i.e.* reduced roaming and/or dwelling, as a substantial decline in the distances travelled is observed over control counterparts. Motility particularly in *C. elegans* treated with 0.10% captopril was restricted and distances travelled are reminiscent of worms in lethargus (Raizen et al., 2008), suggesting captopril may cause rapid satiation and entry in to a resting or quiescent-like state as observed in captopril administered mice.

Speed of travel by C. elegans declined with captopril

The speed of locomotion of *C. elegans* can predict their health span, lifespan and nutritional status and has been shown to decline with age (Angstman, Frank, & Schmitz, 2016; Gallagher, Bjorness, Greene, You, & Avery, 2013; Hahm et al., 2015; Rollins, Howard, Dobbins, Washburn, & Rogers, 2017). The nutritional status of *C. elegans* can impact their behavioural sequence such that satiation causes a reduction in foraging, feeding, and overall movement [speed] to even reach a state of 'satiety-induced quiescence'(You et al., 2008). WT *C. elegans* moving through an OP50 *E. coli* lawn have previously been shown to reach locomotive speeds of up to 128.6±41.6μm s^{-1} (Angstman et al., 2016) and a satiety-induced quiescent state is described when locomotive speed is ≤ 1μm s^{-1}

(Gallagher et al., 2013). Though distinct quantification of satiety in *C. elegans* remains ambiguous, studies have described food quality and availability to cause shifts between proportions of roamers to dwellers along with changes in speeds of movement of worms enabling prediction/assignment of nutritional statuses and levels of satiation (Angstman et al., 2016; Ben Arous, Laffont, & Chatenay, 2009; Gallagher et al., 2013; Shtonda & Avery, 2006; You et al., 2008).

Using the 60 second captures from above, we assessed the speed of locomotion (μm s^{-1}) of WT worms through *E. coli* lawns in response to captopril treatment. Captopril untreated control worms moved at a rate of 142.1±28.6μm s^{-1} to resemble parameters reported by Angstman et al. (2016). Speeds of locomotion declined with captopril treatment where doses of 0.02% and 0.05% accounted for a 9-10% reduction, and 0.10% captopril treatment had the greatest overall impact reducing speeds by 35% over untreated controls. Group maximum speeds also showed the same dwindling trend where captopril treatment resulted in smaller inter-individual variations in movement speeds over controls, i.e. 0.02%, 0.05% and 0.10% captopril groups ± std. dev. was ~10% of that of controls (data not shown). Additionally, we did not observe satiety-induced quiescence in the current study as it known to be suppressed by the presence of other worms (You et al., 2008). Our results are representative of the dependence of locomotive activity on the nutritional status of *C. elegans*, and a decline in locomotive speeds (and distance travelled) between groups infers worms behavioural sequence is like that of satiated animals (Gallagher et al., 2013; Shtonda & Avery, 2006; You et al., 2008).

A significant reduction in locomotive activity corresponds to a reduction in foraging (previously correlated with distances and speeds) and feeding which is possibly as a result of satiety (You et al., 2008). Taken together, captopril treatment of WT *C. elegans* adopted characteristics observed in captopril treated mice that is consistent with (1) a significant reduction in motility and (2) a significant reduction in appetite or rapid-satiation. Results suggest that the response to captopril is conserved in both *C. elegans* and rodents.

Conclusion

In summary, the current study showed that captopril affects body fat accumulation, lipid droplet size, regional lipid deposition, lifespan, stress-responses, age-related muscular degeneration and locomotor activity in WT *C. elegans*. A reduction in TG storage was evident in WT and *flcn-1(lf) C. elegans* but not *daf-16(lf)* strains to suggest *daf-16* is required for captopril's efficacy to suppress body fat accumulation. The increase in lifespan with captopril treatment of WT and *flcn-1(lf)* but not *daf-16(lf)* strains again suggests the lifespan improving affects are independent of *flcn-1* regulation but dependent on *daf-16* signal transduction. Increased pharyngeal pumping with captopril treatment corroborates a suppression of age-related muscular decline which was proportional with a slowing of aging and lifespan. Furthermore, an overall reduction in locomotor activity (distances and speeds travelled) with captopril treatment may signify a suppression of

appetite which may also contribute to reduced body fat accumulation and improvements in lifespan and survival. The physiological response to captopril suggests functional conservation of its target(s) between *C. elegans* and mice, highlighting the requirements for additional studies to clarify potential mechanisms by which captopril causes the aforementioned effects. This study provides new insights in to the mechanisms of fat accumulation and aging and establishes the *C. elegans* as a system in which to investigate current and novel anti-obesity agents before their application to higher animals.

Chapter 6

General discussion

The review of literature presented our current knowledge of obesity and its key symptoms, with particular focus on a Western style hyper caloric diet and its molecular impact on *de novo* lipogenesis and pathways of Ang-II activation. The emergence of dietary salt as an independent risk for the development of obesity and related diseases was also introduced, an area that is currently under intensive investigation. The relationship between obesity, salt, hypertension RAS over-activation was also introduced, which has led to the use of the ACE-inhibitor captopril as an anti-hypertensive therapeutic, where there is suggestion of captopril working as an anti-obesity therapeutic when dietary salt intake is moderated. The work presented in this thesis investigated the interaction effect between captopril and a high-salt diet on bodyweight and body fat regulation in mice, describing differences in plasma metabolite as well as liver and adipose tissue gene expression patterns. In order to ascertain whether the body fat regulatory mechanism of action of captopril was strictly limited to animals possessing a functional RAS, the *C. elegans* was employed and screened for responses that may resemble that of higher animals. This thesis has generated novel data by a range of methods and scientific disciplines that increase our current knowledge of some of the above-mentioned key areas of obesity research. This chapter will summarise some of the major findings of this thesis.

The results of this study showed that disruption of the RAS by way of ACE-inhibition, or more specifically, blockade of ACE-mediated Ang-II synthesis by captopril reversed DIO in C57BL/6J mice maintained on a HFD. This finding agrees with literature proposing captopril may aid in the treatment and understanding of obesity and its symptoms (de Kloet et al., 2009; Premaratna et al., 2011; Weisinger et al., 2009). The combined administration of captopril and salt however abolished these anti-obesity effects, further agreeing with the finding that dietary salt consumption beyond 0.86 mg day^{-1} is non-conducive to weight loss in mouse models of DIO (Radcliffe, 2013). Whilst many of captopril's properties as a weight loss aid is thought to be mediated via its antagonism of the 'active' components of the RAS, we were able to show that in *C. elegans*, an invertebrate model that is devoid of a circulatory system and all but two homologous genes of RAS, one of which is the ACE-like gene *acn-1*, captopril treatment was able to cause significant reductions to body fat content in a DAF-16/FOXO dependent manner, suggesting the molecular targets of captopril *in vivo* may be more extensive than just the ACE/*acn-1*.

The most noteworthy finding of this study was that salt could increase molecular components involved in intracellular signaling mechanisms utilised by Ang-II, despite pharmacological inhibition of Ang-II synthesis by the ACE-inhibitor captopril. This was identified by tissue transcriptomics where in both liver and adipose tissues, the expression of G-protein subunits, *Gnb1*

and *Gnb5*, which integrate signals between AT_1-receptors and Ang-II were upregulated. This was substantiated further by identifying an upregulation in the expression of subsequent and downstream effector molecules including *Plcb1* and *Prkci*, as well as other classically known AT_1-receptor activated tyrosine and serine/threonine kinases previously described by Forrester et al. (2018). This leads to the assumption that salt may employ ACE-independent mechanisms of Ang-II synthesis by which to oppose the weight loss efficacy of captopril. We then investigated proposed alternate enzyme routes of Ang-II synthesis, which led us to chymase (*Cma1*) and cathepsins D (*Ctsd*), G (*Ctsg*) and L (*Ctsl*) as described by Nehme et al. (2019), all of which were upregulated in adipose tissue in response to salt, and although expression in liver tissues tended to increase in response to salt, results were statistically non-differentiable due to sample variations within groups. Salt also interfered with the expression of several genes comprising the counter-regulatory arm of the RAS in adipose tissue, *i.e. Mas1* and *Lipe*, which have previously been associated with the anti-lipogenic effects of captopril (Oh et al., 2012). This highlighted that the potential mechanism of by which salt may interfere with the weight loss efficacy of captopril may still involve local activation of the RAS, albeit without requiring a functional ACE. It would be interesting to screen the enzymatic activities of chymase and cathepsins against the level of circulating and intracellular Ang-II.

This study also offered a plethora of novel findings and ideas which will be discussed further by the integration of metabolomics, transcriptomics and *C. elegans* studies.

Ang-II is reported to enhance the glycolytic capacity of tissues, suggestive of a role for RAS in whole-body metabolism (Kadoguchi et al., 2015; Li & Zhuo, 2017). To this end, the findings of this study showed that most of the captopril modulated genes and metabolites were involved in carbon metabolising pathways, such as glycolysis the PPP, as well as the TCA cycle. In particular, the molecular interaction between captopril and salt appeared to involve counter-regulation of *Hk2*, *Pfkm*, *Taldo1*, *Tkt*, *Rpia*, *Pdg* and *Prps2* mRNA expression in liver tissue (all but *Taldo1* remained unchanged in adipose tissue). A remarkable down-regulation in the expression of these genes that are essential for glycolysis and the pentose-phosphate shunt (PPP) was observed following captopril treatment, which was re-established by salt (*i.e.* upregulated). Glycolysis converts glucose to pyruvate which may be transformed in to acetyl-CoA to enter the TCA cycle (Butterworth, 2005a). Previously, a decrease in pyruvate release from muscle in to the circulation was reported in diabetic patients administered captopril (Jauch et al., 1987), and the current GC-MS measurements confirmed this finding. Running in parallel to glycolysis, the PPP plays a pivotal role in cell growth and DNL by providing metabolite building blocks and up to 60% of the NADPH necessary for maximum lipogenesis (Shrago et al., 1971). In the current study the interaction between captopril and salt involved the deregulation of plasma metabolites of PP origin, and perhaps one of the most interesting discoveries was related to the levels of erythritol in plasma and its striking inverse association with bodyweight, epididymal fat and liver masses, a finding that contrasts the

suppositions of Hootman et al. (2017). The vast majority of (known) hepatic PPP genes (and adipose tissue *Taldo1*) were suppressed by captopril, and combined with other studies suggesting that PPP insufficiencies, particularly of TALDO1, results in increased erythritol content of biofluids which is in line with the findings described in chapter 3 (Boyle et al., 2016; Verhoeven et al., 2001; Wamelink et al., 2008). The current study supports a role for captopril in the suppression of the PPP and a counter-regulatory role for salt to this effect. This is significant in that the PPP together with FASN activation may adapt physiology to an overall pattern of adiposity (Shrago et al., 1971). Whilst there is further merit to investigate this hypothesis, there is indication that the interaction between captopril and salt may entail opposing effects on glycolytic and PPP activity, whereby captopril appeared to suppress whereas salt appeared to support these pathways. Findings are in line with the hypothesis that Ang-II may be a factor in salt's opposition to captopril's repression of carbon metabolism via glycolysis and the PPP.

Previous studies have shown an increased TCA cycle dynamic during obesity (Nagao et al., 2017; Shearer et al., 2008). Moreover, accumulation of the TCA intermediate, succinate, is reported to trigger RAS and hypertension whereas captopril has been reported as opposing succinate's pressor effects (He et al., 2004). Accordingly, our metabolomics results showed that captopril induced significant decreases in plasma TCA metabolites, such as α-hydroxygluconate (derived from α-ketoglutarate) and succinate, whereas citrate tended to accumulate. Our transcriptomics data aligned with these results as captopril appeared to have an inhibitory effect on TCA genes within the liver with a lesser impact on adipose tissue, albeit all of the above-mentioned effects of captopril were abolished in the presence of salt. With reference to our transcriptomics data, captopril decreased liver (but not adipose) tissue expression of *Aco1* mRNA, which may explain some of the significant afore discussed carbohydrate metabolite and mRNA alterations. *Aco1* is reported as an adipogenic marker, catalysing the conversion of citrate to *iso*-citrate, which is a substrate for the $NADP^+$-dependent IDH (generating α-ketoglutarate) where $NADP^+$ is converted into NADPH that is essential for enzymatic reactions of DNL (Moreno et al., 2015; Nam, Park, & Park, 2012). Knockout of aconitase (ACO) in *Drosophila melanogaster* was reported to lead to an increase in citrate whilst fat body, TGs and most metabolites of glycolysis and the TCA cycle, such as pyruvate, α-ketoglutarate and succinate, were reduced (Cheng, Tsuda, Kishita, Sato, & Aigaki, 2013). Although we were unable to locate comparable studies of ACO1 deficiency, similar metabolic profiles have been observed in humans with ACO2 deficiency, which was suggested to be due to accumulated citrate exerting a negative feedback on glycolysis via negative regulation of PFK1 and 2 (Abela et al., 2017). Accordingly, the present study revealed that liver expression of *Pfkm* and adipose *Pfkp* was significantly affected by captopril and salt, and it moreover appears that glucose metabolism may be secondarily affected by citrate via a mechanism that is not yet completely clear, but may involve NADH and H^+ generated from FA oxidation. Together, these results may indicate that captopril treated mice utilise TG as an energy source as evident by their impaired glycolysis and

TCA cycle, whereas salt may oppose these effects by inducing glycolysis and the TCA cycle. Combined, findings continue to implicate RAS in whole-body metabolic processes albeit the extent of its involvement in metabolic pathways remains to be investigated. It would be interesting to investigate the effect of captopril and salt on plasma acetyl-CoA levels via newly developed detection methods (Shurubor et al., 2017) so as to identify whether active FA oxidation is consistent plasma citrate levels, as well as bodyweight and body fat loss effects.

Recent studies suggested that a high-salt intake may cause obesity, hepatic TG accumulation and leptin resistance by stimulating endogenous fructose synthesis and promoting its hydrolysis via the AR–SDH and KHK–ALDOB pathways respectively (Lanaspa et al., 2018). Lanaspa and colleagues have also shown that genetic deficiencies in either pathway results in the accumulation of plasma fructose. The enzyme SDH, encoded by the *Sord* gene, is associated with carbohydrate metabolism, converting intracellular sorbitol (sugar alcohol from glucose) into fructose (El-Kabbani, Darmanin, & Chung, 2004). Liver-type enzyme ALDOB, encoded by the *Aldob* gene, plays a particularly important function in fructose metabolism by catalysing the hydrolysis of fructose-1-phosphate in to precursors that support glycolysis and DNL (Butterworth, 2005a). Fructose feeding in rats has also been associated with systemic and intracellular Ang-II accumulation concurrent with hypertension and body fat gain (Chou, Lin, Chen, & Fang, 2017; Kobayashi et al., 1993). Moreover, Roncal et al. (2009) showed that unlike their control counterparts, fructose-fed mice co-administered captopril exhibited reduced bodyweight and VAT gain. In this study, we identified a striking interaction effect between captopril and salt on plasma fructose levels which related inversely with bodyweights and liver masses of mice. Accordingly, a reduction in hepatic *Sord* mRNA expression in captopril treated mice against that of their salt-administered counterparts, and a reduction in *Aldob* mRNA against controls was observed. These current GC-MS and mRNA measurements supports a role for captopril in the suppression of *de novo* fructose synthesis and hydrolysis, as evidenced by an increase in plasma fructose and decrease in hepatic *Sord* and *Aldob* mRNA expression, thus there is indication that both the AR–SDH and KHK–ALDOB axes may be involved, at least in part, in the weight loss effectiveness of captopril in the absence of salt. Together, findings allude to a complex interaction between salt, Ang-II, fructose and adiposity albeit further clarification is required.

Inositol and 2-ketogluconate metabolites were also strongly associated with the phenotypic characteristics of captopril and salt treated mice, however endogenous mechanisms leading to their biosynthesis is presently unclear. We did not show distinctions in the mRNA expression of previously identified pathways of inositol biosynthesis, albeit increased inositol bioavailability is thought to reflect reductions in lipogenic enzyme activity in connection with PPP and AR/sorbitol modulation, thus remains consistent with the current data (Croze et al., 2015; Croze & Soulage, 2013; Greene et al., 1987; Santamaria et al., 2012; Shimada, Hibino, & Takeshita, 2017). Interestingly, there is no prior reporting of 2-ketogluconate biosynthesis in higher animals, nor has

this metabolite it been linked to adiposity. As described in microorganisms, 2-ketogluconate is synthesised via the oxidation of gluconate via the Entner-Doudoroff pathway (Lockwood et al., 1941), hence we speculated that as in the case with microorganisms, 2-ketogluconate may comprise part of the gluconate shunt in higher animals that may run in parallel to glycolysis and the PPP (Corkins, Wilson, Cocuron, Alonso, & Bird, 2017). We therefore propose the accumulation of inositol and 2-ketogluconate reflects an alternative glucose and gluconate shunt, whereby glucose homeostasis is maintained when DNL pathways are blunted and/or FA oxidising pathways are heightened. Further investigations are required to elucidate endogenous pathways of inositol and 2-ketogluconate synthesis.

The transcriptome analysis of both liver and adipose tissues revealed differential molecular pathways and candidate markers associated with captopril- and salt-induced bodyweight loss and gain, respectively. Interestingly, captopril treatment in conjunction with a normal salt intake significantly downregulated the majority of DEGs (2,055) in the liver whilst upregulating the majority of DEGs (1,487) in adipose tissue, and of course a high-salt intake reversed these effects. This suggests that the signaling targets of captopril and salt are complex and that both tissues play a role in orchestrating whole-body adiposity.

Based on KEGG pathway analysis of the liver transcriptome, it was revealed that key DEGs involved in the interaction between captopril and salt were involved in the cell cycle. As described in chapter 4, the cell cycle refers to processes taking place within cells leading to mitosis (cell division) and is under the control of CDKs and cyclins. Cell cycle dysregulation can lead to uncontrolled cell proliferation and subsequent biomass, and both Ang-II and salt have previously been shown to promote cell cycle progression in VSMCs, HSCs and cardiac cells, whereby Ang-II promoted HSC proliferation and a high-salt diet promoted cardiac hypertrophy via AT_1-receptor-mediated mechanisms (Bataller et al., 2000; Ding et al., 2010; Jahan et al., 1996). While obesity is frequently associated with an increase in liver mass due TG accretion, Yang and colleagues demonstrated an association between obesity and an increase in hepatocyte proliferation relative to apoptosis, leading to increased liver mass which could not be explained merely by lipid accumulation. As such, this process is thought to contribute to obesity-related liver fibrosis (Yang et al., 2001). There is a role for RAS in liver pathology and captopril has previously been reported to inhibit the progression of hepatic fibrosis (as well as lipids) in rats as indicated by reduced hydroxyproline and *Col1a1* mRNA levels (Jonsson et al., 2001), and similarly, *Col1a1* expression was downregulated in the livers of captopril treated mice and was reversely regulated when treatment was administered with salt. Combined, there is indication that captopril may improve liver pathologies by attenuating cell cycle progression, whereas salt may exacerbate these effects. To the best of our knowledge, the effect of salt on liver *Col1a1* expression has not been reported previously.

The p53 signaling pathways was also implicated in the in the interaction between captopril and salt in liver tissue. As described in chapter 4, there is evidence to suggest that p53 plays a pivotal role in obesity and its symptoms, particularly in that of NAFLD via JNK-mediated mechanisms (Derdak et al., 2013; Ferreira et al., 2014; X. L. Liu et al., 2017). Moreover, a positive feedback relationship is reported to exist between Ang-II and the p53 pathway in cardiac cells (Liu et al., 2009). The Ang-II signaling pathway is associated with the production of pro-inflammatory cytokines and other stress responses that may also activate the JNK pathway (Forrester et al., 2018; Mohib et al., 2016). In the present study, an increase in the expression of *Mapk8* (JNK) and several of its downstream molecular targets, such as *Jun*, *Mapk9*, *Stradb* and *Wnt5a*, supported the hypothesis that an increase in Ang-II induced liver inflammation may have been responsible for p53 signaling pathway upregulation in salt administered mice. Taken together, our results suggest that captopril may improve liver pathologies by attenuating p53 signaling, and to the best of our knowledge this if the first study to report such effects in liver tissues.

Additional KEGG pathway analysis of adipose tissue revealed that the most overrepresented pathway was that of the peroxisome. Playing a major role in cellular metabolism, the importance of peroxisomes in the β-oxidation of FAs is highlighted in congenital disorders, *e.g.* Zellweger syndrome, in which peroxisomal FA oxidation is impaired resulting in the accumulation in VLCFAs in tissues throughout the body, impairing multiple organs including the brain and lung function (Weller, Gould, & Valle, 2003). Here we showed that in the absence of a high-salt diet, captopril treated mice displayed a notable increase in the expression of genes encoding proteins responsible for peroxisomal metabolism in adipose tissue. In addition to an upregulation in genes encoding peroxisomal transport systems for metabolites such as retinoid, EETs and ROS, an increase in the expression of four key PTS1 containing genes responsible for the β-oxidation of FAs, including *Abcd2*, *Pxmp2*, *Crat* and *Mlycd*, were heightened by captopril and reversely regulated by salt. These upregulated marker genes suggested that an integral property of captopril leading to reduced fat accumulation may entail an increase in the commitment of epididymal adipose tissues to peroxisomal processes of metabolism over that of mitochondrial processes. This feature of adipose tissues has been reported in C57BL/6J mice displaying natural resistance to DIO (Xie et al., 2011), indicating that an integral characteristic of obesity-resistance may include enhanced peroxisomal metabolism.

It would be interesting to obtain tissue proteomics in order to provide a comprehensive understanding of changes in metabolic pathways, to link alterations of cellular proteins to gene abundances, and to identify potential pathophysiologic mechanisms from various levels by integrating signal transduction, cellular metabolism and phenotype analysis.

Captopril was reported to cause longevity in *C. elegans* via mechanisms that were dependent on the FOXO/*daf-16* transcription factor (Kumar et al., 2016). The novelty of the current study was the

discovery that captopril causes a significant reduction in the body fat content of *C. elegans,* and like the case in mice (Weisinger et al., 2009), the fat reducing capacity of captopril was most prominent in the intestinal (visceral) region of the worm. As with longevity, we showed that body fat reduction in captopril treated *C. elegans* was dependent on the FOXO/*daf-16* transcription factor, comprising a key component of the canonical signal transduction pathway of AMPK. With reference to the transcriptomics study conducted in mice, captopril treatment significantly upregulated the expression of catalytic and non-catalytic subunits of AMPK in adipose (but not liver) tissue, *i.e. Prkaa1* and *Prkaag2*, whereas all isoforms of adipose FOXO remained unchanged. Interestingly in liver tissue, *Prkaa1* and *Prkaag2* remained unaltered and while the expression levels of all FOXO genes tended be higher, results did not reach the statistical threshold (supplementary table S2). While it is tempting to conclude that findings between captopril treated *C. elegans* and mice are inconsistent, it is important to note that whole-body loss-of-function of FOXO/*daf-16*, as the case in the current *C. elegans* model, may not correctly represent natural physiological responses in higher animals (to captopril). It would be interesting to investigate the effect of captopril in the presence of varying titres of *daf-16* RNAi in *C. elegans* in order to determine whether the same effect (as total loss-of-function) is achieved. Albeit in higher animals, as discussed in earlier parts of thesis, WAT has strong interaction with hepatic lipid metabolism via inter-organ cross talk, and according to our transcriptomics data, both tissues appear to orchestrate whole-body adiposity via different and perhaps convergent molecular mechanisms. It would be interesting to investigate the tissue specific effect of captopril on FOXO activity in future. It would also be interesting to investigate whether Agt and Ang-II like peptides exist in the *C. elegans*. Albeit results remain in agreement with the hypothesis that AMPK plays a significant part in the body fat reducing capacities of captopril.

Taken together, *in vivo* it is likely that the molecular targets of captopril are more extensive and has not been completely elucidated. Whether the bodyweight loss effects of captopril are a direct consequence of ACE-inhibition requires further investigation.

.

References

Aarsland, A., Chinkes, D., & Wolfe, R. R. (1997). Hepatic and whole-body fat synthesis in humans during carbohydrate overfeeding. *The American Journal of Clinical Nutrition, 65*(6), 1774-1782. doi:10.1093/ajcn/65.6.1774

AbdAlla, S., Lother, H., Abdel-tawab, A. M., & Quitterer, U. (2001). The angiotensin II AT2 receptor is an AT1 receptor antagonist. *J Biol Chem, 276*(43), 39721-39726. doi:10.1074/jbc.M105253200

Abdelmalek, M. F., Lazo, M., Horska, A., Bonekamp, S., Lipkin, E. W., Balasubramanyam, A., . . . Fatty Liver Subgroup of Look, A. R. G. (2012). Higher dietary fructose is associated with impaired hepatic adenosine triphosphate homeostasis in obese individuals with type 2 diabetes. *Hepatology, 56*(3), 952-960. doi:10.1002/hep.25741

Abela, L., Spiegel, R., Crowther, L. M., Klein, A., Steindl, K., Papuc, S. M., . . . Simmons, T. L. (2017). Plasma metabolomics reveals a diagnostic metabolic fingerprint for mitochondrial aconitase (ACO2) deficiency. *PLoS One, 12*(5), e0176363. doi:10.1371/journal.pone.0176363

ABS. (1995). *How Australians Measure Up*. Canberra: Australian Bureau of Statistics: Australian Government. Retrieved from http://www.abs.gov.au/ausstats/abs@.nsf/mf/4359.0.

ABS, A. Australian Bureau of Statistics. (2008). *Cafes, restaurants and catering services, Australia 2006-07*. Canberra: Australian Bureau of Statistics: Australian Government.

ABS. (2015). *National Health Survey First Results, 2014-15* Canberra: Australian Bureau of Statistics: Australian Government. Retrieved from http://www.abs.gov.au/ausstats/abs@.nsf/mf/4364.0.55.001.

ABS, A. B. o. Statistics. (2017). *Causes of Death, Australia 2016*. Canberra: Australian Bureau of Statistics: Australian Government.

Access Economics. (2008, August 2008). *The growing cost of obesity in 2008: three years on, Diabetes Australia*. Canberra. Retrieved from http://www.diabetesaustralia.com.au/PageFiles/7835/FULLREPORTGrowingCostOfObesity2008.pdf

Achari, A. E., & Jain, S. K. (2017). Adiponectin, a Therapeutic Target for Obesity, Diabetes, and Endothelial Dysfunction. *Int J Mol Sci, 18*(6), 1321. doi:10.3390/ijms18061321

Ackerman, Z., Oron-Herman, M., Grozovski, M., Rosenthal, T., Pappo, O., Link, G., & Sela, B. A. (2005). Fructose-induced fatty liver disease: hepatic effects of blood pressure and plasma triglyceride reduction. *Hypertension, 45*(5), 1012-1018. doi:10.1161/01.hyp.0000164570.20420.67

Afshin, A., Forouzanfar, M. H., Reitsma, M. B., Sur, P., Estep, K., Lee, A., . . . Murray, C. J. L. (2017). Health Effects of Overweight and Obesity in 195 Countries over 25 Years. *N Engl J Med, 377*(1), 13-27. doi:10.1056/NEJMoa1614362

Agudo, J., Martin, M., Roca, C., Molas, M., Bura, A. S., Zimmer, A., . . . Maldonado, R. (2010). Deficiency of CB2 cannabinoid receptor in mice improves insulin sensitivity but increases food intake and obesity with age. *Diabetologia, 53*(12), 2629-2640. doi:10.1007/s00125-010-1894-6

Aguirre, V., Uchida, T., Yenush, L., Davis, R., & White, M. F. (2000). The c-Jun NH(2)-terminal kinase promotes insulin resistance during association with insulin receptor substrate-1 and phosphorylation of Ser(307). *J Biol Chem, 275*(12), 9047-9054. doi:10.1074/jbc.275.12.9047

Aharoni-Simon, M., Hann-Obercyger, M., Pen, S., Madar, Z., & Tirosh, O. (2011). Fatty liver is associated with impaired activity of PPARgamma-coactivator 1alpha (PGC1alpha) and mitochondrial biogenesis in mice. *Lab Invest, 91*(7), 1018-1028. doi:10.1038/labinvest.2011.55

Ai, D., Fu, Y., Guo, D., Tanaka, H., Wang, N., Tang, C., . . . Zhu, Y. (2007). Angiotensin II up-regulates soluble epoxide hydrolase in vascular endothelium in vitro and in vivo. *Proc Natl Acad Sci U S A, 104*(21), 9018-9023. doi:10.1073/pnas.0703229104

AIHW, A. I. o. H. a. Welfare. (2016). *Overweight and Obesity*. Canberra: Australian Government. Retrieved from https://www.aihw.gov.au/getmedia/384eafec-fa90-412d-8c98-b279fddc7911/ah16-4-4-overweight-obesity.pdf.aspx.

AIHW, A. I. o. H. a. W. (2018). *Australia's health 2018*. Canberra.
AIWH. (2017). *Australian Institute of Health and Welfare: How much does Australia spend on health care?*

. Canberra: Australian Government. Retrieved from https://www.aihw.gov.au/getmedia/3a34cf2c-c715-43a8-be44-0cf53349fd9d/20592.pdf.aspx?inline=true.
Aizat, W. M., Dias, D. A., Stangoulis, J. C. R., Able, J. A., Roessner, U., & Able, A. J. (2014). Metabolomics of capsicum ripening reveals modification of the ethylene related-pathway and carbon metabolism. *Postharvest Biology and Technology, 89*, 19-31. doi:10.1016/j.postharvbio.2013.11.004
Alabaster, V. (2002). The fall and rise of in vivo pharmacology. *Trends in Pharmacological Sciences, 23*(1), 13-18. doi:10.1016/s0165-6147(00)01882-4
Alam, H., Williams, T. W., Dumas, K. J., Guo, C., Yoshina, S., Mitani, S., & Hu, P. J. (2010). EAK-7 controls development and lifespan by regulating nuclear DAF-16/FoxO activity. *Cell metabolism, 12*(1), 30-41. doi:10.1016/j.cmet.2010.05.004
Alipourfard, I., Datukishvili, N., & Mikeladze, D. (2019). TNF-alpha Downregulation Modifies Insulin Receptor Substrate 1 (IRS-1) in Metabolic Signaling of Diabetic Insulin-Resistant Hepatocytes. *Mediators Inflamm, 2019*, 3560819. doi:10.1155/2019/3560819
An, J., Muoio, D. M., Shiota, M., Fujimoto, Y., Cline, G. W., Shulman, G. I., . . . Newgard, C. B. (2004). Hepatic expression of malonyl-CoA decarboxylase reverses muscle, liver and whole-animal insulin resistance. *Nat Med, 10*(3), 268-274. doi:10.1038/nm995
An, R. (2016). Fast-food and full-service restaurant consumption and daily energy and nutrient intakes in US adults. *Eur J Clin Nutr, 70*(1), 97-103. doi:10.1038/ejcn.2015.104
Angstman, N. B., Frank, H. G., & Schmitz, C. (2016). Advanced Behavioral Analyses Show that the Presence of Food Causes Subtle Changes in C. elegans Movement. *Front Behav Neurosci, 10*, 60. doi:10.3389/fnbeh.2016.00060
Anselmi, C. V., Malovini, A., Roncarati, R., Novelli, V., Villa, F., Condorelli, G., . . . Puca, A. A. (2009). Association of the FOXO3A locus with extreme longevity in a southern Italian centenarian study. *Rejuvenation Res, 12*(2), 95-104. doi:10.1089/rej.2008.0827
Antin, J., Gibbs, J., Holt, J., Young, R. C., & Smith, G. P. (1975). Cholecystokinin elicits the complete behavioral sequence of satiety in rats. *J Comp Physiol Psychol, 89*(7), 784-790. Retrieved from http://www.ncbi.nlm.nih.gov/pubmed/1176672
Apfeld, J., O'Connor, G., McDonagh, T., DiStefano, P. S., & Curtis, R. (2004). The AMP-activated protein kinase AAK-2 links energy levels and insulin-like signals to lifespan in C. elegans. *Genes Dev, 18*(24), 3004-3009. doi:10.1101/gad.1255404
Apovian, C. M., Aronne, L. J., Bessesen, D. H., McDonnell, M. E., Murad, M. H., Pagotto, U., . . . Endocrine, S. (2015). Pharmacological management of obesity: an endocrine Society clinical practice guideline. *J Clin Endocrinol Metab, 100*(2), 342-362. doi:10.1210/jc.2014-3415
Arauz-Pacheco, C., Parrott, M. A., & Raskin, P. (2002). The treatment of hypertension in adult patients with diabetes. *Diabetes Care, 25*(1), 134-147. doi:10.2337/diacare.25.1.134
Argueta, D. A., & DiPatrizio, N. V. (2017). Peripheral endocannabinoid signaling controls hyperphagia in western diet-induced obesity. *Physiol Behav, 171*, 32-39. doi:10.1016/j.physbeh.2016.12.044
Arita, Y., Kihara, S., Ouchi, N., Takahashi, M., Maeda, K., Miyagawa, J., . . . Matsuzawa, Y. (1999). Paradoxical decrease of an adipose-specific protein, adiponectin, in obesity. *Biochem Biophys Res Commun, 257*(1), 79-83. doi:10.1006/bbrc.1999.0255
Armoni, M., Harel, C., Karni, S., Chen, H., Bar-Yoseph, F., Ver, M. R., . . . Karnieli, E. (2006). FOXO1 represses peroxisome proliferator-activated receptor-gamma1 and -gamma2 gene promoters in primary adipocytes. A novel paradigm to increase insulin sensitivity. *J Biol Chem, 281*(29), 19881-19891. doi:10.1074/jbc.M600320200
Astrup, A. (2005). The satiating power of protein—a key to obesity prevention? *The American Journal of Clinical Nutrition, 82*(1), 1-2. doi:10.1093/ajcn/82.1.1
Astrup, A., Raben, A., & Geiker, N. (2015). The role of higher protein diets in weight control and obesity-related comorbidities. *Int J Obes (Lond), 39*(5), 721-726. doi:10.1038/ijo.2014.216

Baba, M., Hong, S. B., Sharma, N., Warren, M. B., Nickerson, M. L., Iwamatsu, A., . . . Zbar, B. (2006). Folliculin encoded by the BHD gene interacts with a binding protein, FNIP1, and AMPK, and is involved in AMPK and mTOR signaling. *Proc Natl Acad Sci U S A, 103*(42), 15552-15557. doi:10.1073/pnas.0603781103

Bader, M. (2007). The second life of the (pro)renin receptor. *J Renin Angiotensin Aldosterone Syst, 8*(4), 205-208. doi:10.3317/jraas.2007.031

Baker, P. R., 2nd, Boyle, K. E., Koves, T. R., Ilkayeva, O. R., Muoio, D. M., Houmard, J. A., & Friedman, J. E. (2015). Metabolomic analysis reveals altered skeletal muscle amino acid and fatty acid handling in obese humans. *Obesity (Silver Spring), 23*(5), 981-988. doi:10.1002/oby.21046

Bang, S., Kim, S., Dailey, M. J., Chen, Y., Moran, T. H., Snyder, S. H., & Kim, S. F. (2012). AMP-activated protein kinase is physiologically regulated by inositol polyphosphate multikinase. *Proc Natl Acad Sci U S A, 109*(2), 616-620. doi:10.1073/pnas.1119751109

Bankman, J. (2017). The Globalization of Western-style Eating and Its Implications. *Brighter Green*. Retrieved from http://brightergreen.org/wp-content/uploads/2017/12/brighter_green_public_health_paper.pdf

Bao, Y., Zhao, T., Wang, X., Qiu, Y., Su, M., Jia, W., & Jia, W. (2009). Metabonomic variations in the drug-treated type 2 diabetes mellitus patients and healthy volunteers. *J Proteome Res, 8*(4), 1623-1630. doi:10.1021/pr800643w

Barroso, W. A., Victorino, V. J., Jeremias, I. C., Petroni, R. C., Ariga, S. K. K., Salles, T. A., . . . de Souza, H. P. (2018). High-fat diet inhibits PGC-1alpha suppressive effect on NFkappaB signaling in hepatocytes. *Eur J Nutr, 57*(5), 1891-1900. doi:10.1007/s00394-017-1472-5

Bartelt, A., Bruns, O. T., Reimer, R., Hohenberg, H., Ittrich, H., Peldschus, K., . . . Heeren, J. (2011). Brown adipose tissue activity controls triglyceride clearance. *Nat Med, 17*(2), 200-205. doi:10.1038/nm.2297

Bataller, R., Gines, P., Nicolas, J. M., Gorbig, M. N., Garcia-Ramallo, E., Gasull, X., . . . Rodes, J. (2000). Angiotensin II induces contraction and proliferation of human hepatic stellate cells. *Gastroenterology, 118*(6), 1149-1156.

Bedogni, G., Miglioli, L., Masutti, F., Tiribelli, C., Marchesini, G., & Bellentani, S. (2005). Prevalence of and risk factors for nonalcoholic fatty liver disease: the Dionysos nutrition and liver study. *Hepatology, 42*(1), 44-52. doi:10.1002/hep.20734

Ben Arous, J., Laffont, S., & Chatenay, D. (2009). Molecular and sensory basis of a food related two-state behavior in C. elegans. *PLoS One, 4*(10), e7584. doi:10.1371/journal.pone.0007584

Bennett, C. F., Kwon, J. J., Chen, C., Russell, J., Acosta, K., Burnaevskiy, N., . . . Kaeberlein, M. (2017). Transaldolase inhibition impairs mitochondrial respiration and induces a starvation-like longevity response in Caenorhabditis elegans. *PLoS Genet, 13*(3), e1006695. doi:10.1371/journal.pgen.1006695

Bensaid, M., Gary-Bobo, M., Esclangon, A., Maffrand, J. P., Le Fur, G., Oury-Donat, F., & Soubrie, P. (2003). The cannabinoid CB1 receptor antagonist SR141716 increases Acrp30 mRNA expression in adipose tissue of obese fa/fa rats and in cultured adipocyte cells. *Mol Pharmacol, 63*(4), 908-914. doi:10.1124/mol.63.4.908

Berdichevsky, A., Viswanathan, M., Horvitz, H. R., & Guarente, L. (2006). C. elegans SIR-2.1 interacts with 14-3-3 proteins to activate DAF-16 and extend life span. *Cell, 125*(6), 1165-1177. doi:10.1016/j.cell.2006.04.036

Berg, A. H., Combs, T. P., Du, X., Brownlee, M., & Scherer, P. E. (2001). The adipocyte-secreted protein Acrp30 enhances hepatic insulin action. *Nat Med, 7*(8), 947-953. doi:10.1038/90992

Berg, J., Tymoczko, J., & Stryer, L. (2002). The Pentose Phosphate Pathway Generates NADPH and Synthesizes Five-Carbon Sugars. In ***Biochemistry*** (5th edition ed.). New York: W H Freeman. Retrieved from https://www.ncbi.nlm.nih.gov/books/NBK22416/

Bermudez, O. I., & Gao, X. (2010). Greater consumption of sweetened beverages and added sugars is associated with obesity among US young adults. *Ann Nutr Metab, 57*(3-4), 211-218. doi:10.1159/000321542

Bettaieb, A., Nagata, N., AbouBechara, D., Chahed, S., Morisseau, C., Hammock, B. D., & Haj, F. G. (2013). Soluble epoxide hydrolase deficiency or inhibition attenuates diet-induced endoplasmic reticulum stress in liver and adipose tissue. *J Biol Chem, 288*(20), 14189-14199. doi:10.1074/jbc.M113.458414

Bevilacqua, A., & Bizzarri, M. (2018). Inositols in Insulin Signaling and Glucose Metabolism. *Int J Endocrinol, 2018*, 1968450. doi:10.1155/2018/1968450

Bhatnagar, A., Unal, H., Jagannathan, R., Kaveti, S., Duan, Z. H., Yong, S., . . . Karnik, S. S. (2013). Interaction of G-protein betagamma complex with chromatin modulates GPCR-dependent gene regulation. *PLoS One, 8*(1), e52689. doi:10.1371/journal.pone.0052689

Bitkin, E. C., Boyraz, M., Taskin, N., Akcay, A., Ulucan, K., Akyol, M. B., & Akcay, T. (2013). Effects of ACE inhibitors on insulin resistance and lipid profile in children with metabolic syndrome. *J Clin Res Pediatr Endocrinol, 5*(3), 164-169. doi:10.4274/Jcrpe.1020

Bjørnland, T., Langaas, M., Grill, V., & Mostad, I. L. (2017). Assessing gene-environment interaction effects of FTO, MC4R and lifestyle factors on obesity using an extreme phenotype sampling design: Results from the HUNT study. *PLoS One, 12*(4), e0175071. doi:10.1371/journal.pone.0175071

Blanco, A., & Blanco, G. (2017). Metabolism in Some Tissues. In A. Blanco & G. Blanco (Eds.), *Medical Biochemistry* (pp. 447-463): Academic Press. doi:10.1016/b978-0-12-803550-4.00020-3

Bloom, B., & Stetten, D., Jr. (1955). The fraction of glucose catabolized via the glycolytic pathway. *J Biol Chem, 212*(2), 555-563. Retrieved from https://www.ncbi.nlm.nih.gov/pubmed/14353856

Bloomfield, H. E., Kane, R., Koeller, E., Greer, N., MacDonald, R., & Wilt, T. (2015). *Benefits and Harms of the Mediterranean Diet Compared to Other Diets*. Washington (DC): Department of Veterans Affairs (US).

Bolhuis, D. P., Lakemond, C. M., de Wijk, R. A., Luning, P. A., & de Graaf, C. (2012). Effect of salt intensity in soup on ad libitum intake and on subsequent food choice. *Appetite, 58*(1), 48-55. doi:10.1016/j.appet.2011.09.001

Boustany, C. M., Bharadwaj, K., Daugherty, A., Brown, D. R., Randall, D. C., & Cassis, L. A. (2004). Activation of the systemic and adipose renin-angiotensin system in rats with diet-induced obesity and hypertension. *Am J Physiol Regul Integr Comp Physiol, 287*(4), R943-949. doi:10.1152/ajpregu.00265.2004

Boyle, L., Wamelink, M. M. C., Salomons, G. S., Roos, B., Pop, A., Dauber, A., . . . Chung, W. K. (2016). Mutations in TKT Are the Cause of a Syndrome Including Short Stature, Developmental Delay, and Congenital Heart Defects. *Am J Hum Genet, 98*(6), 1235-1242. doi:10.1016/j.ajhg.2016.03.030

Braun-Dullaeus, R. C., Mann, M. J., Ziegler, A., von der Leyen, H. E., & Dzau, V. J. (1999). A novel role for the cyclin-dependent kinase inhibitor p27(Kip1) in angiotensin II-stimulated vascular smooth muscle cell hypertrophy. *The Journal of clinical investigation, 104*(6), 815-823. doi:10.1172/JCI5339

Bravata, D. M., Sanders, L., Huang, J., Krumholz, H. M., Olkin, I., Gardner, C. D., & Bravata, D. M. (2003). Efficacy and safety of low-carbohydrate diets: a systematic review. *JAMA, 289*(14), 1837-1850. doi:10.1001/jama.289.14.1837

Brennan, A. M., & Mantzoros, C. S. (2006). Drug Insight: the role of leptin in human physiology and pathophysiology--emerging clinical applications. *Nat Clin Pract Endocrinol Metab, 2*(6), 318-327. doi:10.1038/ncpendmet0196

Bricca, G., Legedz, L., Nehme, A., Ayari, H., Paultre, C., Hodroj, W., . . . Cerutti, C. (2015). Local Angiotensin Pathways in Human Carotid Atheroma: Towards a Systems Biology Approach. *Conference Papers in Science, 2015*, 1-9. doi:10.1155/2015/593086

Broadhurst, D. I., & Kell, D. B. (2006). Statistical strategies for avoiding false discoveries in metabolomics and related experiments. *Metabolomics, 2*(4), 171-196. doi:10.1007/s11306-006-0037-z

Brooks, D. R., Appleford, P. J., Murray, L., & Isaac, R. E. (2003). An essential role in molting and morphogenesis of Caenorhabditis elegans for ACN-1, a novel member of the angiotensin-converting enzyme family that lacks a metallopeptidase active site. *The Journal of biological chemistry, 278*(52), 52340-52346. doi:10.1074/jbc.M308858200

Brouns, F. (2018). Overweight and diabetes prevention: is a low-carbohydrate-high-fat diet recommendable? *Eur J Nutr, 57*(4), 1301-1312. doi:10.1007/s00394-018-1636-y

Brown, G. T., & Kleiner, D. E. (2016). Histopathology of nonalcoholic fatty liver disease and nonalcoholic steatohepatitis. *Metabolism, 65*(8), 1080-1086. doi:10.1016/j.metabol.2015.11.008

Brown, I. J., Tzoulaki, I., Candeias, V., & Elliott, P. (2009). Salt intakes around the world: implications for public health. *Int J Epidemiol, 38*(3), 791-813. doi:10.1093/ije/dyp139

Brown, W. J., Miller, Y. D., & Miller, R. (2003). Sitting time and work patterns as indicators of overweight and obesity in Australian adults. *Int J Obes Relat Metab Disord, 27*(11), 1340-1346. doi:10.1038/sj.ijo.0802426

Butler, M. G. (2016). Chapter One - Single Gene and Syndromic Causes of Obesity: Illustrative Examples. In Y.-X. Tao (Ed.), *Progress in Molecular Biology and Translational Science* (Vol. 140, pp. 1-45): Academic Press. doi:https://doi.org/10.1016/bs.pmbts.2015.12.003

Butsch, W. S. (2015). Obesity medications: what does the future look like? *Curr Opin Endocrinol Diabetes Obes, 22*(5), 360-366. doi:10.1097/MED.0000000000000192

Butterworth, P. J. (2005a, 2005/07/01). Lehninger: principles of biochemistry (4th edn) D. L. Nelson and M. C. Cox, W. H. Freeman & Co., New York, 1119 pp (plus 17 pp glossary), ISBN 0-7167-4339-6 (2004). *Cell Biochemistry and Function, 23*(4), 293-294. doi:10.1002/cbf.1216 Retrieved from https://doi.org/10.1002/cbf.1216

Butterworth, P. J. (2005b). Lehninger: principles of biochemistry (4th edn) D. L. Nelson and M. C. Cox, W. H. Freeman & Co., New York, 1119 pp (plus 17 pp glossary), ISBN 0-7167-4339-6 (2004). In *Cell Biochemistry and Function* (Vol. 23, pp. 293-294). doi:10.1002/cbf.1216

Cahová, M., Vavrinková, H., Tutterova, M., Meschisvilli, E., & Kazdova, L. (2003). Captopril enhanced insulin-stimulated glycogen synthesis in skeletal muscle but not fatty acid synthesis in adipose tissue of hereditary hypertriglyceridemic rats. *Metabolism, 52*(11), 1406-1412. doi:10.1016/s0026-0495(03)00319-6

Caminhotto, R. d. O., Sertié, R. A. L., Andreotti, S., Campaãa, A. B., & Lima, F. B. (2016). Renin-angiotensin system blockers regulate the metabolism of isolated fat cells in vitro. *Brazilian journal of medical and biological research = Revista brasileira de pesquisas medicas e biologicas, 49*(8), e5409. doi:10.1590/1414-431X20165409

Campbell, R., Tasevska, N., Jackson, K., Sagi-Kiss, V., di Paolo, N., Mindell, J., . . . Kuhnle, G. (2017). *Association between urinary biomarkers of total sugars intake and measures of obesity in a cross-sectional study* (Vol. 12)(PLOS ONE).

Cannon, B., & Nedergaard, J. (2004). Brown adipose tissue: function and physiological significance. *Physiol Rev, 84*(1), 277-359. doi:10.1152/physrev.00015.2003

Cao, X., Yang, F. Y., Xin, Z., Xie, R. R., & Yang, J. K. (2014). The ACE2/Ang-(1-7)/Mas axis can inhibit hepatic insulin resistance. *Mol Cell Endocrinol, 393*(1-2), 30-38. doi:10.1016/j.mce.2014.05.024

Carr, K. A., Lin, H., Fletcher, K. D., Sucheston, L., Singh, P. K., Salis, R. J., . . . Epstein, L. H. (2013). Two functional serotonin polymorphisms moderate the effect of food reinforcement on BMI. *Behav Neurosci, 127*(3), 387-399. doi:10.1037/a0032026

Carroll, W. X., Kalupahana, N. S., Booker, S. L., Siriwardhana, N., Lemieux, M., Saxton, A. M., & Moustaid-Moussa, N. (2013). Angiotensinogen gene silencing reduces markers of lipid accumulation and inflammation in cultured adipocytes. *Front Endocrinol (Lausanne), 4*, 10. doi:10.3389/fendo.2013.00010

Castellini, G., Franzago, M., Bagnoli, S., Lelli, L., Balsamo, M., Mancini, M., . . . Stanghellini, G. (2017). Fat mass and obesity-associated gene (FTO) is associated to eating disorders susceptibility and moderates the expression of psychopathological traits. *PLoS One, 12*(3), e0173560. doi:10.1371/journal.pone.0173560

Castro, A. V. B., Kolka, C. M., Kim, S. P., & Bergman, R. N. (2014). Obesity, insulin resistance and comorbidities – Mechanisms of association. *Arquivos brasileiros de endocrinologia e metabologia, 58*(6), 600-609. Retrieved from http://www.ncbi.nlm.nih.gov/pmc/articles/PMC4423826/

Cazanave, S. C., Elmi, N. A., Akazawa, Y., Bronk, S. F., Mott, J. L., & Gores, G. J. (2010). CHOP and AP-1 cooperatively mediate PUMA expression during lipoapoptosis. *Am J Physiol Gastrointest Liver Physiol, 299*(1), G236-243. doi:10.1152/ajpgi.00091.2010

Ceddia, R. B., Somwar, R., Maida, A., Fang, X., Bikopoulos, G., & Sweeney, G. (2005). Globular adiponectin increases GLUT4 translocation and glucose uptake but reduces glycogen synthesis in rat skeletal muscle cells. *Diabetologia, 48*(1), 132-139. doi:10.1007/s00125-004-1609-y

Ceddia, R. B., William, W. N., Jr., Lima, F. B., Flandin, P., Curi, R., & Giacobino, J. P. (2000). Leptin stimulates uncoupling protein-2 mRNA expression and Krebs cycle activity and inhibits lipid synthesis in isolated rat white adipocytes. *Eur J Biochem, 267*(19), 5952-5958. doi:10.1046/j.1432-1327.2000.01664.x

Cedikova, M., Kripnerova, M., Dvorakova, J., Pitule, P., Grundmanova, M., Babuska, V., . . . Kuncova, J. (2016). Mitochondria in White, Brown, and Beige Adipocytes. *Stem Cells Int, 2016*, 6067349. doi:10.1155/2016/6067349

Chalasani, N., Wilson, L., Kleiner, D. E., Cummings, O. W., Brunt, E. M., Unalp, A., & Network, N. C. R. (2008). Relationship of steatosis grade and zonal location to histological features of steatohepatitis in adult patients with non-alcoholic fatty liver disease. *J Hepatol, 48*(5), 829-834. doi:10.1016/j.jhep.2008.01.016

Chan, J. L., Heist, K., DePaoli, A. M., Veldhuis, J. D., & Mantzoros, C. S. (2003). The role of falling leptin levels in the neuroendocrine and metabolic adaptation to short-term starvation in healthy men. *J Clin Invest, 111*(9), 1409-1421. doi:10.1172/JCI17490

Chang, H.-H. G. (2011). *Mechanisms Underlying the Abnormal Inositol Metabolisms in Diabetes Mellitus* (Biological Science, The University of Auckland, Auckland).

Chen, H., Zhang, L., Li, X., Li, X., Sun, G., Yuan, X., . . . Liu, G. (2013). Adiponectin activates the AMPK signaling pathway to regulate lipid metabolism in bovine hepatocytes. *J Steroid Biochem Mol Biol, 138*, 445-454. doi:10.1016/j.jsbmb.2013.08.013

Chen, M., Lu, B., Li, Y., Wang, Y., Zheng, H., Zhong, D., . . . Xie, Z. (2018). Metabolomics insights into the modulatory effects of long-term compound polysaccharide intake in high-fat diet-induced obese rats. *Nutr Metab (Lond), 15*, 8. doi:10.1186/s12986-018-0246-2

Chen, M. S., Ryan, C. E., & Piwnica-Worms, H. (2003). Chk1 kinase negatively regulates mitotic function of Cdc25A phosphatase through 14-3-3 binding. *Mol Cell Biol, 23*(21), 7488-7497. doi:10.1128/mcb.23.21.7488-7497.2003

Cheng, Z., Tsuda, M., Kishita, Y., Sato, Y., & Aigaki, T. (2013). Impaired energy metabolism in a Drosophila model of mitochondrial aconitase deficiency. *Biochem Biophys Res Commun, 433*(1), 145-150. doi:10.1016/j.bbrc.2013.02.040

Ching Lee, P., & Dixon, J. (2017). Pharmacotherapy for obesity. *Australian Family Physician, 46*, 472-477. Retrieved from http://www.racgp.org.au/afp/2017/july/pharmacotherapy-for-obesity/

Choe, S. S., Huh, J. Y., Hwang, I. J., Kim, J. I., & Kim, J. B. (2016). Adipose Tissue Remodeling: Its Role in Energy Metabolism and Metabolic Disorders. *Front Endocrinol (Lausanne), 7*, 30. doi:10.3389/fendo.2016.00030

Chou, C. L., Lin, H., Chen, J. S., & Fang, T. C. (2017). Renin inhibition improves metabolic syndrome, and reduces angiotensin II levels and oxidative stress in visceral fat tissues in fructose-fed rats. *PLoS One, 12*(7), e0180712. doi:10.1371/journal.pone.0180712

Coates, D. (2003). The angiotensin converting enzyme (ACE). *The international journal of biochemistry & cell biology, 35*(6), 769-773. doi:10.1016/s1357-2725(02)00309-6

Coates, D., Siviter, R., & Isaac, R. E. (2000). Exploring the Caenorhabditis elegans and Drosophila melanogaster genomes to understand neuropeptide and peptidase function. *Biochem Soc Trans, 28*(4), 464-469. Retrieved from http://www.ncbi.nlm.nih.gov/pubmed/10961941

Colagiuri, S., Lee, C. M., Colagiuri, R., Magliano, D., Shaw, J. E., Zimmet, P. Z., & Caterson, I. D. (2010). The cost of overweight and obesity in Australia. *Med J Aust, 192*(5), 260-264. Retrieved from http://www.ncbi.nlm.nih.gov/pubmed/20201759

Collard, F., Baldin, F., Gerin, I., Bolsee, J., Noel, G., Graff, J., . . . Bommer, G. T. (2016). A conserved phosphatase destroys toxic glycolytic side products in mammals and yeast. *Nat Chem Biol, 12*(8), 601-607. doi:10.1038/nchembio.2104

Combs, T. P., Pajvani, U. B., Berg, A. H., Lin, Y., Jelicks, L. A., Laplante, M., . . . Scherer, P. E. (2004). A transgenic mouse with a deletion in the collagenous domain of adiponectin displays elevated circulating adiponectin and improved insulin sensitivity. *Endocrinology, 145*(1), 367-383. doi:10.1210/en.2003-1068

Considine, R. V., Sinha, M. K., Heiman, M. L., Kriauciunas, A., Stephens, T. W., Nyce, M. R., . . . et al. (1996). Serum immunoreactive-leptin concentrations in normal-weight and obese humans. *N Engl J Med, 334*(5), 292-295. doi:10.1056/NEJM199602013340503

Cordain, L., Eaton, S. B., Sebastian, A., Mann, N., Lindeberg, S., Watkins, B. A., . . . Brand-Miller, J. (2005). Origins and evolution of the Western diet: health implications for the 21st century. *Am J Clin Nutr, 81*(2), 341-354. doi:10.1093/ajcn.81.2.341

Cordain, L., Miller, J. B., Eaton, S. B., Mann, N., Holt, S. H., & Speth, J. D. (2000). Plant-animal subsistence ratios and macronutrient energy estimations in worldwide hunter-gatherer diets. *Am J Clin Nutr, 71*(3), 682-692. doi:10.1093/ajcn/71.3.682

Corkins, M. E., Wilson, S., Cocuron, J. C., Alonso, A. P., & Bird, A. J. (2017). The gluconate shunt is an alternative route for directing glucose into the pentose phosphate pathway in fission yeast. *J Biol Chem, 292*(33), 13823-13832. doi:10.1074/jbc.M117.798488

Crandall, D. L., Herzlinger, H. E., Saunders, B. D., Armellino, D. C., & Kral, J. G. (1994). Distribution of angiotensin II receptors in rat and human adipocytes. *J Lipid Res, 35*(8), 1378-1385.

Crestani, S., Gasparotto Junior, A., Marques, M. C., Sullivan, J. C., Webb, R. C., & da Silva-Santos, J. E. (2014). Enhanced angiotensin-converting enzyme activity and systemic reactivity to angiotensin II in normotensive rats exposed to a high-sodium diet. *Vascul Pharmacol, 60*(2), 67-74. doi:10.1016/j.vph.2013.12.001

Croze, M. L., Géloën, A., & Soulage, C. O. (2015). Abnormalities in myo-inositol metabolism associated with type 2 diabetes in mice fed a high-fat diet: benefits of a dietary myo-inositol supplementation. *Br J Nutr, 113*(12), 1862-1875. doi:10.1017/S000711451500121X

Croze, M. L., & Soulage, C. O. (2013). Potential role and therapeutic interests of myo-inositol in metabolic diseases. *Biochimie, 95*(10), 1811-1827. doi:10.1016/j.biochi.2013.05.011

Cui, H., Yang, S., Zheng, M., Liu, R., Zhao, G., & Wen, J. (2017). High-salt intake negatively regulates fat deposition in mouse. *Scientific Reports, 7*(1), 2053. doi:10.1038/s41598-017-01560-3

Cupisti, A., Meola, M., D'Alessandro, C., Bernabini, G., Pasquali, E., Carpi, A., & Barsotti, G. (2007). Insulin resistance and low urinary citrate excretion in calcium stone formers. *Biomed Pharmacother, 61*(1), 86-90. doi:10.1016/j.biopha.2006.09.012

Curtis, R., O'Connor, G., & DiStefano, P. S. (2006). Aging networks in Caenorhabditis elegans: AMP-activated protein kinase (aak-2) links multiple aging and metabolism pathways. *Aging Cell, 5*(2), 119-126. doi:10.1111/j.1474-9726.2006.00205.x

da Silva, A. A., do Carmo, J., Dubinion, J., & Hall, J. E. (2009). The role of the sympathetic nervous system in obesity-related hypertension. *Curr Hypertens Rep, 11*(3), 206-211. doi:10.1007/s11906-009-0036-3

Dalle Molle, R., Fatemi, H., Dagher, A., Levitan, R. D., Silveira, P. P., & Dube, L. (2017). Gene and environment interaction: Is the differential susceptibility hypothesis relevant for obesity? *Neurosci Biobehav Rev, 73*, 326-339. doi:10.1016/j.neubiorev.2016.12.028

Danaei, G., Ding, E. L., Mozaffarian, D., Taylor, B., Rehm, J., Murray, C. J., & Ezzati, M. (2009). The preventable causes of death in the United States: comparative risk assessment of dietary, lifestyle, and metabolic risk factors. *PLoS Med, 6*(4), e1000058. doi:10.1371/journal.pmed.1000058

Danforth, E., Jr. (2000). Failure of adipocyte differentiation causes type II diabetes mellitus? *Nat Genet, 26*(1), 13. doi:10.1038/79111

Darlington, G. J., Ross, S. E., & MacDougald, O. A. (1998). The role of C/EBP genes in adipocyte differentiation. *J Biol Chem, 273*(46), 30057-30060. Retrieved from http://www.ncbi.nlm.nih.gov/pubmed/9804754

Davis, J. N., Hodges, V. A., & Gillham, M. B. (2006). Normal-Weight Adults Consume More Fiber and Fruit than Their Age- and Height-Matched Overweight/Obese Counterparts. *Journal of the American Dietetic Association, 106*(6), 833-840. doi:https://doi.org/10.1016/j.jada.2006.03.013

de Kloet, A. D., Krause, E. G., Kim, D.-H., Sakai, R. R., Seeley, R. J., & Woods, S. C. (2009). The Effect of Angiotensin-Converting Enzyme Inhibition Using Captopril on Energy Balance and Glucose Homeostasis. *Endocrinology, 150*(9), 4114-4123. doi:10.1210/en.2009-0065

de Kloet, A. D., Krause, E. G., & Woods, S. C. (2010). The renin angiotensin system and the metabolic syndrome. *Physiol Behav, 100*(5), 525-534. doi:10.1016/j.physbeh.2010.03.018

De Taeye, B. M., Morisseau, C., Coyle, J., Covington, J. W., Luria, A., Yang, J., . . . Vaughan, D. E. (2010). Expression and regulation of soluble epoxide hydrolase in adipose tissue. *Obesity (Silver Spring), 18*(3), 489-498. doi:10.1038/oby.2009.227

DeClercq, V. C., Goldsby, J. S., McMurray, D. N., & Chapkin, R. S. (2016). Distinct Adipose Depots from Mice Differentially Respond to a High-Fat, High-Salt Diet. *J Nutr, 146*(6), 1189-1196. doi:10.3945/jn.115.227496

Deepa, S. S., Zhou, L., Ryu, J., Wang, C., Mao, X., Li, C., . . . Dong, L. Q. (2011). APPL1 mediates adiponectin-induced LKB1 cytosolic localization through the PP2A-PKCzeta signaling pathway. *Mol Endocrinol, 25*(10), 1773-1785. doi:10.1210/me.2011-0082

den Hartog, G. J., Boots, A. W., Adam-Perrot, A., Brouns, F., Verkooijen, I. W., Weseler, A. R., . . . Bast, A. (2010). Erythritol is a sweet antioxidant. *Nutrition, 26*(4), 449-458. doi:10.1016/j.nut.2009.05.004

Derdak, Z., Villegas, K. A., Harb, R., Wu, A. M., Sousa, A., & Wands, J. R. (2013). Inhibition of p53 attenuates steatosis and liver injury in a mouse model of non-alcoholic fatty liver disease. *J Hepatol, 58*(4), 785-791. doi:10.1016/j.jhep.2012.11.042

Derkach, A., Sampson, J., Joseph, J., Playdon, M. C., & Stolzenberg-Solomon, R. Z. (2017). Effects of dietary sodium on metabolites: the Dietary Approaches to Stop Hypertension (DASH)-Sodium Feeding Study. *Am J Clin Nutr, 106*(4), 1131-1141. doi:10.3945/ajcn.116.150136

Devarajan, S., Yahiro, E., Uehara, Y., Habe, S., Nishiyama, A., Miura, S., . . . Urata, H. (2015). Depressor effect of chymase inhibitor in mice with high salt-induced moderate hypertension. *Am J Physiol Heart Circ Physiol, 309*(11), H1987-1996. doi:10.1152/ajpheart.00721.2014

Dietz, W. H. (1998). Health consequences of obesity in youth: childhood predictors of adult disease. *Pediatrics, 101*(3 Pt 2), 518-525.

Ding, Y., Lv, J., Mao, C., Zhang, H., Wang, A., Zhu, L., . . . Xu, Z. (2010). High-salt diet during pregnancy and angiotensin-related cardiac changes. *J Hypertens, 28*(6), 1290-1297. doi:10.1097/HJH.0b013e328337da8f

Diraison, F., Dusserre, E., Vidal, H., Sothier, M., & Beylot, M. (2002). Increased hepatic lipogenesis but decreased expression of lipogenic gene in adipose tissue in human obesity. *Am J Physiol Endocrinol Metab, 282*(1), E46-51. doi:10.1152/ajpendo.2002.282.1.E46

Divoux, A., Moutel, S., Poitou, C., Lacasa, D., Veyrie, N., Aissat, A., . . . Clement, K. (2012). Mast cells in human adipose tissue: link with morbid obesity, inflammatory status, and diabetes. *J Clin Endocrinol Metab, 97*(9), E1677-1685. doi:10.1210/jc.2012-1532

Diwan, A. G., Kuvalekar, A. A., Dharamsi, S., Vora, A. M., Nikam, V. A., & Ghadge, A. A. (2018). Correlation of Serum Adiponectin and Leptin levels in Obesity and Type 2 Diabetes Mellitus. *Indian J Endocrinol Metab, 22*(1), 93-99. doi:10.4103/ijem.IJEM_491_15

Dixon, J. B., Bhathal, P. S., Jonsson, J. R., Dixon, A. F., Powell, E. E., & O'Brien, P. E. (2003). Pro-fibrotic polymorphisms predictive of advanced liver fibrosis in the severely obese. *J Hepatol, 39*(6), 967-971.

DoH, D. o. Health. (2013). *Healthy weight guide*. Canberra, ACT: Australian Government Department of Health. Retrieved from http://healthyweight.health.gov.au/wps/portal/Home/get-started/are-you-a-healthy-weight/waist-circumference.

Donnelly, K. L., Smith, C. I., Schwarzenberg, S. J., Jessurun, J., Boldt, M. D., & Parks, E. J. (2005). Sources of fatty acids stored in liver and secreted via lipoproteins in patients with nonalcoholic fatty liver disease. *J Clin Invest, 115*(5), 1343-1351. doi:10.1172/JCI23621

Dorman, J. B., Albinder, B., Shroyer, T., & Kenyon, C. (1995). The age-1 and daf-2 genes function in a common pathway to control the lifespan of Caenorhabditis elegans. *Genetics, 141*(4), 1399-1406. Retrieved from http://www.ncbi.nlm.nih.gov/pubmed/8601482

Dornas, W. C., Cardoso, L. M., Silva, M., Machado, N. L., Chianca, D. A., Jr., Alzamora, A. C., . . . Silva, M. E. (2017). Oxidative stress causes hypertension and activation of nuclear factor-kappaB after high-fructose and salt treatments. *Sci Rep, 7*, 46051. doi:10.1038/srep46051

Dornas, W. C., de Lima, W. G., dos Santos, R. C., Guerra, J. F., de Souza, M. O., Silva, M., . . . Silva, M. E. (2013). High dietary salt decreases antioxidant defenses in the liver of fructose-fed insulin-resistant rats. *J Nutr Biochem, 24*(12), 2016-2022. doi:10.1016/j.jnutbio.2013.06.006

Dostal, D. E., & Baker, K. M. (1999). The cardiac renin-angiotensin system: conceptual, or a regulator of cardiac function? *Circ Res, 85*(7), 643-650.

Dowell, P., Otto, T. C., Adi, S., & Lane, M. D. (2003). Convergence of peroxisome proliferator-activated receptor gamma and Foxo1 signaling pathways. *J Biol Chem, 278*(46), 45485-45491. doi:10.1074/jbc.M309069200

Drenjancevic-Peric, I., Jelakovic, B., Lombard, J. H., Kunert, M. P., Kibel, A., & Gros, M. (2011). High-salt diet and hypertension: focus on the renin-angiotensin system. *Kidney Blood Press Res, 34*(1), 1-11. doi:10.1159/000320387

Driscoll, D. J., Miller, J. L., Schwartz, S., & Cassidy, S. B. (1993). Prader-Willi Syndrome. In M. P. Adam, H. H. Ardinger, R. A. Pagon, S. E. Wallace, L. J. H. Bean, K. Stephens & A. Amemiya (Eds.), *GeneReviews((R))* (20301505). Seattle (WA): University of Washington, Seattle

University of Washington, Seattle. GeneReviews is a registered trademark of the University of Washington, Seattle. All rights reserved. Retrieved from http://www.ncbi.nlm.nih.gov/pubmed/20301505

Duan, Q., Song, P., Ding, Y., & Zou, M. H. (2017). Activation of AMP-activated protein kinase by metformin ablates angiotensin II-induced endoplasmic reticulum stress and hypertension in mice in vivo. *Br J Pharmacol, 174*(13), 2140-2151. doi:10.1111/bph.13833

Eisenberg, F., & Parthasarathy, R. (1987). Measurement of biosynthesis of myo-inositol from glucose 6-phosphate. In *Methods in Enzymology* (Vol. 141, pp. 127-143): Academic Press. doi:https://doi.org/10.1016/0076-6879(87)41061-6

Eissing, L., Scherer, T., Tödter, K., Knippschild, U., Greve, J. W., Buurman, W. A., . . . Scheja, L. (2013). De novo lipogenesis in human fat and liver is linked to ChREBP-β and metabolic health. *Nature Communications, 4*, 1528. doi:10.1038/ncomms2537

https://www.nature.com/articles/ncomms2537#supplementary-information

El-Kabbani, O., Darmanin, C., & Chung, R. P. (2004). Sorbitol dehydrogenase: structure, function and ligand design. *Curr Med Chem, 11*(4), 465-476.

El Hadi, H., Frascati, A., Granzotto, M., Silvestrin, V., Ferlini, E., Vettor, R., & Rossato, M. (2016). Infrared thermography for indirect assessment of activation of brown adipose tissue in lean and obese male subjects. *Physiol Meas, 37*(12), N118-N128. doi:10.1088/0967-3334/37/12/N118

Elliott, H. (2006). Epidemiology, aetiology and prognosis of hypertension. *Medicine, 34*(8), 286-289. doi:10.1053/j.mpmed.2006.06.002

Enerback, S. (2010). Human brown adipose tissue. *Cell Metab, 11*(4), 248-252. doi:10.1016/j.cmet.2010.03.008

Engeli, S., Böhnke, J., Gorzelniak, K., Janke, J., Schling, P., Bader, M., . . . Sharma, A. M. (2005). Weight loss and the renin-angiotensin-aldosterone system. *Hypertension, 45*(3), 356-362.

Engeli, S., Boschmann, M., Frings, P., Beck, L., Janke, J., Titze, J., . . . Jordan, J. (2006). Influence of salt intake on renin-angiotensin and natriuretic peptide system genes in human adipose tissue. *Hypertension, 48*(6), 1103-1108. doi:10.1161/01.HYP.0000248837.88749.18

Engelke, U. F., Zijlstra, F. S., Mochel, F., Valayannopoulos, V., Rabier, D., Kluijtmans, L. A., . . . Wevers, R. A. (2010). Mitochondrial involvement and erythronic acid as a novel biomarker in transaldolase deficiency. *Biochim Biophys Acta, 1802*(11), 1028-1035. doi:10.1016/j.bbadis.2010.06.007

Ewing, R., Brownson, R. C., & Berrigan, D. (2006). Relationship between urban sprawl and weight of United States youth. *Am J Prev Med, 31*(6), 464-474. doi:10.1016/j.amepre.2006.08.020

Ewing, R., & Hamidi, S., N. I. o. H. a. S. G. America. (2014). *Measuring Urban Sprawl and Validating Sprawl Measures*. Washington, DC.

Ewing, R., Meakins, G., Hamidi, S., & Nelson, A. C. (2014). Relationship between urban sprawl and physical activity, obesity, and morbidity - update and refinement. *Health Place, 26*, 118-126. doi:10.1016/j.healthplace.2013.12.008

Ewing, R., Schmid, T., Killingsworth, R., Zlot, A., & Raudenbush, S. (2003). Relationship between urban sprawl and physical activity, obesity, and morbidity. *Am J Health Promot, 18*(1), 47-57. doi:10.4278/0890-1171-18.1.47

Fain, J. N., Madan, A. K., Hiler, M. L., Cheema, P., & Bahouth, S. W. (2004). Comparison of the release of adipokines by adipose tissue, adipose tissue matrix, and adipocytes from visceral and subcutaneous abdominal adipose tissues of obese humans. *Endocrinology, 145*(5), 2273-2282. doi:10.1210/en.2003-1336

Fantuzzi, G. (2008). Adiponectin and inflammation: Consensus and controversy. *Journal of Allergy and Clinical Immunology, 121*(2), 326-330. doi:https://doi.org/10.1016/j.jaci.2007.10.018

Farmer, S. R. (2003). The Forkhead Transcription Factor Foxo1: A Possible Link between Obesity and Insulin Resistance. *Molecular Cell, 11*(1), 6-8. doi:https://doi.org/10.1016/S1097-2765(03)00003-0

Farooqi, I. S., & O'Rahilly, S. (2014). Genetic Obesity Syndromes. 23-32. doi:10.1007/978-1-4614-8642-8_2

Feng, D., Yang, C., Geurts, Aron M., Kurth, T., Liang, M., Lazar, J., . . . Cowley, Allen W. (2012). Increased Expression of NAD(P)H Oxidase Subunit p67phox in the Renal Medulla Contributes to Excess Oxidative Stress and Salt-Sensitive Hypertension. *Cell Metabolism, 15*(2), 201-208. doi:https://doi.org/10.1016/j.cmet.2012.01.003

Ferreira, D. M., Afonso, M. B., Rodrigues, P. M., Simao, A. L., Pereira, D. M., Borralho, P. M., . . . Castro, R. E. (2014). c-Jun N-terminal kinase 1/c-Jun activation of the p53/microRNA 34a/sirtuin 1 pathway contributes to apoptosis induced by deoxycholic acid in rat liver. *Mol Cell Biol, 34*(6), 1100-1120. doi:10.1128/mcb.00420-13

Fillmore, N., Levasseur, J. L., Fukushima, A., Wagg, C. S., Wang, W., Dyck, J. R. B., & Lopaschuk, G. D. (2018). Uncoupling of glycolysis from glucose oxidation accompanies the development of heart failure with preserved ejection fraction. *Mol Med, 24*(1), 3. doi:10.1186/s10020-018-0005-x

Fiordaliso, F., Leri, A., Cesselli, D., Limana, F., Safai, B., Nadal-Ginard, B., . . . Kajstura, J. (2001). Hyperglycemia activates p53 and p53-regulated genes leading to myocyte cell death. *Diabetes, 50*(10), 2363-2375. doi:10.2337/diabetes.50.10.2363

Fonseca-Alaniz, M. H., Brito, L. C., Borges-Silva, C. N., Takada, J., Andreotti, S., & Lima, F. B. (2007). High dietary sodium intake increases white adipose tissue mass and plasma leptin in rats. *Obesity (Silver Spring), 15*(9), 2200-2208. doi:10.1038/oby.2007.261

Foretz, M., Pacot, C., Dugail, I., Lemarchand, P., Guichard, C., Le Liepvre, X., . . . Foufelle, F. (1999). ADD1/SREBP-1c is required in the activation of hepatic lipogenic gene expression by glucose. *Mol Cell Biol, 19*(5), 3760-3768. doi:10.1128/mcb.19.5.3760

Forrester, S. J., Booz, G. W., Sigmund, C. D., Coffman, T. M., Kawai, T., Rizzo, V., . . . Eguchi, S. (2018). Angiotensin II Signal Transduction: An Update on Mechanisms of Physiology and Pathophysiology. *Physiol Rev, 98*(3), 1627-1738. doi:10.1152/physrev.00038.2017

Foti, M., & Locati, M. (2017). *Cytokine Effector Functions in Tissues*. San Diego, UNITED STATES: Elsevier Science & Technology.

Fourcade, S., Ruiz, M., Camps, C., Schluter, A., Houten, S. M., Mooyer, P. A., . . . Pujol, A. (2009). A key role for the peroxisomal ABCD2 transporter in fatty acid homeostasis. *Am J Physiol Endocrinol Metab, 296*(1), E211-221. doi:10.1152/ajpendo.90736.2008

Francisco, T., Rodrigues, T. A., Freitas, M. O., Grou, C. P., Carvalho, A. F., Sá-Miranda, C., . . . Azevedo, J. E. (2013). A cargo-centered perspective on the PEX5 receptor-mediated peroxisomal protein import pathway. *The Journal of biological chemistry, 288*(40), 29151-29159. doi:10.1074/jbc.M113.487140

Frantz, E. D. C., Prodel, E., Braz, I. D., Giori, I. G., Bargut, T. C. L., Magliano, D. C., & Nobrega, A. C. L. (2018). Modulation of the renin-angiotensin system in white adipose tissue and skeletal muscle: focus on exercise training. *Clin Sci (Lond), 132*(14), 1487-1507. doi:10.1042/CS20180276

Frayling, T. M., Timpson, N. J., Weedon, M. N., Zeggini, E., Freathy, R. M., Lindgren, C. M., . . . McCarthy, M. I. (2007). A common variant in the FTO gene is associated with body mass index and predisposes to childhood and adult obesity. *Science, 316*(5826), 889-894. doi:10.1126/science.1141634

Frederich, R. C., Jr., Kahn, B. B., Peach, M. J., & Flier, J. S. (1992). Tissue-specific nutritional regulation of angiotensinogen in adipose tissue. *Hypertension, 19*(4), 339-344. doi:10.1161/01.hyp.19.4.339

Friedman, J. M., & Halaas, J. L. (1998). Leptin and the regulation of body weight in mammals. *Nature, 395*(6704), 763-770. doi:10.1038/27376

Friedman, S. L., Neuschwander-Tetri, B. A., Rinella, M., & Sanyal, A. J. (2018). Mechanisms of NAFLD development and therapeutic strategies. *Nat Med, 24*(7), 908-922. doi:10.1038/s41591-018-0104-9

Fruebis, J., Tsao, T. S., Javorschi, S., Ebbets-Reed, D., Erickson, M. R., Yen, F. T., . . . Lodish, H. F. (2001). Proteolytic cleavage product of 30-kDa adipocyte complement-related protein increases fatty acid oxidation in muscle and causes weight loss in mice. *Proc Natl Acad Sci U S A, 98*(4), 2005-2010. doi:10.1073/pnas.041591798

Frühbeck, G., Catalan, V., Rodriguez, A., Ramirez, B., Becerril, S., Salvador, J., . . . Gomez-Ambrosi, J. (2017). Involvement of the leptin-adiponectin axis in inflammation and oxidative stress in the metabolic syndrome. *Sci Rep, 7*(1), 6619. doi:10.1038/s41598-017-06997-0

Fu, Y., Luo, N., Klein, R. L., & Garvey, W. T. (2005). Adiponectin promotes adipocyte differentiation, insulin sensitivity, and lipid accumulation. *J Lipid Res, 46*(7), 1369-1379. doi:10.1194/jlr.M400373-JLR200

Fukuo, Y., Yamashina, S., Sonoue, H., Arakawa, A., Nakadera, E., Aoyama, T., . . . Watanabe, S. (2014). Abnormality of autophagic function and cathepsin expression in the liver from patients with non-alcoholic fatty liver disease. *Hepatol Res, 44*(9), 1026-1036. doi:10.1111/hepr.12282

Furuhashi, M., Ura, N., Higashiura, K., Murakami, H., Tanaka, M., Moniwa, N., . . . Shimamoto, K. (2003). Blockade of the renin-angiotensin system increases adiponectin concentrations in patients with essential hypertension. *Hypertension, 42*(1), 76-81.

Furuhashi, M., Ura, N., Takizawa, H., Yoshida, D., Moniwa, N., Murakami, H., . . . Shimamoto, K. (2004). Blockade of the renin-angiotensin system decreases adipocyte size with improvement in insulin sensitivity. *J Hypertens, 22*(10), 1977-1982.

Galgani, J., & Ravussin, E. (2008). Energy metabolism, fuel selection and body weight regulation. *Int J Obes (Lond), 32 Suppl 7*(Suppl 7), S109-119. doi:10.1038/ijo.2008.246

Gallagher, T., Bjorness, T., Greene, R., You, Y. J., & Avery, L. (2013). The geometry of locomotive behavioral states in C. elegans. *PLoS One, 8*(3), e59865. doi:10.1371/journal.pone.0059865

Gallo-Payet, N., Shum, M., Baillargeon, J.-P., Langlois, M.-F., Wallinder, C., Alterman, M., . . . Carpentier, A. C. (2012). AT2 Receptor Agonists: Exploiting the Beneficial Arm of Ang II Signaling. *Current Hypertension Reviews,* (8), 47-59.

Gao, Z., Hwang, D., Bataille, F., Lefevre, M., York, D., Quon, M. J., & Ye, J. (2002). Serine phosphorylation of insulin receptor substrate 1 by inhibitor kappa B kinase complex. *J Biol Chem, 277*(50), 48115-48121. doi:10.1074/jbc.M209459200

Gastaldelli, A., Gaggini, M., & DeFronzo, R. A. (2017). Role of Adipose Tissue Insulin Resistance in the Natural History of Type 2 Diabetes: Results From the San Antonio Metabolism Study. *Diabetes, 66*(4), 815-822. doi:10.2337/db16-1167

Gavras, H., & Gavras, I. (1988). Angiotensin converting enzyme inhibitors. Properties and side effects. *Hypertension, 11*(3 Pt 2), Ii37-41. doi:10.1161/01.hyp.11.3_pt_2.ii37

Genest, J., Cantin, M., Garcia, R., Thibault, G., Gutkowska, J., Schiffrin, E., . . . Hamet, P. (1983). Extrarenal angiotensin-forming enzymes. *Clin Exp Hypertens A, 5*(7-8), 1065-1080.

Gentile, C. L., Weir, T. L., Cox-York, K. A., Wei, Y., Wang, D., Reese, L., . . . Foster, M. T. (2015). The role of visceral and subcutaneous adipose tissue fatty acid composition in liver pathophysiology associated with NAFLD. *Adipocyte, 4*(2), 101-112. doi:10.4161/21623945.2014.978662

Gesta, S., Bluher, M., Yamamoto, Y., Norris, A. W., Berndt, J., Kralisch, S., . . . Kahn, C. R. (2006). Evidence for a role of developmental genes in the origin of obesity and body fat distribution. *Proc Natl Acad Sci U S A, 103*(17), 6676-6681. doi:10.1073/pnas.0601752103

Gesta, S., Tseng, Y. H., & Kahn, C. R. (2007). Developmental origin of fat: tracking obesity to its source. *Cell, 131*(2), 242-256. doi:10.1016/j.cell.2007.10.004

Gharbi, H., Fabretti, F., Bharill, P., Rinschen, M. M., Brinkkotter, S., Frommolt, P., . . . Muller, R. U. (2013). Loss of the Birt-Hogg-Dube gene product folliculin induces longevity in a hypoxia-inducible factor-dependent manner. *Aging Cell, 12*(4), 593-603. doi:10.1111/acel.12081

Ghazi, A. (2010). *Identifying the novel GTPase function of FLCN and characterizing its role in aging* (Department of Biochemistry, McGill University, Montreal).

Giacchetti, G., Faloia, E., Mariniello, B., Sardu, C., Gatti, C., Camilloni, M. A., . . . Mantero, F. (2002). Overexpression of the renin-angiotensin system in human visceral adipose tissue in normal and overweight subjects. *Am J Hypertens, 15*(5), 381-388. doi:10.1016/s0895-7061(02)02257-4

Giani, J. F., Mayer, M. A., Munoz, M. C., Silberman, E. A., Hocht, C., Taira, C. A., . . . Dominici, F. P. (2009). Chronic infusion of angiotensin-(1-7) improves insulin resistance and hypertension induced by a high-fructose diet in rats. *Am J Physiol Endocrinol Metab, 296*(2), E262-271. doi:10.1152/ajpendo.90678.2008

Gooda Sahib Jambocus, N., Saari, N., Ismail, A., Khatib, A., Mahomoodally, M. F., & Abdul Hamid, A. (2016). An Investigation into the Antiobesity Effects of Morinda citrifolia L. Leaf Extract in High Fat Diet Induced Obese Rats Using a (1)H NMR Metabolomics Approach. *J Diabetes Res, 2016*, 2391592. doi:10.1155/2016/2391592

Goossens, G. H., Blaak, E. E., Arner, P., Saris, W. H. M., & van Baak, M. A. (2006). Angiotensin II: a hormone that affects lipid metabolism in adipose tissue. *International Journal Of Obesity, 31*, 382. doi:10.1038/sj.ijo.0803388

Goossens, G. H., Moors, C. C., van der Zijl, N. J., Venteclef, N., Alili, R., Jocken, J. W., . . . Blaak, E. E. (2012). Valsartan improves adipose tissue function in humans with impaired glucose metabolism: a randomized placebo-controlled double-blind trial. *PLoS One, 7*(6), e39930. doi:10.1371/journal.pone.0039930

Grarup, N., Sandholt, C. H., Hansen, T., & Pedersen, O. (2014). Genetic susceptibility to type 2 diabetes and obesity: from genome-wide association studies to rare variants and beyond. *Diabetologia, 57*(8), 1528-1541. doi:10.1007/s00125-014-3270-4

Greene, D. A., & Lattimer, S. A. (1982). Sodium- and energy-dependent uptake of myo-inositol by rabbit peripheral nerve. Competitive inhibition by glucose and lack of an insulin effect. *J Clin Invest, 70*(5), 1009-1018.

Greene, D. A., Lattimer, S. A., & Sima, A. A. (1987). Sorbitol, phosphoinositides, and sodium-potassium-ATPase in the pathogenesis of diabetic complications. *N Engl J Med, 316*(10), 599-606. doi:10.1056/NEJM198703053161007

Greer, E. L., & Brunet, A. (2009). Different dietary restriction regimens extend lifespan by both independent and overlapping genetic pathways in C. elegans. *Aging Cell, 8*(2), 113-127. doi:10.1111/j.1474-9726.2009.00459.x

Greer, E. L., Dowlatshahi, D., Banko, M. R., Villen, J., Hoang, K., Blanchard, D., . . . Brunet, A. (2007). An AMPK-FOXO pathway mediates longevity induced by a novel method of dietary restriction in C. elegans. *Curr Biol, 17*(19), 1646-1656. doi:10.1016/j.cub.2007.08.047

Greer, E. L., Oskoui, P. R., Banko, M. R., Maniar, J. M., Gygi, M. P., Gygi, S. P., & Brunet, A. (2007). The energy sensor AMP-activated protein kinase directly regulates the mammalian FOXO3 transcription factor. *J Biol Chem, 282*(41), 30107-30119. doi:10.1074/jbc.M705325200

Guh, D. P., Zhang, W., Bansback, N., Amarsi, Z., Birmingham, C. L., & Anis, A. H. (2009). The incidence of co-morbidities related to obesity and overweight: a systematic review and meta-analysis. *BMC Public Health, 9*, 88. doi:10.1186/1471-2458-9-88

Guillemot, L., Levy, A., Raymondjean, M., & Rothhut, B. (2001). Angiotensin II-induced transcriptional activation of the cyclin D1 gene is mediated by Egr-1 in CHO-AT(1A) cells. *J Biol Chem, 276*(42), 39394-39403. doi:10.1074/jbc.M103862200

Hahm, J. H., Kim, S., DiLoreto, R., Shi, C., Lee, S. J., Murphy, C. T., & Nam, H. G. (2015). C. elegans maximum velocity correlates with healthspan and is maintained in worms with an insulin receptor mutation. *Nat Commun, 6*, 8919. doi:10.1038/ncomms9919

Hall, J. E. (1997). Mechanisms of abnormal renal sodium handling in obesity hypertension. *Am J Hypertens, 10*(5 Pt 2), 49s-55s.

Hall, J. E., Hildebrandt, D. A., & Kuo, J. (2001). Obesity hypertension: role of leptin and sympathetic nervous system. *Am J Hypertens, 14*(6 Pt 2), 103S-115S. doi:10.1016/S0895-7061(01)02077-5

Hamdan, II, Afifi, F., & Taha, M. O. (2004). In vitro alpha amylase inhibitory effect of some clinically-used drugs. *Pharmazie, 59*(10), 799-801.

Harp, J. B., & DiGirolamo, M. (1995). Components of the renin-angiotensin system in adipose tissue: changes with maturation and adipose mass enlargement. *J Gerontol A Biol Sci Med Sci, 50*(5), B270-276. doi:10.1093/gerona/50a.5.b270

Harp, J. B., Henry, S. A., & DiGirolamo, M. (2002). Dietary weight loss decreases serum angiotensin-converting enzyme activity in obese adults. *Obes Res, 10*(10), 985-990. doi:10.1038/oby.2002.134

Harris, M. (2013). The metabolic syndrome. *Australian Family Physician, 42*, 524-527. Retrieved from http://www.racgp.org.au/afp/2013/august/the-metabolic-syndrome/

Harte, A., McTernan, P., Chetty, R., Coppack, S., Katz, J., Smith, S., & Kumar, S. (2005). Insulin-mediated upregulation of the renin angiotensin system in human subcutaneous adipocytes is reduced by rosiglitazone. *Circulation, 111*(15), 1954-1961. doi:10.1161/01.CIR.0000161954.17870.5D

Haskell, W. L., Lee, I. M., Pate, R. R., Powell, K. E., Blair, S. N., Franklin, B. A., . . . Bauman, A. (2007). Physical activity and public health: updated recommendation for adults from the American College of Sports Medicine and the American Heart Association. *Med Sci Sports Exerc, 39*(8), 1423-1434. doi:10.1249/mss.0b013e3180616b27

Hattori, T., Murase, T., Takatsu, M., Nagasawa, K., Matsuura, N., Watanabe, S., . . . Nagata, K. (2014). Dietary salt restriction improves cardiac and adipose tissue pathology independently of obesity in a rat model of metabolic syndrome. *J Am Heart Assoc, 3*(6), e001312. doi:10.1161/JAHA.114.001312

Hayes, A. J., Lung, T. W., Bauman, A., & Howard, K. (2017). Modelling obesity trends in Australia: unravelling the past and predicting the future. *Int J Obes (Lond), 41*(1), 178-185. doi:10.1038/ijo.2016.165

He, W., Miao, F. J. P., Lin, D. C. H., Schwandner, R. T., Wang, Z., Gao, J., . . . Ling, L. (2004). Citric acid cycle intermediates as ligands for orphan G-protein-coupled receptors. *Nature, 429*(6988), 188-193. doi:10.1038/nature02488

Hecker, P. A., Mapanga, R. F., Kimar, C. P., Ribeiro, R. F., Jr., Brown, B. H., O'Connell, K. A., . . . Stanley, W. C. (2012). Effects of glucose-6-phosphate dehydrogenase deficiency on the

metabolic and cardiac responses to obesogenic or high-fructose diets. *Am J Physiol Endocrinol Metab, 303*(8), E959-972. doi:10.1152/ajpendo.00202.2012
Hellerstein, M. K., Schwarz, J. M., & Neese, R. A. (1996). Regulation of hepatic de novo lipogenesis in humans. *Annu Rev Nutr, 16*, 523-557. doi:10.1146/annurev.nu.16.070196.002515
Henderson, S. T., Bonafe, M., & Johnson, T. E. (2006). daf-16 protects the nematode Caenorhabditis elegans during food deprivation. *J Gerontol A Biol Sci Med Sci, 61*(5), 444-460. Retrieved from http://www.ncbi.nlm.nih.gov/pubmed/16720740
Henderson, S. T., & Johnson, T. E. (2001). daf-16 integrates developmental and environmental inputs to mediate aging in the nematode Caenorhabditis elegans. *Curr Biol, 11*(24), 1975-1980. doi:https://doi.org/10.1016/S0960-9822(01)00594-2
Herman, M. A., & Samuel, V. T. (2016). The Sweet Path to Metabolic Demise: Fructose and Lipid Synthesis. *Trends Endocrinol Metab, 27*(10), 719-730. doi:10.1016/j.tem.2016.06.005
Herndon, L. A., Schmeissner, P. J., Dudaronek, J. M., Brown, P. A., Listner, K. M., Sakano, Y., . . . Driscoll, M. (2002). Stochastic and genetic factors influence tissue-specific decline in ageing C. elegans. *Nature, 419*, 808. doi:10.1038/nature01135

https://www.nature.com/articles/nature01135#supplementary-information
Herrera, M., & Garvin, J. L. (2010). Angiotensin II stimulates thick ascending limb NO production via AT(2) receptors and Akt1-dependent nitric-oxide synthase 3 (NOS3) activation. *J Biol Chem, 285*(20), 14932-14940. doi:10.1074/jbc.M110.109041
Hiele, M., Ghoos, Y., Rutgeerts, P., & Vantrappen, G. (1993). Metabolism of erythritol in humans: comparison with glucose and lactitol. *Br J Nutr, 69*(1), 169-176.
Higuchi, S., Ohtsu, H., Suzuki, H., Shirai, H., Frank, G. D., & Eguchi, S. (2007). Angiotensin II signal transduction through the AT1 receptor: novel insights into mechanisms and pathophysiology. *Clin Sci (Lond), 112*(8), 417-428. doi:10.1042/CS20060342
Himms-Hagen, J., Melnyk, A., Zingaretti, M. C., Ceresi, E., Barbatelli, G., & Cinti, S. (2000). Multilocular fat cells in WAT of CL-316243-treated rats derive directly from white adipocytes. *Am J Physiol Cell Physiol, 279*(3), C670-681. doi:10.1152/ajpcell.2000.279.3.C670
Hixon, M. L., Obejero-Paz, C., Muro-Cacho, C., Wagner, M. W., Millie, E., Nagy, J., . . . Gualberto, A. (2000). Cks1 mediates vascular smooth muscle cell polyploidization. *J Biol Chem, 275*(51), 40434-40442. doi:10.1074/jbc.M005059200
Hofbauer, K. G. (2002). Molecular pathways to obesity. *Int J Obes Relat Metab Disord, 26 Suppl 2*, S18-27. doi:10.1038/sj.ijo.0802124
Holvoet, P., Rull, A., Garcia-Heredia, A., Lopez-Sanroma, S., Geeraert, B., Joven, J., & Camps, J. (2015). Stevia-derived compounds attenuate the toxic effects of ectopic lipid accumulation in the liver of obese mice: a transcriptomic and metabolomic study. *Food Chem Toxicol, 77*, 22-33. doi:10.1016/j.fct.2014.12.017
Honda, Y., & Honda, S. (1999). The daf-2 gene network for longevity regulates oxidative stress resistance and Mn-superoxide dismutase gene expression in Caenorhabditis elegans. *FASEB J, 13*(11), 1385-1393. doi:10.1096/fasebj.13.11.1385
Hootman, K. C., Trezzi, J. P., Kraemer, L., Burwell, L. S., Dong, X., Guertin, K. A., . . . Cassano, P. A. (2017). Erythritol is a pentose-phosphate pathway metabolite and associated with adiposity gain in young adults. *Proc Natl Acad Sci U S A, 114*(21), E4233-E4240. doi:10.1073/pnas.1620079114
Horiuchi, M., Hayashida, W., Akishita, M., Tamura, K., Daviet, L., Lehtonen, J. Y., & Dzau, V. J. (1999). Stimulation of different subtypes of angiotensin II receptors, AT1 and AT2 receptors, regulates STAT activation by negative crosstalk. *Circ Res, 84*(8), 876-882. doi:10.1161/01.res.84.8.876
Horton, T. J., Drougas, H., Brachey, A., Reed, G. W., Peters, J. C., & Hill, J. O. (1995). Fat and carbohydrate overfeeding in humans: different effects on energy storage. *Am J Clin Nutr, 62*(1), 19-29. doi:10.1093/ajcn/62.1.19
Hotamisligil, G. S. (1999a). Mechanisms of TNF-alpha-induced insulin resistance. *Exp Clin Endocrinol Diabetes, 107*(2), 119-125. doi:10.1055/s-0029-1212086

Hotamisligil, G. S. (1999b). The role of TNFα and TNF receptors in obesity and insulin resistance. *Journal of Internal Medicine, 245*(6), 621-625. doi:10.1046/j.1365-2796.1999.00490.x

Howarth, N. C., Huang, T. T., Roberts, S. B., & McCrory, M. A. (2005). Dietary fiber and fat are associated with excess weight in young and middle-aged US adults. *J Am Diet Assoc, 105*(9), 1365-1372. doi:10.1016/j.jada.2005.06.001

Hsu, A. L., Murphy, C. T., & Kenyon, C. (2003). Regulation of aging and age-related disease by DAF-16 and heat-shock factor. *Science, 300*(5622), 1142-1145. doi:10.1126/science.1083701

Hu, T., Mills, K. T., Yao, L., Demanelis, K., Eloustaz, M., Yancy, W. S., Jr., . . . Bazzano, L. A. (2012). Effects of low-carbohydrate diets versus low-fat diets on metabolic risk factors: a meta-analysis of randomized controlled clinical trials. *Am J Epidemiol, 176 Suppl 7*(Suppl 7), S44-54. doi:10.1093/aje/kws264

Hu, W. Y., Chen, D. G., Chen, S. C., Jin, X. Q., & Wang, H. J. (1996). Effect of chronic captopril treatment on circulating and tissue renin-angiotensin system in SHR rats. *Zhongguo Yao Li Xue Bao, 17*(6), 507-512.

Huang, C., Xiong, C., & Kornfeld, K. (2004). Measurements of age-related changes of physiological processes that predict lifespan of Caenorhabditis elegans. *Proc Natl Acad Sci U S A, 101*(21), 8084-8089. doi:10.1073/pnas.0400848101

Huang, D. Y., & Ichikawa, Y. (1997). Purification and characterization of a novel cytosolic NADP(H)-dependent retinol oxidoreductase from rabbit liver. *Biochim Biophys Acta, 1338*(1), 47-59. doi:10.1016/s0167-4838(96)00183-5

Huang, T., & Hu, F. B. (2015). Gene-environment interactions and obesity: recent developments and future directions. *BMC Med Genomics, 8 Suppl 1*(Suppl 1), S2. doi:10.1186/1755-8794-8-S1-S2

Huang, T. Y., Zheng, D., Houmard, J. A., Brault, J. J., Hickner, R. C., & Cortright, R. N. (2017). Overexpression of PGC-1alpha increases peroxisomal activity and mitochondrial fatty acid oxidation in human primary myotubes. *Am J Physiol Endocrinol Metab, 312*(4), E253-e263. doi:10.1152/ajpendo.00331.2016

Huck, J. H., Verhoeven, N. M., Struys, E. A., Salomons, G. S., Jakobs, C., & van der Knaap, M. S. (2004). Ribose-5-phosphate isomerase deficiency: new inborn error in the pentose phosphate pathway associated with a slowly progressive leukoencephalopathy. *Am J Hum Genet, 74*(4), 745-751. doi:10.1086/383204

Huh, J. Y., Park, Y. J., Ham, M., & Kim, J. B. (2014). Crosstalk between adipocytes and immune cells in adipose tissue inflammation and metabolic dysregulation in obesity. *Mol Cells, 37*(5), 365-371. doi:10.14348/molcells.2014.0074

Hulthén, L., Aurell, M., Klingberg, S., Hallenberg, E., Lorentzon, M., & Ohlsson, C. (2010). Salt intake in young Swedish men. *Public Health Nutr, 13*(5), 601-605. doi:10.1017/S1368980009991431

Huo, Y., Guo, X., Li, H., Xu, H., Halim, V., Zhang, W., . . . Wu, C. (2012). Targeted overexpression of inducible 6-phosphofructo-2-kinase in adipose tissue increases fat deposition but protects against diet-induced insulin resistance and inflammatory responses. *J Biol Chem, 287*(25), 21492-21500. doi:10.1074/jbc.M112.370379

Hwang, B., Jeoung, N. H., & Harris, R. A. (2009). Pyruvate dehydrogenase kinase isoenzyme 4 (PDHK4) deficiency attenuates the long-term negative effects of a high-saturated fat diet. *Biochem J, 423*(2), 243-252. doi:10.1042/BJ20090390

Ikeda, K., Maretich, P., & Kajimura, S. (2018). The Common and Distinct Features of Brown and Beige Adipocytes. *Trends Endocrinol Metab, 29*(3), 191-200. doi:10.1016/j.tem.2018.01.001

Imig, J. D., Zhao, X., Zaharis, C. Z., Olearczyk, J. J., Pollock, D. M., Newman, J. W., . . . Hammock, B. D. (2005). An orally active epoxide hydrolase inhibitor lowers blood pressure and provides renal protection in salt-sensitive hypertension. *Hypertension, 46*(4), 975-981. doi:10.1161/01.hyp.0000176237.74820.75

Isaac, R. E., Siviter, R. J., Stancombe, P., Coates, D., & Shirras, A. D. (2000). Conserved roles for peptidases in the processing of invertebrate neuropeptides. *Biochem Soc Trans, 28*(4), 460-464. Retrieved from http://www.ncbi.nlm.nih.gov/pubmed/10961940

Isakson, P., Hammarstedt, A., Gustafson, B., & Smith, U. (2009). Impaired preadipocyte differentiation in human abdominal obesity: role of Wnt, tumor necrosis factor-alpha, and inflammation. *Diabetes, 58*(7), 1550-1557. doi:10.2337/db08-1770

Itahana, Y., & Itahana, K. (2018). Emerging Roles of p53 Family Members in Glucose Metabolism. *International journal of molecular sciences, 19*(3), 776. doi:10.3390/ijms19030776

Item, F., & Konrad, D. (2012). Visceral fat and metabolic inflammation: the portal theory revisited. *Obes Rev, 13 Suppl 2*, 30-39. doi:10.1111/j.1467-789X.2012.01035.x

Jahan, H., Kobayashi, S., Nishimura, J., & Kanaide, H. (1996). Endothelin-1 and angiotensin II act as progression but not competence growth factors in vascular smooth muscle cells. *European Journal of Pharmacology, 295*(2-3), 261-269. doi:10.1016/0014-2999(95)00653-2

Janzer, A., German, N. J., Gonzalez-Herrera, K. N., Asara, J. M., Haigis, M. C., & Struhl, K. (2014). Metformin and phenformin deplete tricarboxylic acid cycle and glycolytic intermediates during cell transformation and NTPs in cancer stem cells. *Proc Natl Acad Sci U S A, 111*(29), 10574-10579. doi:10.1073/pnas.1409844111

Jauch, K. W., Hartl, W., Guenther, B., Wicklmayr, M., Rett, K., & Dietze, G. (1987). Captopril enhances insulin responsiveness of forearm muscle tissue in non-insulin-dependent diabetes mellitus. *Eur J Clin Invest, 17*(5), 448-454.

Jayasooriya, A. P., Mathai, M. L., Walker, L. L., Begg, D. P., Denton, D. A., Cameron-Smith, D., . . . Weisinger, R. S. (2008). Mice lacking angiotensin-converting enzyme have increased energy expenditure, with reduced fat mass and improved glucose clearance. *Proceedings of the National Academy of Sciences, 105*(18), 6531. Retrieved from http://www.pnas.org/content/105/18/6531.abstract

Jebb, S. A. (1997). Aetiology of obesity. *Br Med Bull, 53*(2), 264-285. Retrieved from http://www.ncbi.nlm.nih.gov/pubmed/9246836

Jeon, S. M., Chandel, N. S., & Hay, N. (2012). AMPK regulates NADPH homeostasis to promote tumour cell survival during energy stress. *Nature, 485*(7400), 661-665. doi:10.1038/nature11066

Jew, S., AbuMweis, S. S., & Jones, P. J. (2009). Evolution of the human diet: linking our ancestral diet to modern functional foods as a means of chronic disease prevention. *J Med Food, 12*(5), 925-934. doi:10.1089/jmf.2008.0268

Jeyakumar, S. M., & Vajreswari, A. (2015). Vitamin A as a key regulator of obesity & its associated disorders: Evidences from an obese rat model. *Indian J Med Res, 141*(3), 275-284. Retrieved from https://www.ncbi.nlm.nih.gov/pubmed/25963488

Jiang, S. Z., Lu, W., Zong, X. F., Ruan, H. Y., & Liu, Y. (2016). Obesity and hypertension. *Exp Ther Med, 12*(4), 2395-2399. doi:10.3892/etm.2016.3667

Jin, E. S., Lee, M. H., Murphy, R. E., & Malloy, C. R. (2018). Pentose phosphate pathway activity parallels lipogenesis but not antioxidant processes in rat liver. *Am J Physiol Endocrinol Metab, 314*(6), E543-e551. doi:10.1152/ajpendo.00342.2017

Johns, D. J., Hartmann-Boyce, J., Jebb, S. A., & Aveyard, P. (2014). Diet or exercise interventions vs combined behavioral weight management programs: a systematic review and meta-analysis of direct comparisons. *J Acad Nutr Diet, 114*(10), 1557-1568. doi:10.1016/j.jand.2014.07.005

Johnson, R. J., Nakagawa, T., Sanchez-Lozada, L. G., Shafiu, M., Sundaram, S., Le, M., . . . Lanaspa, M. A. (2013). Sugar, uric acid, and the etiology of diabetes and obesity. *Diabetes, 62*(10), 3307-3315. doi:10.2337/db12-1814

Jones, B. H., Standridge, M. K., & Moustaid, N. (1997). Angiotensin II increases lipogenesis in 3T3-L1 and human adipose cells. *Endocrinology, 138*(4), 1512-1519. doi:10.1210/endo.138.4.5038

Jonsson, J. R., Clouston, A. D., Ando, Y., Kelemen, L. I., Horn, M. J., Adamson, M. D., . . . Powell, E. E. (2001). Angiotensin-converting enzyme inhibition attenuates the progression of rat hepatic fibrosis. *Gastroenterology, 121*(1), 148-155.

Jonsson, J. R., Frewin, D. B., & Head, R. J. (1994). The Effect of Captopril Treatment and Its Withdrawal on the Gene Expression of the Renin-Angiotensin System. *Blood Pressure, 3*(1-2), 97-105. doi:10.3109/08037059409101528

Jovic, K., Sterken, M. G., Grilli, J., Bevers, R. P. J., Rodriguez, M., Riksen, J. A. G., . . . Snoek, L. B. (2017). Temporal dynamics of gene expression in heat-stressed Caenorhabditis elegans. *PLoS One, 12*(12), e0189445. doi:10.1371/journal.pone.0189445

Jung, O., Brandes, R. P., Kim, I. H., Schweda, F., Schmidt, R., Hammock, B. D., . . . Fleming, I. (2005). Soluble epoxide hydrolase is a main effector of angiotensin II-induced hypertension. *Hypertension, 45*(4), 759-765. doi:10.1161/01.HYP.0000153792.29478.1d

Kadoguchi, T., Kinugawa, S., Takada, S., Fukushima, A., Furihata, T., Homma, T., . . . Tsutsui, H. (2015). Angiotensin II can directly induce mitochondrial dysfunction, decrease oxidative fibre number and induce atrophy in mouse hindlimb skeletal muscle. *Exp Physiol, 100*(3), 312-322. doi:10.1113/expphysiol.2014.084095

Kahn, S. E., Hull, R. L., & Utzschneider, K. M. (2006). Mechanisms linking obesity to insulin resistance and type 2 diabetes. *Nature, 444*(7121), 840-846. doi:10.1038/nature05482

Kalra, A., & Tuma, F. (2019, 2018 Dec 18). *Physiology, Liver*. Retrieved 2019, from https://www.ncbi.nlm.nih.gov/books/NBK535438/

Kalupahana, N., & Moustaid-Moussa, N. (2012). The renin-angiotensin system: a link between obesity, inflammation and insulin resistance. *Obesity Reviews, 13*(2), 136-149. Retrieved from http://0-onlinelibrary.wiley.com.alpha2.latrobe.edu.au/doi/10.1111/j.1467-789X.2011.00942.x/full

Kalupahana, N. S., Massiera, F., Quignard-Boulange, A., Ailhaud, G., Voy, B. H., Wasserman, D. H., & Moustaid-Moussa, N. (2012). Overproduction of angiotensinogen from adipose tissue induces adipose inflammation, glucose intolerance, and insulin resistance. *Obesity (Silver Spring), 20*(1), 48-56. doi:10.1038/oby.2011.299

Kalupahana, N. S., & Moustaid-Moussa, N. (2012). The renin-angiotensin system: a link between obesity, inflammation and insulin resistance. *Obes Rev, 13*(2), 136-149. doi:10.1111/j.1467-789X.2011.00942.x

Kanai, H., Matsuzawa, Y., Kotani, K., Keno, Y., Kobatake, T., Nagai, Y., . . . Tarui, S. (1990). Close correlation of intra-abdominal fat accumulation to hypertension in obese women. *Hypertension, 16*(5), 484-490. doi:10.1161/01.hyp.16.5.484

Kang, C., Yijun, L., Jingtao, D., Changyu, P., Wenhua, Y., Baoan, W., . . . Juming, L. (2015). Effects of telmisartan on lipid metabolisms and proinflammatory factors secretion of differentiated 3T3-L1 adipocytes. *J Renin Angiotensin Aldosterone Syst, 16*(4), 1061-1068. doi:10.1177/1470320313518252

Kang, J. G., Park, C. Y., Kang, J. H., Park, Y. W., & Park, S. W. (2010). Randomized controlled trial to investigate the effects of a newly developed formulation of phentermine diffuse-controlled release for obesity. *Diabetes Obes Metab, 12*(10), 876-882. doi:10.1111/j.1463-1326.2010.01242.x

Kang, M., Yoo, H. J., Kim, M., Kim, M., & Lee, J. H. (2018). Metabolomics identifies increases in the acylcarnitine profiles in the plasma of overweight subjects in response to mild weight loss: a randomized, controlled design study. *Lipids Health Dis, 17*(1), 237. doi:10.1186/s12944-018-0887-1

Kannel, W. B., Brand, N., Skinner, J. J., Jr., Dawber, T. R., & McNamara, P. M. (1967). The relation of adiposity to blood pressure and development of hypertension. The Framingham study. *Ann Intern Med, 67*(1), 48-59. doi:10.7326/0003-4819-67-1-48

Karimani, A. D. V. M., Mamashkhani, Y. D. V. M., Moghadam Jafari, A. P., Akbarabadi, M. D. V. M., & Heidarpour, M. P. (2018). Captopril Attenuates Diazinon-Induced Oxidative Stress: A Subchronic Study in Rats. *Iranian journal of medical sciences, 43*(5), 514-522. Retrieved from https://www.ncbi.nlm.nih.gov/pubmed/30214104

https://www.ncbi.nlm.nih.gov/pmc/articles/PMC6123549/

Karl, J. P., Margolis, L. M., Murphy, N. E., Carrigan, C. T., Castellani, J. W., Madslien, E. H., . . . Pasiakos, S. M. (2017). Military training elicits marked increases in plasma metabolomic signatures of energy metabolism, lipolysis, fatty acid oxidation, and ketogenesis. *Physiol Rep, 5*(17). doi:10.14814/phy2.13407

Karlsson, C., Lindell, K., Ottosson, M., Sjostrom, L., Carlsson, B., & Carlsson, L. M. (1998). Human adipose tissue expresses angiotensinogen and enzymes required for its conversion to angiotensin II. *J Clin Endocrinol Metab, 83*(11), 3925-3929. doi:10.1210/jcem.83.11.5276

Kato, T., Niizuma, S., Inuzuka, Y., Kawashima, T., Okuda, J., Kawamoto, A., . . . Shioi, T. (2012). Analysis of liver metabolism in a rat model of heart failure. *Int J Cardiol, 161*(3), 130-136. doi:10.1016/j.ijcard.2011.07.056

Katsiki, N., Mikhailidis, D. P., & Banach, M. (2018). Leptin, cardiovascular diseases and type 2 diabetes mellitus. *Acta Pharmacol Sin, 39*(7), 1176-1188. doi:10.1038/aps.2018.40

Keller, K., Kolbe, H., Herken, H., & Lange, K. (1976). Glycolysis and glycogen metabolism after inhibition of hexose monophosphate pathway in C6-GLIAL cells. *Naunyn Schmiedebergs Arch Pharmacol, 294*(2), 213-215. Retrieved from https://www.ncbi.nlm.nih.gov/pubmed/138094

Kenyon, C., Chang, J., Gensch, E., Rudner, A., & Tabtiang, R. (1993). A C. elegans mutant that lives twice as long as wild type. *Nature, 366*(6454), 461-464. doi:10.1038/366461a0

Kershaw, E. E., & Flier, J. S. (2004). Adipose tissue as an endocrine organ. *J Clin Endocrinol Metab, 89*(6), 2548-2556. doi:10.1210/jc.2004-0395

Keys, A., Fidanza, F., Karvonen, M. J., Kimura, N., & Taylor, H. L. (1972). Indices of relative weight and obesity. *J Chronic Dis, 25*(6), 329-343.

Khakimov, B., Poulsen, S. K., Savorani, F., Acar, E., Gurdeniz, G., Larsen, T. M., . . . Engelsen, S. B. (2016). New Nordic Diet versus Average Danish Diet: A Randomized Controlled Trial Revealed Healthy Long-Term Effects of the New Nordic Diet by GC-MS Blood Plasma Metabolomics. *J Proteome Res, 15*(6), 1939-1954. doi:10.1021/acs.jproteome.6b00109

Khitan, Z., & Kim, D. H. (2013). Fructose: a key factor in the development of metabolic syndrome and hypertension. *J Nutr Metab, 2013*, 682673. doi:10.1155/2013/682673

Kim, E., Ahn, H., Kim, M. G., Lee, H., & Kim, S. (2017). The Expanding Significance of Inositol Polyphosphate Multikinase as a Signaling Hub. *Mol Cells, 40*(5), 315-321. doi:10.14348/molcells.2017.0066

Kim, H. J., Kim, J. H., Noh, S., Hur, H. J., Sung, M. J., Hwang, J. T., . . . Yoon, S. H. (2011). Metabolomic analysis of livers and serum from high-fat diet induced obese mice. *J Proteome Res, 10*(2), 722-731. doi:10.1021/pr100892r

Kim, J. Y., van de Wall, E., Laplante, M., Azzara, A., Trujillo, M. E., Hofmann, S. M., . . . Scherer, P. E. (2007). Obesity-associated improvements in metabolic profile through expansion of adipose tissue. *J Clin Invest, 117*(9), 2621-2637. doi:10.1172/jci31021

Kim, Y. C., Koo, H. S., Kim, S., & Chin, H. J. (2014). Estimation of Daily Salt Intake through a 24-Hour Urine Collection in Pohang, Korea. *Journal of Korean Medical Science, 29*(Suppl 2), S87-S90. doi:10.3346/jkms.2014.29.S2.S87

Kimball, S. R., Ravi, S., Gordon, B. S., Dennis, M. D., & Jefferson, L. S. (2015). Amino Acid-Induced Activation of mTORC1 in Rat Liver Is Attenuated by Short-Term Consumption of a High-Fat Diet. *J Nutr, 145*(11), 2496-2502. doi:10.3945/jn.115.215491

Kirchner, H., Sinha, I., Gao, H., Ruby, M. A., Schonke, M., Lindvall, J. M., . . . Zierath, J. R. (2016). Altered DNA methylation of glycolytic and lipogenic genes in liver from obese and type 2 diabetic patients. *Mol Metab, 5*(3), 171-183. doi:10.1016/j.molmet.2015.12.004

Kitada, K., Daub, S., Zhang, Y., Klein, J. D., Nakano, D., Pedchenko, T., . . . Titze, J. (2017). High salt intake reprioritizes osmolyte and energy metabolism for body fluid conservation. *J Clin Invest, 127*(5), 1944-1959. doi:10.1172/jci88532

Kitiyakara, C., Chabrashvili, T., Chen, Y., Blau, J., Karber, A., Aslam, S., . . . Wilcox, C. S. (2003). Salt intake, oxidative stress, and renal expression of NADPH oxidase and superoxide dismutase. *J Am Soc Nephrol, 14*(11), 2775-2782.

Kobayashi, R., Nagano, M., Nakamura, F., Higaki, J., Fujioka, Y., Ikegami, H., . . . Ogihara, T. (1993). Role of angiotensin II in high fructose-induced left ventricular hypertrophy in rats. *Hypertension, 21*(6 Pt 2), 1051-1055. doi:10.1161/01.hyp.21.6.1051

Kohlstedt, K., Gershome, C., Trouvain, C., Hofmann, W. K., Fichtlscherer, S., & Fleming, I. (2009). Angiotensin-converting enzyme (ACE) inhibitors modulate cellular retinol-binding protein 1 and adiponectin expression in adipocytes via the ACE-dependent signaling cascade. *Mol Pharmacol, 75*(3), 685-692. doi:10.1124/mol.108.051631

Kojda, G., & Harrison, D. (1999). Interactions between NO and reactive oxygen species: pathophysiological importance in atherosclerosis, hypertension, diabetes and heart failure. *Cardiovasc Res, 43*(3), 562-571. doi:10.1016/s0008-6363(99)00169-8

Kolaczynski, J. W., Ohannesian, J. P., Considine, R. V., Marco, C. C., & Caro, J. F. (1996). Response of leptin to short-term and prolonged overfeeding in humans. *J Clin Endocrinol Metab, 81*(11), 4162-4165. doi:10.1210/jcem.81.11.8923877

Kong, Y. W., Baqar, S., Jerums, G., & Ekinci, E. I. (2016). Sodium and Its Role in Cardiovascular Disease - The Debate Continues. *Front Endocrinol (Lausanne), 7*, 164. doi:10.3389/fendo.2016.00164

Konner, M., & Eaton, S. B. (2010). Paleolithic nutrition: twenty-five years later. *Nutr Clin Pract, 25*(6), 594-602. doi:10.1177/0884533610385702

Kouyama, R., Suganami, T., Nishida, J., Tanaka, M., Toyoda, T., Kiso, M., . . . Ogawa, Y. (2005). Attenuation of diet-induced weight gain and adiposity through increased energy expenditure in mice lacking angiotensin II type 1a receptor. *Endocrinology, 146*(8), 3481-3489. doi:10.1210/en.2005-0003

Kozak, L. P., & Anunciado-Koza, R. (2008). UCP1: its involvement and utility in obesity. *Int J Obes (Lond), 32 Suppl 7*(Suppl 7), S32-38. doi:10.1038/ijo.2008.236

Kristinsson, A., Hardarson, T., Palsson, K., Petursson, M. K., Snorrason, S. P., & Thorgeirsson, G. (1988). Additive effects of moderate dietary salt reduction and captopril in hypertension. *Acta Med Scand, 223*(2), 133-137. doi:doi:10.1111/j.0954-6820.1988.tb15777.x

Krstic, J., Galhuber, M., Schulz, T. J., Schupp, M., & Prokesch, A. (2018). p53 as a Dichotomous Regulator of Liver Disease: The Dose Makes the Medicine. *Int J Mol Sci, 19*(3), 921. doi:10.3390/ijms19030921

Krude, H., Biebermann, H., Luck, W., Horn, R., Brabant, G., & Gruters, A. (1998). Severe early-onset obesity, adrenal insufficiency and red hair pigmentation caused by POMC mutations in humans. *Nat Genet, 19*(2), 155-157. doi:10.1038/509

Krycer, J. R., Yugi, K., Hirayama, A., Fazakerley, D. J., Quek, L. E., Scalzo, R., . . . James, D. E. (2017). Dynamic Metabolomics Reveals that Insulin Primes the Adipocyte for Glucose Metabolism. *Cell Rep, 21*(12), 3536-3547. doi:10.1016/j.celrep.2017.11.085

Kuhnle, G. G., Tasevska, N., Lentjes, M. A., Griffin, J. L., Sims, M. A., Richardson, L., . . . Khaw, K. T. (2015). Association between sucrose intake and risk of overweight and obesity in a prospective sub-cohort of the European Prospective Investigation into Cancer in Norfolk (EPIC-Norfolk). *Public Health Nutr, 18*(15), 2815-2824. doi:10.1017/S1368980015000300

Kumar, S., Dietrich, N., & Kornfeld, K. (2016). Angiotensin Converting Enzyme (ACE) Inhibitor Extends Caenorhabditis elegans Life Span. *PLoS Genet, 12*(2), e1005866. doi:10.1371/journal.pgen.1005866

Kunjara, S., Sochor, M., Greenbaum, A. L., & McLean, P. (1993). Aspects of the regulation of hepatic phosphoribosyl pyrophosphate formation in the obese (ob/ob) mouse: relationship to the pentose phosphate pathway. *Biochem Med Metab Biol, 49*(2), 217-227.

Lai, C. H., Chou, C. Y., Ch'ang, L. Y., Liu, C. S., & Lin, W. (2000). Identification of novel human genes evolutionarily conserved in Caenorhabditis elegans by comparative proteomics. *Genome Res, 10*(5), 703-713. Retrieved from http://www.ncbi.nlm.nih.gov/pubmed/10810093

Lakowski, B., & Hekimi, S. (1998). The genetics of caloric restriction in Caenorhabditis elegans. *Proc Natl Acad Sci U S A, 95*(22), 13091-13096. Retrieved from http://www.ncbi.nlm.nih.gov/pubmed/9789046

Lanaspa, M. A., Ishimoto, T., Li, N., Cicerchi, C., Orlicky, D. J., Ruzycki, P., . . . Johnson, R. J. (2013). Endogenous fructose production and metabolism in the liver contributes to the development of metabolic syndrome. *Nat Commun, 4*, 2434. doi:10.1038/ncomms3434

Lanaspa, M. A., Kuwabara, M., Andres-Hernando, A., Li, N., Cicerchi, C., Jensen, T., . . . Johnson, R. J. (2018). High salt intake causes leptin resistance and obesity in mice by stimulating endogenous fructose production and metabolism. *Proc Natl Acad Sci U S A, 115*(12), 3138-3143. doi:10.1073/pnas.1713837115

Lanaspa, M. A., Sanchez-Lozada, L. G., Cicerchi, C., Li, N., Roncal-Jimenez, C. A., Ishimoto, T., . . . Johnson, R. J. (2012). Uric acid stimulates fructokinase and accelerates fructose metabolism in the development of fatty liver. *PLoS One, 7*(10), e47948. doi:10.1371/journal.pone.0047948

Larsen, T. M., Dalskov, S. M., van Baak, M., Jebb, S. A., Papadaki, A., Pfeiffer, A. F., . . . Genes, P. (2010). Diets with high or low protein content and glycemic index for weight-loss maintenance. *N Engl J Med, 363*(22), 2102-2113. doi:10.1056/NEJMoa1007137

Lazarow, P. B., & De Duve, C. (1976). A fatty acyl-CoA oxidizing system in rat liver peroxisomes; enhancement by clofibrate, a hypolipidemic drug. *Proc Natl Acad Sci U S A, 73*(6), 2043-2046. doi:10.1073/pnas.73.6.2043

Lebeau, P. F., Byun, J. H., Platko, K., MacDonald, M. E., Poon, S. V., Faiyaz, M., . . . Austin, R. C. (2019). Diet-induced hepatic steatosis abrogates cell-surface LDLR by inducing de novo PCSK9 expression in mice. *J Biol Chem, 294*(23), 9037-9047. doi:10.1074/jbc.RA119.008094

Leblanc, E. S., O'Connor, E., Whitlock, E. P., Patnode, C. D., & Kapka, T. (2011). Effectiveness of primary care-relevant treatments for obesity in adults: a systematic evidence review for the U.S. Preventive Services Task Force. *Ann Intern Med, 155*(7), 434-447. doi:10.7326/0003-4819-155-7-201110040-00006

Lee, M., Sorn, S. R., Lee, Y., & Kang, I. (2019). Salt Induces Adipogenesis/Lipogenesis and Inflammatory Adipocytokines Secretion in Adipocytes. *Int J Mol Sci, 20*(1), 160. doi:10.3390/ijms20010160

Lei, Z., Chen, W., Zhang, M., & Napoli, J. L. (2003). Reduction of all-trans-retinal in the mouse liver peroxisome fraction by the short-chain dehydrogenase/reductase RRD: induction by the PPAR alpha ligand clofibrate. *Biochemistry, 42*(14), 4190-4196. doi:10.1021/bi026948i

Leitner, B. P., Huang, S., Brychta, R. J., Duckworth, C. J., Baskin, A. S., McGehee, S., . . . Chen, K. Y. (2017). Mapping of human brown adipose tissue in lean and obese young men. *Proc Natl Acad Sci U S A, 114*(32), 8649-8654. doi:10.1073/pnas.1705287114

Léon, S., Goodman, J. M., & Subramani, S. (2006). Uniqueness of the mechanism of protein import into the peroxisome matrix: transport of folded, co-factor-bound and oligomeric proteins by shuttling receptors. *Biochim Biophys Acta, 1763*(12), 1552-1564. doi:10.1016/j.bbamcr.2006.08.037

Leri, A., Claudio, P. P., Li, Q., Wang, X., Reiss, K., Wang, S., . . . Anversa, P. (1998). Stretch-mediated release of angiotensin II induces myocyte apoptosis by activating p53 that enhances the local renin-angiotensin system and decreases the Bcl-2-to-Bax protein ratio in the cell. *J Clin Invest, 101*(7), 1326-1342. doi:10.1172/jci316

Leri, A., Fiordaliso, F., Setoguchi, M., Limana, F., Bishopric, N. H., Kajstura, J., . . . Anversa, P. (2000). Inhibition of p53 function prevents renin-angiotensin system activation and stretch-mediated myocyte apoptosis. *The American journal of pathology, 157*(3), 843-857. doi:10.1016/S0002-9440(10)64598-1

Leroux, A., Ferrere, G., Godie, V., Cailleux, F., Renoud, M. L., Gaudin, F., . . . Cassard-Doulcier, A. M. (2012). Toxic lipids stored by Kupffer cells correlates with their pro-inflammatory phenotype at an early stage of steatohepatitis. *J Hepatol, 57*(1), 141-149. doi:10.1016/j.jhep.2012.02.028

Lesmana, C. R., Hasan, I., Budihusodo, U., Gani, R. A., Krisnuhoni, E., Akbar, N., & Lesmana, L. A. (2009). Diagnostic value of a group of biochemical markers of liver fibrosis in patients with non-alcoholic steatohepatitis. *J Dig Dis, 10*(3), 201-206. doi:10.1111/j.1751-2980.2009.00386.x

Leung, A., Trac, C., Jin, W., Lanting, L., Akbany, A., Saetrom, P., . . . Natarajan, R. (2013). Novel long noncoding RNAs are regulated by angiotensin II in vascular smooth muscle cells. *Circ Res, 113*(3), 266-278. doi:10.1161/CIRCRESAHA.112.300849

Li, D. J., Huang, F., Ni, M., Fu, H., Zhang, L. S., & Shen, F. M. (2016). alpha7 Nicotinic Acetylcholine Receptor Relieves Angiotensin II-Induced Senescence in Vascular Smooth Muscle Cells by Raising Nicotinamide Adenine Dinucleotide-Dependent SIRT1 Activity. *Arterioscler Thromb Vasc Biol, 36*(8), 1566-1576. doi:10.1161/atvbaha.116.307157

Li, X., & Zhuo, J. (2015). Microarray Profiling of G Protein-coupled Receptor Signaling Responses to Overexpression of An Intracellular Angiotensin II Fusion Protein in Mouse Proximal Tubule Cells. *Faseb Journal, 29*(1_supplement), 971.976. doi:10.1096/fasebj.29.1_supplement.971.6

Li, X. C., & Zhuo, J. L. (2017). Evidence for Mitochondrial AT2 Receptor-Mediated Inhibition of Intracellular Angiotensin II-induced Respiratory and Glycolytic Responses in Mouse Proximal Tubule Cells. *The FASEB Journal, 31*(1_supplement), 854.852-854.852. doi:10.1096/fasebj.31.1_supplement.854.2

Lin, K., Hsin, H., Libina, N., & Kenyon, C. (2001). Regulation of the Caenorhabditis elegans longevity protein DAF-16 by insulin/IGF-1 and germline signaling. *Nat Genet, 28*(2), 139-145. doi:10.1038/88850

Lin, R., Elf, S., Shan, C., Kang, H.-B., Ji, Q., Zhou, L., . . . Chen, J. (2015). 6-Phosphogluconate dehydrogenase links oxidative PPP, lipogenesis and tumour growth by inhibiting LKB1–AMPK signalling. *Nature Cell Biology, 17*, 1484. doi:10.1038/ncb3255

https://www.nature.com/articles/ncb3255#supplementary-information

Liu, J., Liang, S., Liu, X., Brown, J. A., Newman, K. E., Sunkara, M., . . . Graf, G. A. (2012). The absence of ABCD2 sensitizes mice to disruptions in lipid metabolism by dietary erucic acid. *J Lipid Res, 53*(6), 1071-1079. doi:10.1194/jlr.M022160

Liu, J., Lu, W., Shi, B., Klein, S., & Su, X. (2019). Peroxisomal regulation of redox homeostasis and adipocyte metabolism. *Redox biology, 24*, 101167-101167. doi:10.1016/j.redox.2019.101167

Liu, Q., Wang, G., Zhou, G., Tan, Y., Wang, X., Wei, W., . . . Cai, L. (2009). Angiotensin II-induced p53-dependent cardiac apoptotic cell death: its prevention by metallothionein. *Toxicol Lett, 191*(2-3), 314-320. doi:10.1016/j.toxlet.2009.09.015

Liu, S., Kim, T. H., Franklin, D. A., & Zhang, Y. (2017). Protection against High-Fat-Diet-Induced Obesity in MDM2(C305F) Mice Due to Reduced p53 Activity and Enhanced Energy Expenditure. *Cell Rep, 18*(4), 1005-1018. doi:10.1016/j.celrep.2016.12.086

Liu, X. L., Ming, Y. N., Zhang, J. Y., Chen, X. Y., Zeng, M. D., & Mao, Y. M. (2017). Gene-metabolite network analysis in different nonalcoholic fatty liver disease phenotypes. *Exp Mol Med, 49*(1), e283. doi:10.1038/emm.2016.123

Liu, Y., Turdi, S., Park, T., Morris, N. J., Deshaies, Y., Xu, A., & Sweeney, G. (2013). Adiponectin corrects high-fat diet-induced disturbances in muscle metabolomic profile and whole-body glucose homeostasis. *Diabetes, 62*(3), 743-752. doi:10.2337/db12-0687

Livesey, G. (2003). Health potential of polyols as sugar replacers, with emphasis on low glycaemic properties. *Nutr Res Rev, 16*(2), 163-191. doi:10.1079/nrr200371

Lockwood, L. B., Tabenkin, B., & Ward, G. E. (1941). The Production of Gluconic Acid and 2-Keto-Gluconic Acid from Glucose by Species of Pseudomonas and Phytomonas. *J Bacteriol, 42*(1), 51-61. Retrieved from https://www.ncbi.nlm.nih.gov/pubmed/16560442

Loloi, J., Miller, A. J., Bingaman, S. S., Silberman, Y., & Arnold, A. C. (2018). Angiotensin-(1-7) contributes to insulin-sensitizing effects of angiotensin-converting enzyme inhibition in obese mice. *Am J Physiol Endocrinol Metab, 315*(6), E1204-e1211. doi:10.1152/ajpendo.00281.2018

Lönnqvist, F., Arner, P., Nordfors, L., & Schalling, M. (1995). Overexpression of the obese (ob) gene in adipose tissue of human obese subjects. *Nat Med, 1*(9), 950-953.

Lopez-Mejia, I. C., Lagarrigue, S., Giralt, A., Martinez-Carreres, L., Zanou, N., Denechaud, P. D., . . . Fajas, L. (2017). CDK4 Phosphorylates AMPKalpha2 to Inhibit Its Activity and Repress Fatty Acid Oxidation. *Mol Cell, 68*(2), 336-349 e336. doi:10.1016/j.molcel.2017.09.034

Loyer, P., Corlu, A., & Desdouets, C. (2012). Regulation of the hepatocyte cell cycle: signaling pathways and protein kinases. *Int J Hepatol, 2012*, 592354. doi:10.1155/2012/592354

Loza, M. J., McCall, C. E., Li, L., Isaacs, W. B., Xu, J., & Chang, B. L. (2007). Assembly of inflammation-related genes for pathway-focused genetic analysis. *PLoS One, 2*(10), e1035. doi:10.1371/journal.pone.0001035

Lu, H., Wu, C., Howatt, D. A., Balakrishnan, A., Moorleghen, J. J., Chen, X., . . . Daugherty, A. (2016). Angiotensinogen Exerts Effects Independent of Angiotensin II. *Arterioscler Thromb Vasc Biol, 36*(2), 256-265. doi:10.1161/atvbaha.115.306740

Ludewig, A. H., Kober-Eisermann, C., Weitzel, C., Bethke, A., Neubert, K., Gerisch, B., . . . Antebi, A. (2004). A novel nuclear receptor/coregulator complex controls C. elegans lipid metabolism, larval development, and aging. *Genes Dev, 18*(17), 2120-2133. doi:10.1101/gad.312604

Ma, W., Huang, T., Zheng, Y., Wang, M., Bray, G. A., Sacks, F. M., & Qi, L. (2016). Weight-Loss Diets, Adiponectin, and Changes in Cardiometabolic Risk in the 2-Year POUNDS Lost Trial. *J Clin Endocrinol Metab, 101*(6), 2415-2422. doi:10.1210/jc.2016-1207

Ma, Y., He, F. J., & MacGregor, G. A. (2015). High salt intake: independent risk factor for obesity? *Hypertension, 66*(4), 843-849. doi:10.1161/HYPERTENSIONAHA.115.05948

Maeda, K., Okubo, K., Shimomura, I., Funahashi, T., Matsuzawa, Y., & Matsubara, K. (1996). cDNA cloning and expression of a novel adipose specific collagen-like factor, apM1 (AdiPose Most abundant Gene transcript 1). *Biochem Biophys Res Commun, 221*(2), 286-289. doi:10.1006/bbrc.1996.0587

Mair, W., Panowski, S. H., Shaw, R. J., & Dillin, A. (2009). Optimizing dietary restriction for genetic epistasis analysis and gene discovery in C. elegans. *PLoS One, 4*(2), e4535. doi:10.1371/journal.pone.0004535

Mak, H. Y. (2012). Lipid droplets as fat storage organelles in Caenorhabditis elegans: Thematic Review Series: Lipid Droplet Synthesis and Metabolism: from Yeast to Man. *J Lipid Res, 53*(1), 28-33. doi:10.1194/jlr.R021006

Mann, J. (1984). Mechanisms of the antihypertensive action of captopril. *Contributions to Nephrology, 43*, 171-181.

Mann, T., Tomiyama, A. J., Westling, E., Lew, A. M., Samuels, B., & Chatman, J. (2007). Medicare's search for effective obesity treatments: diets are not the answer. *Am Psychol, 62*(3), 220-233. doi:10.1037/0003-066x.62.3.220

Marcus, Y., Shefer, G., Sasson, K., Kohen, F., Limor, R., Pappo, O., . . . Stern, N. (2013). Angiotensin 1-7 as means to prevent the metabolic syndrome: lessons from the fructose-fed rat model. *Diabetes, 62*(4), 1121-1130. doi:10.2337/db12-0792

Martin, G. M., Austad, S. N., & Johnson, T. E. (1996). Genetic analysis of ageing: role of oxidative damage and environmental stresses. *Nat Genet, 13*(1), 25-34. doi:10.1038/ng0596-25

Martinez Steele, E., Baraldi, L. G., Louzada, M. L., Moubarac, J. C., Mozaffarian, D., & Monteiro, C. A. (2016). Ultra-processed foods and added sugars in the US diet: evidence from a nationally representative cross-sectional study. *BMJ Open, 6*(3), e009892. doi:10.1136/bmjopen-2015-009892

Masaki, T., Chiba, S., Yasuda, T., Tsubone, T., Kakuma, T., Shimomura, I., . . . Yoshimatsu, H. (2003). Peripheral, but not central, administration of adiponectin reduces visceral adiposity and upregulates the expression of uncoupling protein in agouti yellow (Ay/a) obese mice. *Diabetes, 52*(9), 2266-2273.

Mason, C. (2000). Transport and health: en route to a healthier Australia? *Med J Aust, 172*(5), 230-232. Retrieved from http://www.ncbi.nlm.nih.gov/pubmed/10776396

Massiéra, F., Bloch-Faure, M., Ceiler, D., Murakami, K., Fukamizu, A., Gasc, J. M., . . . Teboul, M. (2001). Adipose angiotensinogen is involved in adipose tissue growth and blood pressure regulation. *FASEB J, 15*(14), 2727-2729. doi:10.1096/fj.01-0457fje

Massiéra, F., Seydoux, J., Geloen, A., Quignard-Boulange, A., Turban, S., Saint-Marc, P., . . . Teboul, M. (2001). Angiotensinogen-deficient mice exhibit impairment of diet-induced weight gain with alteration in adipose tissue development and increased locomotor activity. *Endocrinology, 142*(12), 5220-5225. doi:10.1210/endo.142.12.8556

Masuo, K., Mikami, H., Ogihara, T., & Tuck, M. L. (2001). Weight reduction and pharmacologic treatment in obese hypertensives. *Am J Hypertens, 14*(6 Pt 1), 530-538. doi:10.1016/s0895-7061(00)01279-6

Mathai, M. L., Naik, S., Sinclair, A. J., Weisinger, H. S., & Weisinger, R. S. (2008). Selective reduction in body fat mass and plasma leptin induced by angiotensin-converting enzyme inhibition in rats. *Int J Obes (Lond), 32*(10), 1576-1584. doi:10.1038/ijo.2008.126

Matsubara, M., Maruoka, S., & Katayose, S. (2002). Inverse relationship between plasma adiponectin and leptin concentrations in normal-weight and obese women. *Eur J*

Endocrinol, 147(2), 173-180. Retrieved from https://www.ncbi.nlm.nih.gov/pubmed/12153737
Matsui, R., Xu, S., Maitland, K. A., Hayes, A., Leopold, J. A., Handy, D. E., . . . Cohen, R. A. (2005). Glucose-6 phosphate dehydrogenase deficiency decreases the vascular response to angiotensin II. *Circulation, 112*(2), 257-263. doi:10.1161/CIRCULATIONAHA.104.499095
Matsusaka, T., Niimura, F., Shimizu, A., Pastan, I., Saito, A., Kobori, H., . . . Ichikawa, I. (2012). Liver angiotensinogen is the primary source of renal angiotensin II. *J Am Soc Nephrol, 23*(7), 1181-1189. doi:10.1681/asn.2011121159
Matteoni, C. A., Younossi, Z. M., Gramlich, T., Boparai, N., Liu, Y. C., & McCullough, A. J. (1999). Nonalcoholic fatty liver disease: a spectrum of clinical and pathological severity. *Gastroenterology, 116*(6), 1413-1419. doi:10.1016/s0016-5085(99)70506-8
McCaleb, M. L., & Sredy, J. (1992). Metabolic abnormalities of the hyperglycemic obese Zucker rat. *Metabolism, 41*(5), 522-525.
McColl, G., Rogers, A. N., Alavez, S., Hubbard, A. E., Melov, S., Link, C. D., . . . Lithgow, G. J. (2010). Insulin-like signaling determines survival during stress via posttranscriptional mechanisms in C. elegans. *Cell Metab, 12*(3), 260-272. doi:10.1016/j.cmet.2010.08.004
McDevitt, R. M., Bott, S. J., Harding, M., Coward, W. A., Bluck, L. J., & Prentice, A. M. (2001). De novo lipogenesis during controlled overfeeding with sucrose or glucose in lean and obese women. *Am J Clin Nutr, 74*(6), 737-746. doi:10.1093/ajcn/74.6.737
McLean, R. M. (2014). Measuring population sodium intake: a review of methods. *Nutrients, 6*(11), 4651-4662. doi:10.3390/nu6114651
McMillan Price, J., & Egger, G. (2017). Nutrition for the Nondietitian. In G. Egger, A. Binns, S. Rössner & M. Sagner (Eds.), *Lifestyle Medicine* (pp. 135-152): Academic Press. doi:10.1016/b978-0-12-810401-9.00008-5
Menikdiwela, K. R., Ramalingam, L., Allen, L., Scoggin, S., Kalupahana, N. S., & Moustaid-Moussa, N. (2019). Angiotensin II Increases Endoplasmic Reticulum Stress in Adipose Tissue and Adipocytes. *Sci Rep, 9*(1), 8481. doi:10.1038/s41598-019-44834-8
Minokoshi, Y., Kim, Y. B., Peroni, O. D., Fryer, L. G., Muller, C., Carling, D., & Kahn, B. B. (2002). Leptin stimulates fatty-acid oxidation by activating AMP-activated protein kinase. *Nature, 415*(6869), 339-343. doi:10.1038/415339a
Mittendorfer, B., Horowitz, J. F., DePaoli, A. M., McCamish, M. A., Patterson, B. W., & Klein, S. (2011). Recombinant human leptin treatment does not improve insulin action in obese subjects with type 2 diabetes. *Diabetes, 60*(5), 1474-1477. doi:10.2337/db10-1302
Miura, S., Ideishi, M., Sakai, T., Motoyama, M., Kinoshita, A., Sasaguri, M., . . . Arakawa, K. (1994). Angiotensin II formation by an alternative pathway during exercise in humans. *J Hypertens, 12*(10), 1177-1181.
Miyaoka, Y., Jin, D., Tashiro, K., Komeda, K., Masubuchi, S., Hirokawa, F., . . . Uchiyama, K. (2017). Chymase inhibitor prevents the development and progression of non-alcoholic steatohepatitis in rats fed a high-fat and high-cholesterol diet. *J Pharmacol Sci, 134*(3), 139-146. doi:10.1016/j.jphs.2017.04.005
Mizunoe, Y., Sudo, Y., Okita, N., Hiraoka, H., Mikami, K., Narahara, T., . . . Higami, Y. (2017). Involvement of lysosomal dysfunction in autophagosome accumulation and early pathologies in adipose tissue of obese mice. *Autophagy, 13*(4), 642-653. doi:10.1080/15548627.2016.1274850
Mohib, M., Hasan, I., Chowdhury, W. H., Chowdhury, N. U., Mohiuddin, S., Sagor, A. T., . . . Alam, A. (2016). Role of Angiotensin II in Hepatic Inflammation through MAPK Pathway: A Review. *J Hep, 2*(2). doi:10.21767/2471-9706.100013
Montague, C. T., Farooqi, I. S., Whitehead, J. P., Soos, M. A., Rau, H., Wareham, N. J., . . . O'Rahilly, S. (1997). Congenital leptin deficiency is associated with severe early-onset obesity in humans. *Nature, 387*(6636), 903-908. doi:10.1038/43185
Moreira, C. C. L., Lourenco, F. C., Mario, E. G., Santos, R. A. S., Botion, L. M., & Chaves, V. E. (2017). Long-term effects of angiotensin-(1-7) on lipid metabolism in the adipose tissue and liver. *Peptides, 92*, 16-22. doi:10.1016/j.peptides.2017.04.004
Moreno, M., Ortega, F., Xifra, G., Ricart, W., Fernandez-Real, J. M., & Moreno-Navarrete, J. M. (2015). Cytosolic aconitase activity sustains adipogenic capacity of adipose tissue

connecting iron metabolism and adipogenesis. *FASEB J, 29*(4), 1529-1539. doi:10.1096/fj.14-258996

Morimoto, H., Mori, J., Nakajima, H., Kawabe, Y., Tsuma, Y., Fukuhara, S., . . . Hosoi, H. (2018). Angiotensin 1-7 stimulates brown adipose tissue and reduces diet-induced obesity. *Am J Physiol Endocrinol Metab, 314*(2), E131-e138. doi:10.1152/ajpendo.00192.2017

Morine, M. J., Tierney, A. C., van Ommen, B., Daniel, H., Toomey, S., Gjelstad, I. M., . . . Roche, H. M. (2011). Transcriptomic coordination in the human metabolic network reveals links between n-3 fat intake, adipose tissue gene expression and metabolic health. *PLoS Comput Biol, 7*(11), e1002223. doi:10.1371/journal.pcbi.1002223

Morris, E. M., Meers, G. M., Booth, F. W., Fritsche, K. L., Hardin, C. D., Thyfault, J. P., & Ibdah, J. A. (2012). PGC-1alpha overexpression results in increased hepatic fatty acid oxidation with reduced triacylglycerol accumulation and secretion. *Am J Physiol Gastrointest Liver Physiol, 303*(8), G979-992. doi:10.1152/ajpgi.00169.2012

Mottillo, S., Filion, K. B., Genest, J., Joseph, L., Pilote, L., Poirier, P., . . . Eisenberg, M. J. (2010). The metabolic syndrome and cardiovascular risk a systematic review and meta-analysis. *J Am Coll Cardiol, 56*(14), 1113-1132. doi:10.1016/j.jacc.2010.05.034

Muir, L. A., Neeley, C. K., Meyer, K. A., Baker, N. A., Brosius, A. M., Washabaugh, A. R., . . . O'Rourke, R. W. (2016). Adipose tissue fibrosis, hypertrophy, and hyperplasia: Correlations with diabetes in human obesity. *Obesity (Silver Spring, Md.), 24*(3), 597-605. doi:10.1002/oby.21377

Muir, L. A., Neeley, C. K., Meyer, K. A., Baker, N. A., Brosius, A. M., Washabaugh, A. R., . . . O'Rourke, R. W. (2016). Adipose tissue fibrosis, hypertrophy, and hyperplasia: Correlations with diabetes in human obesity. *Obesity (Silver Spring), 24*(3), 597-605. doi:10.1002/oby.21377

Mummery, W. K., Schofield, G. M., Steele, R., Eakin, E. G., & Brown, W. J. (2005). Occupational sitting time and overweight and obesity in Australian workers. *Am J Prev Med, 29*(2), 91-97. doi:10.1016/j.amepre.2005.04.003

Mundy, A. L., Haas, E., Bhattacharya, I., Widmer, C. C., Kretz, M., Hofmann-Lehmann, R., . . . Barton, M. (2007). Fat intake modifies vascular responsiveness and receptor expression of vasoconstrictors: Implications for diet-induced obesity. *Cardiovascular Research, 73*(2), 368-375. doi:10.1016/j.cardiores.2006.11.019

Munekata, K., & Sakamoto, K. (Munekata2009). (2009). Forkhead transcription factor Foxo1 is essential for adipocyte differentiation. *In Vitro Cell Dev Biol Anim, 45*(10), 642-651. doi:10.1007/s11626-009-9230-5

Muoio, D. M., Noland, R. C., Kovalik, J. P., Seiler, S. E., Davies, M. N., DeBalsi, K. L., . . . Mynatt, R. L. (2012). Muscle-specific deletion of carnitine acetyltransferase compromises glucose tolerance and metabolic flexibility. *Cell Metab, 15*(5), 764-777. doi:10.1016/j.cmet.2012.04.005

Murphy, A. M., Wong, A. L., & Bezuhly, M. (2015). Modulation of angiotensin II signaling in the prevention of fibrosis. *Fibrogenesis Tissue Repair, 8*, 7. doi:10.1186/s13069-015-0023-z

Murphy, C. T., McCarroll, S. A., Bargmann, C. I., Fraser, A., Kamath, R. S., Ahringer, J., . . . Kenyon, C. (2003). Genes that act downstream of DAF-16 to influence the lifespan of Caenorhabditis elegans. *Nature, 424*(6946), 277-283. doi:10.1038/nature01789

Nadler, S. T., Stoehr, J. P., Schueler, K. L., Tanimoto, G., Yandell, B. S., & Attie, A. D. (2000). The expression of adipogenic genes is decreased in obesity and diabetes mellitus. *Proc Natl Acad Sci U S A, 97*(21), 11371-11376. doi:10.1073/pnas.97.21.11371

Nagao, H., Nishizawa, H., Bamba, T., Nakayama, Y., Isozumi, N., Nagamori, S., . . . Shimomura, I. (2017). Increased Dynamics of Tricarboxylic Acid Cycle and Glutamate Synthesis in Obese Adipose Tissue: IN VIVO METABOLIC TURNOVER ANALYSIS. *J Biol Chem, 292*(11), 4469-4483. doi:10.1074/jbc.M116.770172

Nakae, J., Kitamura, T., Kitamura, Y., Biggs, W. H., 3rd, Arden, K. C., & Accili, D. (2003). The forkhead transcription factor Foxo1 regulates adipocyte differentiation. *Dev Cell, 4*(1), 119-129. doi:https://doi.org/10.1016/S1534-5807(02)00401-X

Nam, W. S., Park, K. M., & Park, J. W. (2012). RNA interference targeting cytosolic NADP(+)-dependent isocitrate dehydrogenase exerts anti-obesity effect in vitro and in vivo. *Biochim Biophys Acta, 1822*(8), 1181-1188. doi:10.1016/j.bbadis.2012.04.003

Narasimhan, S. D., Mukhopadhyay, A., & Tissenbaum, H. A. (2009). InAKTivation of insulin/IGF-1 signaling by dephosphorylation. *Cell Cycle, 8*(23), 3878-3884. doi:10.4161/cc.8.23.10072

Nehme, A., Zouein, F. A., Zayeri, Z. D., & Zibara, K. (2019). An Update on the Tissue Renin Angiotensin System and Its Role in Physiology and Pathology. *J Cardiovasc Dev Dis, 6*(2). doi:10.3390/jcdd6020014

Nesteruk, M., Hennig, E. E., Mikula, M., Karczmarski, J., Dzwonek, A., Goryca, K., . . . Ostrowski, J. (2014). Mitochondrial-related proteomic changes during obesity and fasting in mice are greater in the liver than skeletal muscles. *Funct Integr Genomics, 14*(1), 245-259. doi:10.1007/s10142-013-0342-3

Neuhaus, A., Kooshapur, H., Wolf, J., Meyer, N. H., Madl, T., Saidowsky, J., . . . Erdmann, R. (2014). A novel Pex14 protein-interacting site of human Pex5 is critical for matrix protein import into peroxisomes. *J Biol Chem, 289*(1), 437-448. doi:10.1074/jbc.M113.499707

Ng, D. P. K., Salim, A., Liu, Y., Zou, L., Xu, F. G., Huang, S., . . . Ong, C. N. (2012). A metabolomic study of low estimated GFR in non-proteinuric type 2 diabetes mellitus. *Diabetologia, 55*(2), 499-508. doi:10.1007/s00125-011-2339-6

Ng, M., Fleming, T., Robinson, M., Thomson, B., Graetz, N., Margono, C., . . . Gakidou, E. (2014). Global, regional, and national prevalence of overweight and obesity in children and adults during 1980–2013: a systematic analysis for the Global Burden of Disease Study 2013. *The Lancet, 384*(9945), 766-781. doi:10.1016/s0140-6736(14)60460-8

NHFA. (2017). *Salt and heart healthy eating: position statement*. National Heart Foundation Australia: Melbourne: NHFA. Retrieved from https://www.heartfoundation.org.au/images/uploads/publications/Position_Statement_SaltHealthyEating.pdf

NHMRC. (2013a). *Australian Dietary Guidelines*. Canberra: National Health and Medical Research Council: Department of Health and Ageing. Retrieved from https://www.eatforhealth.gov.au/sites/default/files/files/the_guidelines/n55_australian_dietary_guidelines.pdf.

NHMRC, N. National Health and Medical Research Council. (2013b). *Clinical practice guidelines for the management of overweight and obesity in adults, adolescents and children in Australia*. National Health and Medical Research Council, Melbourne: Australian Government.

NHMRC, D. o. Health. (2017). *Nutrient Reference Values for Australia and New Zealand*. Canberra: Natinal Health and Medical Research Council Australian Government. Retrieved from https://www.nrv.gov.au/home.

Nigro, E., Scudiero, O., Monaco, M. L., Palmieri, A., Mazzarella, G., Costagliola, C., . . . Daniele, A. (2014). New insight into adiponectin role in obesity and obesity-related diseases. *Biomed Res Int, 2014*, 658913. doi:10.1155/2014/658913

Noakes, M., Keogh, J. B., Foster, P. R., & Clifton, P. M. (2005). Effect of an energy-restricted, high-protein, low-fat diet relative to a conventional high-carbohydrate, low-fat diet on weight loss, body composition, nutritional status, and markers of cardiovascular health in obese women. *Am J Clin Nutr, 81*(6), 1298-1306. doi:10.1093/ajcn/81.6.1298

Nuttall, J. M., Motley, A. M., & Hettema, E. H. (2014). Deficiency of the exportomer components Pex1, Pex6, and Pex15 causes enhanced pexophagy in Saccharomyces cerevisiae. *Autophagy, 10*(5), 835-845. doi:10.4161/auto.28259

Ogihara, T., Asano, T., Ando, K., Chiba, Y., Sekine, N., Sakoda, H., . . . Fujita, T. (2001). Insulin Resistance With Enhanced Insulin Signaling in High-Salt Diet-Fed Rats. *Diabetes, 50*(3), 573-583. doi:10.2337/diabetes.50.3.573

Oh, S. W., Koo, H. S., Han, K. H., Han, S. Y., & Chin, H. J. (2017). Associations of sodium intake with obesity, metabolic disorder, and albuminuria according to age. *PLoS One, 12*(12), e0188770. doi:10.1371/journal.pone.0188770

Oh, S. W., Mukhopadhyay, A., Svrzikapa, N., Jiang, F., Davis, R. J., & Tissenbaum, H. A. (2005). JNK regulates lifespan in Caenorhabditis elegans by modulating nuclear

translocation of forkhead transcription factor/DAF-16. *Proc Natl Acad Sci U S A, 102*(12), 4494-4499. doi:10.1073/pnas.0500749102
Oh, Y. B., Kim, J. H., Park, B. M., Park, B. H., & Kim, S. H. (2012). Captopril intake decreases body weight gain via angiotensin-(1-7). *Peptides, 37*(1), 79-85. doi:10.1016/j.peptides.2012.06.005
Ohno, H., Shinoda, K., Spiegelman, B. M., & Kajimura, S. (2012). PPARgamma agonists induce a white-to-brown fat conversion through stabilization of PRDM16 protein. *Cell Metab, 15*(3), 395-404. doi:10.1016/j.cmet.2012.01.019
Okla, M., Zaher, W., Alfayez, M., & Chung, S. (2018). Inhibitory Effects of Toll-Like Receptor 4, NLRP3 Inflammasome, and Interleukin-1beta on White Adipocyte Browning. *Inflammation, 41*(2), 626-642. doi:10.1007/s10753-017-0718-y
Olefsky, J. M. (2000). Treatment of insulin resistance with peroxisome proliferator-activated receptor gamma agonists. *J Clin Invest, 106*(4), 467-472. doi:10.1172/JCI10843
Ono, T., Kamimura, N., Matsuhashi, T., Nagai, T., Nishiyama, T., Endo, J., . . . Kaneda, R. (2017). The histone 3 lysine 9 methyltransferase inhibitor chaetocin improves prognosis in a rat model of high salt diet-induced heart failure. *Sci Rep, 7*, 39752. doi:10.1038/srep39752
Orci, L., Cook, W. S., Ravazzola, M., Wang, M. Y., Park, B. H., Montesano, R., & Unger, R. H. (2004). Rapid transformation of white adipocytes into fat-oxidizing machines. *Proc Natl Acad Sci U S A, 101*(7), 2058-2063. doi:10.1073/pnas.0308258100
Ortega-Prieto, P., & Postic, C. (2019). Carbohydrate Sensing Through the Transcription Factor ChREBP. *Front Genet, 10*, 472. doi:10.3389/fgene.2019.00472
Osgood, K., Krakoff, J., & Thearle, M. (2013). Serum uric acid predicts both current and future components of the metabolic syndrome. *Metab Syndr Relat Disord, 11*(3), 157-162. doi:10.1089/met.2012.0151
Otten, J., Stomby, A., Waling, M., Isaksson, A., Soderstrom, I., Ryberg, M., . . . Olsson, T. (2018). A heterogeneous response of liver and skeletal muscle fat to the combination of a Paleolithic diet and exercise in obese individuals with type 2 diabetes: a randomised controlled trial. *Diabetologia, 61*(7), 1548-1559. doi:10.1007/s00125-018-4618-y
Ouchi, N., & Walsh, K. (2007). Adiponectin as an anti-inflammatory factor. *Clin Chim Acta, 380*(1-2), 24-30. doi:10.1016/j.cca.2007.01.026
Ouedraogo, R., Wu, X., Xu, S. Q., Fuchsel, L., Motoshima, H., Mahadev, K., . . . Goldstein, B. J. (2006). Adiponectin suppression of high-glucose-induced reactive oxygen species in vascular endothelial cells: evidence for involvement of a cAMP signaling pathway. *Diabetes, 55*(6), 1840-1846. doi:10.2337/db05-1174
Pacher, P., & Mechoulam, R. (2011). Is lipid signaling through cannabinoid 2 receptors part of a protective system? *Progress in lipid research, 50*(2), 193-211. doi:10.1016/j.plipres.2011.01.001
Palgunow, D., Klapper, M., & Döring, F. (2012). Dietary restriction during development enlarges intestinal and hypodermal lipid droplets in Caenorhabditis elegans. *PLoS One, 7*(11), e46198. doi:10.1371/journal.pone.0046198
Panowski, S. H., Wolff, S., Aguilaniu, H., Durieux, J., & Dillin, A. (2007). PHA-4/Foxa mediates diet-restriction-induced longevity of C. elegans. *Nature, 447*(7144), 550-555. doi:10.1038/nature05837
Papatheodorou, I., Petrovs, R., & Thornton, J. M. (2014). Comparison of the mammalian insulin signalling pathway to invertebrates in the context of FOXO-mediated ageing. *Bioinformatics, 30*(21), 2999-3003. doi:10.1093/bioinformatics/btu493
Park, H., Kaushik, V. K., Constant, S., Prentki, M., Przybytkowski, E., Ruderman, N. B., & Saha, A. K. (2002). Coordinate regulation of malonyl-CoA decarboxylase, sn-glycerol-3-phosphate acyltransferase, and acetyl-CoA carboxylase by AMP-activated protein kinase in rat tissues in response to exercise. *J Biol Chem, 277*(36), 32571-32577. doi:10.1074/jbc.M201692200
Park, H. M., Park, K. T., Park, E. C., Kim, S. I., Choi, M. S., Liu, K. H., & Lee, C. H. (2017). Mass Spectrometry-Based Metabolomic and Lipidomic Analyses of the Effects of Dietary Platycodon grandiflorum on Liver and Serum of Obese Mice under a High-Fat Diet. *Nutrients, 9*(1). doi:10.3390/nu9010071

Park, J., Rho, H. K., Kim, K. H., Choe, S. S., Lee, Y. S., & Kim, J. B. (2005). Overexpression of glucose-6-phosphate dehydrogenase is associated with lipid dysregulation and insulin resistance in obesity. *Mol Cell Biol, 25*(12), 5146-5157. doi:10.1128/MCB.25.12.5146-5157.2005

Park, S., Sadanala, K. C., & Kim, E. K. (2015). A Metabolomic Approach to Understanding the Metabolic Link between Obesity and Diabetes. *Mol Cells, 38*(7), 587-596. doi:10.14348/molcells.2015.0126

Park, S. Y., Karki, S., Saggese, S. M., Zuriaga, M. A., Carmine, B., Hess, D., . . . Gokce, N. (2017). Angiotensin II-mediated vasoconstriction of the visceral adipose tissue vasculature is linked to systemic hypertension in obesity. *Faseb Journal, 31*(1_supplement), 684.686-684.686. doi:10.1096/fasebj.31.1_supplement.684.6

Patra, K. C., & Hay, N. (2014). The pentose phosphate pathway and cancer. *Trends Biochem Sci, 39*(8), 347-354. doi:10.1016/j.tibs.2014.06.005

Patrick, L. G. (2005). *An Introduction to Medicinal Chemistry (Third Edition)* (Vol. 6): Oxford University Press.

Paul, M., Wagner, J., & Dzau, V. J. (1993). Gene expression of the renin-angiotensin system in human tissues. Quantitative analysis by the polymerase chain reaction. *The Journal of Clinical Investigation, 91*(5), 2058-2064. doi:10.1172/JCI116428

Paz-Filho, G., Mastronardi, C. A., & Licinio, J. (2015). Leptin treatment: facts and expectations. *Metabolism, 64*(1), 146-156. doi:10.1016/j.metabol.2014.07.014

Pedrosa, A. G., Francisco, T., Bicho, D., Dias, A. F., Barros-Barbosa, A., Hagmann, V., . . . Azevedo, J. E. (2018). Peroxisomal monoubiquitinated PEX5 interacts with the AAA ATPases PEX1 and PEX6 and is unfolded during its dislocation into the cytosol. *J Biol Chem, 293*(29), 11553-11563. doi:10.1074/jbc.RA118.003669

Peraldi, P., & Spiegelman, B. (1998). TNF-alpha and insulin resistance: summary and future prospects. *Mol Cell Biochem, 182*(1-2), 169-175. doi:10.1023/A:1006865715292

Pereira, M. G., Souza, L. L., Becari, C., Duarte, D. A., Camacho, F. R., Oliveira, J. A., . . . Costa-Neto, C. M. (2013). Angiotensin II-independent angiotensin-(1-7) formation in rat hippocampus: involvement of thimet oligopeptidase. *Hypertension, 62*(5), 879-885. doi:10.1161/HYPERTENSIONAHA.113.01613

PHE, D. o. H. a. S. Care. (2018). *Calorie reduction: The scope and ambition for action*. London: Public Health England.

Pi-Sunyer, X., Astrup, A., Fujioka, K., Greenway, F., Halpern, A., Krempf, M., . . . Prediabetes, N. N. S. G. (2015). A Randomized, Controlled Trial of 3.0 mg of Liraglutide in Weight Management. *N Engl J Med, 373*(1), 11-22. doi:10.1056/NEJMoa1411892

Pigeyre, M., Yazdi, F. T., Kaur, Y., & Meyre, D. (2016). Recent progress in genetics, epigenetics and metagenomics unveils the pathophysiology of human obesity. *Clin Sci (Lond), 130*(12), 943-986. doi:10.1042/CS20160136

Platta, H. W., El Magraoui, F., Bäumer, B. E., Schlee, D., Girzalsky, W., & Erdmann, R. (2009). Pex2 and pex12 function as protein-ubiquitin ligases in peroxisomal protein import. *Mol Cell Biol, 29*(20), 5505-5516. doi:10.1128/MCB.00388-09

Poekes, L., Lanthier, N., & Leclercq, I. A. (2015). Brown adipose tissue: a potential target in the fight against obesity and the metabolic syndrome. *Clin Sci (Lond), 129*(11), 933-949. doi:10.1042/CS20150339

Porta-de-la-Riva, M., Fontrodona, L., Villanueva, A., & Ceron, J. (2012). Basic Caenorhabditis elegans methods: synchronization and observation. *J Vis Exp,* (64), e4019. doi:10.3791/4019

Portillo-Sanchez, P., Bril, F., Maximos, M., Lomonaco, R., Biernacki, D., Orsak, B., . . . Cusi, K. (2015). High Prevalence of Nonalcoholic Fatty Liver Disease in Patients With Type 2 Diabetes Mellitus and Normal Plasma Aminotransferase Levels. *J Clin Endocrinol Metab, 100*(6), 2231-2238. doi:10.1210/jc.2015-1966

Possik, E., Jalali, Z., Nouet, Y., Yan, M., Gingras, M. C., Schmeisser, K., . . . Pause, A. (2014). Folliculin regulates ampk-dependent autophagy and metabolic stress survival. *PLoS Genet, 10*(4), e1004273. doi:10.1371/journal.pgen.1004273

Postic, C., & Girard, J. (2008). Contribution of de novo fatty acid synthesis to hepatic steatosis and insulin resistance: lessons from genetically engineered mice. *J Clin Invest, 118*(3), 829-838. doi:10.1172/jci34275

Pouliot, M. C., Despres, J. P., Lemieux, S., Moorjani, S., Bouchard, C., Tremblay, A., . . . Lupien, P. J. (1994). Waist circumference and abdominal sagittal diameter: best simple anthropometric indexes of abdominal visceral adipose tissue accumulation and related cardiovascular risk in men and women. *Am J Cardiol, 73*(7), 460-468. doi:https://doi.org/10.1016/0002-9149(94)90676-9

Powles, J., Fahimi, S., Micha, R., Khatibzadeh, S., Shi, P., Ezzati, M., . . . Chronic Diseases Expert, G. (2013). Global, regional and national sodium intakes in 1990 and 2010: a systematic analysis of 24 h urinary sodium excretion and dietary surveys worldwide. *BMJ Open, 3*(12), e003733. doi:10.1136/bmjopen-2013-003733

Premaratna, S., Manickam, E., Begg, D., Rayment, D., Hafandi, A., Jois, M., . . . Weisinger, R. (2011). Angiotensin-converting enzyme inhibition reverses diet-induced obesity, insulin resistance and inflammation in C57BL/6J mice. *International journal of obesity, 36*(2), 233-243.

Premaratna, S. D., Manickam, E., Begg, D. P., Rayment, D. J., Hafandi, A., Jois, M., . . . Weisinger, R. S. (2012). Angiotensin-converting enzyme inhibition reverses diet-induced obesity, insulin resistance and inflammation in C57BL/6J mice. *International journal of obesity, 36*(2), 233-243. doi:10.1038/ijo.2011.95

PwC. (2015). *Weighing the cost of obesity: a case for action*. Retrieved from https://www.pwc.com.au/pdf/weighing-the-cost-of-obesity-final.pdf

Qi, Y., Takahashi, N., Hileman, S. M., Patel, H. R., Berg, A. H., Pajvani, U. B., . . . Ahima, R. S. (2004). Adiponectin acts in the brain to decrease body weight. *Nat Med, 10*(5), 524-529. doi:10.1038/nm1029

Qiu, F., & Zhang, Y. Q. (2019). Metabolic effects of mulberry branch bark powder on diabetic mice based on GC-MS metabolomics approach. *Nutr Metab (Lond), 16*(1), 10. doi:10.1186/s12986-019-0335-x

Qureshi, K., & Abrams, G. A. (2007). Metabolic liver disease of obesity and role of adipose tissue in the pathogenesis of nonalcoholic fatty liver disease. *World J Gastroenterol, 13*(26), 3540-3553. doi:10.3748/wjg.v13.i26.3540

Radcliffe, J. (2013). *TREATMENT OF OBESITY WITH ACE-INHIBITORY COMPOUNDS: EFFECTS OF CAPTOPRIL AND CULINARY HERBS AND SPICES, AND THE INTERACTION EFFECT WITH DIETARY SALT* (Agriculture, La Trobe University, Melbourne).

Raizen, D. M., Zimmerman, J. E., Maycock, M. H., Ta, U. D., You, Y.-j., Sundaram, M. V., & Pack, A. I. (2008). Lethargus is a Caenorhabditis elegans sleep-like state. *Nature, 451*, 569. doi:10.1038/nature06535

https://www.nature.com/articles/nature06535#supplementary-information

Ran, J., Hirano, T., & Adachi, M. (2004). Chronic ANG II infusion increases plasma triglyceride level by stimulating hepatic triglyceride production in rats. *Am J Physiol Endocrinol Metab, 287*(5), E955-961. doi:10.1152/ajpendo.00199.2004

Ran, J., Hirano, T., Fukui, T., Saito, K., Kageyama, H., Okada, K., & Adachi, M. (2006). Angiotensin II infusion decreases plasma adiponectin level via its type 1 receptor in rats: an implication for hypertension-related insulin resistance. *Metabolism, 55*(4), 478-488. doi:10.1016/j.metabol.2005.10.009

Rao, K. R., Lal, N., & Giridharan, N. V. (2014). Genetic & epigenetic approach to human obesity. *Indian J Med Res, 140*(5), 589-603. Retrieved from http://www.ncbi.nlm.nih.gov/pubmed/25579139

Ravinet Trillou, C., Delgorge, C., Menet, C., Arnone, M., & Soubrie, P. (2004). CB1 cannabinoid receptor knockout in mice leads to leanness, resistance to diet-induced obesity and enhanced leptin sensitivity. *Int J Obes Relat Metab Disord, 28*(4), 640-648. doi:10.1038/sj.ijo.0802583

Recinos, A., 3rd, Carr, B. K., Bartos, D. B., Boldogh, I., Carmical, J. R., Belalcazar, L. M., & Brasier, A. R. (2004). Liver gene expression associated with diet and lesion development

in atherosclerosis-prone mice: induction of components of alternative complement pathway. *Physiol Genomics, 19*(1), 131-142. doi:10.1152/physiolgenomics.00146.2003
Reddy, M. K., Baskaran, K., & Molteni, A. (1995). Inhibitors of Angiotensin-Converting Enzyme Modulate Mitosis and Gene Expression in Pancreatic Cancer Cells. *Proceedings of the Society for Experimental Biology and Medicine, 210*(3), 221-226. doi:10.3181/00379727-210-43942
Reinehr, T., Roth, C., Menke, T., & Andler, W. (2004). Adiponectin before and after Weight Loss in Obese Children. *The Journal of Clinical Endocrinology & Metabolism, 89*(8), 3790-3794. doi:10.1210/jc.2003-031925
Rena, G., Hardie, D. G., & Pearson, E. R. (2017). The mechanisms of action of metformin. *Diabetologia, 60*(9), 1577-1585. doi:10.1007/s00125-017-4342-z
Rodgers, R. J., Tschop, M. H., & Wilding, J. P. (2012). Anti-obesity drugs: past, present and future. *Dis Model Mech, 5*(5), 621-626. doi:10.1242/dmm.009621
Rohatgi, N., Nielsen, T. K., Bjørn, S. P., Axelsson, I., Paglia, G., Voldborg, B. G., . . . Rolfsson, O. (2014). Biochemical characterization of human gluconokinase and the proposed metabolic impact of gluconic acid as determined by constraint based metabolic network analysis. *PLoS One, 9*(6), e98760. doi:10.1371/journal.pone.0098760
Rollins, J. A., Howard, A. C., Dobbins, S. K., Washburn, E. H., & Rogers, A. N. (2017). Assessing Health Span in Caenorhabditis elegans: Lessons From Short-Lived Mutants. *J Gerontol A Biol Sci Med Sci, 72*(4), 473-480. doi:10.1093/gerona/glw248
Rolls, B. J., Hetherington, M., & Burley, V. J. (1988). The specificity of satiety: the influence of foods of different macronutrient content on the development of satiety. *Physiol Behav, 43*(2), 145-153. doi:https://doi.org/10.1016/0031-9384(88)90230-2
Rolls, B. J., Kim-Harris, S., Fischman, M. W., Foltin, R. W., Moran, T. H., & Stoner, S. A. (1994). Satiety after preloads with different amounts of fat and carbohydrate: implications for obesity. *Am J Clin Nutr, 60*(4), 476-487. doi:10.1093/ajcn/60.4.476
Rompe, F., Artuc, M., Hallberg, A., Alterman, M., Stroder, K., Thone-Reineke, C., . . . Steckelings, U. M. (2010). Direct angiotensin II type 2 receptor stimulation acts anti-inflammatory through epoxyeicosatrienoic acid and inhibition of nuclear factor kappaB. *Hypertension, 55*(4), 924-931. doi:10.1161/hypertensionaha.109.147843
Roncal, C. A., Reungjui, S., Sanchez-Lozada, L. G., Mu, W., Sautin, Y. Y., Nakagawa, T., & Johnson, R. J. (2009). Combination of captopril and allopurinol retards fructose-induced metabolic syndrome. *Am J Nephrol, 30*(5), 399-404. doi:10.1159/000235731
Rosa, G., Di Rocco, P., Manco, M., Greco, A. V., Castagneto, M., Vidal, H., & Mingrone, G. (2003). Reduced PDK4 expression associates with increased insulin sensitivity in postobese patients. *Obes Res, 11*(2), 176-182. doi:10.1038/oby.2003.28
Rosell, M., Kaforou, M., Frontini, A., Okolo, A., Chan, Y. W., Nikolopoulou, E., . . . Christian, M. (2014). Brown and white adipose tissues: intrinsic differences in gene expression and response to cold exposure in mice. *Am J Physiol Endocrinol Metab, 306*(8), E945-964. doi:10.1152/ajpendo.00473.2013
Rosen, E. D., & MacDougald, O. A. (2006). Adipocyte differentiation from the inside out. *Nat Rev Mol Cell Biol, 7*(12), 885-896. doi:10.1038/nrm2066
Roussel, E., Drolet, M. C., Lavigne, A. M., Arsenault, M., & Couet, J. (2018). Multiple short-chain dehydrogenases/reductases are regulated in pathological cardiac hypertrophy. *FEBS Open Bio, 8*(10), 1624-1635. doi:10.1002/2211-5463.12506
Ruan, H., & Dong, L. Q. (2016). Adiponectin signaling and function in insulin target tissues. *J Mol Cell Biol, 8*(2), 101-109. doi:10.1093/jmcb/mjw014
Ryden, M., Andersson, D. P., Bergstrom, I. B., & Arner, P. (2014). Adipose tissue and metabolic alterations: regional differences in fat cell size and number matter, but differently: a cross-sectional study. *J Clin Endocrinol Metab, 99*(10), E1870-1876. doi:10.1210/jc.2014-1526
Sabir, J. S. M., El Omri, A., Shaik, N. A., Banaganapalli, B., Hajrah, N. H., Zrelli, H., . . . Khan, M. (2019). The genetic association study of TP53 polymorphisms in Saudi obese patients. *Saudi Journal of Biological Sciences*. doi:10.1016/j.sjbs.2019.04.006
Sacerdoti, D., Singh, S. P., Schragenheim, J., Bellner, L., Vanella, L., Raffaele, M., . . . Abraham, N. G. (2018). Development of NASH in Obese Mice is Confounded by Adipose Tissue

Increase in Inflammatory NOV and Oxidative Stress. *Int J Hepatol, 2018*, 3484107. doi:10.1155/2018/3484107

Sacks, F. M., Bray, G. A., Carey, V. J., Smith, S. R., Ryan, D. H., Anton, S. D., . . . Williamson, D. A. (2009). Comparison of weight-loss diets with different compositions of fat, protein, and carbohydrates. *N Engl J Med, 360*(9), 859-873. doi:10.1056/NEJMoa0804748

Sacksteder, K. A., Morrell, J. C., Wanders, R. J., Matalon, R., & Gould, S. J. (1999). MCD encodes peroxisomal and cytoplasmic forms of malonyl-CoA decarboxylase and is mutated in malonyl-CoA decarboxylase deficiency. *J Biol Chem, 274*(35), 24461-24468. doi:10.1074/jbc.274.35.24461

Saha, A. K., Schwarsin, A. J., Roduit, R., Masse, F., Kaushik, V., Tornheim, K., . . . Ruderman, N. B. (2000). Activation of malonyl-CoA decarboxylase in rat skeletal muscle by contraction and the AMP-activated protein kinase activator 5-aminoimidazole-4-carboxamide-1-beta -D-ribofuranoside. *J Biol Chem, 275*(32), 24279-24283. doi:10.1074/jbc.C000291200

Sai, C., Yunhan, J., Zhao, J., Yu, Z., Yun, Z., Zhezhe, C., . . . Ruiyan, M. (2019). Cyclin Dependent Kinase 1 (CDK1) Activates Cardiac Fibroblasts via Directly Phosphorylating Paxillin at Ser244. *Int Heart J, 60*(2), 374-383. doi:10.1536/ihj.18-073

Saiki, A., Ohira, M., Endo, K., Koide, N., Oyama, T., Murano, T., . . . Shirai, K. (2009). Circulating angiotensin II is associated with body fat accumulation and insulin resistance in obese subjects with type 2 diabetes mellitus. *Metabolism, 58*(5), 708-713. doi:10.1016/j.metabol.2009.01.013

Sall, J., Pettersson, A. M., Bjork, C., Henriksson, E., Wasserstrom, S., Linder, W., . . . Goransson, O. (2017). Salt-inducible kinase 2 and -3 are downregulated in adipose tissue from obese or insulin-resistant individuals: implications for insulin signalling and glucose uptake in human adipocytes. *Diabetologia, 60*(2), 314-323. doi:10.1007/s00125-016-4141-y

Samuels-Lev, Y., O'Connor, D. J., Bergamaschi, D., Trigiante, G., Hsieh, J. K., Zhong, S., . . . Lu, X. (2001). ASPP proteins specifically stimulate the apoptotic function of p53. *Mol Cell, 8*(4), 781-794. doi:https://doi.org/10.1016/S1097-2765(01)00367-7

Sanchez-Lozada, L. G., Andres-Hernando, A., Garcia-Arroyo, F. E., Cicerchi, C., Li, N., Kuwabara, M., . . . Lanaspa, M. A. (2019). Uric acid activates aldose reductase and the polyol pathway for endogenous fructose and fat production causing development of fatty liver in rats. *J Biol Chem, 294*(11), 4272-4281. doi:10.1074/jbc.RA118.006158

Santamaria, A., Giordano, D., Corrado, F., Pintaudi, B., Interdonato, M. L., Vieste, G. D., . . . D'Anna, R. (2012). One-year effects of myo-inositol supplementation in postmenopausal women with metabolic syndrome. *Climacteric, 15*(5), 490-495. doi:10.3109/13697137.2011.631063

Santos, E. L., de Picoli Souza, K., da Silva, E. D., Batista, E. C., Martins, P. J., D'Almeida, V., & Pesquero, J. B. (2009). Long term treatment with ACE inhibitor enalapril decreases body weight gain and increases life span in rats. *Biochem Pharmacol, 78*(8), 951-958. doi:10.1016/j.bcp.2009.06.018

Santos, E. L., de Picoli Souza, K., Guimaraes, P. B., Reis, F. C., Silva, S. M., Costa-Neto, C. M., . . . Pesquero, J. B. (2008). Effect of angiotensin converting enzyme inhibitor enalapril on body weight and composition in young rats. *Int Immunopharmacol, 8*(2), 247-253. doi:10.1016/j.intimp.2007.07.021

Santos, F. L., Esteves, S. S., da Costa Pereira, A., Yancy, W. S., Jr., & Nunes, J. P. (2012). Systematic review and meta-analysis of clinical trials of the effects of low carbohydrate diets on cardiovascular risk factors. *Obes Rev, 13*(11), 1048-1066. doi:10.1111/j.1467-789X.2012.01021.x

Santos, R. A., Simoes e Silva, A. C., Maric, C., Silva, D. M., Machado, R. P., de Buhr, I., . . . Walther, T. (2003). Angiotensin-(1-7) is an endogenous ligand for the G protein-coupled receptor Mas. *Proc Natl Acad Sci U S A, 100*(14), 8258-8263. doi:10.1073/pnas.1432869100

Santos, S. H., Fernandes, L. R., Mario, E. G., Ferreira, A. V., Porto, L. C., Alvarez-Leite, J. I., . . . Santos, R. A. (2008). Mas deficiency in FVB/N mice produces marked changes in lipid and glycemic metabolism. *Diabetes, 57*(2), 340-347. doi:10.2337/db07-0953

Sartorius, K., Sartorius, B., Madiba, T. E., & Stefan, C. (2018). Does high-carbohydrate intake lead to increased risk of obesity? A systematic review and meta-analysis. *BMJ Open, 8*(2), e018449. doi:10.1136/bmjopen-2017-018449

Satapati, S., Sunny, N. E., Kucejova, B., Fu, X., He, T. T., Mendez-Lucas, A., . . . Burgess, S. C. (2012). Elevated TCA cycle function in the pathology of diet-induced hepatic insulin resistance and fatty liver. *J Lipid Res, 53*(6), 1080-1092. doi:10.1194/jlr.M023382

Schmelzer, K. R., Kubala, L., Newman, J. W., Kim, I. H., Eiserich, J. P., & Hammock, B. D. (2005). Soluble epoxide hydrolase is a therapeutic target for acute inflammation. *Proc Natl Acad Sci U S A, 102*(28), 9772-9777. doi:10.1073/pnas.0503279102

Schmieder, R. E., Hilgers, K. F., Schlaich, M. P., & Schmidt, B. M. (2007). Renin-angiotensin system and cardiovascular risk. *Lancet, 369*(9568), 1208-1219. doi:10.1016/S0140-6736(07)60242-6

Schmitt, E., Boutros, R., Froment, C., Monsarrat, B., Ducommun, B., & Dozier, C. (2006). CHK1 phosphorylates CDC25B during the cell cycle in the absence of DNA damage. *J Cell Sci, 119*(Pt 20), 4269-4275. doi:10.1242/jcs.03200

Schuchard, J., Winkler, M., Stolting, I., Schuster, F., Vogt, F. M., Barkhausen, J., . . . Raasch, W. (2015). Lack of weight gain after angiotensin AT1 receptor blockade in diet-induced obesity is partly mediated by an angiotensin-(1-7)/Mas-dependent pathway. *Br J Pharmacol, 172*(15), 3764-3778. doi:10.1111/bph.13172

Sechi, L. A., Griffin, C. A., Giacchetti, G., Valentin, J. P., Llorens-Cortes, C., Corvol, P., & Schambelan, M. (1996). Tissue-specific regulation of type 1 angiotensin II receptor mRNA levels in the rat. *Hypertension, 28*(3), 403-408.

Seiler, S. E., Martin, O. J., Noland, R. C., Slentz, D. H., DeBalsi, K. L., Ilkayeva, O. R., . . . Muoio, D. M. (2014). Obesity and lipid stress inhibit carnitine acetyltransferase activity. *J Lipid Res, 55*(4), 635-644. doi:10.1194/jlr.M043448

Seip, R. L., Volek, J. S., Windemuth, A., Kocherla, M., Fernandez, M. L., Kraemer, W. J., & Ruano, G. (2008). Physiogenomic comparison of human fat loss in response to diets restrictive of carbohydrate or fat. *Nutr Metab (Lond), 5*, 4. doi:10.1186/1743-7075-5-4

Seok, H., Sohn, T. S., & Son, H. S. (2014). Po352 Raas Blockades Modulate Glucose-Stimulated Angiotensin Ii Expression in 3t3-L1 Adipocyte. *Diabetes Research and Clinical Practice, 106*, S227. doi:10.1016/s0168-8227(14)70646-1

Shearer, J., Duggan, G., Weljie, A., Hittel, D. S., Wasserman, D. H., & Vogel, H. J. (2008). Metabolomic profiling of dietary-induced insulin resistance in the high fat-fed C57BL/6J mouse. *Diabetes Obes Metab, 10*(10), 950-958. doi:10.1111/j.1463-1326.2007.00837.x

Shenoy, S. K., & Lefkowitz, R. J. (2005). Angiotensin II-stimulated signaling through G proteins and beta-arrestin. *Sci STKE, 2005*(311), cm14. doi:10.1126/stke.3112005cm14

Shimada, M., Hibino, M., & Takeshita, A. (2017). Dietary supplementation with myo-inositol reduces hepatic triglyceride accumulation and expression of both fructolytic and lipogenic genes in rats fed a high-fructose diet. *Nutr Res, 47*, 21-27. doi:10.1016/j.nutres.2017.08.005

Shimoura, C. G., Lincevicius, G. S., Nishi, E. E., Girardi, A. C., Simon, K. A., Bergamaschi, C. T., & Campos, R. R. (2017). Increased Dietary Salt Changes Baroreceptor Sensitivity and Intrarenal Renin-Angiotensin System in Goldblatt Hypertension. *Am J Hypertens, 30*(1), 28-36. doi:10.1093/ajh/hpw107

Shrago, E., Glennon, J. A., & Gordon, E. S. (1971). Comparative aspects of lipogenesis in mammalian tissues. *Metabolism, 20*(1), 54-62. doi:https://doi.org/10.1016/0026-0495(71)90059-X

Shtonda, B. B., & Avery, L. (2006). Dietary choice behavior in Caenorhabditis elegans. *J Exp Biol, 209*(Pt 1), 89-102. doi:10.1242/jeb.01955

Shurubor, Y. I., D'Aurelio, M., Clark-Matott, J., Isakova, E. P., Deryabina, Y. I., Beal, M. F., . . . Krasnikov, B. F. (2017). Determination of Coenzyme A and Acetyl-Coenzyme A in Biological Samples Using HPLC with UV Detection. *Molecules, 22*(9). doi:10.3390/molecules22091388

Simoes e Silva, A. C., Silveira, K. D., Ferreira, A. J., & Teixeira, M. M. (2013). ACE2, angiotensin-(1-7) and Mas receptor axis in inflammation and fibrosis. *Br J Pharmacol, 169*(3), 477-492. doi:10.1111/bph.12159

Simões, E. S. A. C., Miranda, A. S., Rocha, N. P., & Teixeira, A. L. (2017). Renin angiotensin system in liver diseases: Friend or foe? *World J Gastroenterol, 23*(19), 3396-3406. doi:10.3748/wjg.v23.i19.3396

Singh, V. P., Le, B., Bhat, V. B., Baker, K. M., & Kumar, R. (2007). High-glucose-induced regulation of intracellular ANG II synthesis and nuclear redistribution in cardiac myocytes. *Am J Physiol Heart Circ Physiol, 293*(2), H939-948. doi:10.1152/ajpheart.00391.2007

Sjostrom, L., Narbro, K., Sjostrom, C. D., Karason, K., Larsson, B., Wedel, H., . . . Swedish Obese Subjects, S. (2007). Effects of bariatric surgery on mortality in Swedish obese subjects. *N Engl J Med, 357*(8), 741-752. doi:10.1056/NEJMoa066254

Slamkova, M., Zorad, S., & Krskova, K. (2016). Alternative renin-angiotensin system pathways in adipose tissue and their role in the pathogenesis of obesity. *Endocr Regul, 50*(4), 229-240. doi:10.1515/enr-2016-0025

Smith, K. J., McNaughton, S. A., Gall, S. L., Blizzard, L., Dwyer, T., & Venn, A. J. (2009). Takeaway food consumption and its associations with diet quality and abdominal obesity: a cross-sectional study of young adults. *Int J Behav Nutr Phys Act, 6*(1), 29. doi:10.1186/1479-5868-6-29

Snyder, H. S., Sakaan, S. A., March, K. L., Siddique, O., Cholankeril, R., Cummings, C. D., . . . Cholankeril, G. (2018). Non-alcoholic Fatty Liver Disease: A Review of Anti-diabetic Pharmacologic Therapies. *J Clin Transl Hepatol, 6*(2), 168-174. doi:10.14218/JCTH.2017.00050

Song, Z., Xiaoli, A. M., & Yang, F. (2018). Regulation and Metabolic Significance of De Novo Lipogenesis in Adipose Tissues. *Nutrients, 10*(10), 1383. doi:10.3390/nu10101383

Spreadbury, I. (2012). Comparison with ancestral diets suggests dense acellular carbohydrates promote an inflammatory microbiota, and may be the primary dietary cause of leptin resistance and obesity. *Diabetes Metab Syndr Obes, 5*, 175-189. doi:10.2147/DMSO.S33473

Sprenger, G. A., Schorken, U., Sprenger, G., & Sahm, H. (1995). Transketolase A of Escherichia coli K12. Purification and properties of the enzyme from recombinant strains. *Eur J Biochem, 230*(2), 525-532.

Springer, S. C., Silverstein, J., Copeland, K., Moore, K. R., Prazar, G. E., Raymer, T., . . . American Academy of, P. (2013). Management of type 2 diabetes mellitus in children and adolescents. *Pediatrics, 131*(2), e648-664. doi:10.1542/peds.2012-3496

Standeven, K. F., Hess, K., Carter, A. M., Rice, G. I., Cordell, P. A., Balmforth, A. J., . . . Grant, P. J. (2011). Neprilysin, obesity and the metabolic syndrome. *International journal of obesity (2005), 35*(8), 1031-1040. doi:10.1038/ijo.2010.227

Stanley, T. K. (2013). *Prevention and Reversal of Diet Induced Obesity in C57BL/6J Mice by Captopril* (La Trobe University, Melbourne).

Starodub, N. F., & Samokhina, L. M. (2013). The activities of endothelial elastase and cathepsin G in rats at oxidative stress caused by heavy metals salts. *Advances in Biological Chemistry, 03*(02), 208-214. doi:10.4236/abc.2013.32026

Steffen, L. M., Dai, S., Fulton, J. E., & Labarthe, D. R. (2009). Overweight in children and adolescents associated with TV viewing and parental weight: Project HeartBeat! *Am J Prev Med, 37*(1 Suppl), S50-55. doi:10.1016/j.amepre.2009.04.017

Stegbauer, J., & Coffman, T. M. (2011). New insights into angiotensin receptor actions: from blood pressure to aging. *Curr Opin Nephrol Hypertens, 20*(1), 84-88. doi:10.1097/MNH.0b013e3283414d40

Stetten, M. R., & Topper, Y. J. (1953). Pathways from gluconic acid to glucose in vivo. *J Biol Chem, 203*(2), 653-664.

Stincone, A., Prigione, A., Cramer, T., Wamelink, M. M. C., Campbell, K., Cheung, E., . . . Ralser, M. (2015). The return of metabolism: biochemistry and physiology of the pentose phosphate pathway. *Biological reviews of the Cambridge Philosophical Society, 90*(3), 927-963. doi:10.1111/brv.12140

Strable, M. S., & Ntambi, J. M. (2010). Genetic control of de novo lipogenesis: role in diet-induced obesity. *Crit Rev Biochem Mol Biol, 45*(3), 199-214. doi:10.3109/10409231003667500

Strazzullo, P., & Galletti, F. (2004). Impact of the renin–angiotensin system on lipid and carbohydrate metabolism. *Current Opinion in Nephrology and Hypertension, 13*, 325–332. doi:10.1097/01.mnh.0000126799.46712.ae

Stubbs, J., Ferres, S., & Horgan, G. (2000). Energy density of foods: effects on energy intake. *Crit Rev Food Sci Nutr, 40*(6), 481-515. doi:10.1080/10408690091189248

Sun, J., Luo, J., Ruan, Y., Xiu, L., Fang, B., Zhang, H., . . . Chen, H. (2016). Free Fatty Acids Activate Renin-Angiotensin System in 3T3-L1 Adipocytes through Nuclear Factor-kappa B Pathway. *J Diabetes Res, 2016*, 1587594. doi:10.1155/2016/1587594

Sun, W., Alexander, T., Man, Z., Xiao, F., Cui, F., & Qi, X. (2018). Enhancing 2-Ketogluconate Production of Pseudomonas plecoglossicida JUIM01 by Maintaining the Carbon Catabolite Repression of 2-Ketogluconate Metabolism. *Molecules, 23*(10), 2629. doi:10.3390/molecules23102629

Sutphin, G. L., & Kaeberlein, M. (2009). Measuring Caenorhabditis elegans life span on solid media. *J Vis Exp*, (27), 1152. doi:10.3791/1152

Swartz, S. L., Williams, G. H., Hollenberg, N. K., Levine, L., Dluhy, R. G., & Moore, T. J. (1980). Captopril-induced changes in prostaglandin production: relationship to vascular responses in normal man. *J Clin Invest, 65*(6), 1257-1264. doi:10.1172/JCI109788

Szklarczyk, D., Gable, A. L., Lyon, D., Junge, A., Wyder, S., Huerta-Cepas, J., . . . Mering, C. V. (2019). STRING v11: protein-protein association networks with increased coverage, supporting functional discovery in genome-wide experimental datasets. *Nucleic Acids Res, 47*(D1), D607-d613. doi:10.1093/nar/gky1131

Tabbi-Anneni, I., Buchanan, J., Cooksey, R. C., & Abel, E. D. (2008). Captopril normalizes insulin signaling and insulin-regulated substrate metabolism in obese (ob/ob) mouse hearts. *Endocrinology, 149*(8), 4043-4050. doi:10.1210/en.2007-1646

Takamura, T., Misu, H., Matsuzawa-Nagata, N., Sakurai, M., Ota, T., Shimizu, A., . . . Kaneko, S. (2008). Obesity Upregulates Genes Involved in Oxidative Phosphorylation in Livers of Diabetic Patients. *Obesity, 16*(12), 2601-2609. doi:10.1038/oby.2008.419

Takamura, T., Misu, H., Matsuzawa-Nagata, N., Sakurai, M., Ota, T., Shimizu, A., . . . Kaneko, S. (2008). Obesity upregulates genes involved in oxidative phosphorylation in livers of diabetic patients. *Obesity (Silver Spring), 16*(12), 2601-2609. doi:10.1038/oby.2008.419

Takeshita, Y., Takamura, T., Ando, H., Hamaguchi, E., Takazakura, A., Matsuzawa-Nagata, N., & Kaneko, S. (2008). Cross talk of tumor necrosis factor-alpha and the renin-angiotensin system in tumor necrosis factor-alpha-induced plasminogen activator inhibitor-1 production from hepatocytes. *Eur J Pharmacol, 579*(1-3), 426-432. doi:10.1016/j.ejphar.2007.11.016

Takizawa, C. G., & Morgan, D. O. (2000). Control of mitosis by changes in the subcellular location of cyclin-B1-Cdk1 and Cdc25C. *Curr Opin Cell Biol, 12*(6), 658-665.

Tamura, K., Chiba, E., Yokoyama, N., Sumida, Y., Yabana, M., Tamura, N., . . . Umemura. (1999). Renin–angiotensin system and fibronectin gene expression in Dahl Iwai salt-sensitive and salt-resistant rats. *Hypertension, 17*(1), 81-89.

Tanimoto, K., Sugiyama, F., Goto, Y., Ishida, J., Takimoto, E., Yagami, K., . . . Murakami, K. (1994). Angiotensinogen-deficient mice with hypotension. *J Biol Chem, 269*(50), 31334-31337.

Tanner, C. J., Barakat, H. A., Dohm, G. L., Pories, W. J., MacDonald, K. G., Cunningham, P. R., . . . Houmard, J. A. (2002). Muscle fiber type is associated with obesity and weight loss. *Am J Physiol Endocrinol Metab, 282*(6), E1191-1196. doi:10.1152/ajpendo.00416.2001

Tappy, L. (2018). Fructose-containing caloric sweeteners as a cause of obesity and metabolic disorders. *J Exp Biol, 221*(Pt Suppl 1). doi:10.1242/jeb.164202

Taskin, E., & Guven, C. (2017). Local Renin-Angiotensin System at Liver and Crosstalk with Hepatic Diseases. In *Renin-Angiotensin System - Past, Present and Future*. doi:10.5772/65919

Te Morenga, L., Mallard, S., & Mann, J. (2012). Dietary sugars and body weight: systematic review and meta-analyses of randomised controlled trials and cohort studies. *BMJ, 346*, e7492. doi:10.1136/bmj.e7492

Tejesvi, M. V., Kini, K. R., Prakash, H. S., Subbiah, V., & Shetty, H. S. (2008). Antioxidant, antihypertensive, and antibacterial properties of endophytic Pestalotiopsis species from

medicinal plants. *Canadian Journal of Microbiology, 54*(9), 769-780. doi:10.1139/W08-070

Tencerova, M., Aouadi, M., Vangala, P., Nicoloro, S. M., Yawe, J. C., Cohen, J. L., . . . Czech, M. P. (2015). Activated Kupffer cells inhibit insulin sensitivity in obese mice. *FASEB J, 29*(7), 2959-2969. doi:10.1096/fj.15-270496

Than, A., Xu, S., Li, R., Leow, M. K., Sun, L., & Chen, P. (2017). Angiotensin type 2 receptor activation promotes browning of white adipose tissue and brown adipogenesis. *Signal Transduct Target Ther, 2*, 17022. doi:10.1038/sigtrans.2017.22

Timmons, J. A., Wennmalm, K., Larsson, O., Walden, T. B., Lassmann, T., Petrovic, N., . . . Cannon, B. (2007). Myogenic gene expression signature establishes that brown and white adipocytes originate from distinct cell lineages. *Proc Natl Acad Sci U S A, 104*(11), 4401-4406. doi:10.1073/pnas.0610615104

Timofeev, O., Cizmecioglu, O., Settele, F., Kempf, T., & Hoffmann, I. (2010). Cdc25 phosphatases are required for timely assembly of CDK1-cyclin B at the G2/M transition. *J Biol Chem, 285*(22), 16978-16990. doi:10.1074/jbc.M109.096552

Tipnis, S. R., Hooper, N. M., Hyde, R., Karran, E., Christie, G., & Turner, A. J. (2000). A human homolog of angiotensin-converting enzyme. Cloning and functional expression as a captopril-insensitive carboxypeptidase. *J Biol Chem, 275*(43), 33238-33243. doi:10.1074/jbc.M002615200

Torlone, E., Rambotti, A. M., Perriello, G., Botta, G., Santeusanio, F., Brunetti, P., & Bolli, G. B. (1991). ACE-inhibition increases hepatic and extrahepatic sensitivity to insulin in patients with Type 2 (non-insulin-dependent) diabetes mellitus and arterial hypertension. *Diabetologia, 34*(2), 119-125. doi:10.1007/BF00500383

Traversy, G., & Chaput, J. P. (2015). Alcohol Consumption and Obesity: An Update. *Curr Obes Rep, 4*(1), 122-130. doi:10.1007/s13679-014-0129-4

Tsouko, E., Khan, A. S., White, M. A., Han, J. J., Shi, Y., Merchant, F. A., . . . Frigo, D. E. (2014). Regulation of the pentose phosphate pathway by an androgen receptor–mTOR-mediated mechanism and its role in prostate cancer cell growth. *Oncogenesis, 3*, e103. doi:10.1038/oncsis.2014.18

https://www.nature.com/articles/oncsis201418#supplementary-information

Tsuchiya, K., Yoshimoto, T., Hirono, Y., Tateno, T., Sugiyama, T., & Hirata, Y. (2006). Angiotensin II induces monocyte chemoattractant protein-1 expression via a nuclear factor-kappaB-dependent pathway in rat preadipocytes. *Am J Physiol Endocrinol Metab, 291*(4), E771-778. doi:10.1152/ajpendo.00560.2005

Tsukuda, K., Mogi, M., Iwanami, J., Kanno, H., Nakaoka, H., Wang, X. L., . . . Horiuchi, M. (2016). Enhancement of Adipocyte Browning by Angiotensin II Type 1 Receptor Blockade. *PLoS One, 11*(12), e0167704. doi:10.1371/journal.pone.0167704

Tullet, J. M., Araiz, C., Sanders, M. J., Au, C., Benedetto, A., Papatheodorou, I., . . . Gems, D. (2014). DAF-16/FoxO directly regulates an atypical AMP-activated protein kinase gamma isoform to mediate the effects of insulin/IGF-1 signaling on aging in Caenorhabditis elegans. *PLoS Genet, 10*(2), e1004109. doi:10.1371/journal.pgen.1004109

Turner, A. J., & Hooper, N. M. (2002). The angiotensin–converting enzyme gene family: genomics and pharmacology. *Trends in Pharmacological Sciences, 23*(4), 177-183. doi:10.1016/s0165-6147(00)01994-5

Uehara, M., Kishikawa, H., Isami, S., Kisanuki, K., Ohkubo, Y., Miyamura, N., . . . Shichiri, M. (1994). Effect on insulin sensitivity of angiotensin converting enzyme inhibitors with or without a sulphydryl group: bradykinin may improve insulin resistance in dogs and humans. *Diabetologia, 37*(3), 300-307. Retrieved from http://www.ncbi.nlm.nih.gov/pubmed/8174845

Uetake, Y., Ikeda, H., Irie, R., Tejima, K., Matsui, H., Ogura, S., . . . Shimosawa, T. (2015). High-salt in addition to high-fat diet may enhance inflammation and fibrosis in liver steatosis induced by oxidative stress and dyslipidemia in mice. *Lipids Health Dis, 14*, 6. doi:10.1186/s12944-015-0002-9

Umemura, S., Nyui, N., Tamura, K., Hibi, K., Yamaguchi, S., Nakamaru, M., . . . Ishii, M. (1997). Plasma angiotensinogen concentrations in obese patients. *Am J Hypertens, 10*(6), 629-633. doi:10.1016/s0895-7061(97)00053-8

Unger, R. H., & Orci, L. (2002). Lipoapoptosis: its mechanism and its diseases. *Biochim Biophys Acta, 1585*(2-3), 202-212. doi:10.1016/s1388-1981(02)00342-6

USDA. (2002). *Dietary reference intakes for energy, carbohydrate, fiber, fat, fatty acids, cholesterol, protein, and amino acids (macronutrients)*. Washington, DC: Institute of Medicine, Food and Nutrition Board: National Academy Press.

Valenti, L., Fracanzani, A. L., Dongiovanni, P., Santorelli, G., Branchi, A., Taioli, E., . . . Fargion, S. (2002). Tumor necrosis factor alpha promoter polymorphisms and insulin resistance in nonalcoholic fatty liver disease. *Gastroenterology, 122*(2), 274-280. doi:10.1053/gast.2002.31065

Van Gilst, M. R., Hadjivassiliou, H., Jolly, A., & Yamamoto, K. R. (2005). Nuclear hormone receptor NHR-49 controls fat consumption and fatty acid composition in C. elegans. *PLoS Biol, 3*(2), e53. doi:10.1371/journal.pbio.0030053

van Harmelen, V., Elizalde, M., Ariapart, P., Bergstedt-Lindqvist, S., Reynisdottir, S., Hoffstedt, J., . . . Arner, P. (2000). The association of human adipose angiotensinogen gene expression with abdominal fat distribution in obesity. *Int J Obes Relat Metab Disord, 24*(6), 673-678.

Vandelanotte, C., Sugiyama, T., Gardiner, P., & Owen, N. (2009). Associations of leisure-time internet and computer use with overweight and obesity, physical activity and sedentary behaviors: cross-sectional study. *J Med Internet Res, 11*(3), e28. doi:10.2196/jmir.1084

Vapola, M. H., Rokka, A., Sormunen, R. T., Alhonen, L., Schmitz, W., Conzelmann, E., . . . Hiltunen, J. K. (2014). Peroxisomal membrane channel Pxmp2 in the mammary fat pad is essential for stromal lipid homeostasis and for development of mammary gland epithelium in mice. *Developmental Biology, 391*(1), 66-80. doi:https://doi.org/10.1016/j.ydbio.2014.03.022

Vatner, D. F., Majumdar, S. K., Kumashiro, N., Petersen, M. C., Rahimi, Y., Gattu, A. K., . . . Shulman, G. I. (2015). Insulin-independent regulation of hepatic triglyceride synthesis by fatty acids. *Proceedings of the National Academy of Sciences, 112*(4), 1143. doi:10.1073/pnas.1423952112

Veilleux, A., Caron-Jobin, M., Noel, S., Laberge, P. Y., & Tchernof, A. (2011). Visceral adipocyte hypertrophy is associated with dyslipidemia independent of body composition and fat distribution in women. *Diabetes, 60*(5), 1504-1511. doi:10.2337/db10-1039

Veldhorst, M. A., Nieuwenhuizen, A. G., Hochstenbach-Waelen, A., Westerterp, K. R., Engelen, M. P., Brummer, R. J., . . . Westerterp-Plantenga, M. S. (2009). Effects of high and normal soyprotein breakfasts on satiety and subsequent energy intake, including amino acid and 'satiety' hormone responses. *Eur J Nutr, 48*(2), 92-100. doi:10.1007/s00394-008-0767-y

Verhoeven, N. M., Huck, J. H., Roos, B., Struys, E. A., Salomons, G. S., Douwes, A. C., . . . Jakobs, C. (2001). Transaldolase deficiency: liver cirrhosis associated with a new inborn error in the pentose phosphate pathway. *American journal of human genetics, 68*(5), 1086-1092. doi:10.1086/320108

Villarroya, F., Cereijo, R., Gavalda-Navarro, A., Villarroya, J., & Giralt, M. (2018). Inflammation of brown/beige adipose tissues in obesity and metabolic disease. *J Intern Med, 284*(5), 492-504. doi:10.1111/joim.12803

Vrablik, T. L., Petyuk, V. A., Larson, E. M., Smith, R. D., & Watts, J. L. (2015). Lipidomic and proteomic analysis of Caenorhabditis elegans lipid droplets and identification of ACS-4 as a lipid droplet-associated protein. *Biochim Biophys Acta, 1851*(10), 1337-1345. doi:10.1016/j.bbalip.2015.06.004

Wadden, T. A., Berkowitz, R. I., Sarwer, D. B., Prus-Wisniewski, R., & Steinberg, C. (2001). Benefits of lifestyle modification in the pharmacologic treatment of obesity: a randomized trial. *Arch Intern Med, 161*(2), 218-227. doi:10.1001/archinte.161.2.218

Wahlby, C., Conery, A. L., Bray, M. A., Kamentsky, L., Larkins-Ford, J., Sokolnicki, K. L., . . . O'Rourke, E. J. (2014). High- and low-throughput scoring of fat mass and body fat distribution in C. elegans. *Methods, 68*(3), 492-499. doi:10.1016/j.ymeth.2014.04.017

Wamelink, M. M., Struys, E. A., & Jakobs, C. (2008). The biochemistry, metabolism and inherited defects of the pentose phosphate pathway: a review. *J Inherit Metab Dis, 31*(6), 703-717. doi:10.1007/s10545-008-1015-6

Wang, L., Hou, E., Wang, Z., Sun, N., He, L., Chen, L., . . . Tian, Z. (2014). Analysis of metabolites in plasma reveals distinct metabolic features between Dahl salt-sensitive rats and consomic SS.13(BN) rats. *Biochemical and biophysical research communications, 450*(1), 863-869. doi:10.1016/j.bbrc.2014.06.089

Wang, L., Lv, Y., Yao, H., Yin, L., & Shang, J. (2015). Curcumin prevents the non-alcoholic fatty hepatitis via mitochondria protection and apoptosis reduction. *Int J Clin Exp Pathol, 8*(9), 11503-11509. Retrieved from https://www.ncbi.nlm.nih.gov/pubmed/26617882

Wang, L., Manson, J. E., Gaziano, J. M., Liu, S., Cochrane, B., Cook, N. R., . . . Sesso, H. D. (2012). Plasma adiponectin and the risk of hypertension in white and black postmenopausal women. *Clin Chem, 58*(10), 1438-1445. doi:10.1373/clinchem.2012.191080

Wang, M., Xu, Y., Liu, J., Ye, J., Yuan, W., Jiang, H., . . . Wan, J. (2017). Recent Insights into the Biological Functions of Sestrins in Health and Disease. *Cellular Physiology and Biochemistry, 43*(5), 1731-1741. doi:10.1159/000484060

Wang, M. Y., Lee, Y., & Unger, R. H. (1999). Novel form of lipolysis induced by leptin. *J Biol Chem, 274*(25), 17541-17544. doi:10.1074/jbc.274.25.17541

Wang, R. F., Wang, X. B., & Zhuang, L. W. (2016). Gene expression profiling reveals key genes and pathways related to the development of non-alcoholic fatty liver disease. *Annals of Hepatology, 15*(2), 190-199. doi:10.5604/16652681.1193709

Wang, S., Pan, M. H., Hung, W. L., Tung, Y. C., & Ho, C. T. (2019). From white to beige adipocytes: therapeutic potential of dietary molecules against obesity and their molecular mechanisms. *Food Funct, 10*(3), 1263-1279. doi:10.1039/c8fo02154f

Wang, Y., Chu, C., Wang, K. K., Hu, J. W., Yan, Y., Lv, Y. B., . . . Mu, J. J. (2018). Effect of Salt Intake on Plasma and Urinary Uric Acid Levels in Chinese Adults: An Interventional Trial. *Sci Rep, 8*(1), 1434. doi:10.1038/s41598-018-20048-2

Wang, Y., Liu, X., Zhang, C., & Wang, Z. (2018). High salt diet induces metabolic alterations in multiple biological processes of Dahl salt-sensitive rats. *J Nutr Biochem, 56*, 133-141. doi:10.1016/j.jnutbio.2018.01.007

Watanabe, G., Lee, R. J., Albanese, C., Rainey, W. E., Batlle, D., & Pestell, R. G. (1996). Angiotensin II activation of cyclin D1-dependent kinase activity. *J Biol Chem, 271*(37), 22570-22577. doi:10.1074/jbc.271.37.22570

Webber, J. (2003). Energy balance in obesity. *Proc Nutr Soc, 62*(2), 539-543.

Weidemann, B. J., Voong, S., Morales-Santiago, F. I., Kahn, M. Z., Ni, J., Littlejohn, N. K., . . . Grobe, J. L. (2015). Dietary Sodium Suppresses Digestive Efficiency via the Renin-Angiotensin System. *Sci Rep, 5*, 11123. doi:10.1038/srep11123

Weinkove, D., Halstead, J. R., Gems, D., & Divecha, N. (2006). Long-term starvation and ageing induce AGE-1/PI 3-kinase-dependent translocation of DAF-16/FOXO to the cytoplasm. *BMC Biol, 4*(1), 1. doi:10.1186/1741-7007-4-1

Weisinger, R. S., Stanley, T. K., Begg, D. P., Weisinger, H. S., Spark, K. J., & Jois, M. (2009). Angiotensin converting enzyme inhibition lowers body weight and improves glucose tolerance in C57BL/6J mice maintained on a high fat diet. *Physiol Behav, 98*(1-2), 192-197. doi:10.1016/j.physbeh.2009.05.009

Weiss, R., Bremer, A. A., & Lustig, R. H. (2013). What is metabolic syndrome, and why are children getting it? *Ann N Y Acad Sci, 1281*(1), 123-140. doi:10.1111/nyas.12030

Weller, S., Gould, S. J., & Valle, D. (2003). Peroxisome biogenesis disorders. *Annu Rev Genomics Hum Genet, 4*(1), 165-211. doi:10.1146/annurev.genom.4.070802.110424

Wells, J. C. (2012). The evolution of human adiposity and obesity: where did it all go wrong? *Dis Model Mech, 5*(5), 595-607. doi:10.1242/dmm.009613

Westin, M. A., Hunt, M. C., & Alexson, S. E. (2008). Short- and medium-chain carnitine acyltransferases and acyl-CoA thioesterases in mouse provide complementary systems for transport of beta-oxidation products out of peroxisomes. *Cell Mol Life Sci, 65*(6), 982-990. doi:10.1007/s00018-008-7576-6

Weyer, C., Funahashi, T., Tanaka, S., Hotta, K., Matsuzawa, Y., Pratley, R. E., & Tataranni, P. A. (2001). Hypoadiponectinemia in obesity and type 2 diabetes: close association with insulin resistance and hyperinsulinemia. *J Clin Endocrinol Metab, 86*(5), 1930-1935. doi:10.1210/jcem.86.5.7463

WHO. (2015). *Guidelines: Sugar intake for adults and children*. Geneva: World Health Organization.
WHO. (2018, 10/07/2018). *Obesity and Overweight*. Retrieved from http://www.who.int/news-room/fact-sheets/detail/obesity-and-overweight
Wilkin, T. J., & Voss, L. D. (2004). Metabolic syndrome: maladaptation to a modern world. *J R Soc Med, 97*(11), 511-520. doi:10.1258/jrsm.97.11.511
Willcox, B. J., Donlon, T. A., He, Q., Chen, R., Grove, J. S., Yano, K., . . . Curb, J. D. (2008). FOXO3A genotype is strongly associated with human longevity. *Proc Natl Acad Sci U S A, 105*(37), 13987-13992. doi:10.1073/pnas.0801030105
William, W. N., Jr., Ceddia, R. B., & Curi, R. (2002). Leptin controls the fate of fatty acids in isolated rat white adipocytes. *J Endocrinol, 175*(3), 735-744. doi:10.1677/joe.0.1750735
Williamson, J. R. (1966). Mechanism for the stimulation in vivo of hepatic gluconeogenesis by glucagon. *Biochem J, 101*(1), 11c-14c. doi:10.1042/bj1010011c
Winkler, M., Schuchard, J., Stolting, I., Vogt, F. M., Barkhausen, J., Thorns, C., . . . Raasch, W. (2016). The brain renin-angiotensin system plays a crucial role in regulating body weight in diet-induced obesity in rats. *Br J Pharmacol, 173*(10), 1602-1617. doi:10.1111/bph.13461
Wolf, G., & Wenzel, U. O. (2004). Angiotensin II and cell cycle regulation. *Hypertension, 43*(4), 693-698. doi:10.1161/01.HYP.0000120963.09029.ca
Wree, A., Kahraman, A., Gerken, G., & Canbay, A. (2011). Obesity Affects the Liver – The Link between Adipocytes and Hepatocytes. *Digestion, 83*(1-2), 124-133. doi:10.1159/000318741
Wu, C., Xu, Y., Lu, H., Howatt, D. A., Balakrishnan, A., Moorleghen, J. J., . . . Daugherty, A. (2015). Cys18-Cys137 disulfide bond in mouse angiotensinogen does not affect AngII-dependent functions in vivo. *Hypertension, 65*(4), 800-805. doi:10.1161/hypertensionaha.115.05166
Wu, J., Bostrom, P., Sparks, L. M., Ye, L., Choi, J. H., Giang, A. H., . . . Spiegelman, B. M. (2012). Beige adipocytes are a distinct type of thermogenic fat cell in mouse and human. *Cell, 150*(2), 366-376. doi:10.1016/j.cell.2012.05.016
Wu, L., Zhang, L., Li, B., Jiang, H., Duan, Y., Xie, Z., . . . Li, J. (2018). AMP-Activated Protein Kinase (AMPK) Regulates Energy Metabolism through Modulating Thermogenesis in Adipose Tissue. *Front Physiol, 9*, 122. doi:10.3389/fphys.2018.00122
Wynne, B. M., Chiao, C. W., & Webb, R. C. (2009). Vascular Smooth Muscle Cell Signaling Mechanisms for Contraction to Angiotensin II and Endothelin-1. *J Am Soc Hypertens, 3*(2), 84-95. doi:10.1016/j.jash.2008.09.002
Xie, F., Jia, L., Lin, M., Shi, Y., Yin, J., Liu, Y., . . . Meng, Q. (2015). ASPP2 attenuates triglycerides to protect against hepatocyte injury by reducing autophagy in a cell and mouse model of non-alcoholic fatty liver disease. *J Cell Mol Med, 19*(1), 155-164. doi:10.1111/jcmm.12364
Xie, W. D., Wang, H., Zhang, J. F., Li, J. N., Can, Y., Qing, L., . . . Zhang, Y. O. (2011). Enhanced peroxisomal beta-oxidation metabolism in visceral adipose tissues of high-fat diet-fed obesity-resistant C57BL/6 mice. *Exp Ther Med, 2*(2), 309-315. doi:10.3892/etm.2011.208
Xu, J., Nakamura, M. T., Cho, H. P., & Clarke, S. D. (1999). Sterol regulatory element binding protein-1 expression is suppressed by dietary polyunsaturated fatty acids. A mechanism for the coordinate suppression of lipogenic genes by polyunsaturated fats. *J Biol Chem, 274*(33), 23577-23583. doi:10.1074/jbc.274.33.23577
Xu, Y., Wang, W., Wang, M., Liu, X., Lee, M. H., Wang, M., . . . Chen, W. (2018). High Salt Intake Attenuates Breast Cancer Metastasis to Lung. *J Agric Food Chem, 66*(13), 3386-3392. doi:10.1021/acs.jafc.7b05923
Xu, Z. P., Wawrousek, E. F., & Piatigorsky, J. (2002). Transketolase haploinsufficiency reduces adipose tissue and female fertility in mice. *Mol Cell Biol, 22*(17), 6142-6147. doi:10.1128/MCB.22.17.6142-6147.2002
Xue, J., & Ideraabdullah, F. Y. (2016). An assessment of molecular pathways of obesity susceptible to nutrient, toxicant and genetically induced epigenetic perturbation. *The Journal of nutritional biochemistry, 30*, 1-13. doi:10.1016/j.jnutbio.2015.09.002

Yahagi, N., Shimano, H., Matsuzaka, T., Sekiya, M., Najima, Y., Okazaki, S., . . . Yamada, N. (2004). p53 involvement in the pathogenesis of fatty liver disease. *J Biol Chem, 279*(20), 20571-20575. doi:10.1074/jbc.M400884200

Yalcin, A., Clem, B. F., Imbert-Fernandez, Y., Ozcan, S. C., Peker, S., O'Neal, J., . . . Chesney, J. (2014). 6-Phosphofructo-2-kinase (PFKFB3) promotes cell cycle progression and suppresses apoptosis via Cdk1-mediated phosphorylation of p27. *Cell Death Dis, 5*, e1337. doi:10.1038/cddis.2014.292

Yamashita, H., Takenoshita, M., Sakurai, M., Bruick, R. K., Henzel, W. J., Shillinglaw, W., . . . Uyeda, K. (2001). A glucose-responsive transcription factor that regulates carbohydrate metabolism in the liver. *Proc Natl Acad Sci U S A, 98*(16), 9116-9121. doi:10.1073/pnas.161284298

Yamauchi, T., Kamon, J., Waki, H., Terauchi, Y., Kubota, N., Hara, K., . . . Kadowaki, T. (2001). The fat-derived hormone adiponectin reverses insulin resistance associated with both lipoatrophy and obesity. *Nature Medicine, 7*(8), 941-946. doi:10.1038/90984

Yan, M., Audet-Walsh, É., Manteghi, S., Dufour, C. R., Walker, B., Baba, M., . . . Pause, A. (2016). Chronic AMPK activation via loss of FLCN induces functional beige adipose tissue through PGC-1α/ERRα. *Genes & Development, 30*(9), 1034-1046. doi:10.1101/gad.281410.116

Yanase, S., Yasuda, K., & Ishii, N. (2002). Adaptive responses to oxidative damage in three mutants of Caenorhabditis elegans (age-1, mev-1 and daf-16) that affect life span. *Mech Ageing Dev, 123*(12), 1579-1587. Retrieved from http://www.ncbi.nlm.nih.gov/pubmed/12470895

Yang, Q., Graham, T. E., Mody, N., Preitner, F., Peroni, O. D., Zabolotny, J. M., . . . Kahn, B. B. (2005). Serum retinol binding protein 4 contributes to insulin resistance in obesity and type 2 diabetes. *Nature, 436*(7049), 356-362. doi:10.1038/nature03711

Yang, S., Lin, H. Z., Hwang, J., Chacko, V., & Diehl, A. (2001). Hepatic Hyperplasia in Noncirrhotic Fatty Livers: Is Obesity-related Hepatic Steatosis a Premalignant Condition? *Cancer Research and Treatment, 61*, 5016–5023.

Yang, T., Aquino, V., Lobaton, G. O., Li, H., Colon-Perez, L., Goel, R., . . . Raizada, M. K. (2019). Sustained Captopril-Induced Reduction in Blood Pressure Is Associated With Alterations in Gut-Brain Axis in the Spontaneously Hypertensive Rat. *J Am Heart Assoc, 8*(4), e010721. doi:10.1161/JAHA.118.010721

Yang, W., Kelly, T., & He, J. (2007). Genetic epidemiology of obesity. *Epidemiol Rev, 29*, 49-61. doi:10.1093/epirev/mxm004

Yasue, S., Masuzaki, H., Okada, S., Ishii, T., Kozuka, C., Tanaka, T., . . . Nakao, K. (2010). Adipose tissue-specific regulation of angiotensinogen in obese humans and mice: impact of nutritional status and adipocyte hypertrophy. *Am J Hypertens, 23*(4), 425-431. doi:10.1038/ajh.2009.263

Ye, J. (2013). Mechanisms of insulin resistance in obesity. *Front Med, 7*(1), 14-24. doi:10.1007/s11684-013-0262-6

Yi, S. S., Firestone, M. J., & Beasley, J. M. (2015). Independent associations of sodium intake with measures of body size and predictive body fatness. *Obesity (Silver Spring), 23*(1), 20-23. doi:10.1002/oby.20912

Yiannikouris, F., Karounos, M., Charnigo, R., English, V. L., Rateri, D. L., Daugherty, A., & Cassis, L. A. (2012). Adipocyte-specific deficiency of angiotensinogen decreases plasma angiotensinogen concentration and systolic blood pressure in mice. *Am J Physiol Regul Integr Comp Physiol, 302*(2), R244-251. doi:10.1152/ajpregu.00323.2011

Yiannikouris, F., Wang, Y., Shoemaker, R., Larian, N., Thompson, J., English, V. L., . . . Cassis, L. A. (2015). Deficiency of angiotensinogen in hepatocytes markedly decreases blood pressure in lean and obese male mice. *Hypertension, 66*(4), 836-842. doi:10.1161/HYPERTENSIONAHA.115.06040

Yoshiji, H., Kuriyama, S., Yoshii, J., Ikenaka, Y., Noguchi, R., Nakatani, T., . . . Fukui, H. (2001). Angiotensin-II type 1 receptor interaction is a major regulator for liver fibrosis development in rats. *Hepatology, 34*(4 Pt 1), 745-750. doi:10.1053/jhep.2001.28231

You, Y. J., & Avery, L. (2012). Appetite Control: worm's-eye-view. *Animal Cells Syst (Seoul), 16*(5), 351-356. doi:10.1080/19768354.2012.716791

You, Y. J., Kim, J., Raizen, D. M., & Avery, L. (2008). Insulin, cGMP, and TGF-beta signals regulate food intake and quiescence in C. elegans: a model for satiety. *Cell Metab, 7*(3), 249-257. doi:10.1016/j.cmet.2008.01.005

Young, L., & Barnason, S. (2016). Uptake of Dietary Sodium Restriction by Overweight and Obese Patients After Cardiac Revascularization. *Rehabil Nurs, 41*(3), 149-157. doi:10.1002/rnj.205

Younossi, Z. M., Koenig, A. B., Abdelatif, D., Fazel, Y., Henry, L., & Wymer, M. (2016). Global epidemiology of nonalcoholic fatty liver disease-Meta-analytic assessment of prevalence, incidence, and outcomes. *Hepatology, 64*(1), 73-84. doi:10.1002/hep.28431

Yunbae, P., Yonggeun, H., Seokyong, K., Tom, P., Robert, V. F., & Joseph, L. (1998). In vivo Chiro-Inositol Metabolism in the Rat: A Defect in Chiro-Inositol Synthesis from Myo-Inositol and an Increased Incorporation of Chiro-[³H]Inositol into Phospholipid in the Goto-Kakizaki (G.K.) Rat. *Mol. Cells, 8*(3), 301-309.

Zeggini, E., Weedon, M. N., Lindgren, C. M., Frayling, T. M., Elliott, K. S., Lango, H., . . . Hattersley, A. T. (2007). Replication of genome-wide association signals in UK samples reveals risk loci for type 2 diabetes. *Science, 316*(5829), 1336-1341. doi:10.1126/science.1142364

Zhang, B., Berger, J., Hu, E., Szalkowski, D., White-Carrington, S., Spiegelman, B. M., & Moller, D. E. (1996). Negative regulation of peroxisome proliferator-activated receptor-gamma gene expression contributes to the antiadipogenic effects of tumor necrosis factor-alpha. *Molecular Endocrinology, 10*(11), 1457-1466. doi:10.1210/mend.10.11.8923470

Zhang, F., Xu, X., Zhang, Y., Zhou, B., He, Z., & Zhai, Q. (2013). Gene expression profile analysis of type 2 diabetic mouse liver. *PLoS One, 8*(3), e57766. doi:10.1371/journal.pone.0057766

Zhang, M., Zhao, Y., Li, Z., & Wang, C. (2018). Pyruvate dehydrogenase kinase 4 mediates lipogenesis and contributes to the pathogenesis of nonalcoholic steatohepatitis. *Biochem Biophys Res Commun, 495*(1), 582-586. doi:10.1016/j.bbrc.2017.11.054

Zhang, S., Hulver, M. W., McMillan, R. P., Cline, M. A., & Gilbert, E. R. (2014). The pivotal role of pyruvate dehydrogenase kinases in metabolic flexibility. *Nutr Metab (Lond), 11*(1), 10. doi:10.1186/1743-7075-11-10

Zhang, X., Wang, J., Li, J., Yu, Y., & Song, Y. (2018). A positive association between dietary sodium intake and obesity and central obesity: results from the National Health and Nutrition Examination Survey 1999-2006. *Nutr Res, 55*, 33-44. doi:10.1016/j.nutres.2018.04.008

Zhang, Y., Guo, K.-Y., Diaz, P. A., Heo, M., & Leibel, R. L. (2002). Determinants of leptin gene expression in fat depots of lean mice. *American Journal of Physiology-Regulatory, Integrative and Comparative Physiology, 282*(1), R226-R234. doi:10.1152/ajpregu.00392.2001

Zhang, Y., Proenca, R., Maffei, M., Barone, M., Leopold, L., & Friedman, J. M. (1994). Positional cloning of the mouse obese gene and its human homologue. *Nature, 372*(6505), 425-432. doi:10.1038/372425a0

Zhang, Y., Somers, K. R., Becari, C., Polonis, K., Pfeifer, M. A., Allen, A. M., . . . Singh, P. (2018). Comparative Expression of Renin-Angiotensin Pathway Proteins in Visceral Versus Subcutaneous Fat. *Front Physiol, 9*, 1370. doi:10.3389/fphys.2018.01370

Zhao, H., Shen, J., Djukovic, D., Daniel-MacDougall, C., Gu, H., Wu, X., & Chow, W. H. (2016). Metabolomics-identified metabolites associated with body mass index and prospective weight gain among Mexican American women. *Obesity science & practice, 2*(3), 309-317. doi:10.1002/osp4.63

Zhao, Y., Gilliat, A. F., Ziehm, M., Turmaine, M., Wang, H., Ezcurra, M., . . . Gems, D. (2017). Two forms of death in ageing Caenorhabditis elegans. *Nat Commun, 8*, 15458. doi:10.1038/ncomms15458

Zhou, L., Yu, M., Arshad, M., Wang, W., Lu, Y., Gong, J., . . . Xu, L. (2018). Coordination Among Lipid Droplets, Peroxisomes, and Mitochondria Regulates Energy Expenditure Through the CIDE-ATGL-PPARalpha Pathway in Adipocytes. *Diabetes, 67*(10), 1935-1948. doi:10.2337/db17-1452

Zhou, Y. T., Wang, Z. W., Higa, M., Newgard, C. B., & Unger, R. H. (1999). Reversing adipocyte differentiation: implications for treatment of obesity. *Proceedings of the National Academy of Sciences of the United States of America*, *96*(5), 2391-2395. doi:10.1073/pnas.96.5.2391

Zhu, H., Bhagatwala, J., Pollock, N. K., Parikh, S., Gutin, B., Stallmann-Jorgensen, I., . . . Dong, Y. (2015). High sodium intake is associated with short leukocyte telomere length in overweight and obese adolescents. *Int J Obes (Lond)*, *39*(8), 1249-1253. doi:10.1038/ijo.2015.51

Zhu, H., Pollock, N. K., Kotak, I., Gutin, B., Wang, X., Bhagatwala, J., . . . Dong, Y. (2014). Dietary sodium, adiposity, and inflammation in healthy adolescents. *Pediatrics*, *133*(3), e635-642. doi:10.1542/peds.2013-1794

Zhu, S., Cheng, G., Zhu, H., & Guan, G. (2015). A study of genes involved in adipocyte differentiation. *J Pediatr Endocrinol Metab*, *28*(1-2), 93-99. doi:10.1515/jpem-2014-0002

Zorad, S., Dou, J. T., Benicky, J., Hutanu, D., Tybitanclova, K., Zhou, J., & Saavedra, J. M. (2006). Long-term angiotensin II AT1 receptor inhibition produces adipose tissue hypotrophy accompanied by increased expression of adiponectin and PPARgamma. *Eur J Pharmacol*, *552*(1-3), 112-122. doi:10.1016/j.ejphar.2006.08.062

Zorad, S., Fickova, M., Zelezna, B., Macho, L., & Kral, J. G. (1995). The role of angiotensin II and its receptors in regulation of adipose tissue metabolism and cellularity. *Gen Physiol Biophys*, *14*(5), 383-391.

Zusman, R. M. (1987). Effects of converting-enzyme inhibitors on the renin-angiotensin-aldosterone, bradykinin, and arachidonic acid-prostaglandin systems: correlation of chemical structure and biologic activity. *Am J Kidney Dis*, *10*(1 Suppl 1), 13-23. Retrieved from http://www.ncbi.nlm.nih.gov/pubmed/3037886

Appendix

Specialty Feeds

3150 Great Eastern Hwy
Glen Forrest
Western Australia 6071
p: +61 8 9298 8111
F: +61 8 9298 8700
Email: info@specialtyfeeds.com

Diet SF00-219 — **21% Fat, 0.15% Cholesterol Semi-Pure Rodent Diet**

A semi-pure high fat diet formulation for laboratory rats and mice based formulated to mimic a "Western fast food diet". This diet was originally formulated to be equivalent to *Harlan Teklad* TD88137 or *Research Diets* Western Diet D12079B. Some modifications have been made to the original formulation to suit locally available raw materials.

- This Diet was developed to generate arteriosclerotic lesions in a range of susceptible mice strains.

Calculated Nutritional Parameters	
Protein	19.0%
Total Fat	21.0%
Crude Fibre	4.7%
AD Fibre	4.7%
Digestible Energy	19.4 MJ / Kg
% Total calculated digestible energy from lipids	40.0%
% Total calculated digestible energy from protein	17.0%

Ingredients	
Casein (Acid)	195 g/Kg
Sucrose	341 g/Kg
Clarified Butter (Ghee)	210 g/Kg
Cellulose	50 g/Kg
Wheat Starch	154 g/Kg
L Methionine	3.0 g/Kg
Calcium Carbonate	17.1 g/Kg
Sodium Chloride	2.6 g/Kg
AIN93 Trace Minerals	1.4 g/Kg
Potassium Citrate	2.6 g/Kg
Potassium Dihydrogen Phosphate	6.9 g/Kg
Potassium Sulphate	1.6 g/Kg
Choline Chloride (75%)	2.5 g/Kg
SF00-219 Vitamins	10 g/Kg
Cholesterol	1.5 g/Kg
Oxicap E2	0.04 g/Kg

Diet Form and Features

- Semi pure high fat diet. 12 mm diameter pellets.
- Pack size 1.5 Kg trays, vacuum packed in oxygen impermeable plastic bags, under nitrogen. Bags are packed into cardboard cartons to protect them during transit. Smaller pack quantity on request.
- Diet suitable for irradiation but not suitable for autoclave.
- Lead time 2 weeks for non-irradiation or 4 weeks for irradiation.

ISO 9001 SGS JAS-ANZ FEEDSAFE ACCREDITED FEED MANUFACTURER

Calculated Amino Acids	
Valine	1.20%
Leucine	1.80%
Isoleucine	0.80%
Threonine	0.80%
Methionine	0.80%
Cysteine	0.06%
Lysine	1.50%
Phenylalanine	1.00%
Tyrosine	1.00%
Tryptophan	0.30%
Histidine	0.59%

Calculated Total Minerals	
Calcium	0.60%
Phosphorous	0.30%
Magnesium	0.10%
Sodium	0.12%
Chloride	0.16%
Potassium	0.40%
Sulphur	0.23%
Iron	80 mg/Kg
Copper	7.0 mg/Kg
Iodine	0.2 mg/Kg
Manganese	20 mg/Kg
Cobalt	No data
Zinc	52 mg/Kg
Molybdenum	0.15 mg/Kg
Selenium	0.3 mg/Kg
Cadmium	No data
Chromium	1.0 mg/Kg
Fluoride	1.0 mg/Kg
Lithium	0.1 mg/Kg
Boron	2.3 mg/Kg
Nickel	0.5 mg/Kg
Vanadium	0.1 mg/Kg

Calculated Total Vitamins	
Vitamin A (Retinol)	11 650 IU/Kg
Vitamin D (Cholecalciferol)	1 100 IU/Kg
Vitamin E (a Tocopherol acetate)	64 mg/Kg
Vitamin K (Menadione)	12.5 mg/Kg
Vitamin C (Ascorbic acid)	700 mg/Kg
Vitamin B1 (Thiamine)	11 mg/Kg
Vitamin B2 (Riboflavin)	11 mg/Kg
Niacin (Nicotinic acid)	50 mg/Kg
Vitamin B6 (Pryridoxine)	11 mg/Kg
Pantothenic Acid	34 mg/Kg
Biotin	200 ug/Kg
Folic Acid	1 mg/Kg
Inositol	55 mg/Kg
Vitamin B12 (Cyancobalamin)	18 ug/Kg
Choline	3 860 mg/Kg

Calculated Fatty Acid Composition	
Saturated Fats C12:0 or less	1.80%
Myristic Acid 14:0	2.60%
Palmitic Acid 16:0	7.00%
Stearic Acid 18:0	2.40%
Palmitoleic Acid 16:1	0.40%
Oleic Acid 18:1	5.50%
Gadoleic Acid 20:1	No data
Linoleic Acid 18:2 n6	0.40%
a Linolenic Acid 18:3 n3	0.20%
Arachadonic Acid 20:4 n6	Trace
Total n3	0.35%
Total n6	0.41%
Cholesterol	0.15%
Total Mono Unsaturated Fats	6.23%
Total Polyunsaturated Fats	0.77%
Total Saturated Fats	13.99%

Calculated data uses information from typical raw material composition. **Diet post treatment by irradiation or auto clave could change these parameters.** It could be expected that individual batches of diet will vary from this figure. We are happy to provide full calculated nutritional information for all of our products, however we would like to emphasise that these diets have been specifically designed for manufacture by Specialty Feeds.